

T
24-77
MOH

STUDIES OF THE SANDS OF A PART OF THE THAR DESERT IN DISTRICT JAISALMER, RAJASTHAN

University of Roorkee, Roorkee
Certified that the above thesis/
Dissertation has been accepted for the
award of Degree of Doctor of
Philosophy / Master of Engineering
Geology vide notification
No. Ex/...../1965 (Degree) dated... 01/01/78
[Signature]
Assistant Registrar (Exam.)

THESIS SUBMITTED
By
P. C. MOHAN

FOR THE DEGREE OF DOCTOR OF PHILOSOPHY
in
APPLIED GEOLOGY

UNIVERSITY OF ROORKEE CENTRAL LIBRARY
175315 ✓
Date — 30-12-78
ROORKEE



DEPARTMENT OF GEOLOGY & GEOPHYSICS
UNIVERSITY OF ROORKEE
ROORKEE (INDIA)

August, 1977

FRONTISPIECE - A view of barchan dune field at
Dhanana, district Jaisalmer, Rajasthan.





Certificate

The thesis entitled 'STUDIES OF THE SANDS OF A PART OF THE THAR DESERT IN DISTRICT JAISALMER, RAJASTHAN' presented by Sri P. C. Mohan, for the award of the Degree of Doctor of Philosophy in Applied Geology, embodies results of investigations carried out by him from January, 1973 to August, 1977 under our supervision and guidance. This is further to certify that this work has not been submitted for the award of any other degree.

B. Parkash

(B. PARKASH)
M. Tech., Ph.D.
Reader
Department of Geology
and Geophysics
University of Roorkee
Roorkee - 247672
India

R. S. Mithal 8/9/77

(R. S. MITHAL)
M.Sc., Ph.D., D.I.C.
Professor and Head
Department of Geology
and Geophysics
University of Roorkee
Roorkee - 247672
India

ACKNOWLEDGEMENTS

The author feels pleasure in taking this opportunity to express his profound indebtedness to Dr.R.S. Mithal, Professor and Head, Department of Geology and Geophysics, University of Roorkee, for making available all possible facilities, taking keen interest in the fulfilment of this work and giving invaluable guidance during the course of this study.

The author intends to acknowledge his thanks to Dr. B. Prakash, Reader, Department of Geology and Geophysics, University of Roorkee, Roorkee, for initiating the present investigations and for his guidance and criticism throughout this work.

It will not be out of place to say that this work would not have been completed without the perpetual assistance, criticism and encouragement of Dr.S.K. Pathak, Reader in Hydraulics, Department of Civil Engineering, University of Roorkee, Roorkee and Sri Narendra Puri, Lecturer in Structural Engineering, Department of Civil Engineering, University of Roorkee, Roorkee. Credit for all the computer programming is due to Sri Narendra Puri. The author expresses his sincere gratitude to them.

It is a pleasant duty to acknowledge the invaluable help most willingly given in many ways by Drs. V.K. Gaur,

V.K.S. Dave, R.K. Geol, B.B.S. Singhal, N.G.K. Nair,
R.P. Gupta, S.S. Srivastava and A.K. Pachori.

The author feels thankful to Sri A.K. Awasthi, Lecturer,
Department of Geology and Geophysics, University of Roorkee,
for his fruitful discussions and assistance.

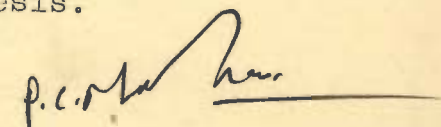
Grateful thanks are due to Sri Jagdish Srivastava,
Research Scholar, Department of Geology and Geophysics,
for his generous help throughout the present work.

Sincere thanks are also due to Sri O.P. Kalia for
carrying out photographic work.

The author expresses his profound thanks to Border
Security Force, Jaisalmer, for giving all help and facili-
ties in the field. The financial assistance extended by the
University Grants Commission is gratefully acknowledged.

The author is also thankful to Sri Kamesh Gupta and
Sri R.C. Sharma for their endurance during the preparation
of drawings and typing.

With much more than gratitude I acknowledge the
contributions of Mrs. Shobha Mohan who not only endured
with forbearance and good humor the long ordeal of this
investigation but also assisted in various capacities
throughout the preparation of this thesis.



(P.C. MOHAN)

STUDIES OF THE SANDS OF A PART OF
THE THAR DESERT IN DISTRICT JAISALMER
RAJASTHAN

A B S T R A C T

The Thar desert in India occupies about 155,000 sq.km of western Rajasthan. During recent times it has attracted investigators with varied types of problems including those of defence, traction and geomorphology. However, geological and geotechnical aspects have received scant attention. The present study is an attempt to fill this gap.

In this investigation an exhaustive and systematic sedimentological study of desert areas around Sam, Dhanana, Lunar and Murar in Jaisalmer district has been made. Various bedforms, namely, ripples, barchans, transverse dunes, longitudinal dunes and sand piles have been described and their probable origin is discussed.

Samples collected from the various bedforms and sand flats have been analysed for (i) textural attributes of sand grains, (ii) mineralogical composition and (iii) engineering properties of the desert sands.

Grain size distribution, roundness and sphericity of the desert sands have been investigated in detail. For statistical analysis of grain size data, graphical moments for central tendency, dispersion, symmetry and peakedness of the distributions have been calculated with the help of a digital computer, using various formulae given by different

workers. The intermediate percentile values used in these formulae were calculated by interpolating between the experimental points using normal distribution. Plots of the statistical parameters have been made and their correlations discussed and interpreted in terms of grain size populations and modes of transport. In addition, spatial variability of grain size parameters in the area, and also within the barchans, has been studied.

Fields of the various environments have been delineated on plots between different grain size parameters by different investigators. Grain size parameters from the area under investigation have been plotted on some of these diagrams such as C-M diagrams, skewness-mean size diagram, mean size standard deviation diagram, Md vs. QDa diagram, QDa vs. Ska diagram etc., with a view to evaluate their efficacy as accurate environment indicators.

Heavy and light minerals of the desert sands have been identified and detailed petrographic modal analyses made. Variations of constituent modes with grain size and in space have been studied with a view to determine the provenance of the sands.

Determination of the various engineering properties of the sands is an essential step for any engineering project in deserts. Representative samples from different localities of the area have been subjected to shear strength and compaction tests. Also maximum dry density and optimum moisture content were

determined. Further, to investigate the mortar properties of the desert sands, samples were mixed with cement and water for casting cubes in ratios prescribed by the Indian Standards Code.

These sand cement cubes were then autoclaved and tested for compressive strength by Universal Testing Machine. The data so obtained were then analysed and correlated with the grain size parameters. Permeability of a few typical samples has been determined. The soil groups of desert sands of the area have also been determined.

In brief, emphasis throughout the study is on a closer understanding of the **energy-environment** relationship which manifests in grain size parameters, bedforms, grain attributes and petrography of the area.

C O N T E N T S

Chapter	Page
CERTIFICATE	... i
ACKNOWLEDGEMENTS	... ii
ABSTRACT	... iv
LIST OF FIGURES	... xii
LIST OF TABLES	... xviii
1. INTRODUCTION	... 1
1.1 Rationale	... 1
1.2 Area of study	... 2
1.3 Climate	... 4
1.3.1 Rainfall	... 4
1.3.2 Temperature	... 4
1.3.3 Humidity	... 5
1.4 Vegetation	... 5
1.5 Physiography	... 6
1.6 Drainage	... 7
1.7 Geology of the area	... 8
1.8 Previous work	... 12
1.9 Scope of the present work	... 14
2. REVIEW OF ORIGIN AND CHARACTERISTICS OF DESERT ENVIRONMENTS WITH SPECIAL REFERENCE TO THE THAR DESERT	... 20
2.1 Theories of desert formation	... 20
2.2 The Thar desert	... 21
2.2.1 Origin of the Thar desert	... 22
2.2.2 Age of the Thar desert	... 25
2.2.3 Expansion or contraction of the Thar desert	... 27
3. BEDFORMS	... 29
3.1 Introduction	... 29

Chapter	Page
3.2 Bedforms of the area	... 30
3.2.1 Ripples	... 30
3.2.1.1 Mechanism of ripple formation	... 38
3.2.2 Dunes	... 41
3.2.2.1 Barchans	... 42
3.2.2.2 Mechanism of formation of barchans	... 48
3.2.2.3 Wind eddies and barchans	... 49
3.2.2.4 Transverse dunes	... 51
3.2.2.5 Origin of transverse dunes	... 53
3.2.2.6 Longitudinal dunes	... 53
3.2.2.7 Origin of longitudinal dunes	... 57
3.2.3 Sand piles	... 58
3.3 Relationship between wind direction and dune orientation	... 59
4. TEXTURAL STUDIES	... 67
4.1 Introduction	... 67
4.2 Grain size analysis	... 67
4.2.1 Purpose	... 67
4.2.2 Collection of samples	... 68
4.2.3 Sample preparation and sieving	... 69
4.2.4 Analysis and presentation of data	... 72
4.2.5 Comparison of graphical grain size parameters	...102
4.2.6 Variation of grain size parameters	...109
4.2.6.1 Mean size	...109
4.2.6.2 Sorting	...110
4.2.6.3 Skewness	...110
4.2.6.4 Kurtosis	...115
4.2.7 Parametric interrelationships	...116
4.2.7.1 Mean size versus sorting	...116
4.2.7.2 Mean size versus skewness	...118
4.2.7.3 Skewness versus kurtosis	...120
4.2.7.4 Mean size versus kurtosis	...120
4.2.7.5 Sorting versus skewness	...123

Chapter	Page
4.2.8 Variation of grain size in different bedforms and sand flats	... 123
4.2.9 Variation of grain size parameters within barchan dunes	... 127
4.2.10 Spatial variation of grain size parameters	... 132
4.2.11 Evaluation of grain size parameters for the recognition of desert environment	... 137
4.2.11.1 Metric based system of Buller and McManus (1972)	... 138
4.2.11.2 C-M pattern	... 141
4.2.11.3 Mean size versus standard deviation diagram of Friedman (1961)	... 143
4.2.11.4 Skewness versus mean diameter diagrams of Friedman (1961) and Moiola and Weiser (1968)	... 143
4.2.11.5 $\sqrt{\sigma^2}$ versus $\frac{s(Ku)}{s(Mz)} \cdot s(\sigma^2)$ plot of Sahu (1964)	... 146
4.2.12 Grain size populations in aeolian sediments	... 149
4.3 Study of roundness	... 155
4.3.1 Procedure	... 155
4.3.2 Operator experiment	... 156
4.3.3 Results of roundness study	... 158
4.4 Study of sphericity of quartz grain	... 161
4.4.1 Introduction	... 161
4.4.2 Procedure of study	... 162
4.4.3 Distribution of sphericity values	... 163
4.4.4 Mean and standard deviation of sphericity values	... 169
5. PETROGRAPHIC STUDIES	... 173
5.1 Introduction	... 173

Chapter	Page
5.2 Light minerals	... 173
5.2.1 Method of study	... 173
5.2.2 Description of light mineral constituents	... 176
5.2.2.1 Quartz	... 176
5.2.2.2 Chert	... 178
5.2.2.3 K-Feldspars	... 178
5.2.2.4 Plagioclase feldspars	... 181
5.2.2.5 Calcite	... 182
5.2.2.6 Aragonite	... 182
5.2.3 Variation of modal composition with grain size	... 182
5.2.4 Areal variation of constituent modes	... 182
5.2.5 Classification of sands	... 185
5.3 Heavy minerals	... 187
5.3.1 Method of study	... 187
5.3.2 Description of heavy minerals	... 188
5.3.2.1 Hornblende	... 188
5.3.2.2 Kyanite	... 192
5.3.2.3 Staurolite	... 192
5.3.2.4 Sphene	... 192
5.3.2.5 Rutile	... 193
5.3.2.6 Other minerals	... 193
5.3.3 Areal variation of heavy mineral frequencies	... 193
5.4 Provenance of the aeolian sands	... 194
6. ENGINEERING PROPERTIES	... 198
6.1 Introduction	... 198
6.2 Laboratory investigations	... 199
6.2.1 Mortar compressive strength	... 199
6.2.2 Compaction	... 205
6.2.3 Shear Strength	... 213
6.2.4 Permeability	... 214

Chapter	Page
7. SUMMARY AND CONCLUSIONS221
7.1 Summary	... 221
7.2 Conclusions	... 232
7.3 Suggestions for further study	... 236
REFERENCES	... 238
APPENDICES	... 251
I Description of sample locations	... 251
II Percentages of weight retained on different sieves	... 256
III Interpolated percentile values in phi units	... 259
IV Mean grain size values (phi units) as estimated by different formulae	... 268
V Standard deviation values (phi units) as estimated by different formulae	... 271
VI Skewness values as estimated by different formulae	... 274
VII Kurtosis values as estimated by different formulae	... 277
VIII Metric values of median (Md), standard deviation (QDa) and skewness (Ska) for use in diagrams of Buller and McManus (1972)	... 280

LIST OF FIGURES

Figure	Page
FRONTISPIECE A view of barchan dune field at Dhanana, district Jaisalmer, Rajasthan	
1.1 Location map of the area	... 3
1.2 Regional geological setup of western Rajasthan	... 9
1.3 Sample location map	... 15
3.1 Typical ripples in the area	... 31
3.2 Sinuous asymmetrical ripples are observed in area A. Sand shadows behind pebbles are observed in region B. Location near Dhanana	... 32
3.3 Two sets of ripples with crests trending almost at right angles to each other formed at the back of a barchan. Crests of some ripples are discontinuous and those of others show bifurcation. Ripples are truncated by sand avalanche. Location near Dhanana	... 33
3.4 Flat crested, arcuate, asymmetrical ripples at the back of a barchan in a dune field. Barchans can be seen in the background. Location near Dhanana	... 34
3.5 Ripples of different wave lengths and amplitudes are developed in areas A, B and C. Boundary between areas B and C is denticulated. Barchans are observed in the background. Location near point 43 in figure 1.3	... 36
3.6 Histograms showing distributions of wavelength, amplitude and ripple index of aeolian ripples	... 37
3.7 Plot of ripple amplitude H vs. wavelength λ (Plot includes 46 observations, extreme values being omitted)	... 39
3.8 Plot of ripple amplitude H vs. ripple index λ/H . Plot includes 48 observations.	... 40
3.9 Plot of ripple wavelength vs. ripple index λ/H . Plot includes all the 49 observations	... 40,

Figure	Page
3.10 Leeward view of barchans. Location near Dhanana	... 43
3.11 Typical barchans of the area.	... 44
3.12 Foresets of cross-bedding exposed in a cut made by wind in a barchan. The foresets dip at about 30° in a northerly direction. Location near Dhanana	... 47
3.13 Wind eddies around the barchans	... 50
3.14 Wavy parallel ripples on transverse dunes having sinuous crests. Location near Sam	... 52
3.15 Histograms showing distribution of lengths of longitudinal dunes	... 54
3.16 Horizontal, parallel laminations exposed in a cut made by wind in a longitudinal dune. The cut is roughly parallel to the crest of the dune. Location near Murar	... 55
3.17 Horizontal, parallel laminations exposed in a cut made by wind in a longitudinal dune. The lower half of the face contains a small scale, solitary crossbed. The cut is roughly parallel to the dune axis. Location near Murar	... 56
3.18 Orientation of sand accumulations in the area of study	... 61
3.19 Normal percentage frequencies of wind direction at Jodhpur	... 63
3.20 Normal percentage frequencies of wind direction at Barmer	... 64
3.21 Normal percentage frequencies of wind direction at Bikaner	... 65
4.1 A photograph of the sample splitter. 1/32 of the sample poured at the top is collected on the left side and the rest in the front	... 70
4.2 A photograph of the transfer funnel. The funnel is fitted with a vibrator. The sieve to be emptied is put at the top in upside down position	... 71
4.3- Cumulative frequency curves for grain size distributions	... 73-
4.30	100

28 pages - ?
6/5/70

Figure	Page
4.31 Histograms showing distributions of the various measures of mean grain size	... 103
4.32 Histograms showing distributions of the various measures of sorting	... 104
4.33 Histograms showing distributions of the various measures of skewness	... 105
4.34 Histograms showing distributions of the various measures of kurtosis	... 106
4.35 Photomicrograph (A) and cumulative frequency curve (B) for sample 63. The sample is from a sand pile. It has a mean size of 2.80 ϕ and shows good sorting ($\sigma = 0.17\phi$)	... 111
4.36 Photomicrograph (A) and cumulative frequency curve (B) of sample 103. The sample is from a barchan having a mean size of 3.00 ϕ . It shows good sorting ($\sigma = 0.25 \phi$)	... 112
4.37 Photomicrograph (A) and cumulative frequency curve (B) of sample 77. The sample is from windward side of a barchan. It has a mean size of 3.12 ϕ	... 113
4.38 Photomicrograph (A) and cumulative frequency curve (B) of sample 2 with a mean size 2.78 ϕ and showing poor sorting ($\sigma = 0.71 \phi$). The sample is collected from the trough of a ripple	... 114
4.39 Variation of σ with Mz	... 117
4.40 Variation of Sk with Mz	... 119
4.41 Variation of Ku with Sk	... 121
4.42 Variation of Ku with Mz	... 122
4.43 Variation of σ with Sk	... 124
4.44 Bar diagrams showing distributions of mean size Mz and standard deviation σ in different bedforms and sand flats	... 125
4.45 Bar diagrams showing distributions of skewness Sk and kurtosis Ku in different bedforms and sand flats	... 126
4.46 Variation of mean size with normalised height in barchans	... 128

Figure	Page
4.47 Variation of standard deviation with normalized height in barchans	... 129
4.48 Variation of skewness with normalised height in barchans	... 130
4.49 Variation of kurtosis with normalized height in barchans	... 131
4.50 Contours of Mz (ϕ units)	... 133
4.51 Contours of σ (ϕ units)	... 134
4.52 Contours of Sk	... 135
4.53 Contours of Ku	... 136
4.54 Plot of samples from the present study on Md-QDa diagram of Bullar and McManus (1972)	... 139
4.55 Ska-QDa diagram of Bullar and McManus (1972)	... 140
4.56 Plot of samples from the present study of Ska-QDa diagram. Dotted line indicates the boundary of the samples	... 140
4.57 (a) Passega's (1964) C-M diagram	... 142
(b) Plot of samples in C-M diagram	... 142
4.58 Plot of samples from the present study on mean size vs. standard deviation diagram of Friedman (1961) alongwith Moiola and Weiser (1968) sample points	... 144
4.59 Plot of samples from the present study on skewness vs. mean size diagram with superimposed boundaries between beach and inland dune sediments after Friedman (1961) and Moiola and Weiser (1968)	... 145
4.60 Plot of samples from the present study on mean size vs. skewness diagram with superimposed boundary between coastal and inland dunes after Moiola and Weiser (1968)	... 147
4.61 Log Log plot of $\sqrt{\sigma^2}$ vs. $\frac{s(Ku)}{s_{Mz}} \cdot s(\sigma^2)$ showing the differentiation between the environments of deposition after Sahu (1964) with the plot of present samples	... 148

Figure	Page
4.62a Histograms showing distributions of amounts of populations A and C in dunes and sand piles	... 150
4.62b Diagrammatic representation to explain the observed grain size characteristics of samples studied by mixing of two distinct populations with $\bar{X} = 2.75\phi$, $\sigma = 0.2\phi$ and $\bar{X} = 3.75\phi$, $\sigma = 0.25\phi$ respectively	... 153
4.63 Variation of mean roundness of quartz grains with grain size in different samples	... 159
4.64 Cumulative per cent frequency curves for sphericity values of quartz grains of different fractions of sample 5	... 164
4.65 Cumulative per cent frequency curves for sphericity values of quartz grains of different size fractions of sample 32.	... 165
4.66 Cumulative per cent frequency curves for sphericity values of quartz grains of different size fractions of sample 33	... 166
4.67 Cumulative per cent frequency curves for sphericity values of quartz grains of different size fractions of sample 38	... 167
4.68 Cumulative per cent frequency curves for sphericity values of quartz grains of different size fractions of sample 77	... 168
4.69 Variation of mean sphericity values with grain size in different samples \pm one standard deviation range is shown by vertical lines	... 170
5.1- Histograms showing distributions of	... 174
5.2 light minerals in different slides	... 175
5.3 Plot of different +120 mesh fractions and samples in the diamond diagram of Basu et al. (1975) for provenance determination	... 180
5.4 Plot of samples on Folk's (1968b) triangular diagram for classifying sandstones	... 186

Figure	Page
5.5 Histograms showing distributions of heavy minerals in different size fractions of samples 24 and 77	... 190
5.6 Histograms showing distributions of heavy minerals in samples from different locations	... 191
6.1 Autoclave for high pressure steam curing	... 201
6.2 Variation of compressive strength with grain size parameters	... 203- 204
6.3- Variation of dry density with water content ratio	... 207- 209
6.6 Variation of maximum dry density with grain size parameters	... 212
6.7 Variation of shear stress with normal stress	... 215
6.8 Variation of shear stress with normal stress	... 216
6.9 Variation of permeability with grain size parameters	... 219
6.10 Variation of permeability with distance	... 220

(109 figs)

LIST OF TABLES

Table No.	Page
1.1 General stratigraphic succession of western Rajasthan. Modified after Krishnan (1968, p.361)	... 11
3.1 Morphometric parameters of barchans	... 45
3.2 Mean wind speed (km/hr)	... 62
4.1 Formulae for computing graphical grain size parameters after different workers	... 101
4.2 Comparison of graphical measures for mean size	... 107
4.3 Comparison of graphical measures for standard deviation	... 107
4.4 Comparison of graphical measures for skewness	... 108
4.5 Comparison of graphical measures for kurtosis	... 108
4.6 Variation of grain size parameters in the various bedforms and sand flats	... 127
4.7 Values of $\bar{X}\rho$ for different slides and operators	... 156
4.8 Operator experiment data subjected to Analysis of Variance	... 157
4.9 Mean and standard deviation of roundness values of quartz grains of the various fractions of different samples	... 160
4.10 Mean, standard deviation and type of distribution of sphericity values.	... 171
5.1 Modal analysis of different slides and samples	... 179
5.2 Comparison of light mineral constituents in +120 mesh fraction to determine whether they are all from the same population	... 184
5.3 Percentages of different minerals in heavy mineral fractions	... 189
5.4 Comparison of heavy mineral frequencies in +230 mesh fractions to determine whether they are all from the same population	... 195
6.1 Properties of A.C.C. Portland Cement	... 200
6.2 Bulk sample data	... 211

CHAPTER-1

I N T R O D U C T I O N1.1 RATIONALE

The Thar desert of India has remained neglected perhaps due to difficult terrain and hostile climatic conditions. Consequently, scant information is available regarding the nature and behaviour of sands. Lately, the problems posed by this vast destitute of sand have come to prominence due to its strategic location near the international border, particularly from defence and traction view points.

The area is almost virgin and there is a great potential for its future development. Keeping these points into consideration coupled with the author's interest in the vast expanse of sands typifying aeolian environment, where winds have free play in shaping and modifying the desert surface, the present type area was selected for detailed investigations presented in this dissertation.

It is hoped that the studies of bedforms and their orientation and textural, petrographic and geotechnical investigations of the aeolian sands should provide an insight into the processes responsible for the initiation, growth and maintenance of the deserts, aeolian transport and deposition, and the possibility of desert contraction or expansion, if any. The study of engineering

properties of the sands will be of use for future engineering works that may be carried out in this area.

It is also hoped that this work may attract the attention of more workers to probe the mysteries of the deserts for the betterment of mankind.

1.2 AREA OF STUDY

The area under investigation covers a part of the Thar desert falling between latitudes $26^{\circ}30'$ to $26^{\circ}52'$ and longitudes $70^{\circ}0'$ to $70^{\circ}33'$. The village Sam lies in the northeast of the area which extends to the southwest right upto international Indo-Pakistan border including remote border outposts like Murar, Dhanana and Lunar (Fig. 1.1). In all, it occupies about 3,000 square kilometers of the arid expanse in the district of Jaisalmer (Lat. $26^{\circ}55'N$, Long. $70^{\circ}56'E$), Rajasthan. It falls under the Survey of India sheet numbers 40 J/1, 40 J/2, 40 J/5, 40 J/6, 40 J/9 and 40 J/10. The largest city in the vicinity of the area is Jaisalmer which supports a population of about 30,000 and is well connected with Jodhpur (Lat. $26^{\circ}18'N$, Long. $73^{\circ}01'E$).

The area is conveniently approachable from Jaisalmer which is connected by a metalled road to Sam and Dhanana. However, rest of the interior is accessible with the help of a camel or a power vehicle.

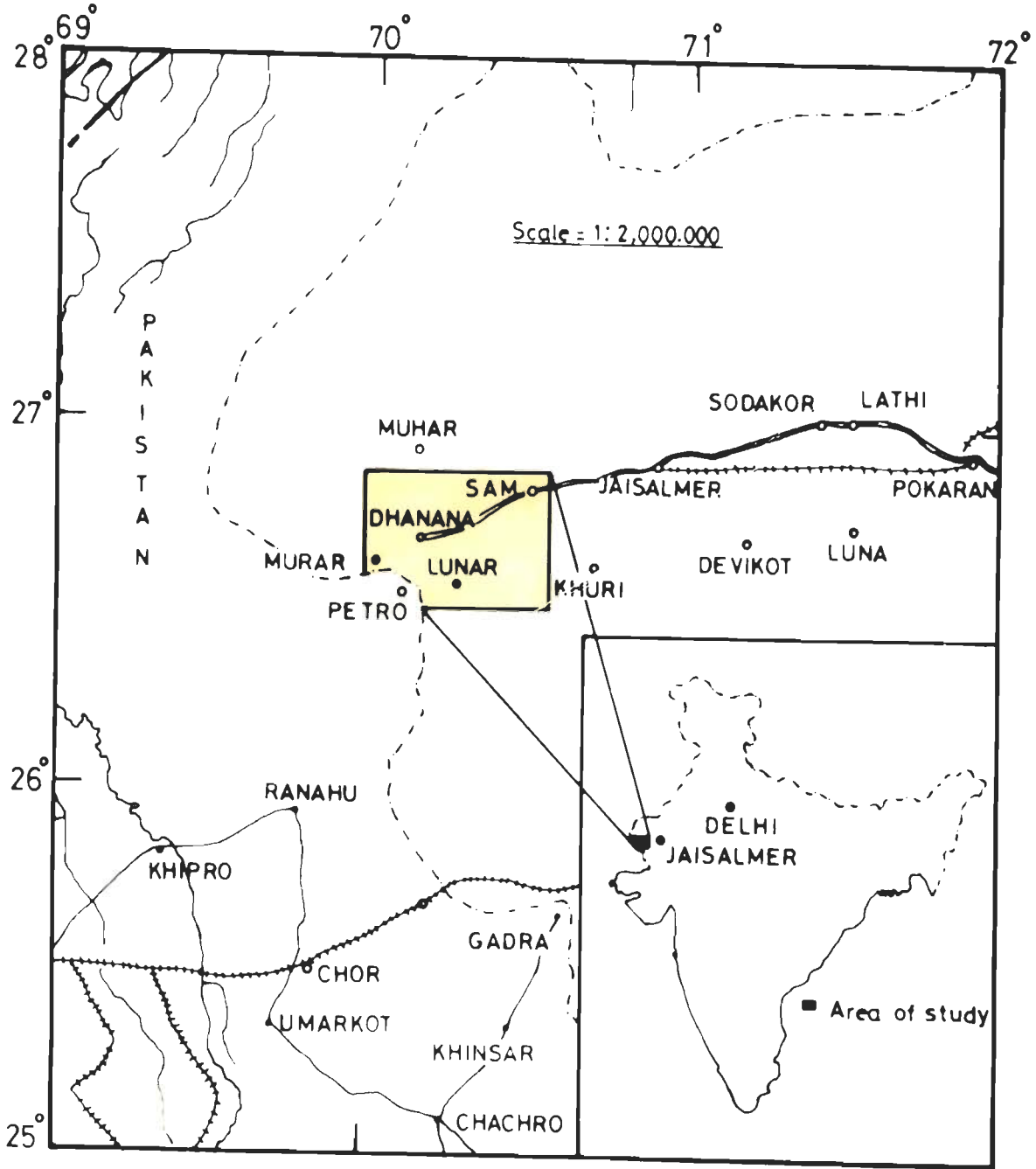


Fig.1.1— Location map of the area.

1.3 CLIMATE

The general characteristics of the Thar desert are typical of a hot desert such as slight rainfall, large variability of rainfall, large diurnal variation of temperatures and high maximum temperatures during summers, large evaporation, nonorigin of any permanent river, scanty vegetation, practically no agriculture, dependence of man on animals and a sparse and nomadic population (Pramanik, 1952).

1.3.1 Rainfall

The annual rainfall in the Thar desert is less than 25 cm. The average rainfall of western Rajasthan is 24.83 cm with the highest rainfall from 77.5 cm to the lowest rainfall 4.7 cm with a coefficient of variability 49 (Pramanik, 1952). Though the average rainfall is low, intense and sporadic falls may occur pouring large quantities of water in a considerably short duration of time. Torrential rains have been reported from deserts when the rainfall equals to one and a half times or even more of the annual rainfall in a single day (Pramanik, 1952). According to Pramanik (1952) Jaisalmer has more daily intensity of rainfall in monsoon as compared to places like Calcutta and Bombay which are situated in rainy regions.

1.3.2 Temperature

The temperatures in the Thar desert are of extreme

nature. Winters are quite cold with temperatures going 2°C to 5°C below zero. Similarly summers are characterised by intense heat with strong hot winds. Due to rocks and sandy nature of the soils lacking sufficient vegetation cover and dry atmosphere with clear skies, the variation of high day temperature to low night temperature is considerable and with a sharp change. The mean maximum temperature in May is 38°C to 46°C over most part of Rajasthan with a mean minimum at 24°C to 27°C (Pramanik, 1952).

1.3.3 Humidity

In winters the relative humidity is generally 50% to 60% in the morning hours and 25% to 35% in the afternoon hours. During summers humidity is in general 35% to 60% in the morning hours and 10% to 30% in the afternoon hours except for the month of June which has higher mean value due to the advent of rainy season near its end (Pramanik, 1952).

1.4 VEGETATION

In general the area lacks vegetation and there is near absence of trees. However, there are sparse and scanty patches of shrubs, thorny bushes and wild grasses. It is a vast barren land showing a typical desert destitute with thin population. There are some tiny settlements scattered in the desert and the major occupation of the inhabitants is cattle rearing (mainly cows). Some of the

villages have grown around tiny wells dug in clusters of 8 to 10 in number which are commonly called 'Boris'. Water table occurs at twenty to thirty metres depth and these wells usually get dried up in summers. The inhabitants move to other areas with their herds during summers and in times of drought, which are fairly common.

1.5 PHYSIOGRAPHY

Regionally, the area consists of low relief with scarps of yellow limestones around the city of Jaisalmer. Most of the area is of undulating topography consisting of barren rock wastes with occasional mounds of sands forming different types of dunes. The area around the city of Jaisalmer is dissected by numerous 'nallas' and gullies giving rise to ephemeral rivulets like the Mussurdi which flows in northwestern direction. Similarly, the Kakni river and its tributaries flow towards north. As one moves towards Murar (Fig.1.3), sand accumulations increase steadily with a general tendency of the sand cover to thicken in the southwest until Dhanana where barchans and scifs practically cover the entire area and the true sandy desert starts. The interdune areas are comparatively firm and flat which occasionally get a darker colour tone due to surface accumulation of small ferruginous concretions.

In general, it may be concluded that the various physiographic features have largely been controlled by

7
climate typical of a wind governed terrain.

1.6 DRAINAGE

Drainagewise the area can be divided into two major units controlled by the lithology i.e. (i) consisting of compact rock wastes and (ii) wind blown sediments forming dunes. The area, for obvious reasons, is not drained by any perennial river. The drainage is mostly internal. On the barren rocky desert, as around Jaisalmer, the drainage pattern is dendritic. A number of small 'nallas' and rivulets start from rocky slopes and culminate into a local depression forming small ponds which may remain dry through most of the year. The chief water tanks around Jaisalmer are Gadi Sar, Govind Sar, Gulab Sagar, Sudha Sar, Kheta Sar, Gajroop Sagar, Mobta Sar, Amar Sagar etc.

On the hill slopes deep ravines have been cut by 'nallas' which flow in the rainy season. At places these 'nallas' have cut deep channels in the wind deposited sands. Elsewhere, there may be formation of alluvial cones adjoining comparatively high scarps where the 'nallas' have reworked the wind blown sediments.

In the sandy desert there is no well established drainage pattern and no 'nallas' or gulley cuttings are observed due to quick and easy mobility of sands by strong summer wind currents.

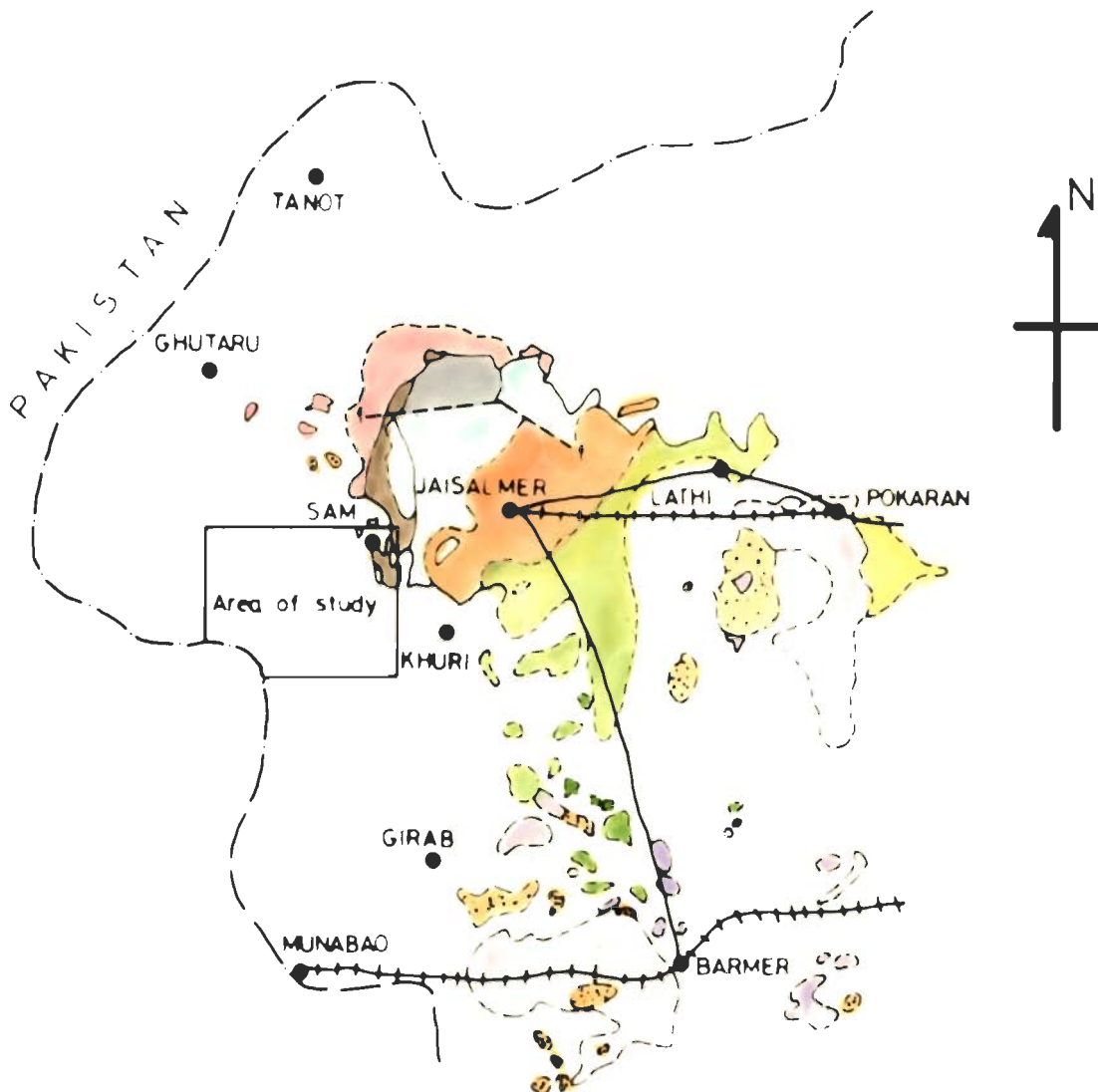
1.7 GEOLOGY OF THE AREA

The regional geological setup is shown in Figure 1.2. The oldest rocks exposed in the Jaisalmer district are Malani suite of igneous rocks which consist of granites and rhyolites. These are overlain unconformably by the Vindhyan composed of dolomites with cherty layers.

The fossiliferous Badhaura Formation, consisting of yellow calcareous sandstones and brown clays, occur as isolated patches overlying unconformably on the Vindhyan. These are thought to be of Permo-Carboniferous age. Though no exposures of Triassic sediments are known, Permo-Triassic sequence has been recorded in the subsurface (Das Gupta, 1975b).

The Jurassic sequence is represented by the Lathi Beds (L. Jurassic), Jaisalmer Beds (Callovian to Oxfordian), Baisakhi Beds (Oxfordian to Kimmeridgian) and Badesar Beds (Upper Jurassic). The Lathi Beds, which are 330 m thick, consist chiefly of sandstones with some layers of limestone in the upper parts. The Jaisalmer Beds are 160 m thick. These are formed of buff to yellow oolitic and shell limestones and calcareous sandstones. The Baisakhi Beds are 600 m thick and consist of gypseous shales and sandstones. A 110 to 300 meter thick horizon, consisting of ferruginous sandstones and grits, constitutes the Badesar Beds.

The Parihar Sandstones which are 600 to 850 m thick are thought to be of Lower Cretaceous age. These consist of ferruginous and feldspathic sandstones and quartzites.



Scale 1:2,000,000

LEGEND

- Recent
 - Bandah and Khuiala beds
 - Abur beds
 - Parihar sandstones
 - Badasar beds
 - Jaisalmer limestones and Baisakhi beds
 - Lathi beds
 - Vindhya
 - Rhyolites
 - Granites
- } Malani suite
- f-----f Fault

Fig 12. Regional Geological Setup Of Western Rajasthan

(Modified after G.S.I. map, 1962)

A comparatively thin formation of about 60 to 90 m consisting of brown to yellow shell limestone with subordinate bands of grit, clays and shales constitutes the Abur Beds. These belong to the Aptian age. The Bandah and Khuiala Beds of Eocene age, about 50 m thick, rest unconformably over the Abur Beds. They consist of siliceous limestones with Fuller's earth and clay.

The Shumar Beds, about 30 to 316 m thick, rest unconformably over the Bandah and Khuiala Beds. These consist of ferricrusted, bouldery, arenaceous limestones, sandstones and limestones. These are the youngest formation belonging to the Sub-Recent age. It has not been possible to include Shumar Beds in the geological map (Fig.1.2) since the published geological maps are of small scale and indistinct. Rest of the area is mainly covered by unconsolidated, sandy soils constituting the aeolian sediments. These are thought to be of Recent age. Table 1.1 gives general stratigraphic succession in the Jaisalmer district as determined by various workers of Geological Survey of India and Oil and Natural Gas Commission (Narayanan, 1964; Lukose, 1972; Das Gupta, 1973; Lukose, 1974; Lukose and Misra, 1974; Das Gupta et al. 1974; Das Gupta, 1975a, b; Pareek, 1975; Verma, 1975).

The Mesozoic and Tertiary rocks form a gentle arch which plunges towards Mari in Sindh, Pakistan, in the northwest direction. The whole sedimentary sequence thickens in the west and northwest and attains a thickness

Table 1.1- General stratigraphic succession of Western Rajasthan. Modified after Krishnan (1968, p.361).

Formation	Thickness	Lithology	Age
Unconsolidated Sediments		Aeolian Sediments	Recent
----- Unconformity -----			
Shumar Beds	30-316 m	Ferricrusted, bouldery arenaceous limestones, sandstones and limestones	?Sub-Recent
----- Unconformity -----			
Bandah and Khuiala Beds	?50 m	Siliceous limestones with fuller's earth and clay	Eocene
----- Unconformity -----			
Abur Beds	60-90 m	Limestone, subordinate grits, clays and shales	Low.Cretaceous(Aptian)
Parihar Sandstones	?600-850 m	Ferruginous and feldspathic sandstones and quartzites overlapped at places by Eocene beds	Low.Cretaceous(Neocomian)
Badesar Beds	110-300 m	Ferruginous sandstones and grits	Up. Jurassic
Baisakhi Beds	600 m	Sandstones and Shales (gypseous)	Up. Jurassic (Oxfordian to Kimmeridgian)
Jaisalmer Beds	160 m	Buff to yellow oolitic and shell limestones and calcareous sandstones	Up Jurassic (Callovian to Oxfordian)
Lathi Beds	330 m	Sandstones and some layers of limestones in the upper part	Low.Jurassic
----- Unconformity -----			
Badhaura Formation		Yellow, calcareous sandstones, brown clays	Permo-Carboniferous
----- Unconformity -----			
Vindhyan		Grey dolomite with chert layers and nodules	Pre-Cambrian
----- Unconformity -----			
Malani Formation		Rhyolites and granites	Pre-Cambrian

of about 6,000 m. A large fault on the western side of the arch is indicated by geophysical surveys (Krishnan, 1968, p.362).

1.8 PREVIOUS WORK

The area under investigation has remained practically neglected from the geological view point perhaps due to its remote location, lack of transport facilities and climatic hazards, though some work has been initiated by the Central Arid Zone Research Institute (CAZRI), Jodhpur in some other parts of the Thar desert.

Frere (1870) and Blanford (1876) are the early workers who reported that most of the Thar desert is occupied by parallel longitudinal dunes. Blanford (1876) was the first to establish the parallelism of the present wind direction and longitudinal dunes.

The Planning Commission of India reported in the First Five Year Plan (Anon., 1952) that the Thar desert had been advancing outwards in a great convex arc at an alarming rate of 0.8 km per year. This resulted in a symposium on the Rajputana desert i.e. the Indian part of the Thar desert, in March, 1952 organised by the National Institute of Sciences (now Indian National Science Academy) in an effort to discuss suitable steps to arrest its unchecked outward march. A symposium on the problems of the Thar desert and a workshop on the desert geology had been organised by the UNESCO and Geological Survey of India in 1964 and 1975 respectively.

More recently Gupta and Prakash (1975) have compiled environmental aspects of the Thar desert in the form of a book. All these works are referred to appropriately in the text.

Most of the workers like Banerji (1952), Pramanik (1952), Kendrew (1961) and Krishnan (1968) have suggested climatic conditions for the origin of the Thar desert. Roy and Pandey (1970) and Ahmad (1975) advocate an important role of tectonism in its genesis. Bryson and Baerreis (1967) think that atmospheric dust caused by human activity may trigger an extreme dry cycle. Wadia (1955,1960) thought that the general desiccation following the Pleistocene glaciation as the major cause of the desert.

Studies on geomorphology and land-use planning in the marginal areas of the desert have been mainly undertaken by the CAZRI and the Geological Survey of India. Various dune forms and landforms of the Luni Basin have been described by Pande et al.(1964), Ghose et al.(1966), Singh(1969-70), Verstappen et al.(1969); Singh et al.(1971) and Ghosh (1975). Dunes and geomorphological land units of the Bikaner district are described by Singh et al.(1975). Bhattacharya (1956) has discussed the nature and origin of dunes on the western side of Mount Abu. Land forms of the northern part of Jaisalmer have been described by Babu and Rao (1974). Morphometric analyses of drainage basins of the desert have been made by Singh et al.(1969-71), Pandey et al.(1972),

Singh and Ghose (1973) and Ramadurai and Gupta (1975).

Holland and Christie (1909) think that salt contents of the salt lakes of the Thar desert have been brought from the Rann of Kutch by wind. Godbole (1952) postulates that salt basins are relics of the extended area of the Arabian sea. Pandey and Chatterji (1970) find that location of some of the Ranns (saline depressions) is controlled by faults. Ghose (1964,1965) thinks that these Ranns are due to internal drainage and salts are obtained by chemical weathering of adjoining rocks.

Gupta (1958) and Rao (1962) have described mineralogy of the desert sands. Ghosh (1952) and Chakarabarti (1968) have studied grain size distributions. Roy and Pandey (1970) have reviewed the problem of expansion of the Thar desert.

1.9 SCOPE OF THE PRESENT WORK

In the present study, an exhaustive and systematic sedimentological analysis and geotechnical investigations of the desert sands in areas around Sam, Dhanana, Lunar and Murar in Jaisalmer district have been made. Various bedforms like seifs, barchans, transverse dunes, ripples and sand piles have been recognised and all the geometric dimensions necessary for defining their shape and any special features noted.

More than one hundred samples have been collected. Locations of the samples are shown in Figure 1.3 and



Fig.1.3_ Sample location map.

descriptions regarding their position on the bedforms are given in Appendix I. Locations of a few samples collected from areas near Ramgarh ($27^{\circ}23' : 70^{\circ}30'$) and Ludharwa ($70^{\circ}48'30'' : 26^{\circ}25'0''$) which do not fall in Figure 1.3 are also given in Appendix I. The samples have been analysed for the following aspects:

- (i) Textural attributes of sand grains, that is, grain size, roundness and sphericity,
- (ii) Mineralogical composition, and
- (iii) Engineering properties and behaviour.

All the findings regarding the above aspects have been systematically presented in this work which consists of seven chapters. Chapter 1 entitled 'INTRODUCTION' describes the location, accessibility, climate, vegetation, geomorphology, drainage, geology of the area under investigation and a brief review of the relevant previous work on the Thar desert.

Chapter 2 with the title 'REVIEW OF ORIGIN AND CHARACTERISTICS OF DESERT ENVIRONMENTS WITH SPECIAL REFERENCE TO THE THAR DESERT' describes various views about the formation of deserts of the World and the Thar desert in particular. The controversial problems of age of the Thar desert and its expansion and contraction are critically reviewed.

Chapter 3 titled as 'BEDFORMS' includes areal distribution of bedforms, their geometry and orientation with respect to the prevailing wind direction and grain size variation within the different

bedforms.

Chapter 4 entitled 'TEXTURAL STUDIES' exhaustively deals with grain size analysis and grain attributes such as grain roundness and sphericity. Desert sand samples were analysed for grain size distribution studies using ASTM sieves. For statistical analysis, the graphical moments were determined for central tendency, dispersion, symmetry and peakedness of the distributions. Moment measures using the various formulae are calculated with the help of a computer and compared. The required percentile values used in the calculation of moment measures are determined by interpolating between the adjacent experimental points using normal distribution. Modality of sand samples of the area has been studied from the cumulative curves plotted on arithmetic-probability paper. Plots of grain size statistical parameters have been made and their correlations discussed and interpreted in terms of grain size populations and processes of transportation by wind. Regional variability of the various statistical parameters in the desert area is probably being reported for the first time in the present work. Spatial variability of the various grain size parameters within barchans is critically analysed.

Diagrams of plots between different grain size parameters have been given by different researchers and fields for various environments have been delineated on these plots. Grain size statistical parameters obtained

from the desert sands of the area under investigation have been plotted on C-M diagram, QDa-Md diagram, QDa-SKa diagram etc., with a view to develop grain size analysis as an accurate environmental indicator.

For grain roundness studies, slides of representative samples are made and roundness of quartz grains in each slide is determined by visual comparison method. Accuracy and consistency of the visual comparison method are also evaluated. Variation of roundness in the area and with grain size in individual samples has been analysed in the study. Also sphericity of the aeolian sands has been studied by measuring axial ratio of quartz grains from half phi fractions of a few sand samples.

Chapter 5, which bears the title 'PETROGRAPHIC STUDIES' deals with separation and detection of both light and heavy minerals in the representative sand samples of the area. Light and heavy mineral slides are made and petrographical and modal analysis is carried out. Mineralogical data so collected is then analysed to study their variability in space and with grain size and also to establish provenance of the sands.

Chapter 6 entitled 'ENGINEERING PROPERTIES' constitutes a very important applied aspect of the present investigation. Determination of the various engineering properties of sands is an inevitable step preceding any construction project in deserts. Representative sand samples from different

localities of the area have been subjected to shear strength and compaction tests in order to evaluate their suitability for foundations. To investigate mortar making properties of the desert sands, representative sand samples of the area were mixed with cement and water in the ratios prescribed by Indian Standards Code and cubes casted. These sand-cement cubes were autoclaved and then tested for compressive strength by Universal Testing Machine. Compressive strength data so obtained were then analyzed and correlated with grain size parameters. The hydrologic potential of desert sand samples was also evaluated by subjecting these to permeability tests.

The final Chapter 7 is titled as 'SUMMARY AND CONCLUSIONS' which summarises the findings of Chapters 1 to 6. The salient results of the investigations are brought out and important conclusions are drawn. Finally suggestions for further studies in sedimentology of the Indian desert are outlined.

The present thesis thus embodies a systematic study of the desert sands in the western part of Rajasthan. The emphasis throughout the work is on a closer understanding of the energy-environment relationships which manifest variously in bedforms, grain size parameters, grain attributes and petrography and engineering properties of the sands of the area.

CHAPTER-2

REVIEW OF ORIGIN AND CHARACTERISTICS OF DESERT
ENVIRONMENTS WITH SPECIAL REFERENCE
TO THE THAR DESERT

2.1 THEORIES OF DESERT FORMATION

Deserts are the reflections of climatic conditions which are responsible for their creation, growth and sustenance. Thus all those factors which influence climatic conditions ultimately also affect the formation and location of the deserts. The atmospheric conditions have their origin from the planetary system of high and low pressure belts. There is circulation of winds between the hot equatorial regions and the cooler polar areas. The existence of high pressure belts 30° north and south of equator causes clear skies which are not favourable to rains.

The deserts of the world are the result of one or many conditions like geographic location, topographic barriers and their orientation with respect to the direction of moisture laden winds, the effect of oceanic currents, low relief of the area or natural winds with insufficient moisture. Roy and Pandey(1970) suggest three different situations and conditions such as (i) the presence of persistent anticyclonic conditions (North African desert), (ii) impinging of cold ocean currents on the coasts (Peru desert, Namib desert) and (iii) topographic barriers which shut out the moisture laden winds (Gobi desert).

Most of the deserts of the world are located in regions where moist winds either originate or pass over land areas under clear skies causing little or no rains. Whenever they are obstructed by any land barrier such as a mountain range the rain occurs whereas desiccating conditions remain prevalent in the leezone. Australian desert and the Kalahari desert of South Africa are the examples.

2.2 THE THAR DESERT

A considerably large area (about 640 km long and 160 km wide) of the western and southwestern Rajasthan, India, and Sind, Pakistan form the Great Indian Desert which is called the Thar desert. The desert, in general, is covered by a several meter thick sand which at places thickens, thins or is absent to bare the rocky floor. The sands are moved by the predominantly southwest winds to form various types of dunes and other characteristic desert bedforms. The desert gradually grades into a semi-arid region on its northern and eastern borders.

The whole region starting from the western coast of north Africa to the Thar desert in the east appears to be almost meteorologically homogeneous (Sajnani, 1964) with nearly identical physiographic and anthrogeographical conditions (Roy and Pandey, 1970). Thus the Thar desert seems to be the eastern limit of a large desert tract which includes the North African Sahara and Arabian deserts also.

2.2.1 Origin of the Thar Desert

The chief causes which are thought to be responsible for the origin of the Thar desert are:

- (a) Geographical location in the desert belt of the world,
- (b) Topographical factors,
- (c) Meteorological factors,
- (d) Tectonism and
- (e) Other factors.

(a) Geographical location in the desert belt of the world — Most of the deserts of the world lie in a belt between 30° north and south of equator. Generally, these are low pressure areas characterised by clear skies which are not conducive to rainfalls. The Thar area of India also falls in this region. Therefore, the occurrence of desert here is not unexpected. In fact, it has been thought as an eastern limit of a great desert that includes even African Sahara (Sajnani, 1964).

(b) Topographical factors — The main factors which influence the climate of the Indian subcontinent as a whole and also constitute one of the major causes of origin of the Thar desert are the location of the high Himalayas, the Kirthars and the Sulaiman mountain ranges and the Tibetan plateau (Roy and Pandey, 1970). The cumulative effect of these natural barriers is such that the western part of Rajasthan gets very meagre rainfall. Similarly, whatever moisture is left from the moist winds passing over the Ganges plains

gets precipitated on the eastern flanks of the Aravallis, whereas desiccating conditions prevail in the west beyond (Glennie, 1970, p.5).

(c) Meteorological factors — The chief climatic causes responsible for the origin of the Thar desert are the presence of low pressure over western part of India and central part of Pakistan, dry northwest upper air and shallow southwest monsoon currents (Roy and Pandey, 1970).

According to Banerji (1952) the mechanism of monsoon in India is influenced by a pressure gradient setup between a low pressure over the Thar desert and a relatively high pressure in the south Indian Ocean. The low pressure is attributed to higher temperatures resulting from the bare desert rocks and sands that get quickly heated and to the hydrodynamic consequence caused by the natural barrier to the airflow by the Himalayan, the Sulaiman and the Kirthar ranges in the form of a 'corner' (Roy and Pandey, 1970).

Moist air can cause precipitation only when it cools and condenses by ascending up. But according to Ramanathan (1972) and Pramanik (1952) there exists dry, warm, subsiding, anticyclonic air over the Thar desert and its neighbourhood which overlies the maritime shallow surface winds drawn in during the monsoons. Thus the ascending moist airs are absorbed by these anticyclonic winds thereby dissipating clouds, if any. Pramanik (1952) states that so long these

anticyclonic winds prevail over the Thar desert there is little possibility of increase in the rainfall in this region.

The monsoon from the Arabian Sea is strong only south of The Gulf of Cambay and almost fades out in the north. Hence a very feeble monsoon air passes over the Thar desert. Winds coming across the Arabian sea loose most of their moisture by travelling over North Africa and Abyssinian plateau. This makes it amply clear that due to either complete denial or very weak monsoons desertic environment thrives in the Thar region.

(d) Tectonism — The Thar region experienced faulting and regional domal upwarping in association with complementary rising of the Aravallis in the Holocene times. Faulting resulted in a horst in Rajasthan and a graben in Sind. As a consequence to this the arm of the sea occupying the Thar region was forced out. There resulted a massive course shifting of rivers like the Indus, the Sutlej and the Beas westward. This caused floods which destroyed Mohanjodaro and Harappa civilizations. Headward erosion of the Jamuna captured the river Drishadwati. The head-waters of the Saraswati were affected by the rising Himalayas which could not succeed in cutting through the Siwalik barrier (Ahmad, 1975).

Thus massive course shifting of the life sustaining rivers of the region coupled with total loss of rivers like

Drishadwati and Saraswati partly due to tectonism, rendered the area a desert. Of course, general worldwide warming up of the climate following the Pleistocene glaciation is also one of the contributory factors (Ahmad, 1975).

(e) Other factors — Massive deforestation, unplanned grazing of animals and unplanned cultivations are the other reasons which add to the aridity of the region. Bryson and Baerries (1967) think that the dust cover raised by excessive human activity is the cause for the spread of the desert.

2.2.2 Age of the Thar Desert

Wadia (1956, 1959) thinks that the Asian deserts are a product of the Post-Pleistocene glaciation aridity phenomenon, and these may be as young as 10,000 to 20,000 years in age.

Roy and Pandey (1970) argue that climatic condition like scanty or no rainfall due to very feeble monsoon over the Rajasthan desert region is the ultimate cause which is responsible for the formation of the desert. Also the present monsoon system was established in the Indian sub-continent during Mid. Miocene period when the Himalayan ranges came into existence. Different lithologies deposited from the Eocene to Pleistocene in this region are indicative of the period of desert formation. Thus the Thar desert came into existence during the Mid. Miocene, though its development was thwarted temporarily by humid climates (Ahmad, 1969). The prevalence

of aridity during the Mid. Miocene in the southwestern desert of North America (Axelrod, 1950; Axelrod and Ting, 1960) is cited as a supporting evidence.

Recent geophysical studies of the Indian ocean (McKenzie and Sclater, 1971; Fisher et al., 1971; Sclater and Harrison, 1971; Laughton et al., 1972) have made it possible to trace the movement of the Indian Peninsula with time. Paleogeographic reconstruction based on these studies by Laughton et al. (1972, Fig. 4) suggest that the equator passed through areas around Madras during the Middle Miocene indicating thereby that the part of Indian Peninsula now occupied by the Thar desert was way down to the south and probably lay in a humid, moist region. Thus it seems that the Thar desert per se could not be older than the time when the Peninsula came to occupy more or less the present position.

The presence of the Pleistocene Bap Boulder Bed in Rajasthan and Sub-Recent Shumar Formation of alluvial origin with a subsurface thickness of more than 300 m in the heart of the desert suggest that humid conditions prevailed in the area till Sub-Recent times.

Historical evidence regarding the age of the desert is rather unequivocal and has been reviewed by Gupta and Prakash (1975). However, Singh et al. (1974) have reported on the basis of pollen studies from the saline lake cores that more than 10,000 years B.P., intense arid conditions prevailed and that between 10,000 and 3,000 years B.P. climate

Archaeological
evidence

was rather humid. Since 3000 years B.P. climate has become arid again.

Goudie et al. (1973) have suggested that in this region stabilized dunes are formed whenever rainfall per annum exceeds 25 cm and active ones if rainfall is less than 25 cm. It will be shown later that the area has stabilized as well as active dunes. It is suggested that the Thar desert probably came into existence more than 10,000 years back and old dunes were formed, which were stabilized during the humid period that followed. Fresh, active dunes have developed since the onset of the present aridity cycle starting some 3000 years back.

2.2.3 Expansion or Contraction of the Thar Desert

It has long been feared that the Thar desert is encroaching on the fertile lands in its immediate neighbourhood. The Planning Commission reported in the First Five Year Plan (Anon., 1952) that the Thar desert is advancing in a great convex arch towards Delhi and Aligarh at the rate of about 0.8 km per year.

Roy and Pandey (1970) argue against the expansion of the desert. According to them if the rate of advancement is taken as 0.8 km per year, then the present boundary should have been 40 km ahead of what it is today. They further argue that if the age of the desert is taken as 5,000 years, as thought by many workers, and the rate of advance as 0.8 km per year then by now the desert would have advanced to at

least the foothills of the Himalayas if not upto somewhere in central Asia.

Meteorological data of the past 70 years suggest no climatological change over the Thar desert and adjoining areas which should be if the desert were advancing (Pramanik, 1952). Rao (1961) examines rainfall data of 80 years of the Thar desert and opines that there is no significant change in the annual regional rainfall of arid Rajasthan.

The present study also suggests that the sands of the Thar desert were brought in by the rivers which shifted their courses westwards, thus leaving the sediments behind for the free play of winds. It appears that no significant expansion of the desert is taking place.

CHAPTER-3

B E D F O R M S3.1 INTRODUCTION

Bedform is a regularly repeated surface feature which develops invariably on the wind blown sand deposits. These resemble with the pattern developed under water. Bedforms have been reported to develop on loess (Rozycki, 1967), in alluvium or even solid rock (Grove, 1960; Wilson, 1971). Cornish (1974) has reported them to develop on snow.

Different bedforms reported by various desert workers are wind formed draas, dunes, ripples, megaripples, gravel ridges, current lineations, sand ribbons, parallel ridges, linguoid dunes, criss-cross lines, net works and oblique echelon lines.

Some basic irregularity on the ground surface or some local disturbance in the wind stream may initiate a particular bedform. This pattern then grows in size and migrates downwind from the site of its origin. Some of the irregularities which may be the ultimate cause of origin of a particular pattern may be listed as a rock outcrop, bush, man made structure, lithology of the surface rock, some erosional or topographical feature, a termite mound or even the older bedforms. A local turbulence of the wind current or change in grain size of the sands may result into a particular type of pattern. Similarly size, shape and orientation of these nuclei

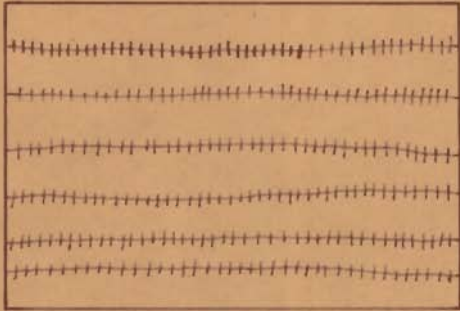
may trigger a mechanism which results in different bedforms.

3.2 BEDFORMS OF THE AREA

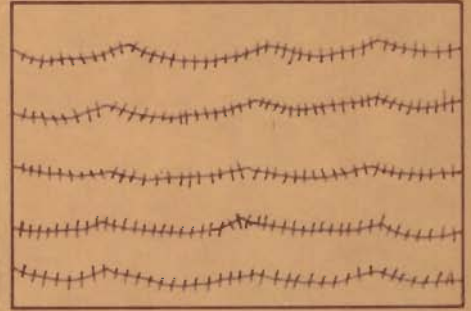
In the area under investigation, mainly three types of bedforms—ripples, dunes and sand piles, are observed. A brief description of these is attempted below.

3.2.1 Ripples

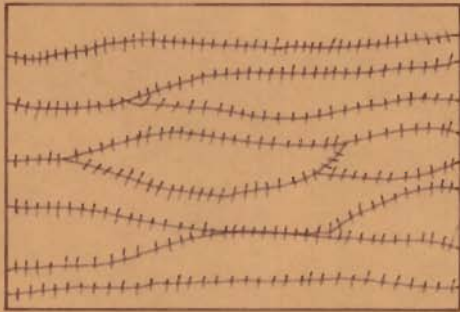
Ripples are present ubiquitously in the area. These are asymmetrical in nature and may occur in long straight ridges (Fig.3.1a). Generally the ripples tend to occur as parallel ridges with wavy crest lines (Figs.3.1b,3.2). Another interesting sedimentary structure is sand shadow observed in Figure 3.2 developed behind pebbles. Wavy ripples may run continuously along their general strike for over 30m. Sometimes it has been observed that ripples branch out from the crests (Figs.3.1c, 3.3). When they branch, it is the crest that bifurcates. The branch of the ripple may join and merge in the adjoining crestline. At times, branching is such that a sort of island of low lying trough is enclosed (Fig.3.1c). Also ripple crests may occur as crescentic ridges which may be called as arcuate ripples (Fig.3.1d). Well developed arcuate ripples are observed in the dune field at Dhanana (Fig.3.4). There is a general tendency of the arcuate ripples to straighten and attain the shape of parallel ripples which are transverse to the dominant wind direction.



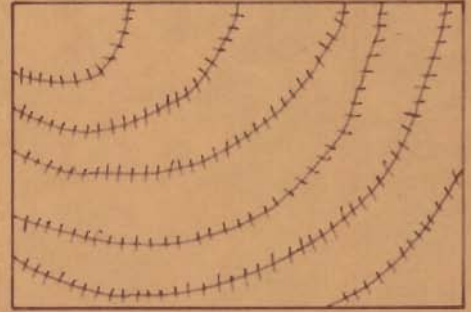
(a) Straight parallel ripples



(b) Wavy parallel ripples



(c) Branching ripples



(d) Arcuate ripples

Fig.31 - Typical ripples in the area.

Fig. 3.2_ Sinuous asymmetrical ripples are observed in area A. Sand shadows behind pebbles are observed in region B. Location near Dhanana.

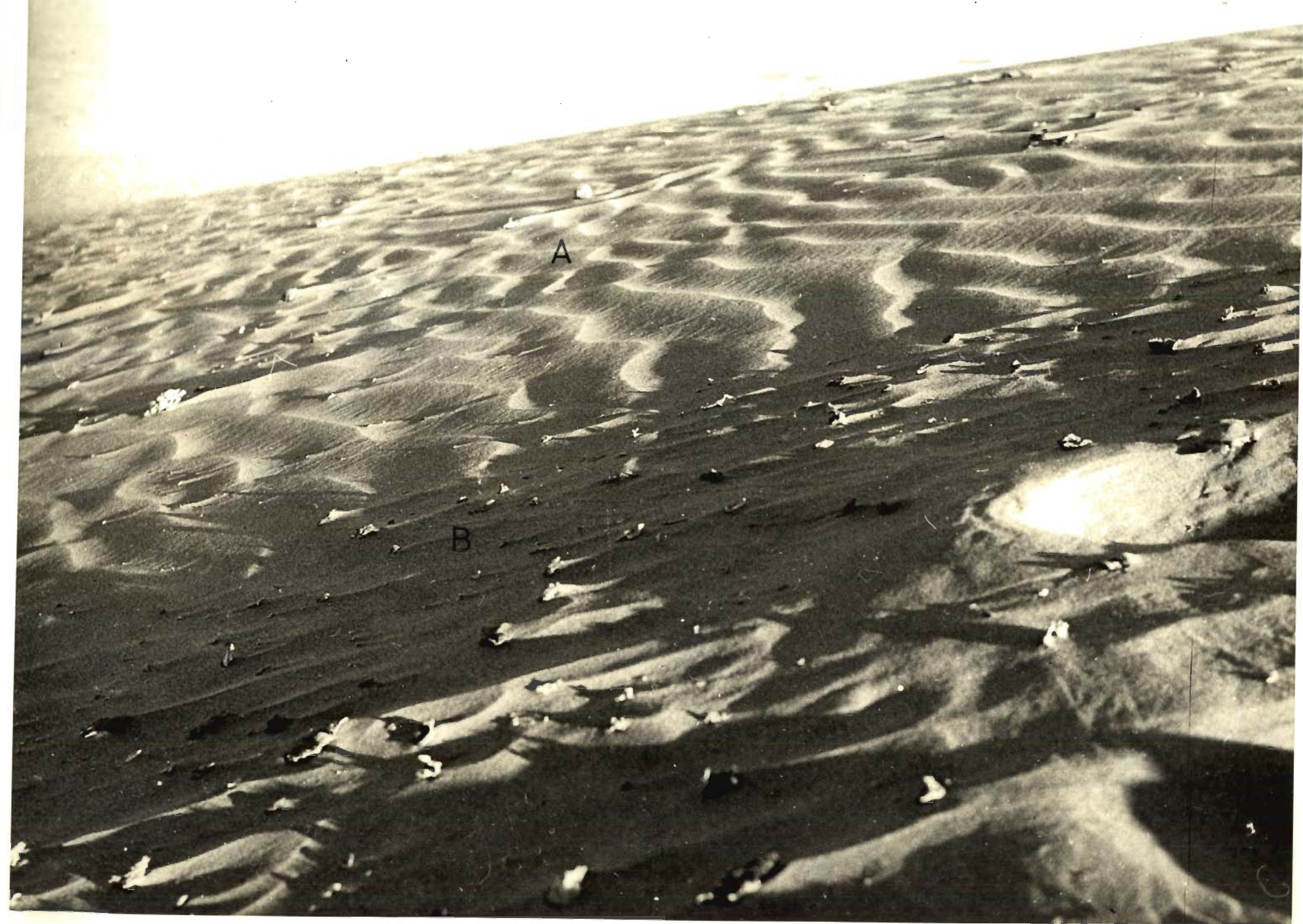


Fig.3.3_ Two sets of ripples with crests trending almost at right angles to each other formed at the back of a barchan. Crests of some ripples are discontinuous and those of others show bifurcation. Ripples are truncated by sand avalanche. Location near Dhanana.



Fig.3.4_ Flat crested, arcuate, asymmetrical ripples at the back of a barchan in a dune field. Barchans can be seen in the background. Location near Dhanana.



Crests of the ripples are composed of coarse grains whereas troughs are composed of comparatively finer grains. As an example, grain size analysis of samples 1 and 2 collected from the crest and trough of a ripple near Sam shows mean size of 1.78ϕ and 2.79ϕ respectively.

The ripples may show abrupt change in wave length and amplitude in downwind direction. Similarly ripples with contrasted morphology may occur in juxtaposition. In such a case the boundaries between these ripples are generally denticulated (Fig.3.5). It is of interest to note that at both these places the same wind regime prevails. This marked change in the ripple characteristics may be due to the variation in the grain size. An increase in grain size corresponds to increase in wave length. Also, it has been observed that the ripples are rather poorly developed in coarser sediments while the finer sands support skins which are ornamented with well formed ripples.

In the area under investigation, the wave length λ and amplitude H of typical ripples from different locations have been measured and ripple index λ/H calculated. Figure 3.6 gives histograms showing distributions of λ , H and λ/H . Aeolian ripples have mean wave length and amplitude of 12.1 cm and 0.64 cm respectively and a mean ripple index of 20.1. In comparison with the present study, Bagnold (1954) and Sharp (1963) found that for aeolian ripples wave length ranged from 25 cm to 20 m and amplitude varied from 2.5 cm to

Fig.3.5_ Ripples of different wave lengths and amplitudes are developed in areas A, B and C. Boundary between areas B and C is denticulated. Barchans are observed in the background. Location near point 43 in figure 1.3.



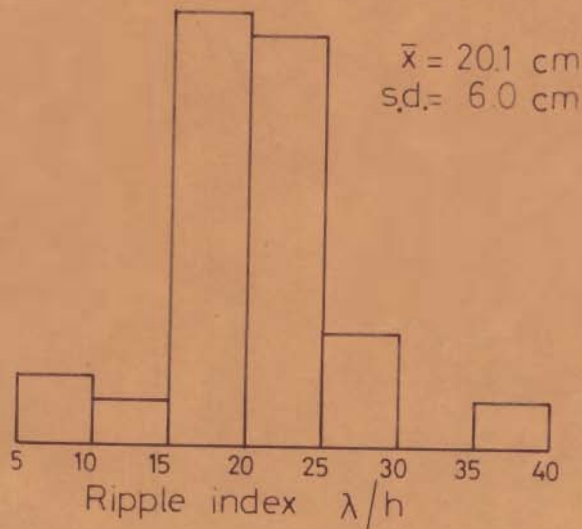
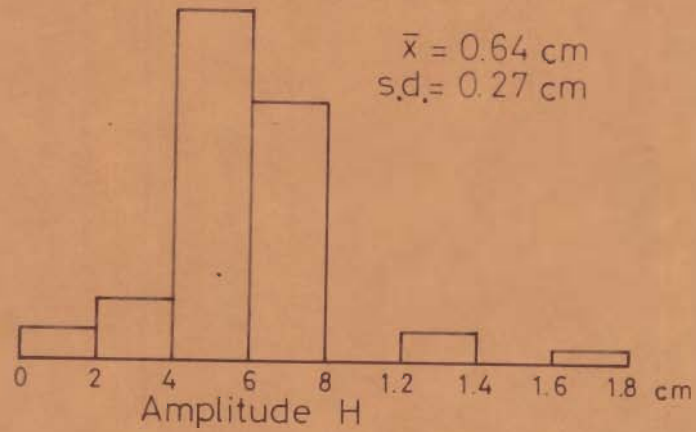
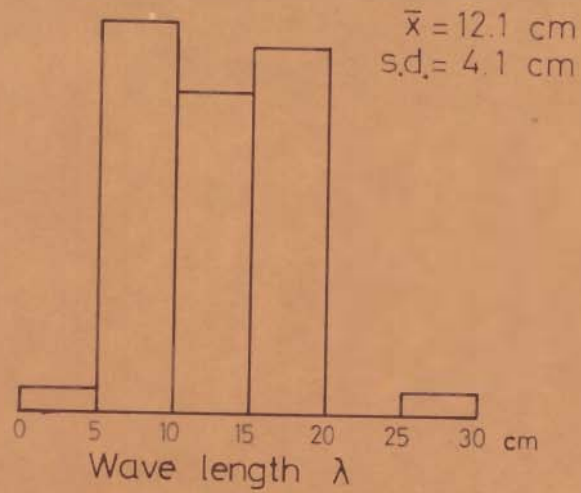


Fig.3.6 _ Histograms showing distributions of wave length, amplitude and ripple index of aeolian ripples.

60 cm. The ripple index was found to have a range of 10 to 70.

In order to find out as to whether any correlation exists between λ , H and λ/H , three plots of H versus λ , λ/H versus H and λ/H versus λ have been prepared (Figs. 3.7-3.9).

Figure 3.7 depicts the variation of H with λ . It is observed that in the range of λ from 4.5 cm to 9.0 cm, the ripple amplitude increases steeply from 0.2 cm to 0.5 cm. Thereafter the increase in H is quite small with increase in λ . For example, corresponding to an increase in λ from 9.0 cm to 17.0 cm, there is only an increase in H from 0.5 cm to 0.8 cm.

The nature of variation of ripple index with amplitude is shown in Figure 3.8. The value of λ/H first decreases rapidly with H and then after a certain critical value of H (4.0 cm to 4.8 cm), the ratio λ/H starts increasing with further increase in λ .

Figure 3.9 shows the variation of λ/H with λ . The ripple index λ/H increases more or less linearly with H .

3.2.1.1 Mechanism of Ripple Formation

The mechanism of ripple formation in fine sand was best studied by Bagnold (1941) in wind tunnel experiments and his ideas are summarised here. Wind blown sand moves

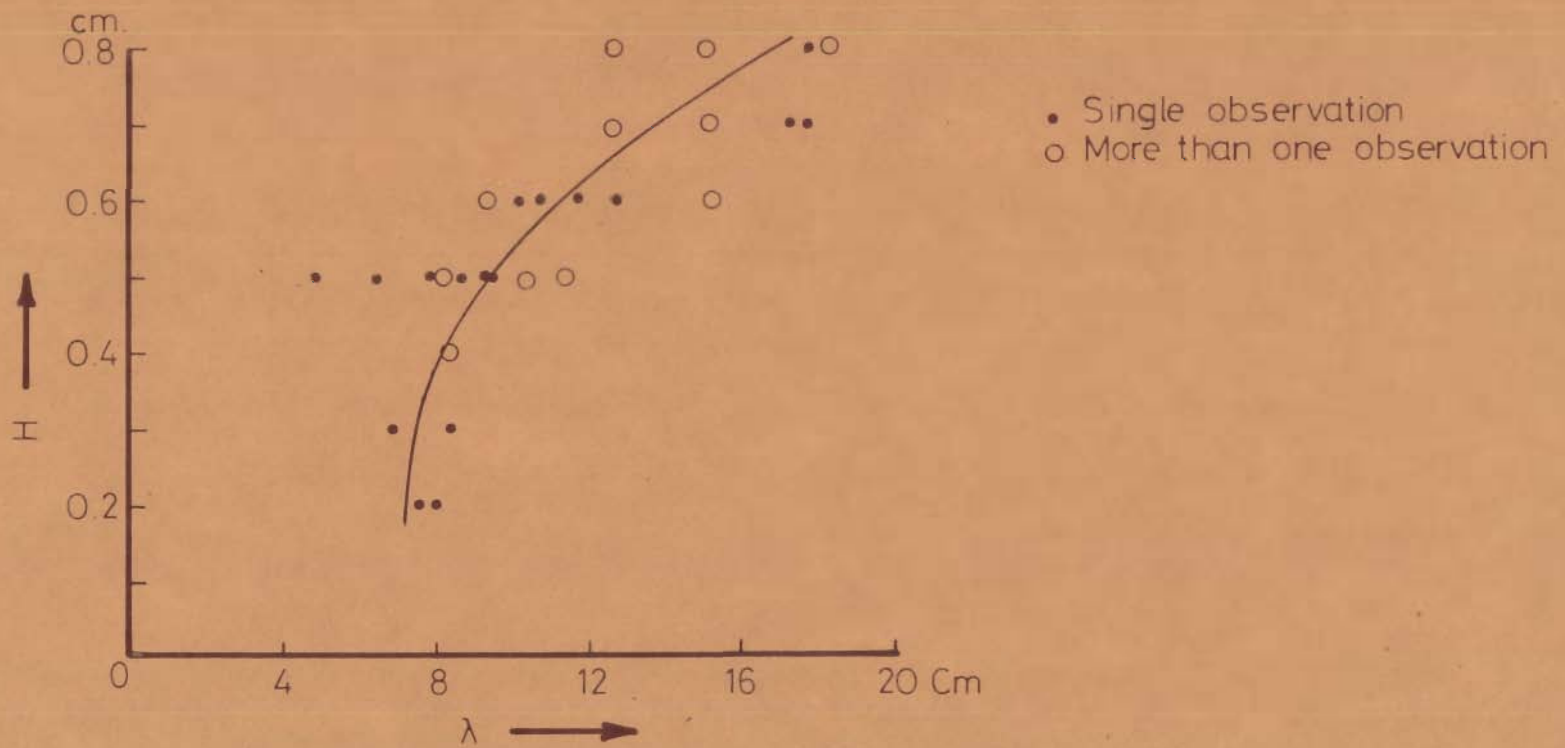


Fig 3.7_Plot of ripple amplitude H vs. wave length λ (Plot includes 46 observations, extreme values being omitted).

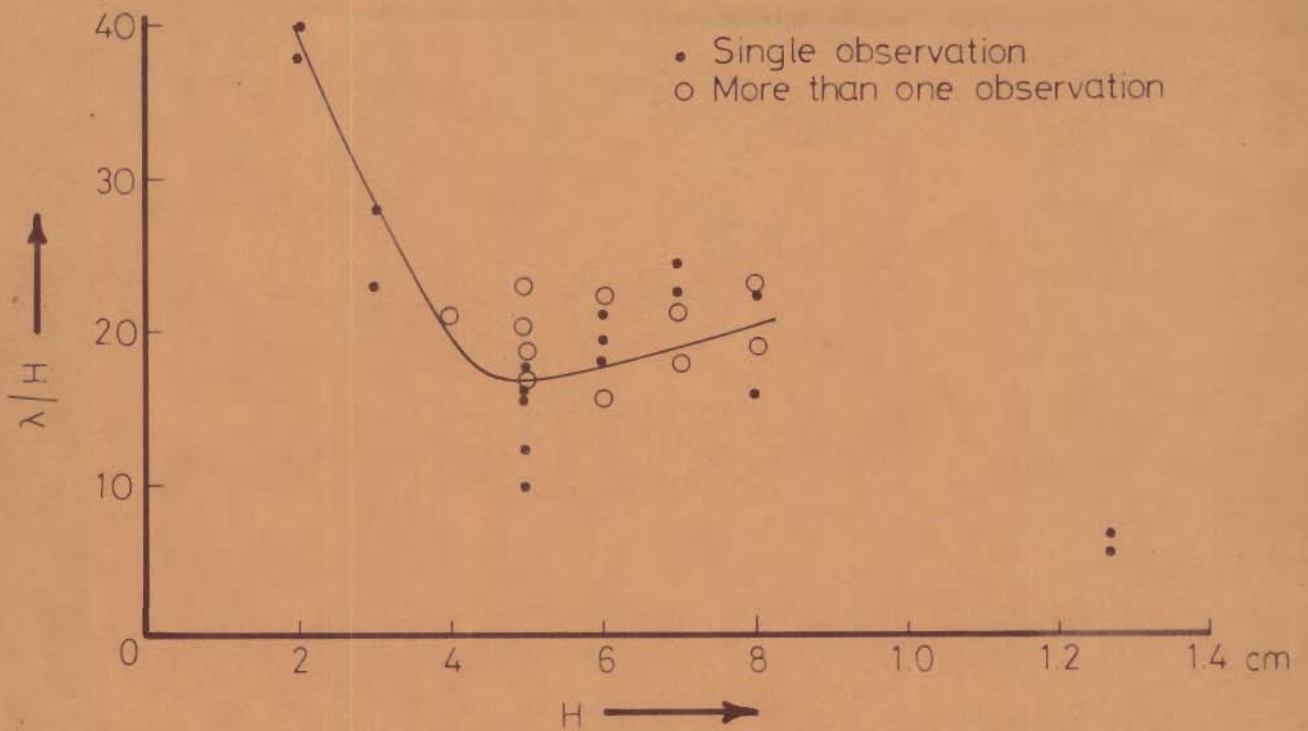


Fig.3.8_Plot of ripple amplitude H vs.ripple index λ/H . Plot includes 48 observations.

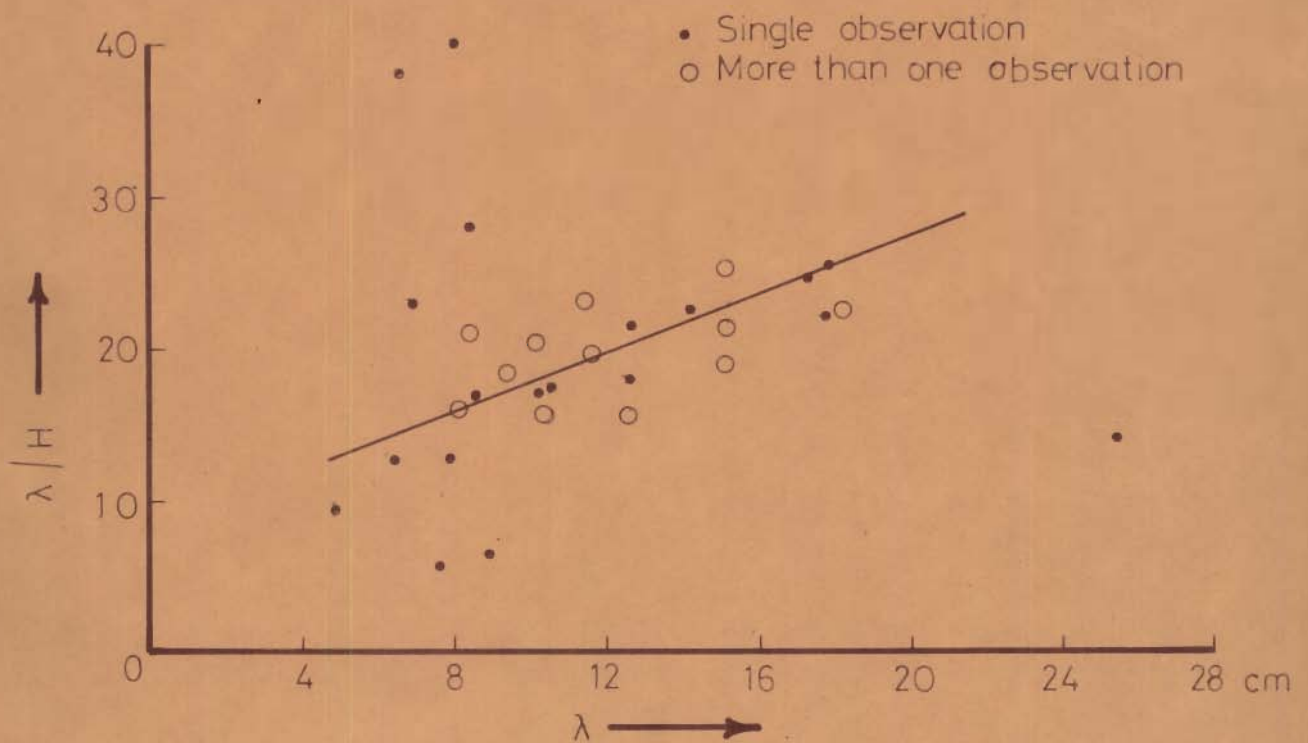


Fig.3.9_Plot of ripple wave length vs. ripple index λ/H . Plot includes all the 49 observations.

largely by saltation. The lengths of the jumps of a particular grain size vary a little from the mean path length which is a function of grain size and wind velocity. Once the saltation starts, any irregularity on the ground surface receives greater bombardment of landing grains on its windward side. Since it has greater angle of incidence with the grain paths, this results in a second zone of denser bombardment downwind at a distance of the mean jump length. This cycle may repeat itself several times downwind before fading out under random processes.

Zones of high and low bombardment are obviously the zones of high and low transport and also zones of erosion and deposition. If such a system gets established once, it would grow until the rate of sand transport at all points on the windward slopes had increased due to increasing angle of incidence with the sand flow. The angle of incidence will increase till it attains a dynamic equilibrium. The ripples thus formed will migrate downwind without changing their shape. The wave length λ of the ripples corresponds to mean jump length.

3.2.2 Dunes

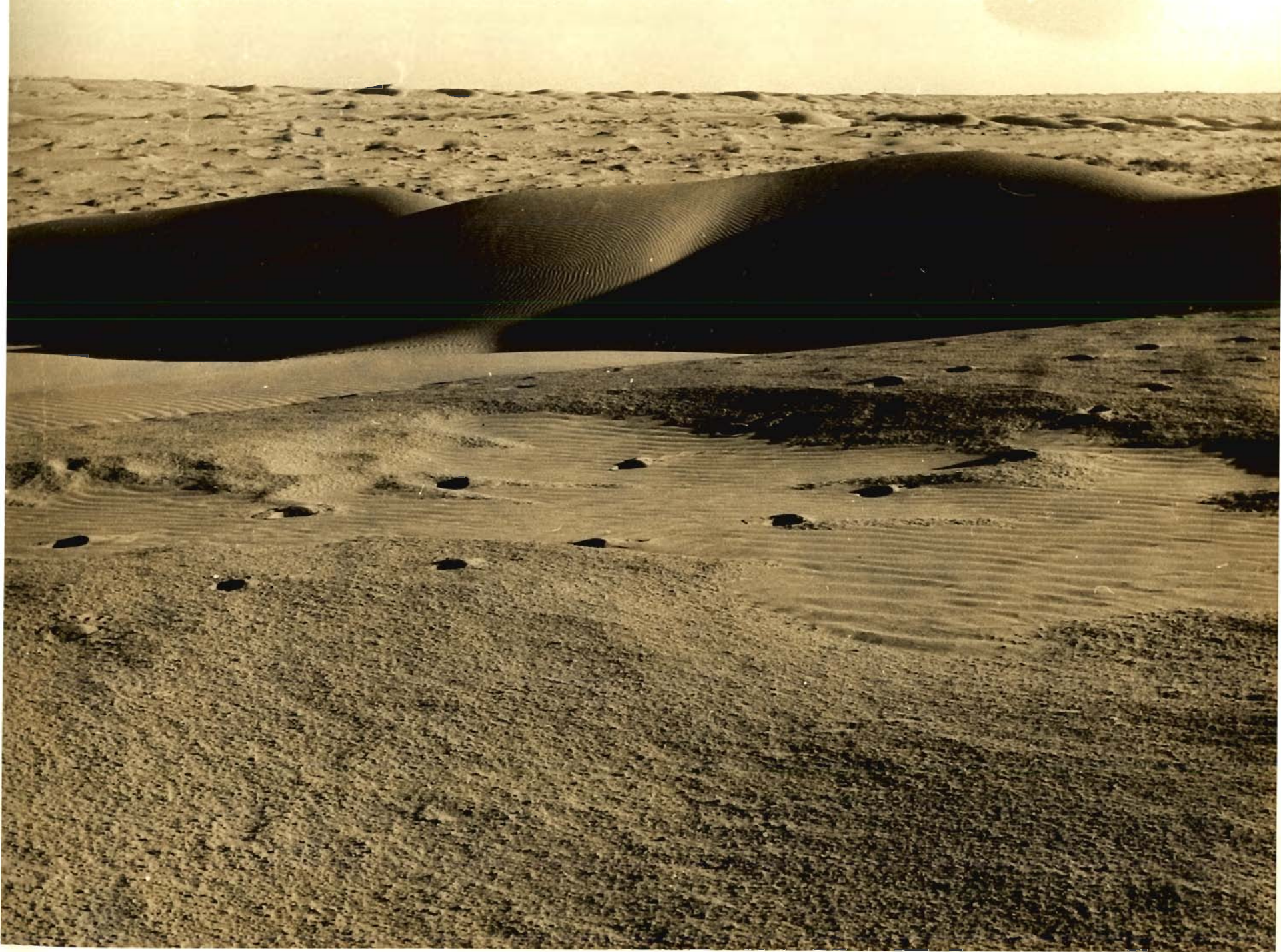
Mainly three types of dunes are encountered in the area, namely, (i) Barchans, (ii) Transverse dunes, and (iii) Longitudinal dunes or seifs.

3.2.2.1 Barchans

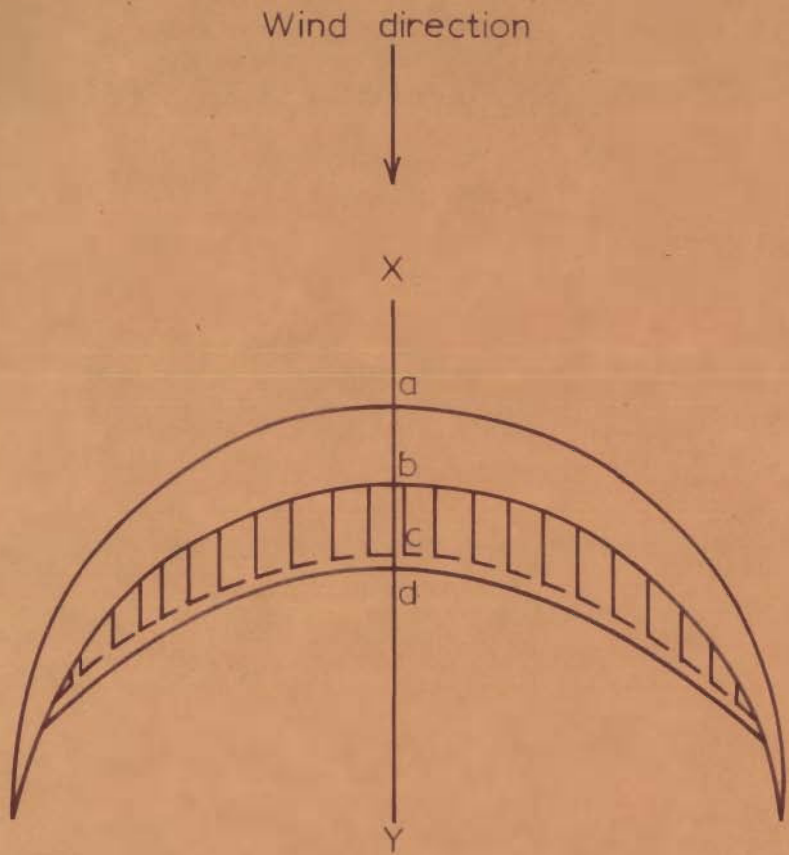
It has been observed that barchans occur as marginal types of dunes. They attain their zenith in comparatively small areas bordering the region occupied mainly by longitudinal dunes. It appears that crescentic dunes prefer to form on comparatively firm ground or on shallow sands where the bottom of firm ground is closeby. The relatively small area covered by barchans together with their preferential marginal occurrence on comparatively firm ground or thin sand cover may perhaps be due to insufficient sand supply. The skins of barchans are ubiquitously rippled. Figure 3.10 shows leeward view of barchans near Dhanana.

Table 3.1 gives morphometric measurements of four barchans of Sam area. The windward sides of these dunes make angles of 15° to 20° and the leeward sides 26° to 32° . At most places leeside does not attain angle of 32° which is the angle of repose of these sands. It has been observed that a narrow band (0.5 m to 1 m wide) with a higher angle of slope (about 32°) invariably occurs at the foot of the leeslope making a sharp contact line with the ground surface (Fig. 3.11, points c,d). Slope lengths measured from the highest point on the crest to the beginning of the slope near the ground surface on windward and leeward sides are 6 to 14 m and 3 to 10 m respectively. Height of dunes varies from 2 to 10 m or even more in Dhanana dune field. Barchans of Lunar area are quite grown up and attain heights upto 10 to

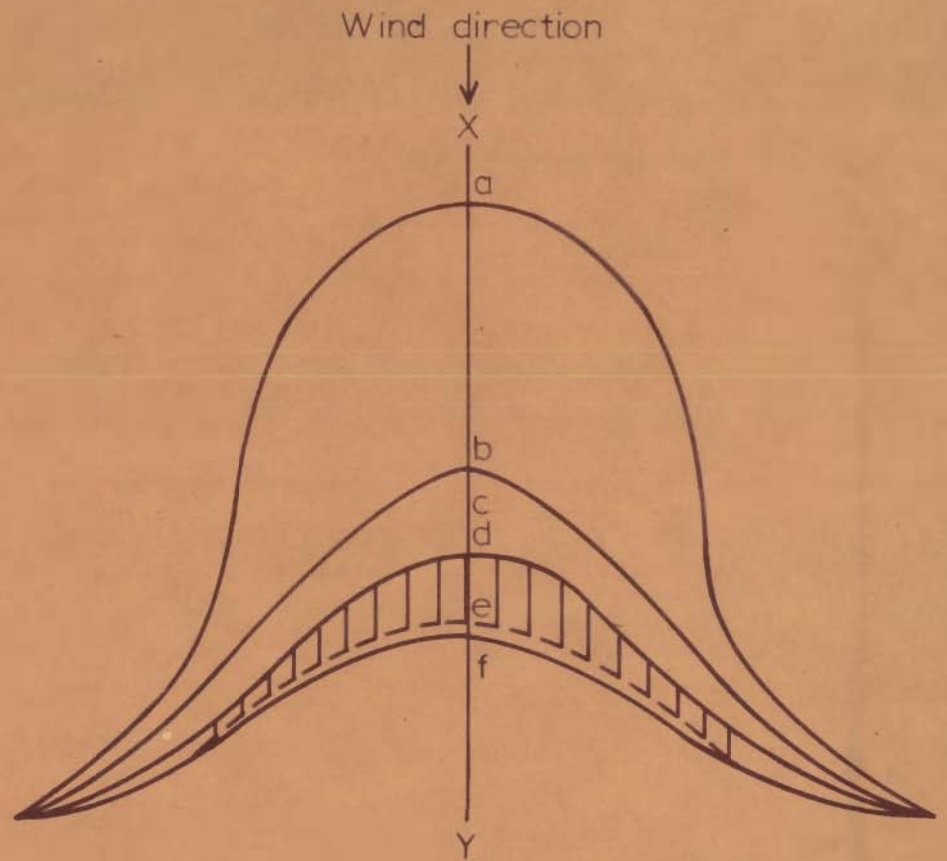
Fig. 3.10 _ Leeward view of barchans.
Location near Dhanana.



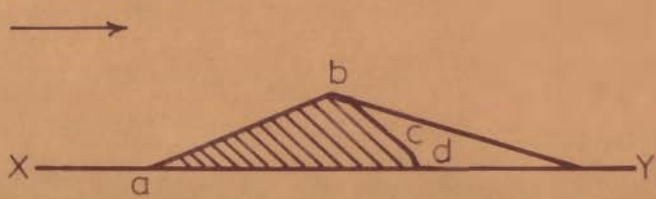
(a) Crescentic barchan



(b) Hat-shape barchan

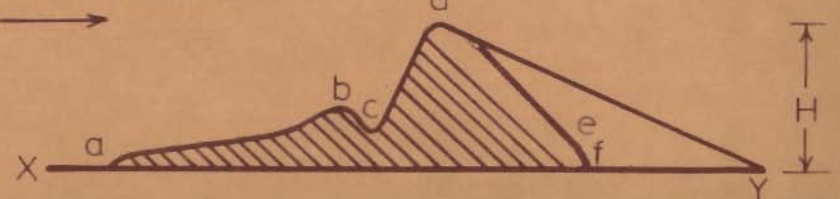


Wind direction



Section along X-Y

Wind direction



Section along X-Y

Fig.311 - Typical Barchans of the area

12 m above the ground surface.

Table 3.1- Morphometric parameters of barchans

Sample Location in Fig.1.3	Dune Characteristics				
	Length L	Breadth B	Height H	Windward slope θ_1	Leeward slope θ_2
3	20.0 m	16.7 m	1.8 m	15°	26°
5	69.7 m	60.0 m	1.7 m	20°	32°
7	90.0 m	73.3 m	6.7 m	20°	31°
8	83.3 m	73.3 m	5.0 m	20°	32°

- Length L - the distance measured parallel to the wind direction between the tip of horn and the beginning of windward slope,
- Breadth B - the distance between tips of horns measured at right angles to the wind direction.
- Height H - the maximum height of the crest above general ground surface,
- Slopes θ_1 and θ_2 - measurements parallel to the wind direction from the highest point on the crest.

A barchan may get stabilized due to the cohesion imparted by the moisture and compaction. In such a case it may get partially or completely buried under the consignments of sands of the subsequent seasons. Thus two families of barchans may be recognised in the area — first, that may be called as active dunes, which are loose enough to respond to the shepherding action of the winds, and the second, stabilized dunes which are apparently belonging

to the previous years.

It is difficult to study the internal structure of active dunes since pitting leads to sliding of loose sediment. In the stabilized dunes, wind has scooped pits and trenches at places to expose internal lamination (Fig.3.12), which is more or less conformable to the slip face. The internal structure of a dune gets more distinct on a surface which has been reworked by the wind.

Chiefly two types of active barchans are recognised, each with its characteristic shape. The first type is more or less perfect crescent in shape (Fig.3.11a). The second variety, not reported earlier, has a shape which can be compared to a hat with curved flanks. A narrow trench, 2 to 3 m down the crest line traverses the windward slope with the deepest point at C (Fig.3.11b). The depth of this trench varies from 0.5 to 1.5 m, from dune to dune. The trench opens up on flanks of the dune. Such hat shape dunes are well developed near Sam but were not found either in Dhanana or Lunar dune fields. The difference in the morphology of these barchans may be summarised as below:

<u>Crescentic Barchans</u>	<u>Hat-shape Barchans</u>
(i) Perfect crescent	(i) Appears like a hat, the domal convexity of which faces the wind direction.
(ii) Flanks are arcuate with convex side facing the wind direction	(ii) Flanks are concave on the sides.

Fig.3.12_ Foresets of cross-bedding exposed in a cut made by wind in a barchan. The foresets dip at about 30° in a northerly direction. Location near Dhanana.



- | | |
|--|--|
| (iii) Windward slope continuous without any trench | (iii) Windward slope has a narrow trench some distance down from the crest. |
| (iv) Slope angle of windward side is gentler than the lee slope. | (iv) A high angle windward face starts dipping till it terminates in the trench. |

3.2.2.2 Mechanism of Formation of Barchans

Mechanism of formation of barchans is a complex process which is influenced by the sand and wind characteristics. However, formation of barchans may be visualized in the following three stages.

(i) Initiation or nucleation stage — Any irregularity of the ground surface or a chance turbulence in the wind current may trigger off a process which may initiate a sandy patch hardly resembling its future crescentic form. This may be called as the embryonic stage. The size, shape and orientation of the nucleus may determine the type of future barchan. With the subsequent onslaught of fresh consignments of sand the patch grows into a tiny mound with a round elevated head and tapering but downwind swept arms. Here a resemblance to a barchan appears.

(ii) Youth Stage — Addition of fresh consignments continue to pile up as wind alters its velocity after reaching raised surface of the sand mound. A gentler windward slope develops with a steeper slip face in the leeward side which steepens to angle of repose with the continued piecemeal consignments of sediments across the crest line

from the windward side. The barchan is well established. This is a stage when the barchan attains a dynamic equilibrium with the prevalent environmental conditions. Main wind current, in assistance with the lee and windward eddies, gives finishing touches to the morphology of the dune which may start migrating. Their typical crescentic shape may be ascribed to the differential rate of migration of the central part and the horns.

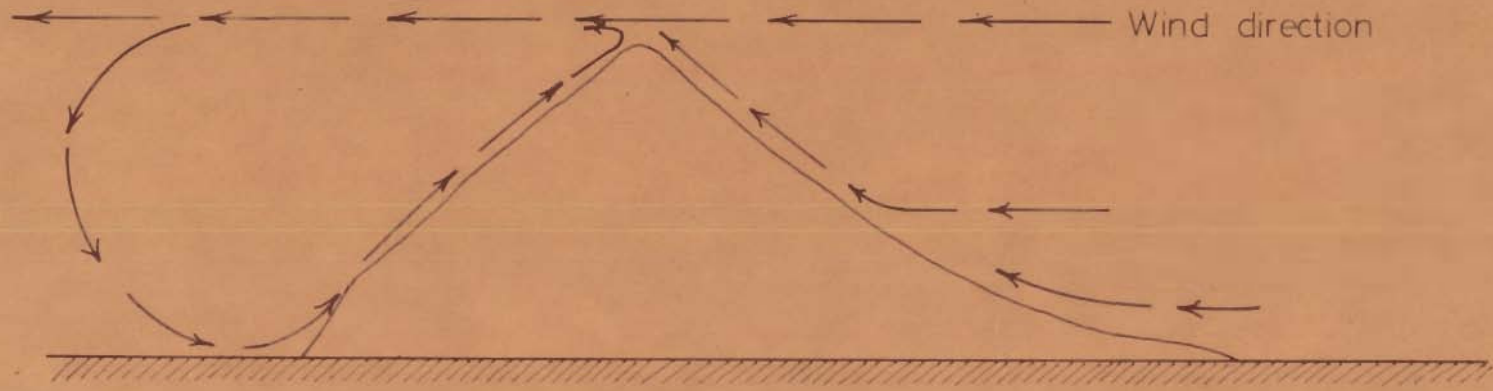
(iii) Old Stage — In this stage barchans may attain a relative stabilization due to cohesion imparted by moisture and compaction of deeper parts. A barchan may get distorted if wind direction changes or it is subjected to winds from different directions.

3.2.2.3 Wind Eddies and Barchans

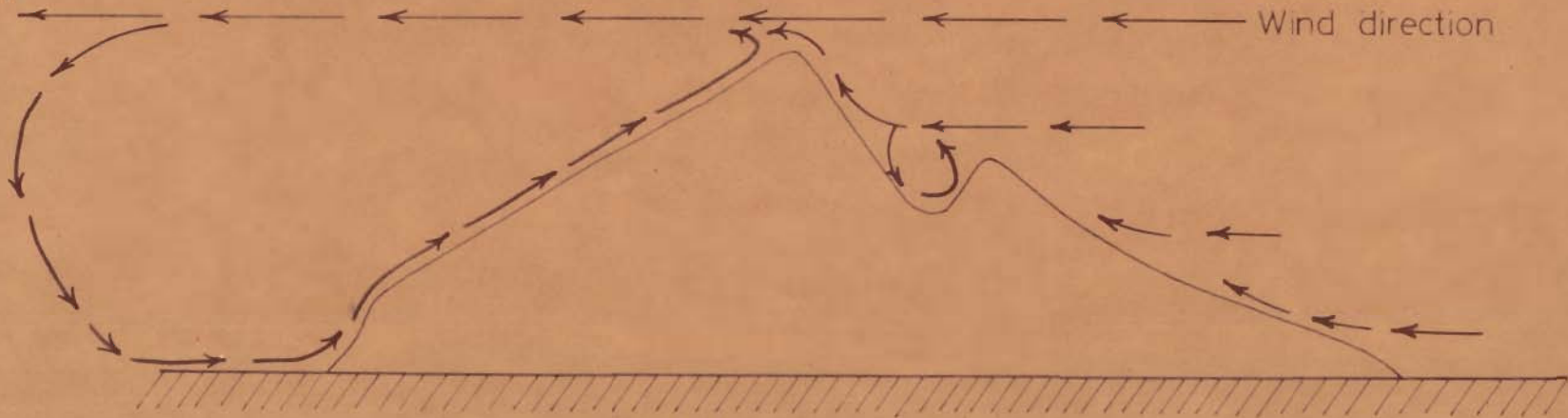
Existence of wind eddies in the strong to moderate winds blowing over barchans are well recognised and are attributed to sudden break in slope at the crest of the dunes (Cornish, 1897, 1914; Hoyt, 1966). Occurrence of lee eddies and windward eddies has also been observed in the present area. A schematic representation is shown in Figures 3.13a and 3.13b. Following evidences may be cited in favour of the existence of lee eddies:

- (a) When dust was dropped it followed the trend of eddy as shown in Figures 3.13a and 3.13b.
- (b) Modification of leeslope near its foot.

175 315



(a) Crescentic dune



(b) Hat-shape dune

Fig.313 _Wind eddies around the barchans.

- (c) Well swept ground of the shadow zone.
- (d) Existence of sharp contact line of leeslope with the ground surface.

It appears that a windward eddy also occurs (Fig.13.3b) which scoops a shallow trench and modifies the morphology of the windward slope on a hat shaped barchan.

3.2.2.4 Transverse Dunes

These are huge dunes resembling ripples with wavy crest lines which are transverse to the dominant wind direction. These develop on sand piles where the thickness of sand is considerable. The length of a single crest line may exceed 50 m. Well developed transverse dunes are found near Sam. Transverse dunes may be sinuous with their crest lines broken at places (Fig.3.14). The total percentage of transverse dunes is very meagre in the area. There is absolutely no difference in the morphology of transverse dunes of Sam and Dabri areas. Here too, windward slope is gentler as compared to the leeslope which is slightly less than the angle of repose. Transverse dunes too, like other types of dunes, support a rippled skin. Barchans and transverse dunes may occur together where the former may form on flat ground surface while the latter may extend from the ground surface up the sand piles but always striking more or less at right angles to the dominant wind direction.

Fig.3.14_Wavy, parallel ripples on transverse
dunes having sinuous crests.
Location near Sam.



3.2.2.5 Origin of Transverse Dunes

Observations in the area under study indicate that two adjacent barchans may join laterally at the horns making a deep re-entrant angle in-between. With further deposition of sands the re-entrant may get buried and ultimately may disappear altogether. Consequently crest lines of two adjoining crescents may become one to form a wavy summit line thus developing a huge transverse dune, but it does not preclude their independent development.

3.2.2.6 Longitudinal Dunes

The area southwest and north of Dhanana is occupied by longitudinal dunes. These dunes usually attain heights of about 10 m or more and have a mean length of 8.8 km as measured between two farthest ends. Figure 3.15 depicts a histogram showing distribution of lengths of longitudinal dunes in Dhanana area as measured from topographic maps. These dunes trend approximately SW-NE. These form 'Y' shaped bifurcations and invariably 'Y' opens in the southwest direction that is facing the wind direction. Flat interdune areas have widths ranging from 0.1 to 0.2 km and may be occupied by barchans. Seif dunes under consideration are stabilized and these may be eroded by wind at places exposing internal lamination. Figures 3.16 and 3.17 show horizontal internal laminations of these dunes in trenches cut by wind. Directions of the trenches are approximately

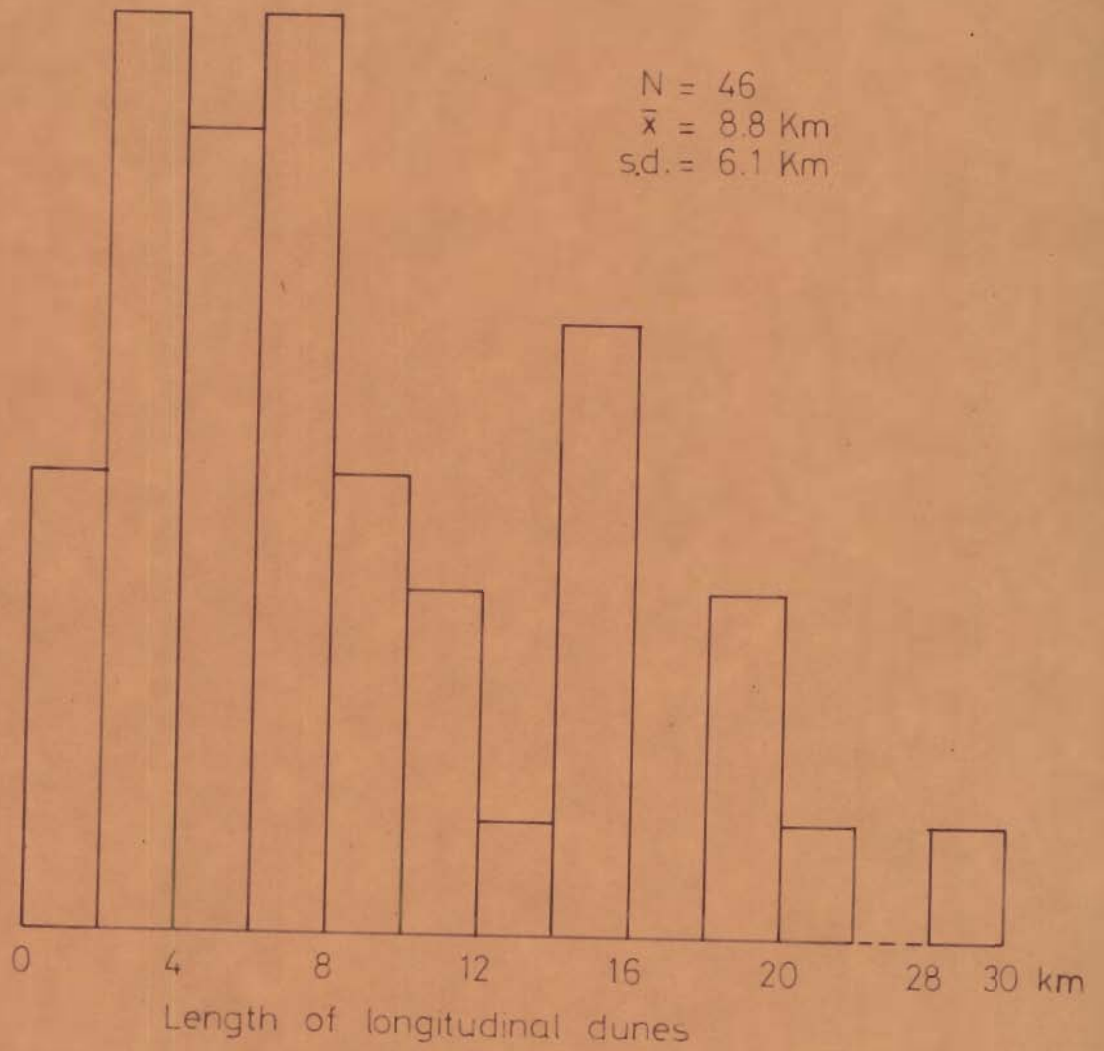


Fig.3.15_Histograms showing distribution of lengths of longitudinal dunes.

Fig.3.16_Horizontal, parallel laminations exposed in a cut made by wind in a longitudinal dune. The cut is roughly parallel to the crest of the dune. Location near Murar.



Fig.3.17_Horizontal, parallel laminations exposed in a cut made by wind in a longitudinal dune. The lower half of the face contains a small scale, solitary crossbed. The cut is roughly parallel to the dune axis. Location near Murar.



parallel to the dune axes.

3.2.2.7 Origin of Longitudinal Dunes

Frere (1870) felt that longitudinal dunes were produced when the predominant winds furrow the sand and deposit them on the ridges in between.

Blanford (1876) thought the longitudinal dunes of the Thar desert to be erosional features. Enquest (1932) suggested that longitudinal dunes are formed on thick sands with deep water table. Melton (1940) suggested the term 'windrift dunes' since wind excavated blowouts in thick sands to build long parallel ridges.

Bagnold (1953) gave the idea of helicoidal air flow to explain the mechanism of formation of longitudinal dunes. According to him if moving wind is heated, convection will form paired roller-vortices in the lower atmosphere with their axes horizontal and trending in the wind direction. Such a movement will tend to sweep the sand from troughs and pile them on the intervening dunes. This process involves partly erosion and partly deposition. Folk (1971 a,b) also thought that similar mechanism was responsible for the formation of longitudinal dunes and obtained experimental evidence for the bifurcation angle of these dunes. Glennie (1970) considers that other conditions being equal, barchans develop at slow to moderate winds while seifs are formed at higher wind velocities. Stronger winds during the Pleistocene

glaciation resulted in abundant seif formation.

Certain aspects about the relationship of longitudinal dunes and the wind directions are discussed further in Section 3.3.

3.2.3 Sand Piles

Large irregular sand accumulations are designated as sand piles. Many such sand bodies are found in the area which may be a couple of hundred meters in maximum length and a few meters high above the general ground surface. Sandpiles are essentially stabilized sand accumulations. At places, these have been reworked and sand has been piled into transverse and barchan dunes which may be associated with them. These are especially abundant in Lunar and Dabri areas and are associated with regular barchans and transverse dunes.

Origin of sand piles is not clear. Their general stabilized nature, predominant SW-NE trend which has been recorded in the topographic maps as linear sand accumulations coupled with the occurrence of well established longitudinal dunes in the near vicinity suggest that these sand piles are probably low longitudinal dunes which are rather difficult to recognize in the field because of their relatively low heights.

Some of the sand piles are, of course, definitely buried and stabilized barchans as observed in the field.

3.3 RELATIONSHIP BETWEEN WIND DIRECTION AND DUNE ORIENTATION

Blanford (1876) was the first to establish parallelism of longitudinal dunes and the present wind direction in the Thar desert. Similar relationship between the wind direction and the longitudinal dunes have been reported from Egyptian and Libyan deserts by Ball (1927) , Bagnold (1931,1933), Kadar (1934) and others, and from the Australian desert by Madigan (1930, 1936, in Folk 1971a). Melton (1940) and Glennie (1970) thought that strong winds of constant direction were necessary for the windrift dunes. Other workers like Madigan (1930, 1938,1946, in Folk, 1971a), Wingate (1934), King (1956, 1960), Veevers and Wells (1961) and Folk (1971a) have also emphasized the parallelism of seifs with one predominant wind direction, but also stressed the importance of secondary cross winds in producing crestal asymmetry and in the shepherding effect of transporting sands from troughs onto dunes.

Most workers think that a strong constant wind from one principal direction is necessary for the formation of barchans (Verlaque, 1958; Finkal, 1959; Long and Sharp, 1964; Hastenrata, 1967; Clos-Arceuduc, 1967).

Bagnold (1941) proposed that two or more wind patterns at an angle were necessary for the formation of longitudinal dunes which become aligned with the resultant wind direction. Later workers like Cooper (1958), Durand de Cabiac (1958) and

McKee and Tibbitts (1964) seem to confirm this view by studies in different deserts. Striem (1954) found Israelite seifs to be parallel to the yearly resultant wind direction.

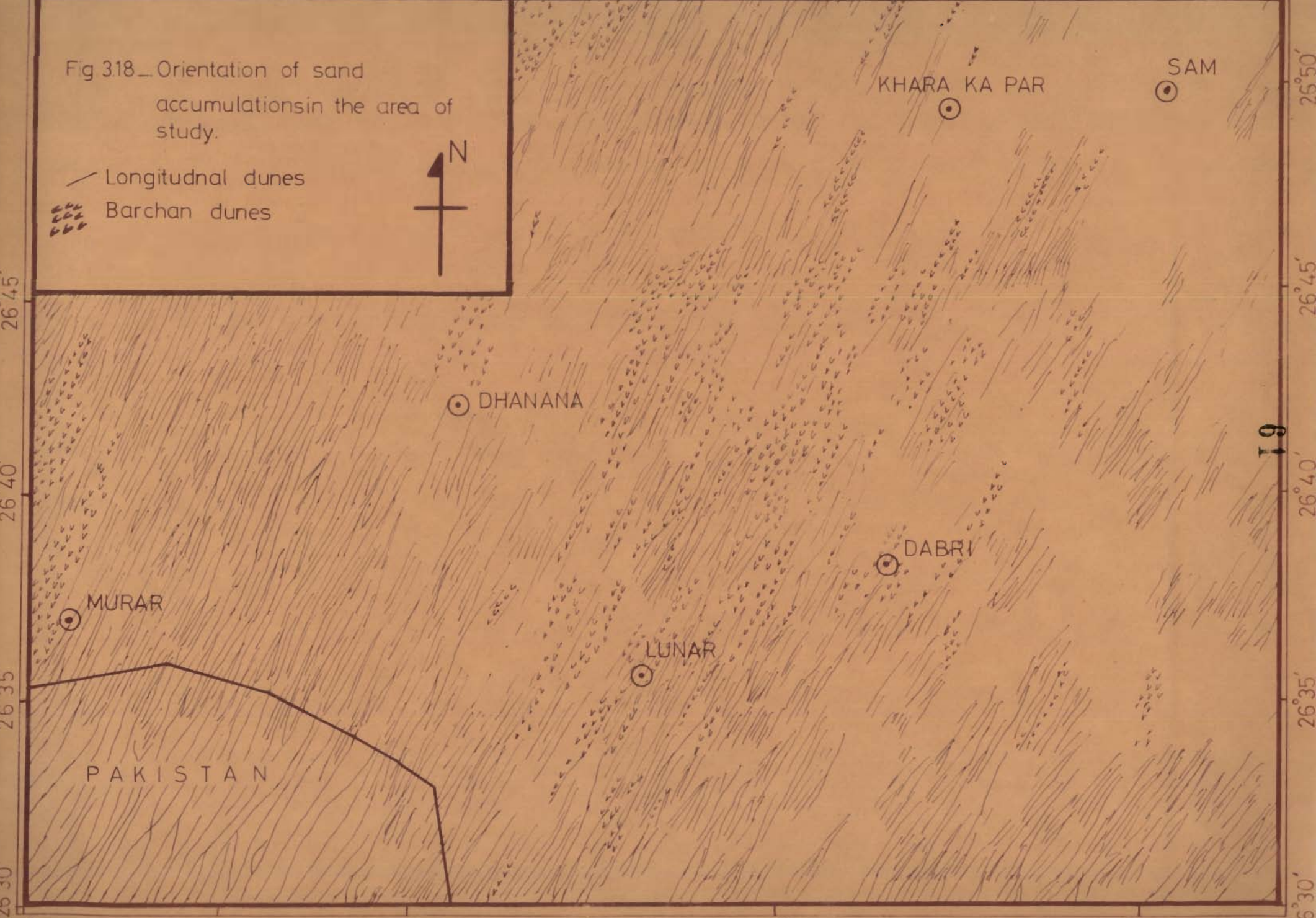
More recently Wilson (1972,1973) questioned earlier explanations of aeolian bedforms. He believed that patterns in aeolian bedforms result from the three dimensional geometry of fluid flow in which there were flow transverse (wave like) and flow parallel (helical, vortex) types of secondary motion. Combination of these yield flow transverse, flow parallel, sinistral and dextral flow oblique bedform elements. Thus seifs may be at an angle to a dominant flow which is determined by the geometry of secondary flow.

Warren (1976) thought that the friction at the earth's surface induces deflection of ground wind from geostrophic direction and the progressive change with height is known as the 'Ekman Spiral'. Dune fields with rougher surfaces and higher altitudes than the neighbouring areas may show such deflections from the wind direction.

Figure 3.18 shows the sand body elongations in the area under study as obtained from 1:50,000 scale topographic sheets of the Survey of India. Thus net sediment transport direction of $N 5^{\circ}E$ to $N 30^{\circ}E$ can be seen. It may be emphasized that both the stabilised and active dunes give similar sediment transport direction indicating thereby that the same wind regime has been prevailing since the formation of stabilized dune system.

Fig 318—Orientation of sand accumulations in the area of study.

— Longitudinal dunes
Barchan dunes



Figures 3.19 to 3.21 show normal percentage frequencies of wind direction in the form of rose diagrams at Jodhpur ($26^{\circ}18'$: $73^{\circ}01'$), Barmer ($25^{\circ}45'$: $71^{\circ}23'$) and Bikaner ($28^{\circ}00'$: $73^{\circ}18'$) using the Climatological Tables of the Meteorological Office, Bombay (Anon., 1953). The percentages of number of days under eight compass directions have been taken into consideration.

The main wind speed for each month is given in Table 3.2. The data are obtained from the Climatological Tables of Meteorological Office, Bombay.

Table 3.2 — Mean wind speed (km/hr).

Station	Jan	Feb	Mar.	April	May	June	July	Aug.	Sept.	Oct.	Nov.	Dec.
Jodhpur	10	10	10	10	16	20	19	14	11	8	8	9
Barmer	8	8	9	9	10	12	11	9	9	8	6	6
Bikaner	5	6	7	8	10	12	11	10	9	6	4	4

The resultant wind directions at Jodhpur and Barmer in the months of May, June, July and August are S 43 W, S 47 W, S 47 W, S 47 W and S 38 W, S 49 W, S 49 W, S 46 W and S 45 W respectively (Pramanik, 1952). At Jodhpur 12, 21 and 18 percent of the total days of May, June and July respectively have the wind speed range of 20.92 - 61.15 km/hr. At Barmer 15, 15 and 6 per cent of the total number of days of May, June and July have similar range of wind speed (Pandey et al. 1964). During winter months, northwesterly

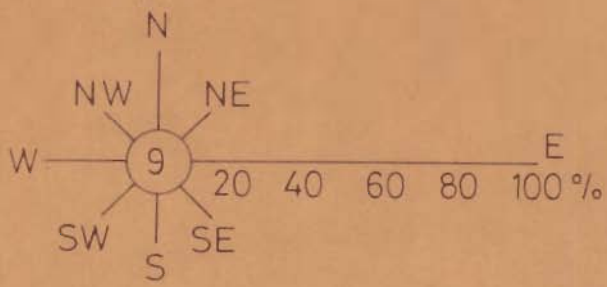
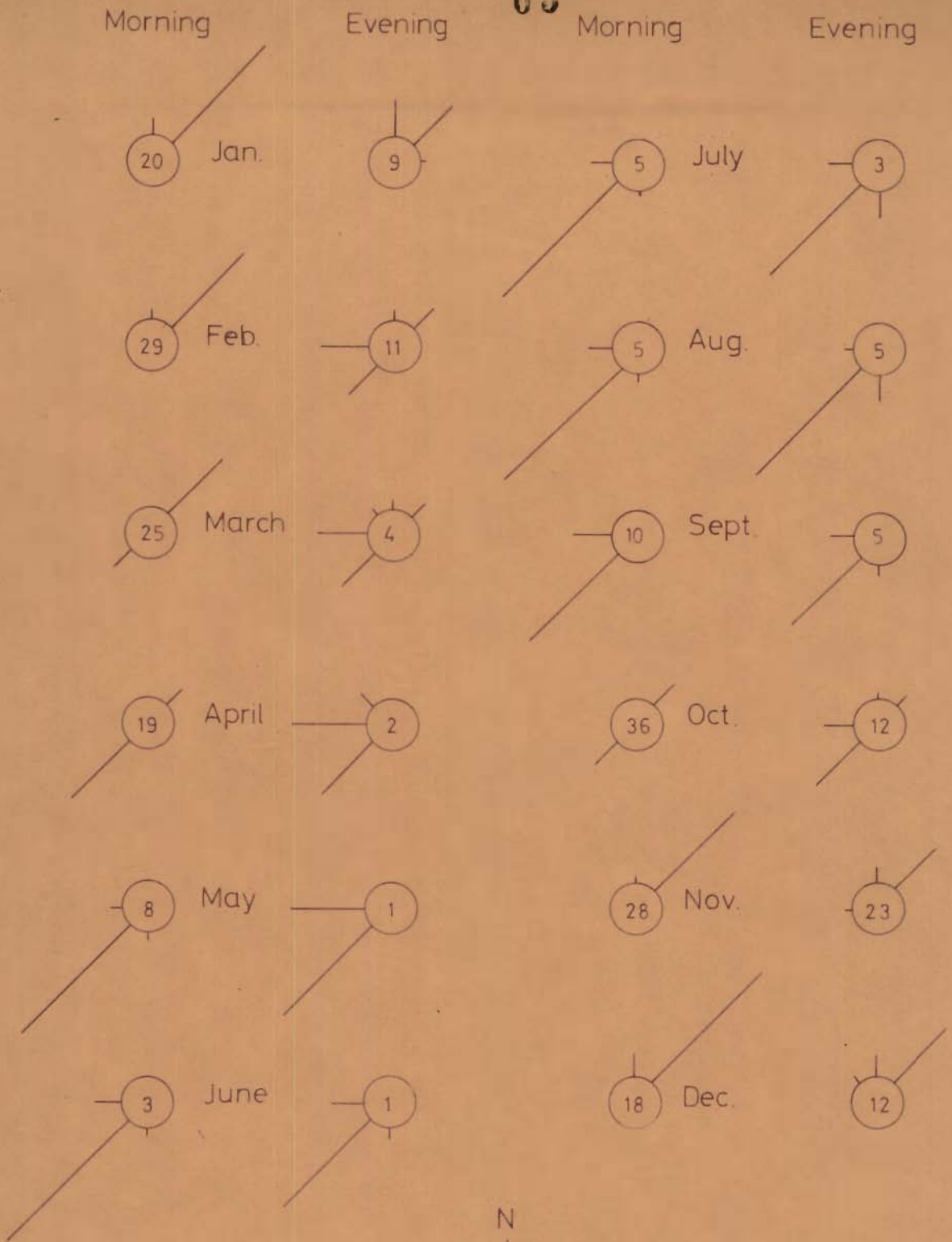


Fig.3.19 – Normal percentage frequencies of wind direction at Jodhpur

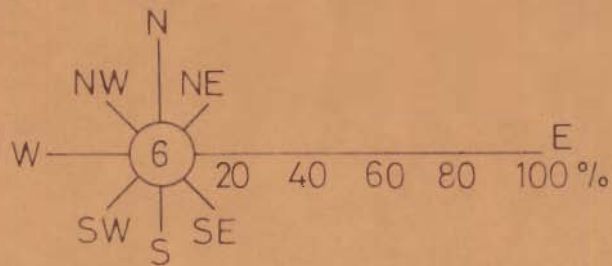
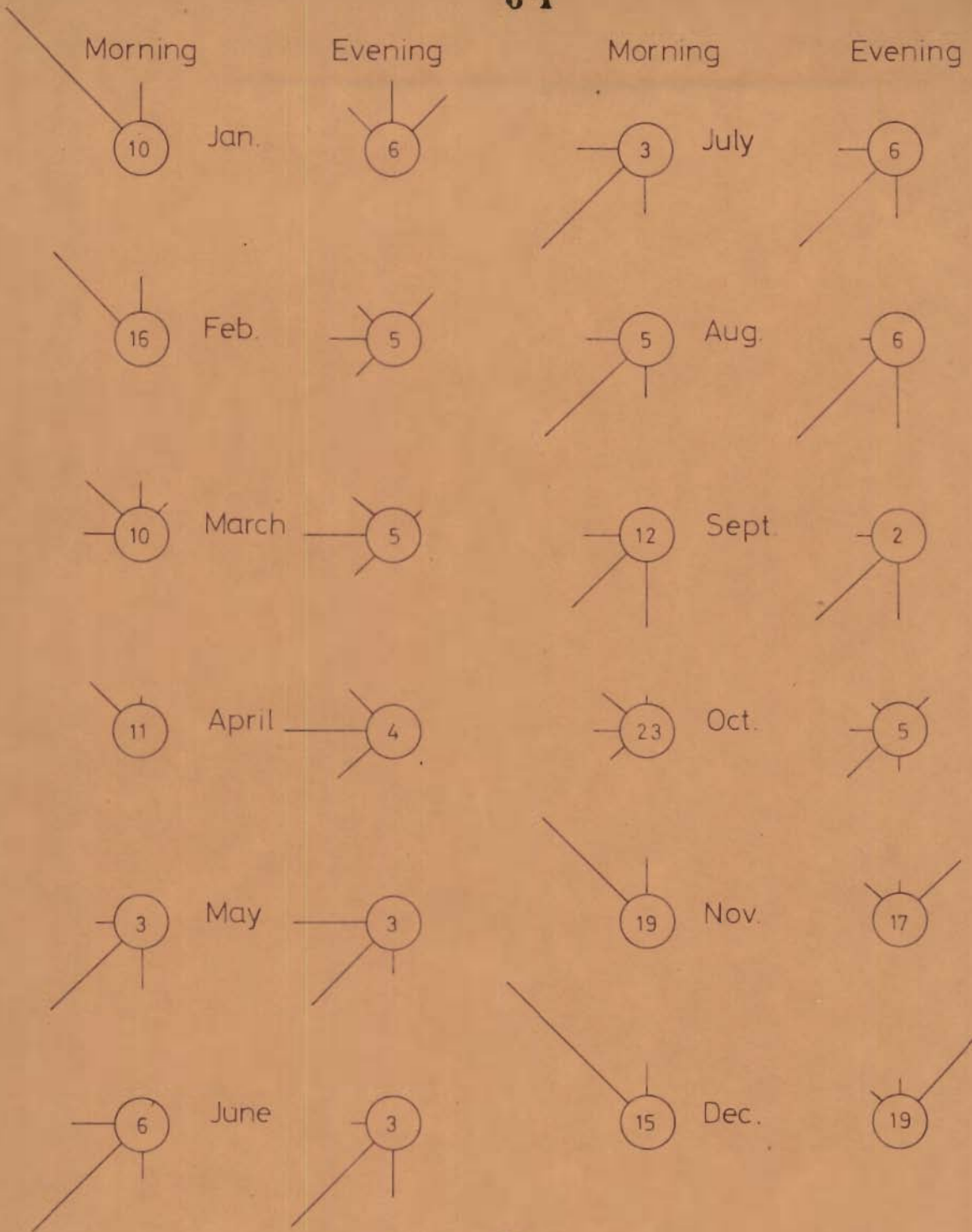
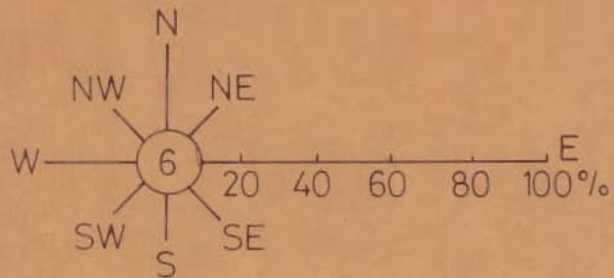
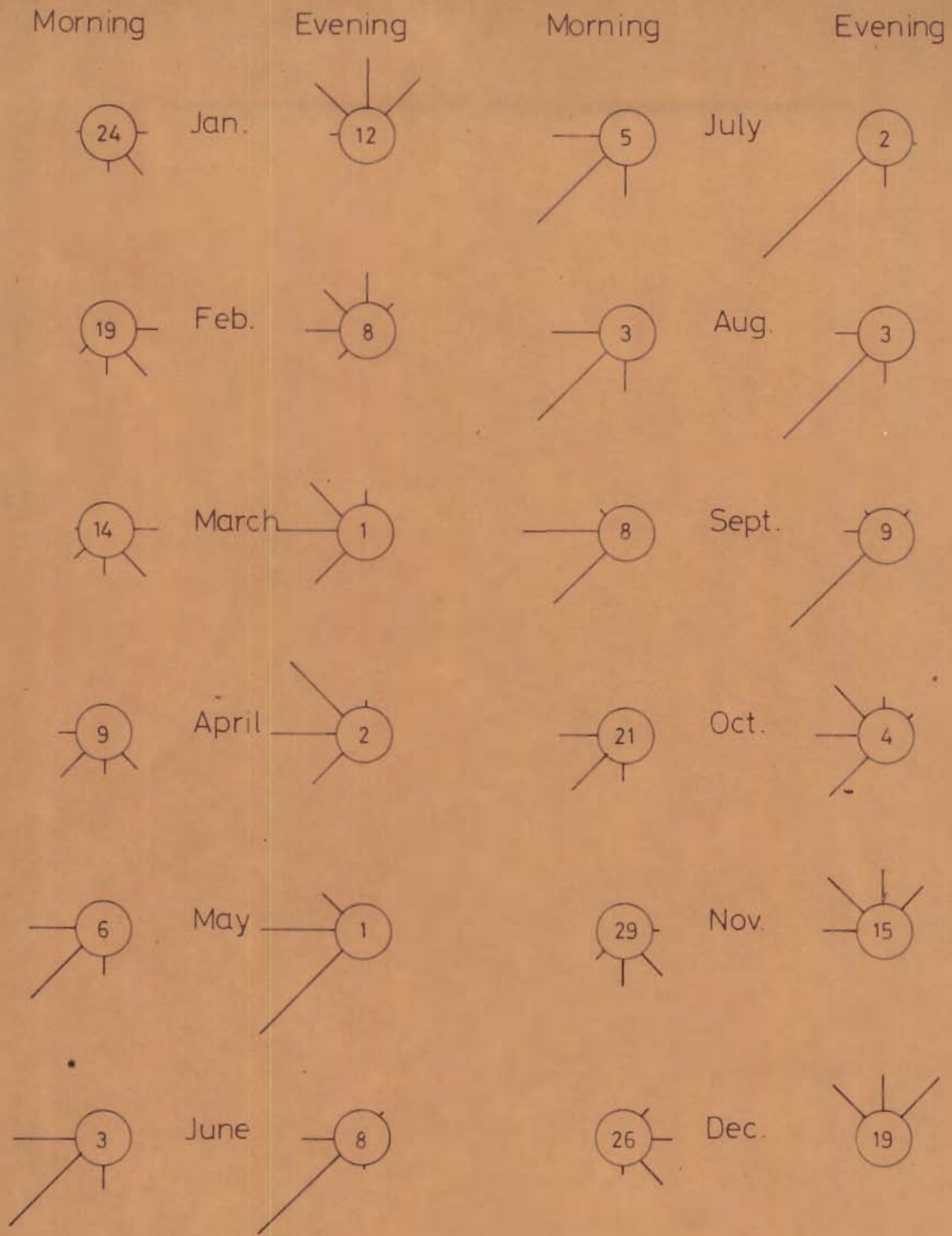


Fig.320 - Normal percentage frequencies of wind direction at Barmer



6 - Frequency per cent of calm winds

Fig.3.21 - Normal percentage frequencies of wind direction at Bikaner

and northeasterly winds predominate which cannot shift sands since they are considerably weak. Similar conditions prevail at Bikaner also.

Thus, it can be concluded that summer winds commonly from S 43°W to S 47°W direction are important factors that control the formation of bedforms. This study shows that longitudinal dunes and barchans give net sediment transport direction which is consistently 15° north of the resultant of dominant summer winds. This deflection is probably due to 'Ekman Spiral' effect described by Warren (1976).

CHAPTER-4

TEXTURAL STUDIES4.1 INTRODUCTION

Each environmental setup with its complex set of physical and chemical variables leaves a distinct imprint on the sediments deposited in it. The present chapter attempts to evaluate textural attributes of the desert sediments so that these might be used for recognizing similar environments in the stratigraphic column. Chiefly grain size, roundness and sphericity have been studied and are described below.

4.2 GRAIN SIZE ANALYSIS4.2.1 Purpose

Sediments of alluvial, beach and shallow marine environments have been studied in fair detail for their grain size distributions using modern statistical parameters. However, there is a great paucity of systematic analyses of sediments of inland desert dunes. A few limited studies have been made of these sediments. Alimen (1957) and Chavaillon (1964) have studied Saharan desert samples for mean size and sorting. Moiola and Weiser (1968) studied thirty sand samples from several deserts and showed the relationship between different parameters. Wait (1969, in Folk, 1971a) and Folk (1971a) studied variation of grain size parameters of dunes

west of Texas (U.S.A.) and Simpson desert respectively. Folk (1966, 1968a) and Skocek and Saadallah (1972) emphasize widespread occurrence of bimodal sediments in deserts. Skocek and Saadallah (1972) find that statistical grain size parameters of aeolian sands of Iraq show a larger variation than previously thought. Baillieul (1975) concludes that cover sands in different parts of Botswana are largely derived locally on the basis of study of mineralogy and grain size distribution.

The present study attempts a detailed analysis of areal distribution and interrelationship of the various grain size parameters and their possible use in distinguishing desert sediments from sediments of other environments. It also investigates grain size distribution in different parts of barchans.

4.2.2 Collection of Samples

Sand samples were collected from different locations in the area which are shown in Figure 1.3 and their details are given in Appendix I. Samples were collected from the various desert bedforms i.e. barchans, transverse dunes, ripples and sand piles and flat interdune areas. Generally thin top layer was removed and 0.5 kg of sand, from surface to 8 cm depth, was taken. Fairly large number of samples were collected from the different parts of barchans.

4.2.3 Sample Preparation and Sieving

Field samples were split to obtain 30 to 80 gm of representative sub-sample. A mechanical splitter was designed and fabricated to obtain the sub-sample of required size (Fig.4.1). The sample is poured at the top hopper and in passing through the splitter, it gets halved five times to give $1/32$ of the original sample in one container and the rest in the other. The splitter is fitted with a 50 cycle electrical vibrator having a variable amplitude device to hasten the splitting process.

ASTM sieves with $1/2\phi$ interval were used to analyse the samples. The samples were shaken for ten minutes on a rotap. Another device which may be called a transfer-funnel (Fig.4.2) was designed and fabricated for transferring the various sample fractions retained on different sieves into weighing containers. The transfer-funnel is a big metallic funnel mounted on a stand with the funnel angle more than 45° . This is also fitted with a 50 cycle electrical vibrator to quicken the transfer of material from a sieve, which is put up side down on the funnel fitting in the spring clips, to the weighing containers. This device keeps losses of sediments due to clogging of sieves to a minimum.

Various sample fractions were accurately weighed upto one hundredth of a gm and the data are given in Appendix II.

Fig. 4.1_ A photograph of the sample splitter.
1/32 of the sample poured at the top is
collected on the left side and the rest
in the front.



Fig.4.2_A photograph of the transfer funnel
The funnel is fitted with a vibrator.
The sieve to be emptied is put at
the top in up side down position.



4.2.4 Analysis and Presentation of Data

Grain size data were analysed using an IBM 1620 computer. Cumulative per cent frequencies were calculated and plotted on arithmetic probability papers as given in Figures 4.3 - 4.30. Further analysis of grain size data could be carried out by two approaches. First method is to compute moment measures using all the grain size fractions. The second method is that of graphical computations. In the latter technique, a cumulative percentile curve is plotted and the various percentile values are read from it to compute the different moment statistics.

In the present study, the second method has been preferred because as pointed out by McBride (1971, p.118-119) computational technique cannot handle 'open ended' distributions well. Secondly the assumption, that all the grains within a size class are assumed to be distributed as if they have a grain size equal to the middle point of that size grade, is not strictly true. Also, results obtained from the graphical computation can be compared well with those published in literature, as this method is most popular with geologists.

Graphical grain size measures were calculated by using a computer. A cumulative per cent frequency curve was obtained by fitting normal curves between adjacent observation points and then the various percentile values needed for calculations of different graphical measures were obtained which are listed in Appendix III. A number of graphical

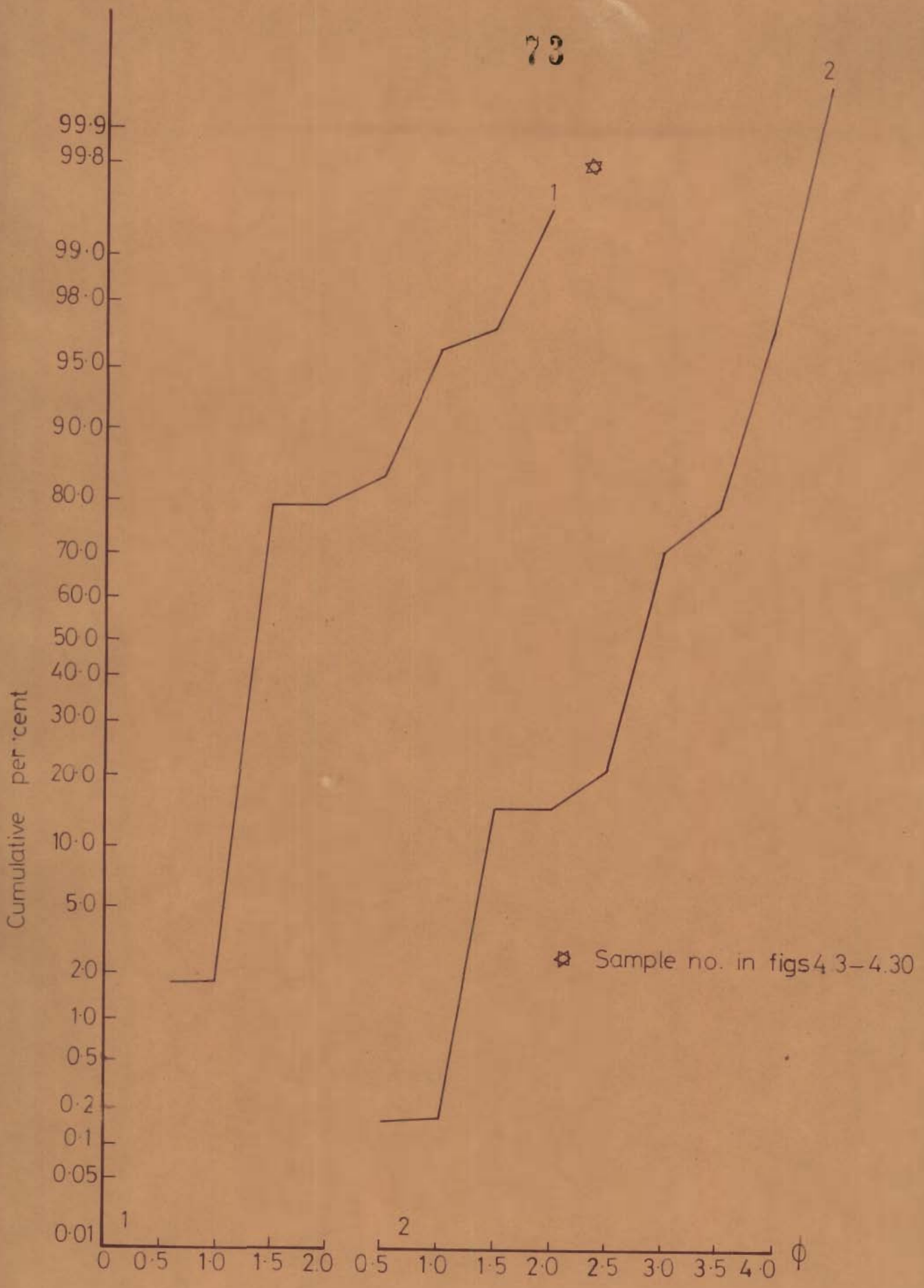


FIG.4-3. Cumulative frequency curves for grain size distributions.

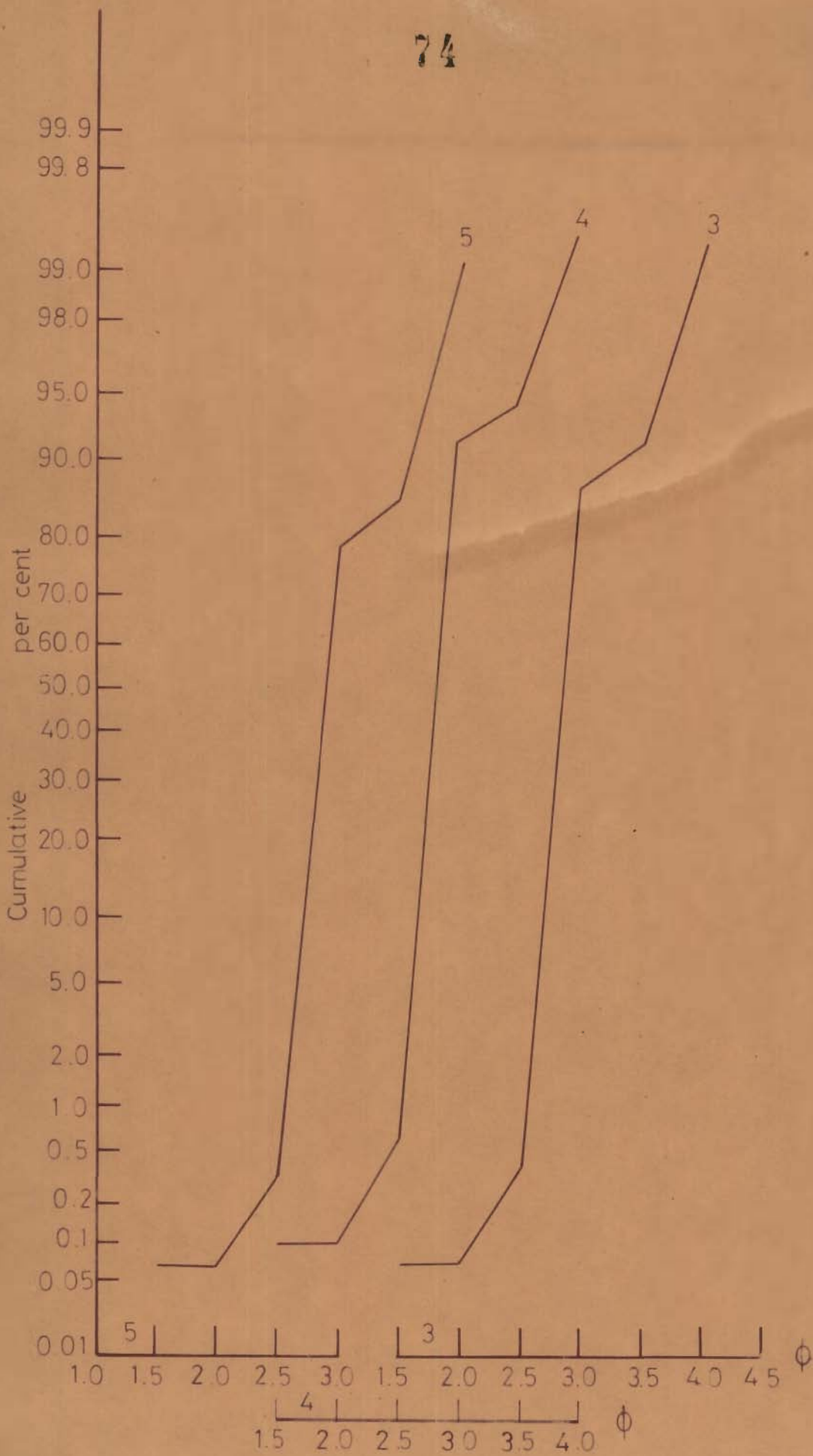


Fig.4.4_Cumulative frequency cruves for grain size distributions.

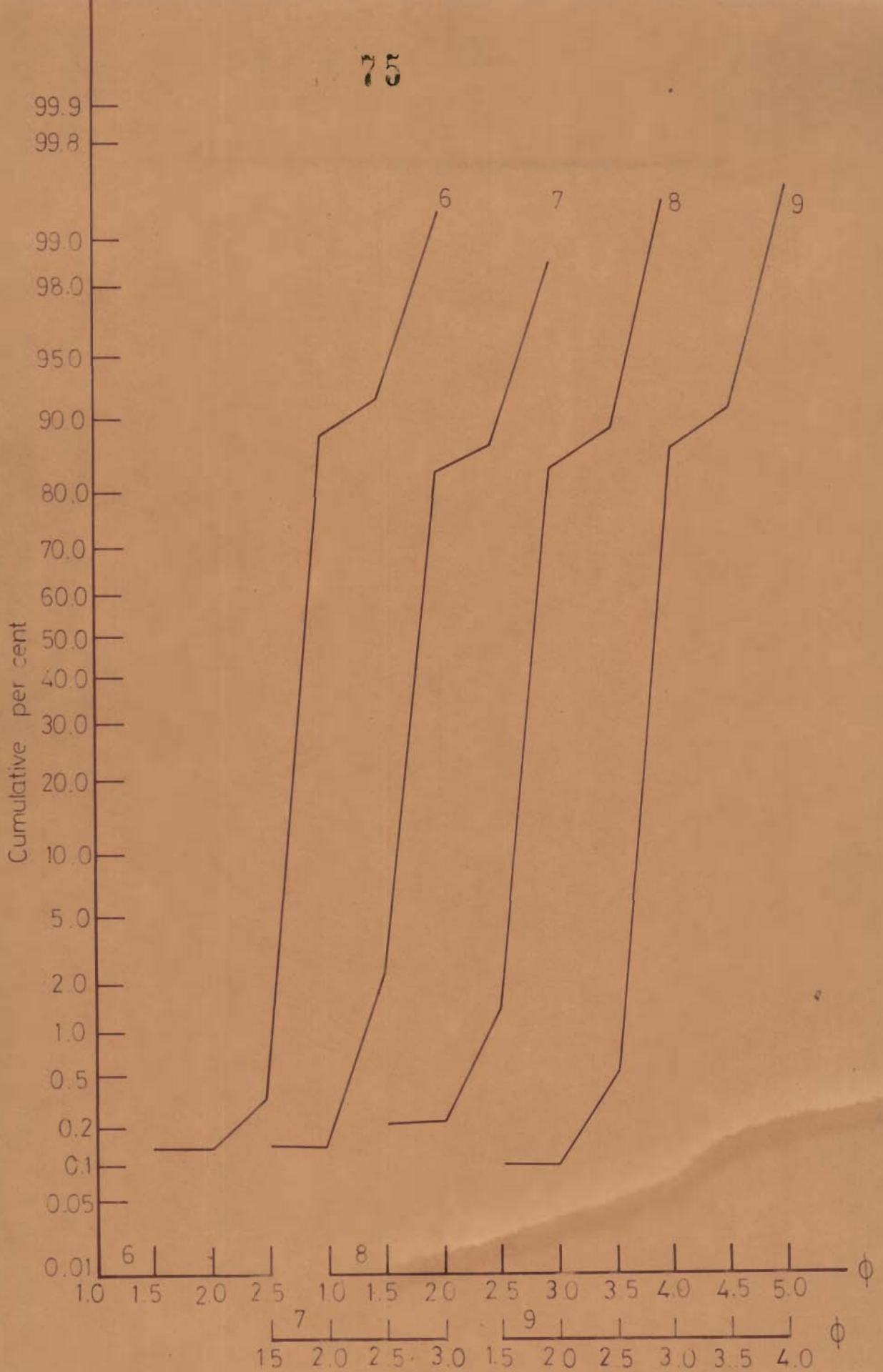


Fig.4.5_Cumulative frequency curves for grain size distributions.

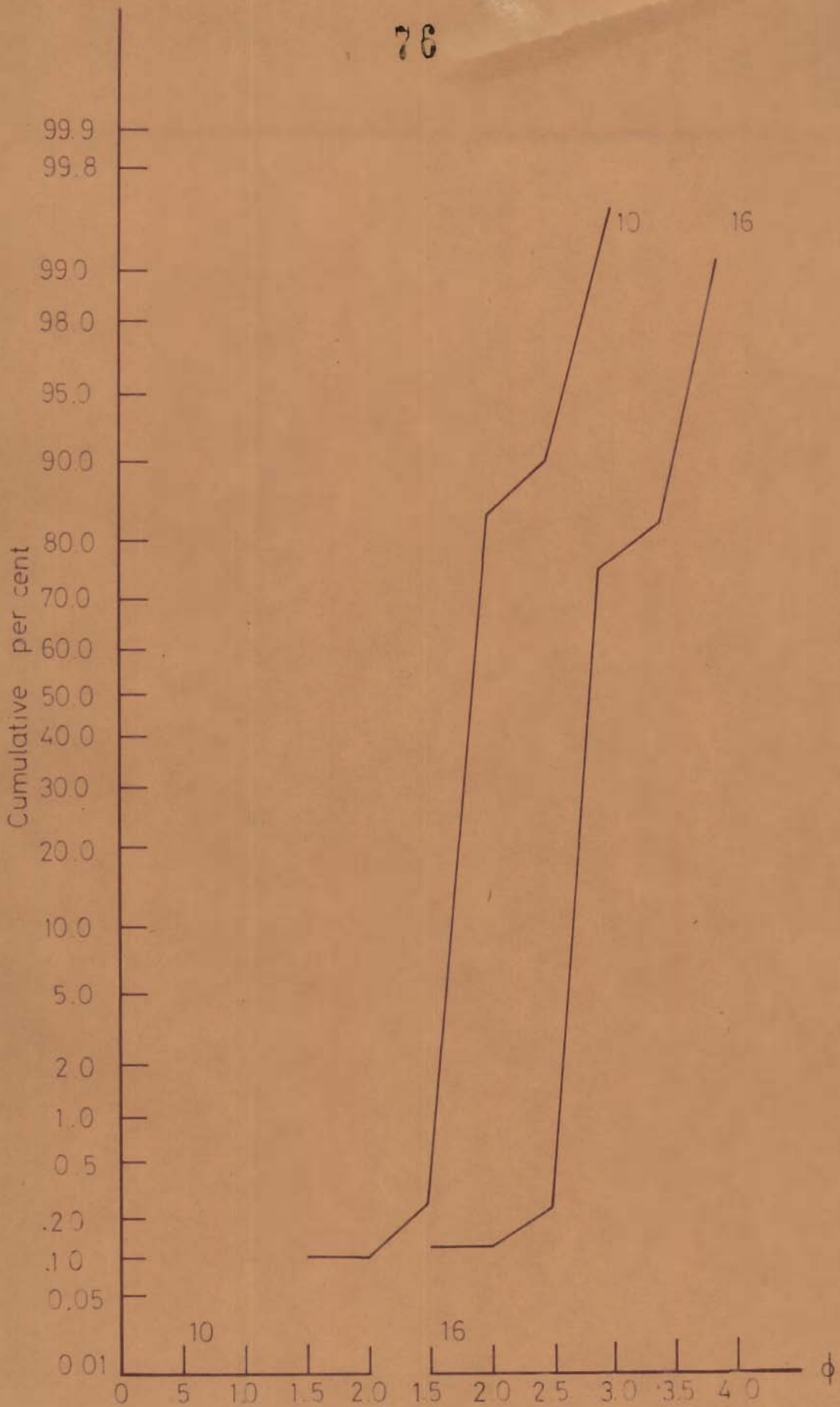


Fig 4.6_Cumulative frequency curves for grain size distributions.

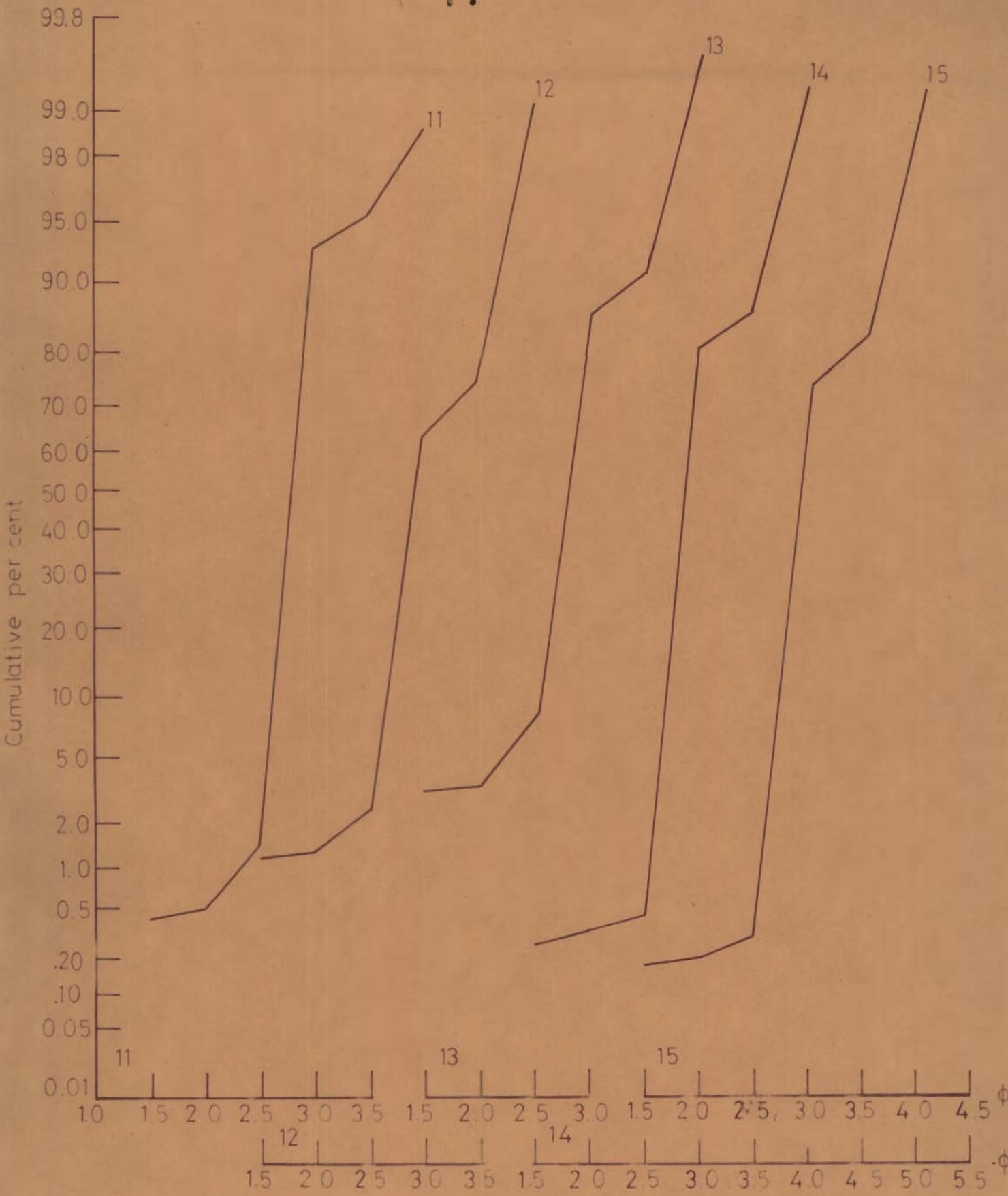


Fig.4.7_ Cumulative frequency curves for grain size distributions.

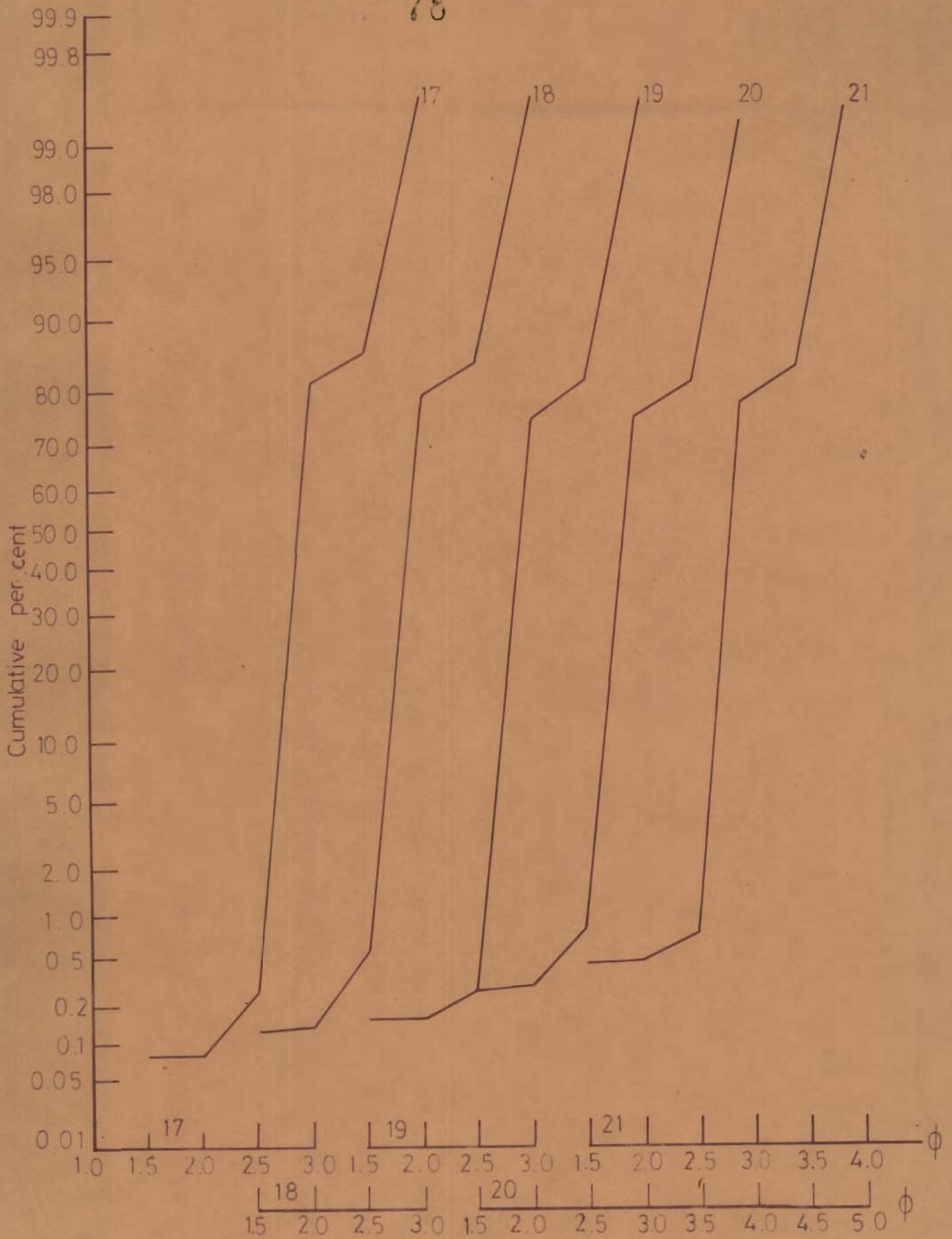


FIG.4.8 - Cumulative frequency curves for grain size distributions.

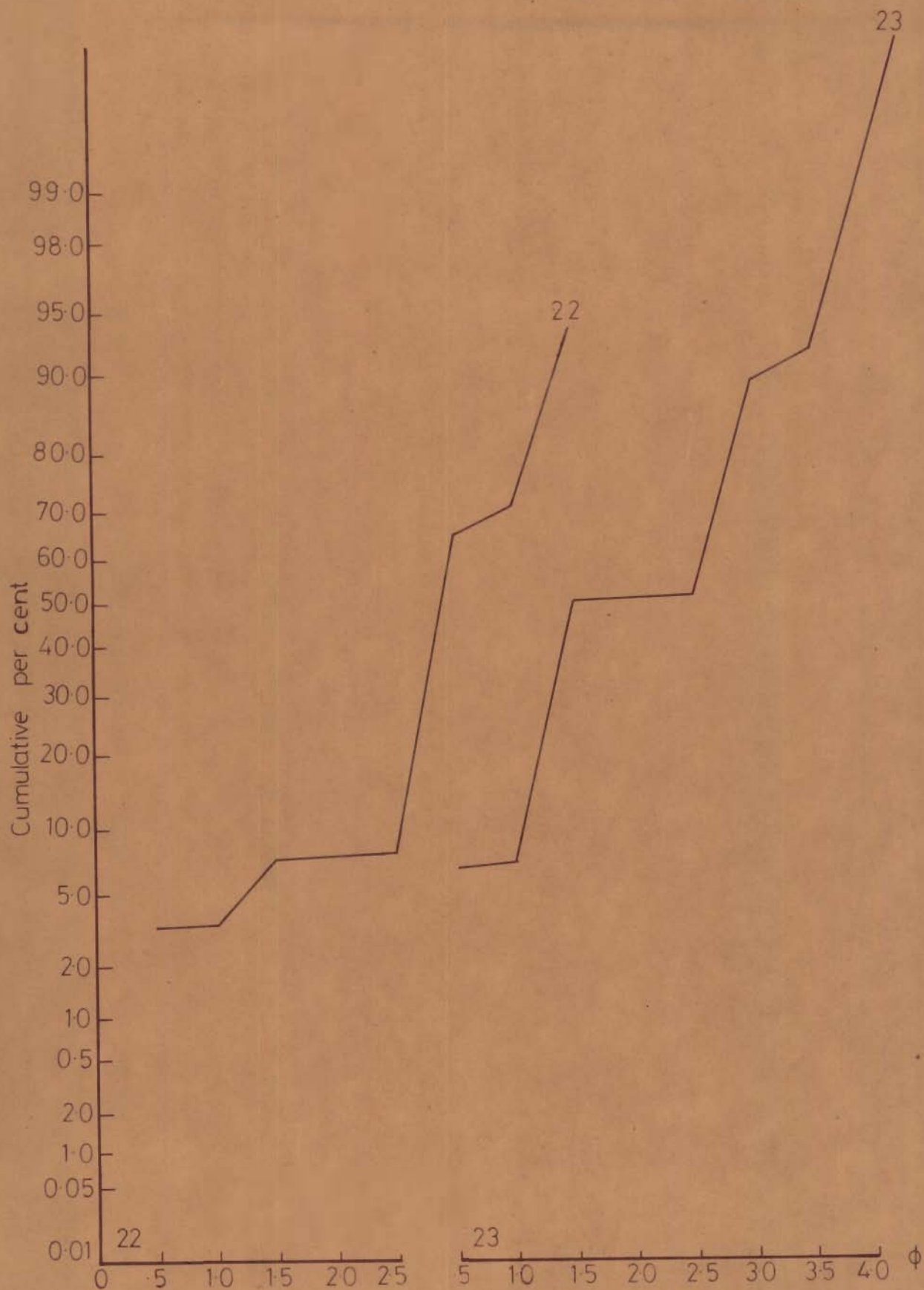


Fig.4.9_Cumulative frequency curves for grain size distributions.

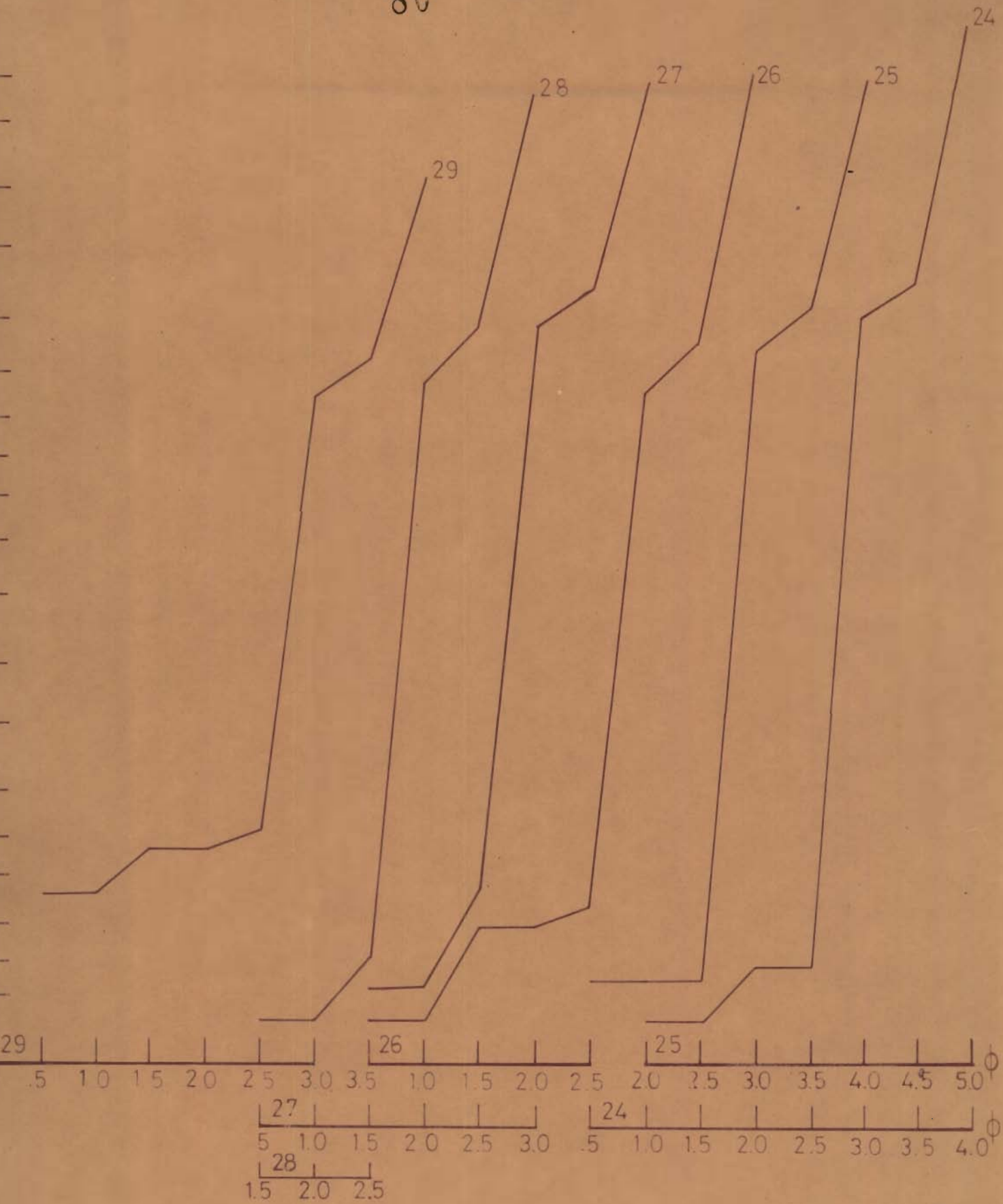


FIG.4-10_ Cumulative frequency curves for grain size distributions.

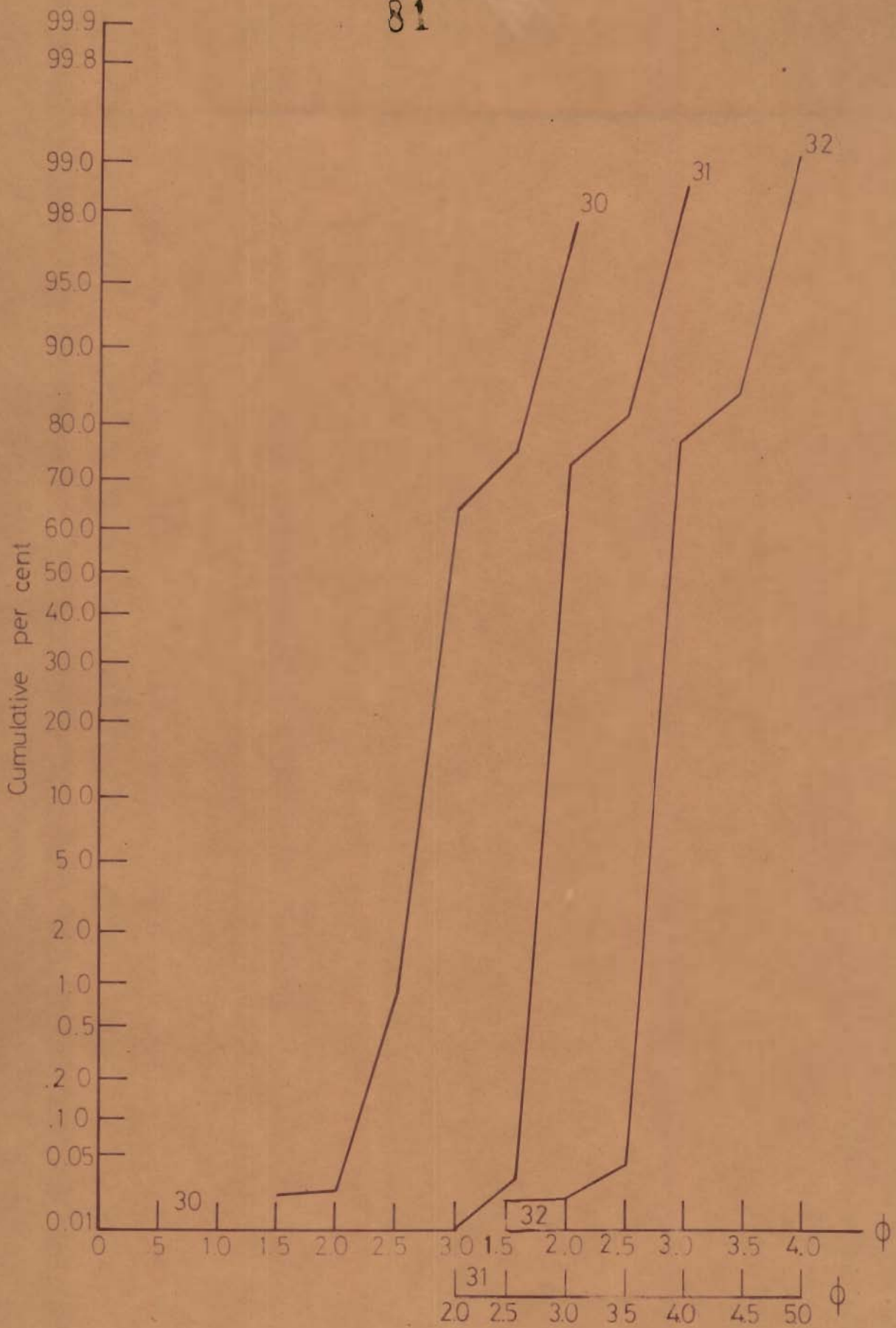


FIG. 4.11 - Cumulative frequency curves for grain size distribution.

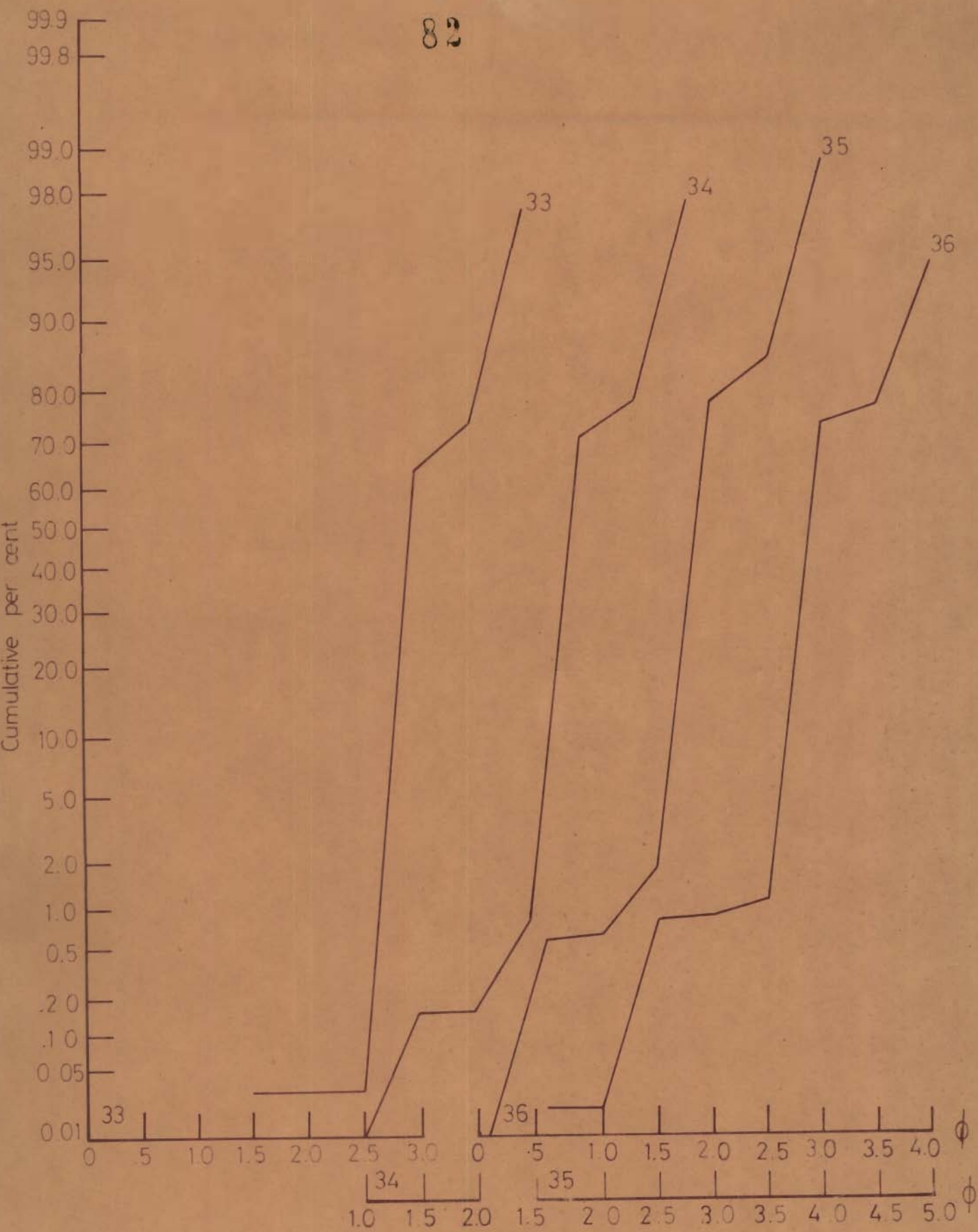


FIG.4.12 _ Cumulative frequency curves for grain size distributions.

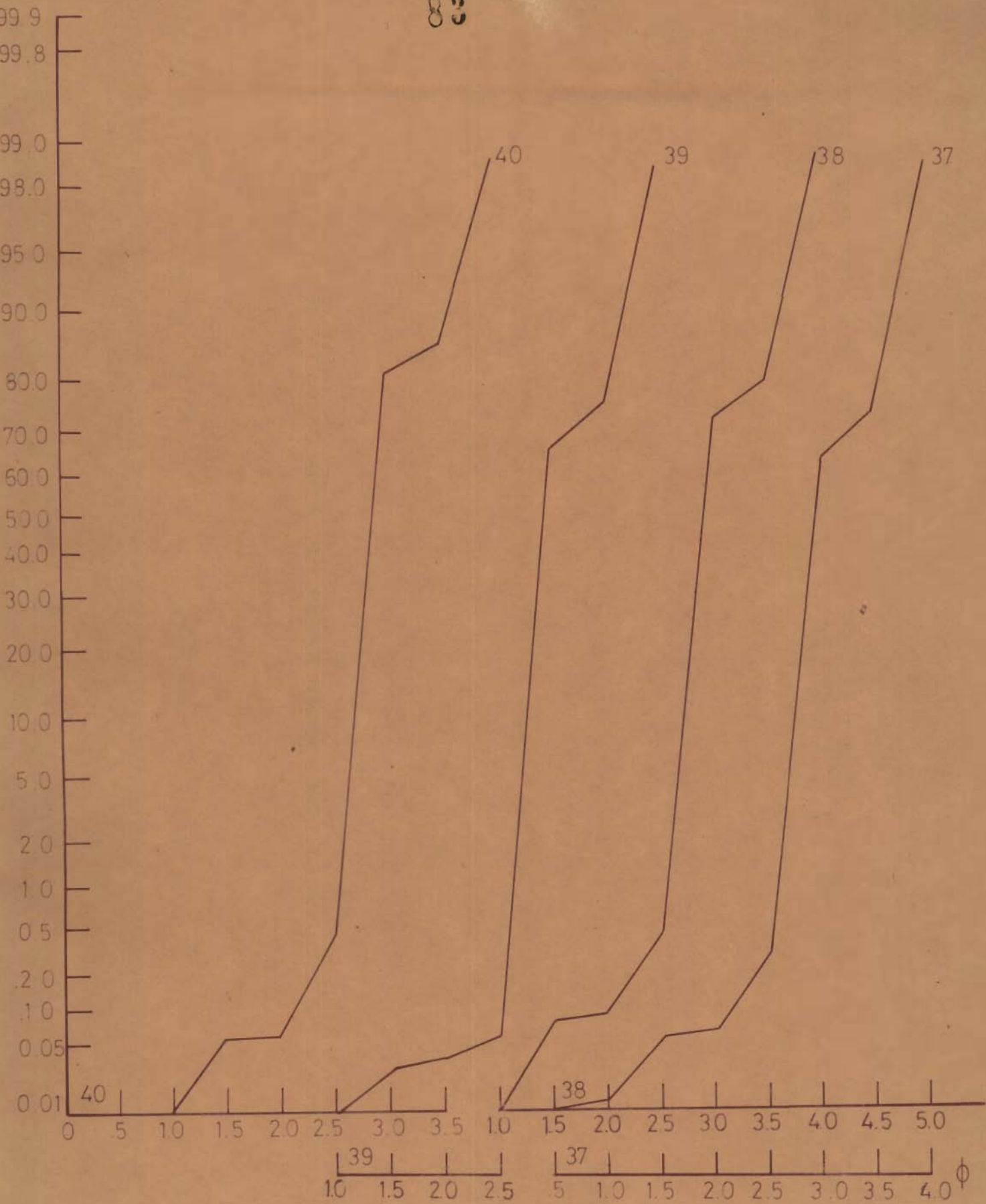


FIG.4.13 -Cumulative frequency curves for grain size distributions.



FIG. 4.14 Cumulative frequency curves for grain size distributions.

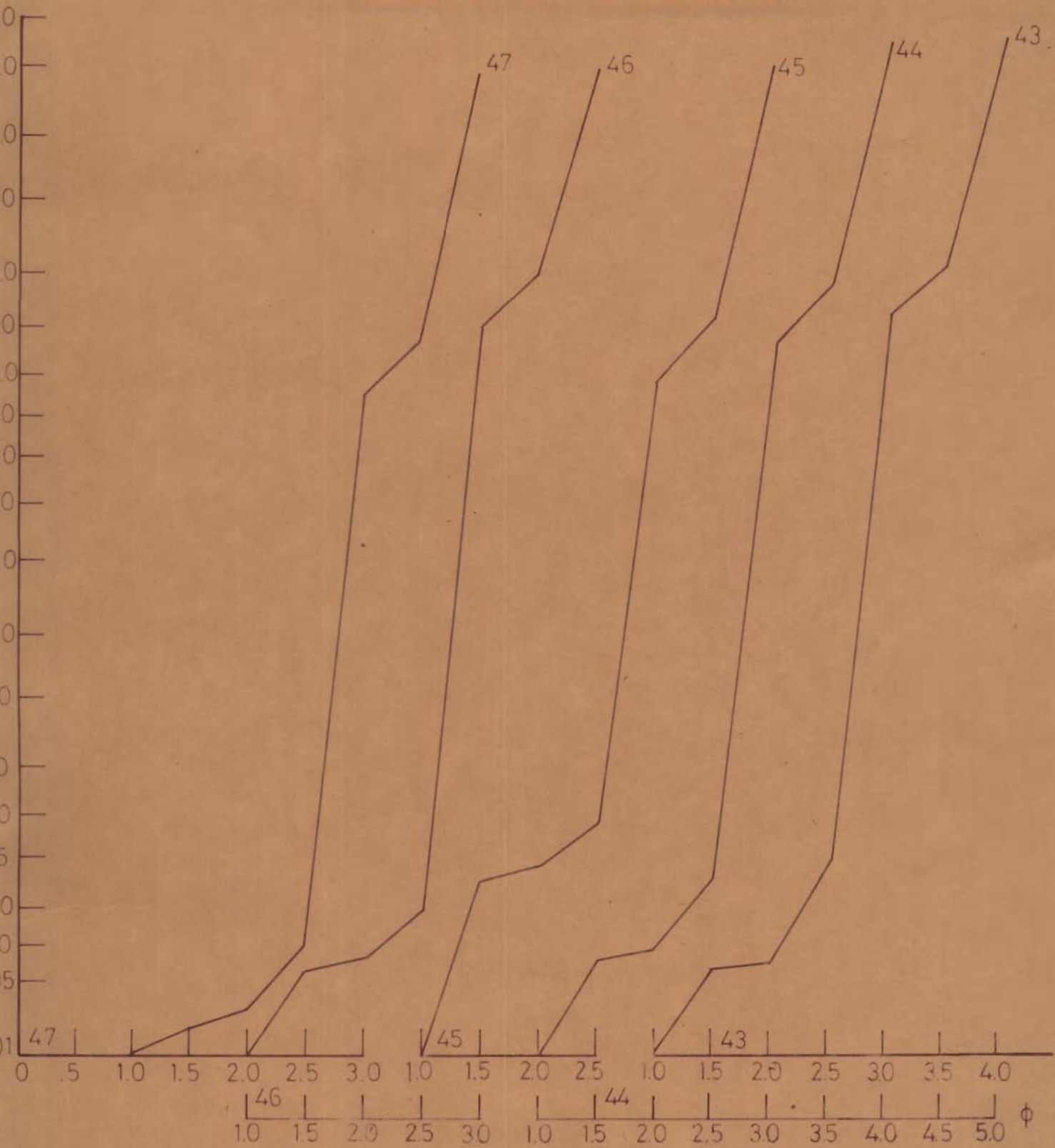
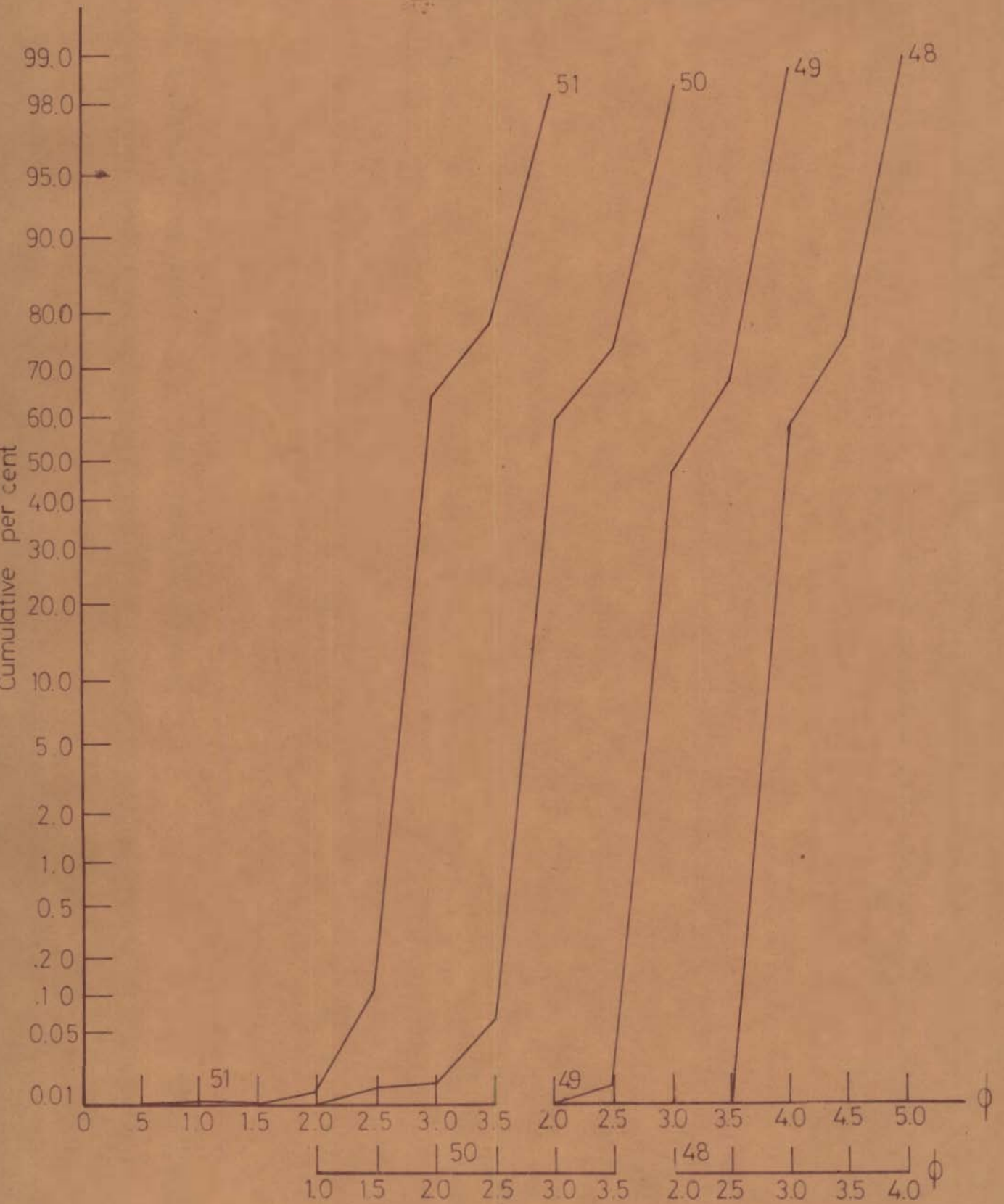


FIG.4.15 - Cumulative frequency curves for grain size distributions.



6.4.16 - Cumulative frequency curves for grain size distributions.

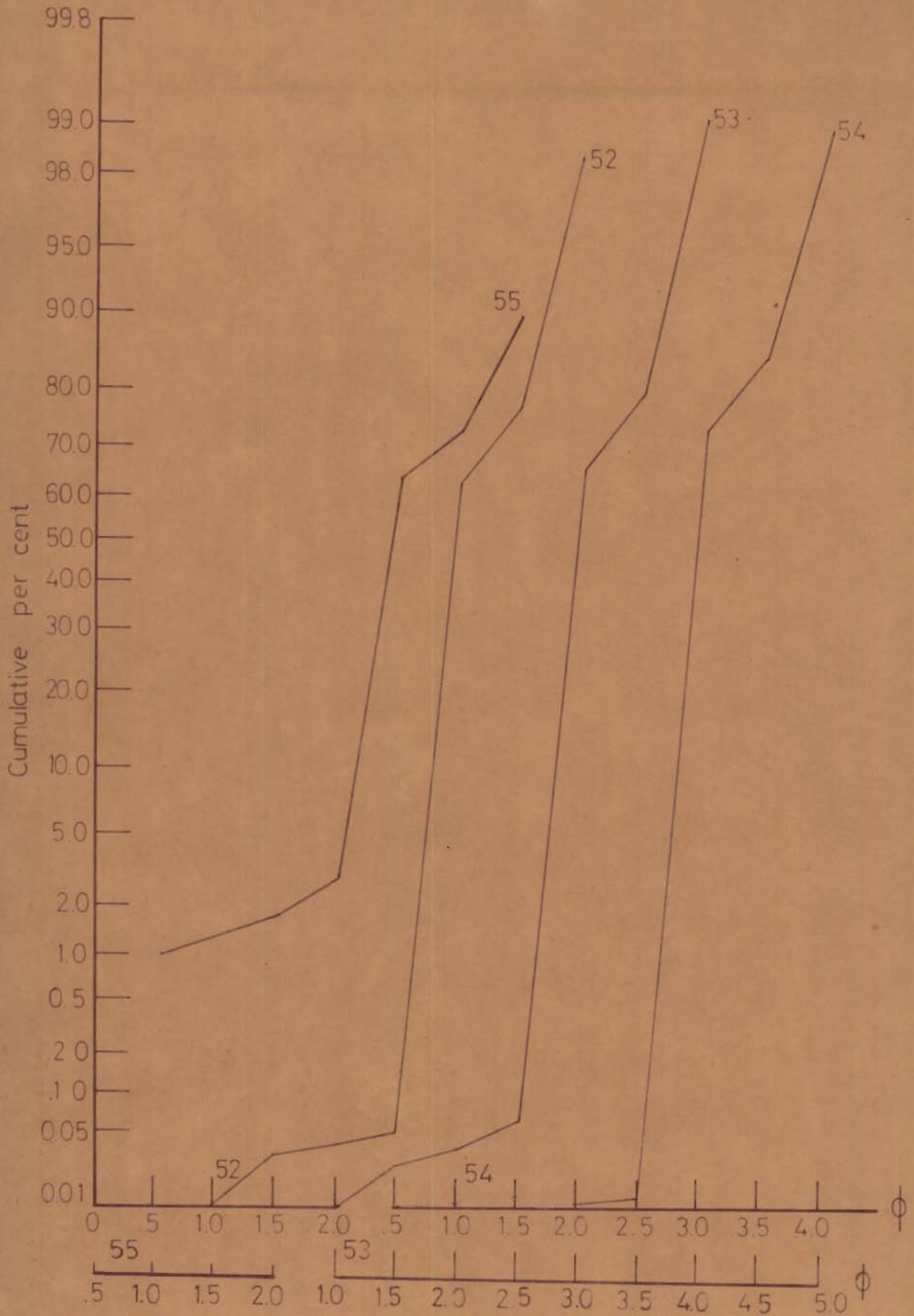


FIG.4.17 - Cumulative frequency curves for grain size distributions.

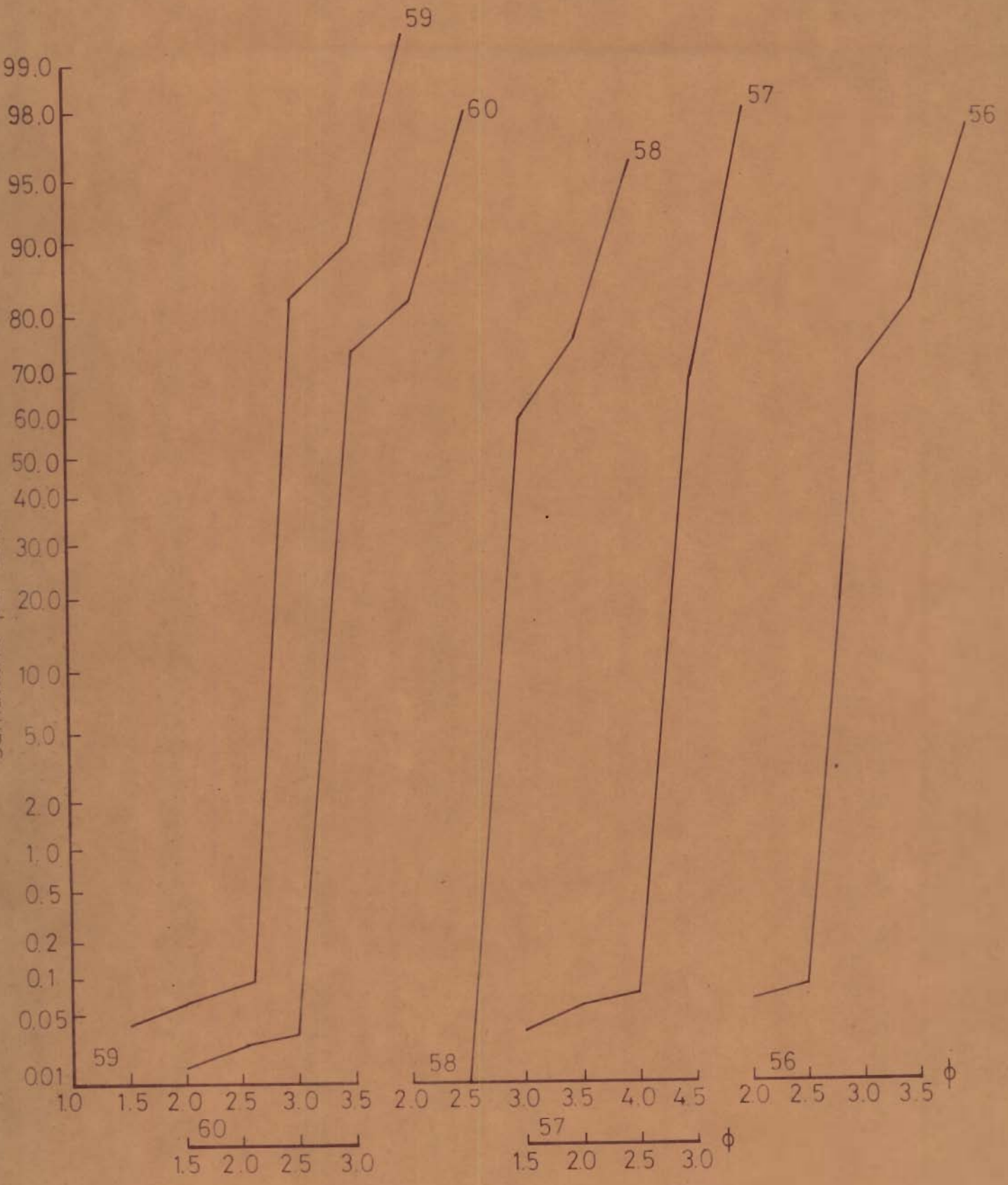


Fig.4.18_ Cumulative frequency curves for grain size distributions.

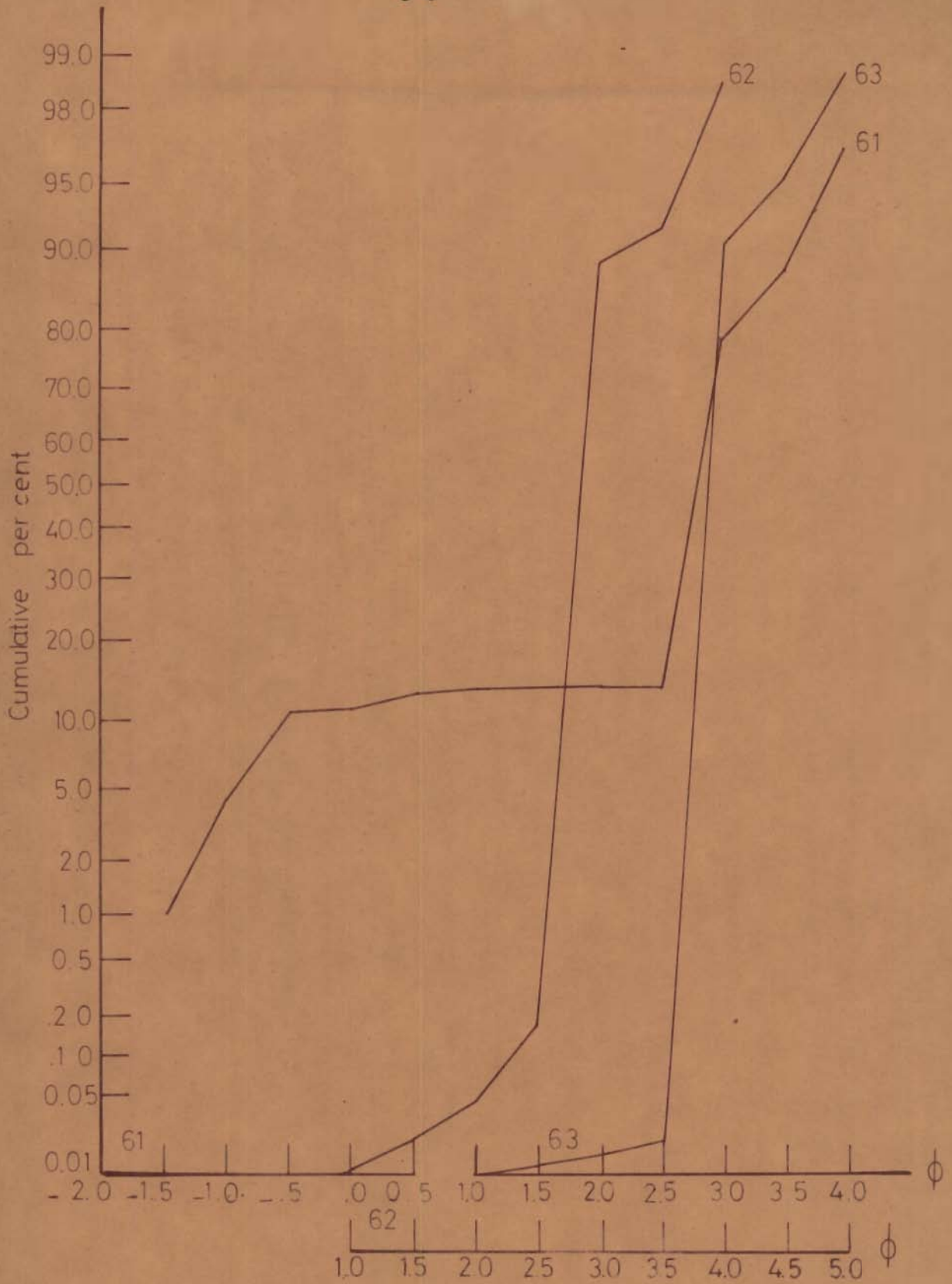


FIG.4.19 - Cumulative frequency curves for grain size distributions.

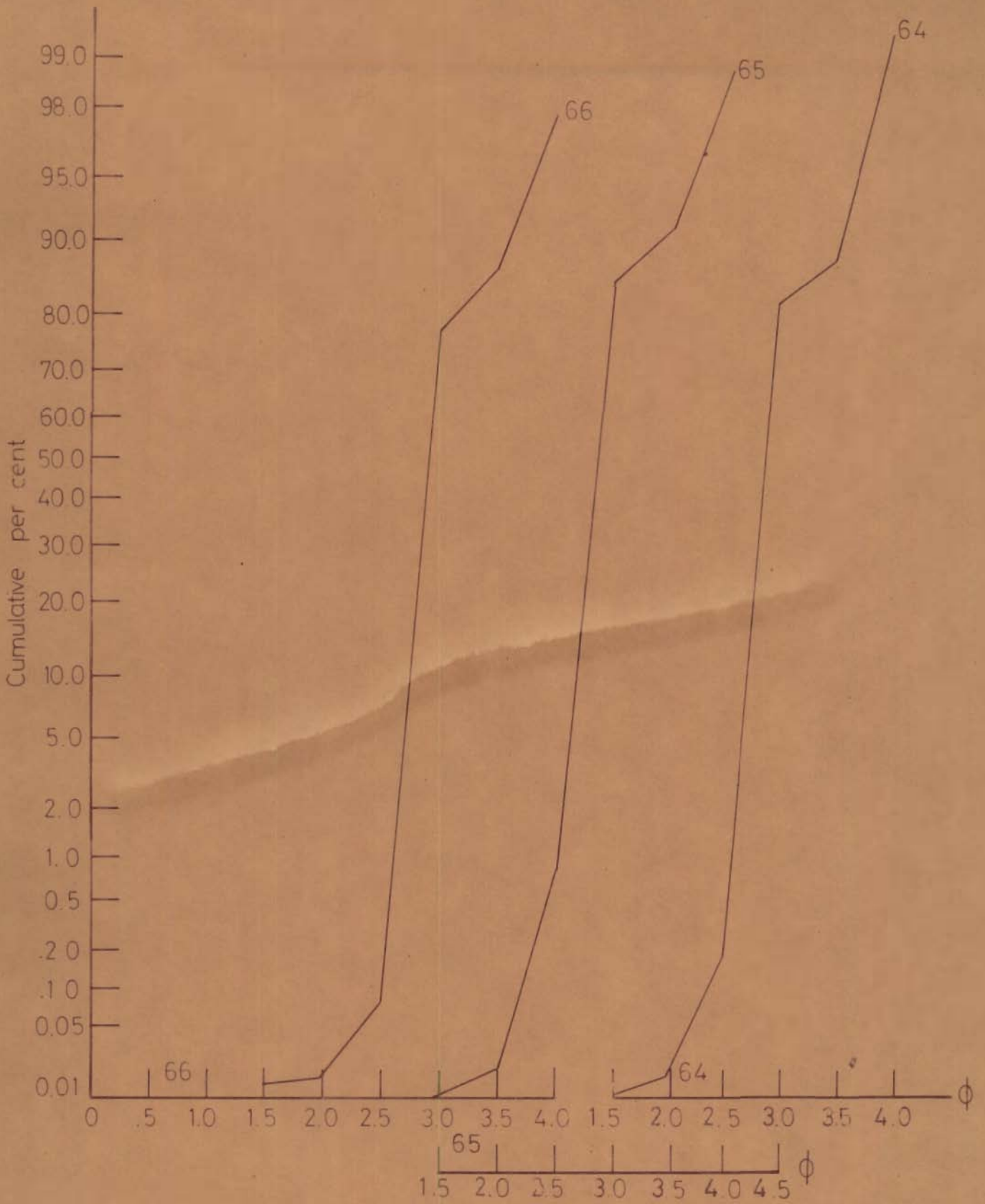


FIG.4 20 - Cumulative frequency curves for grain size distributions.

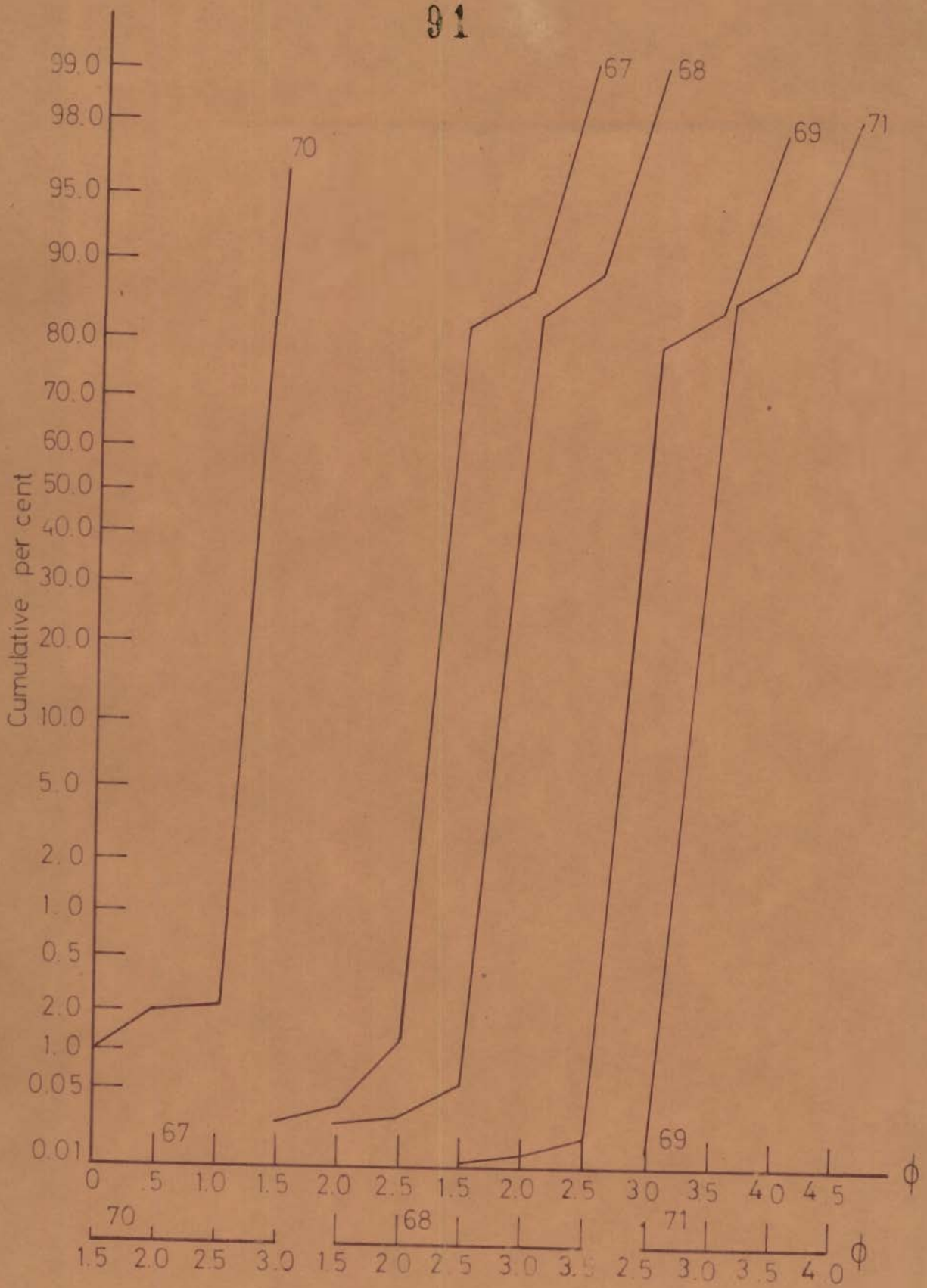


FIG 4.21 - Cumulative frequency curves for grain size distributions.

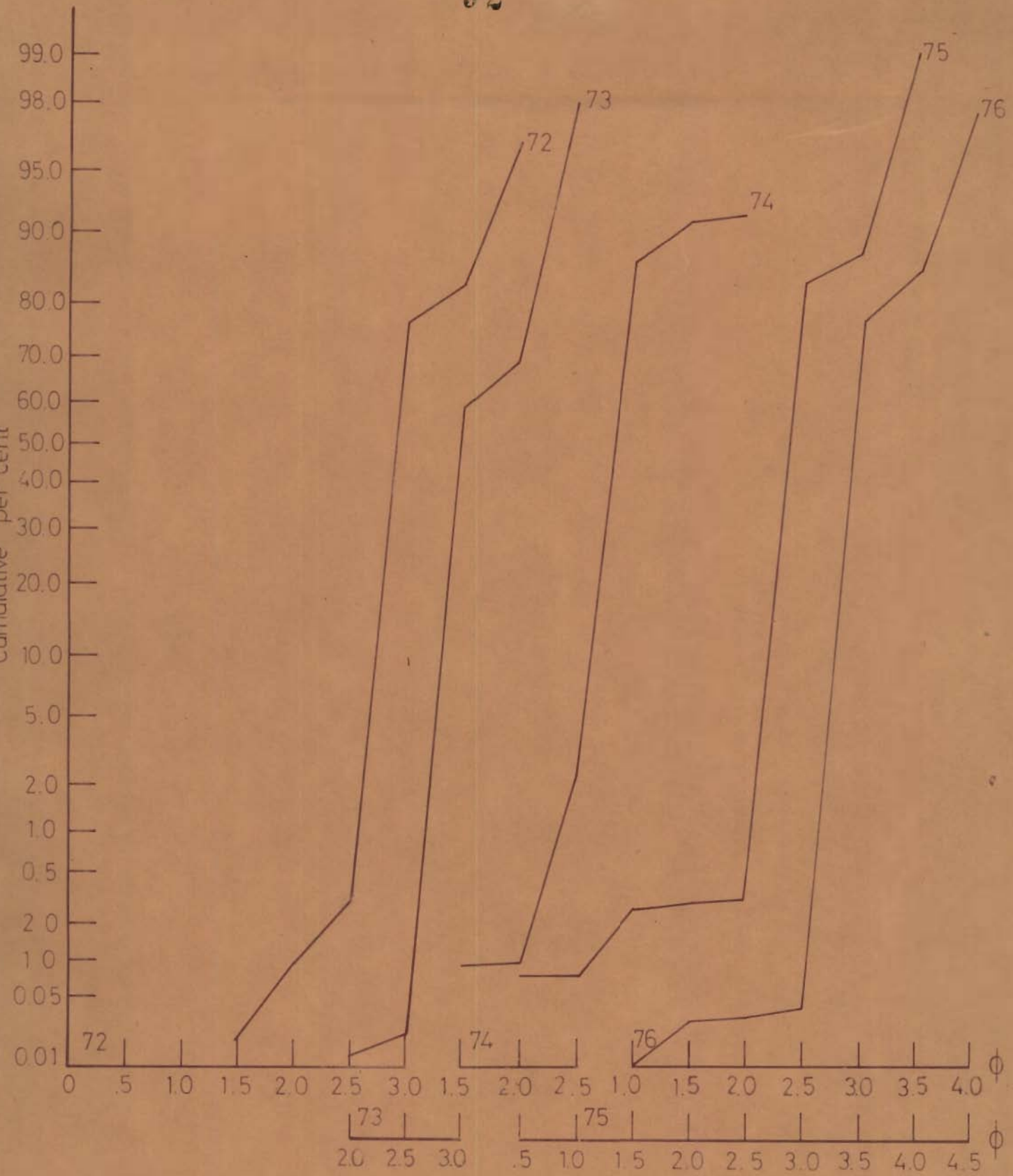


FIG 4.22 - Cumulative frequency curves for grain size distributions.

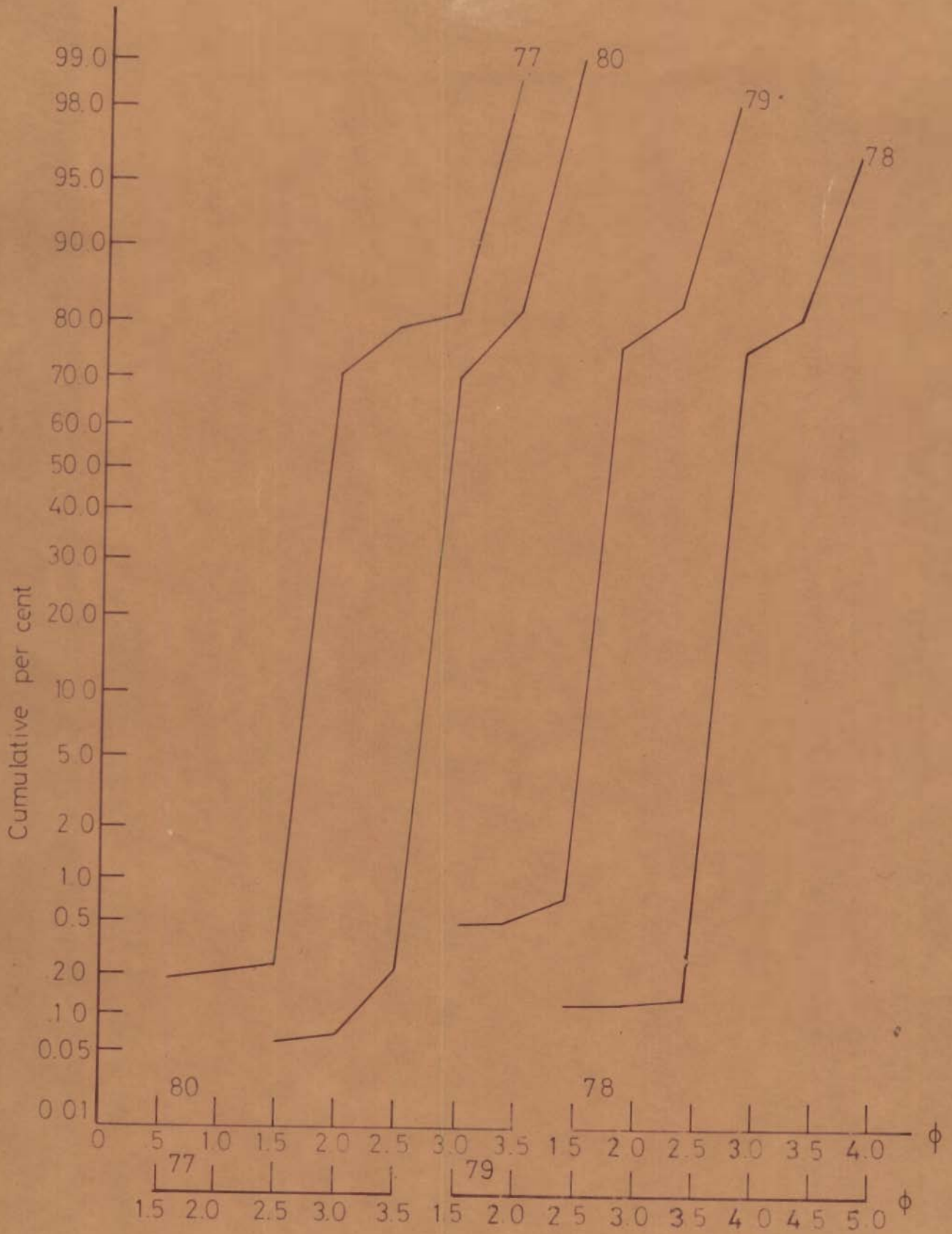


Fig.4.23_Cumulative frequency curves for grain size distributions.

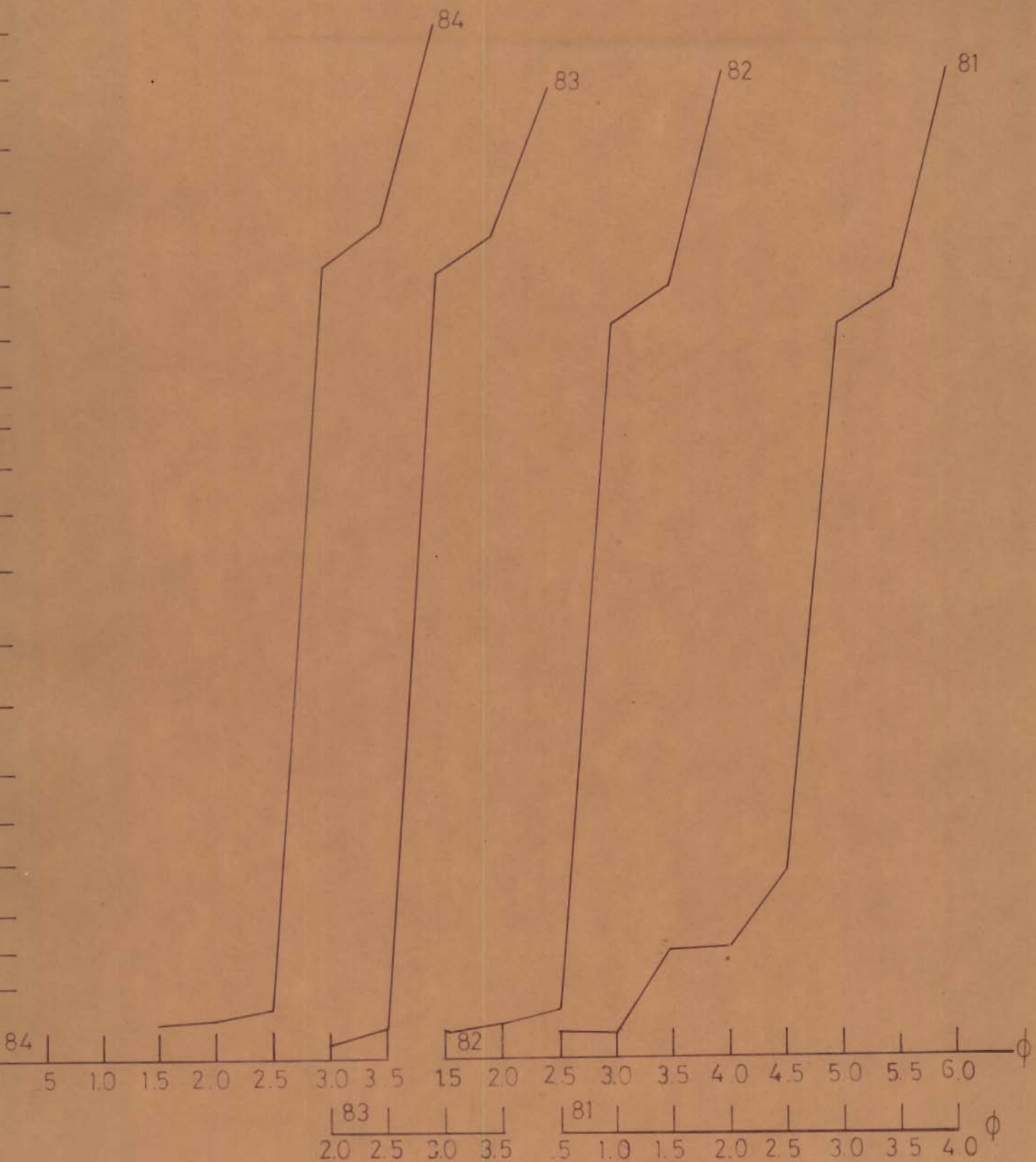


FIG.4.24 - Cumulative frequency curves for grain size distributions.

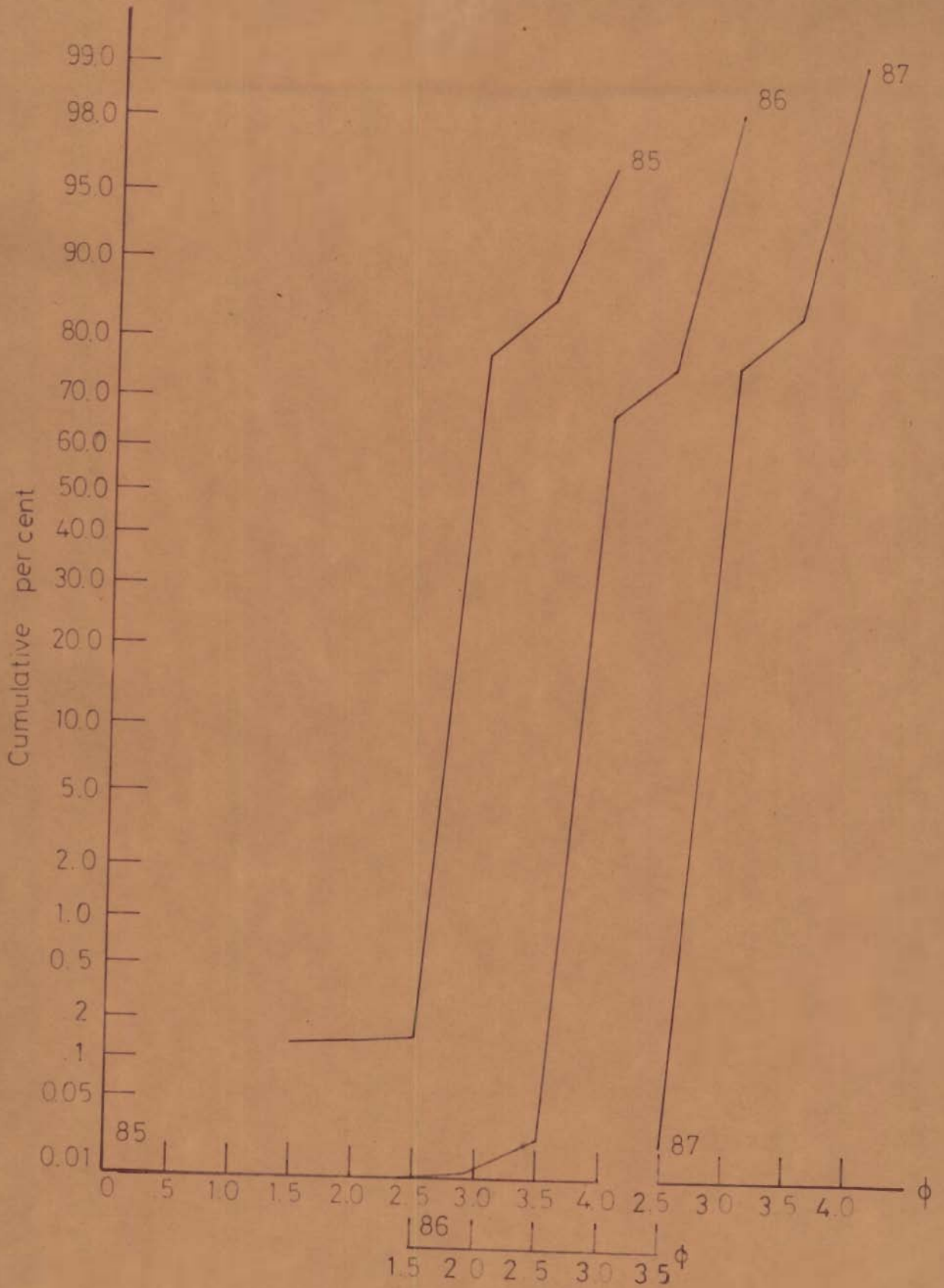


Fig.4.25_ Cumulative frequency curves for grain size distribution

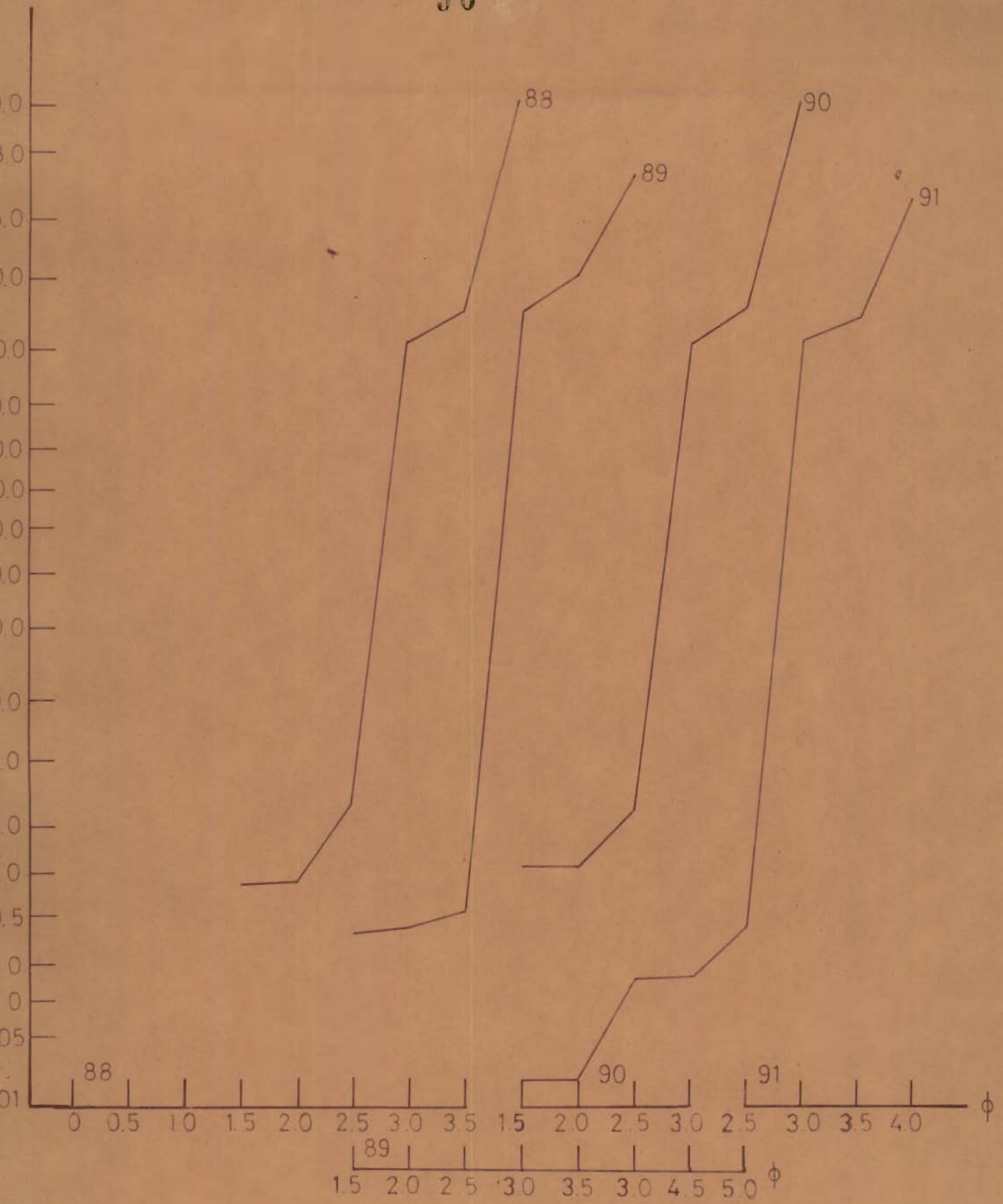


Fig.4.26_Cumulative frequency curves for grain size distributions.

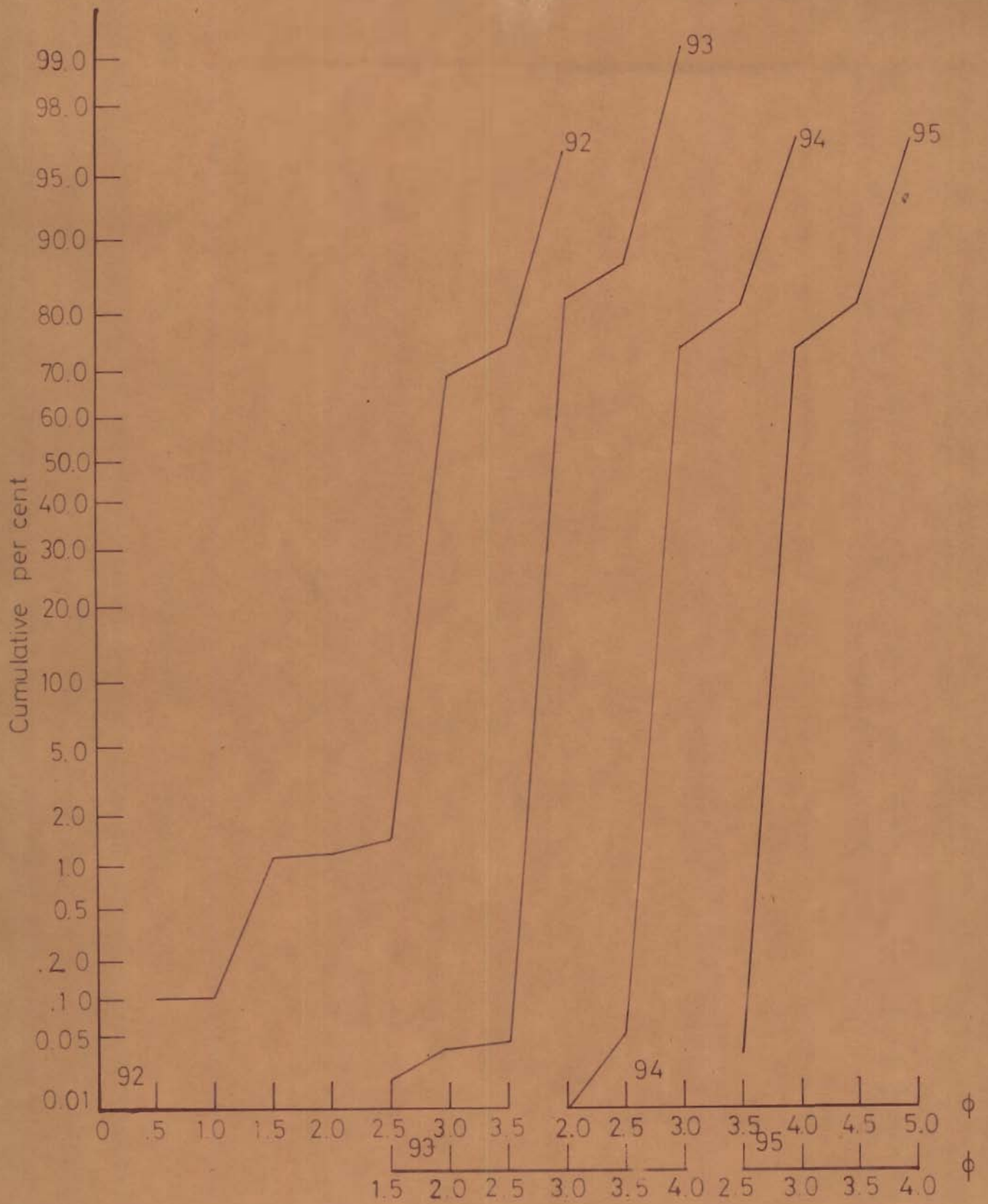


Fig.4.27_Cumulative frequency curves for grain size distributions.

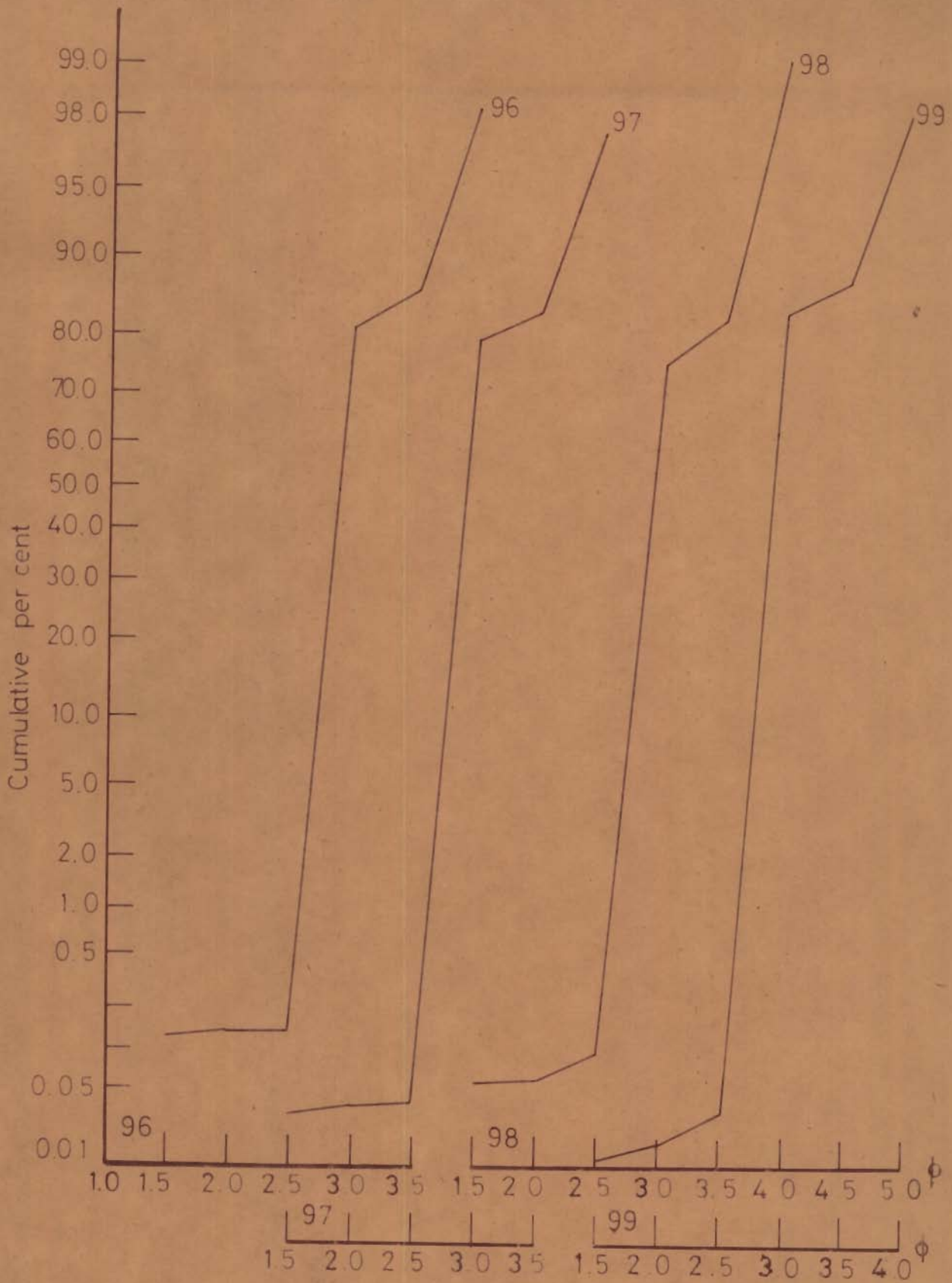


Fig.4.28 - Cumulative frequency curves for grain size distributions

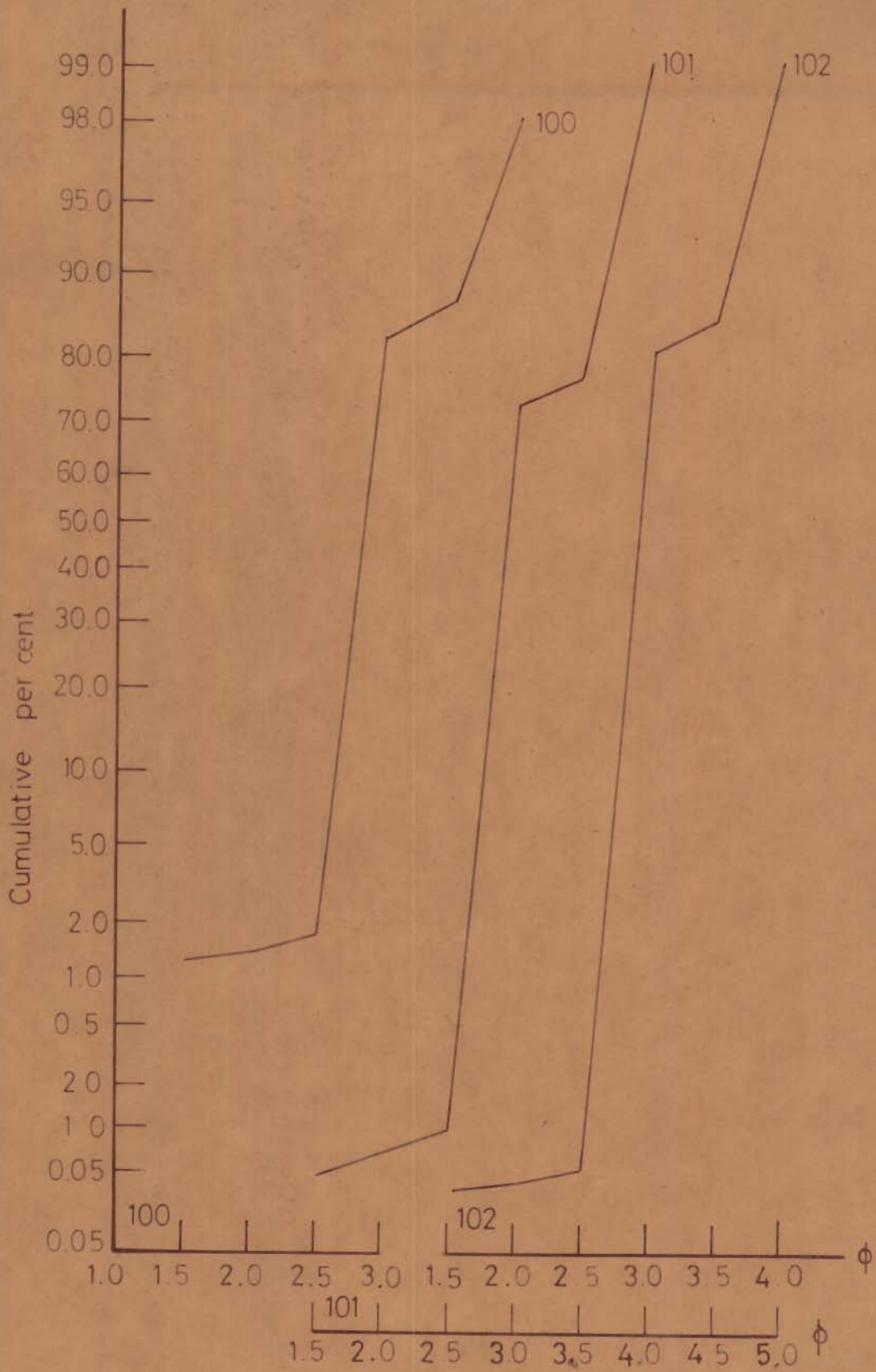


Fig.4.29 - Cumulative frequency curves for grain size distributions

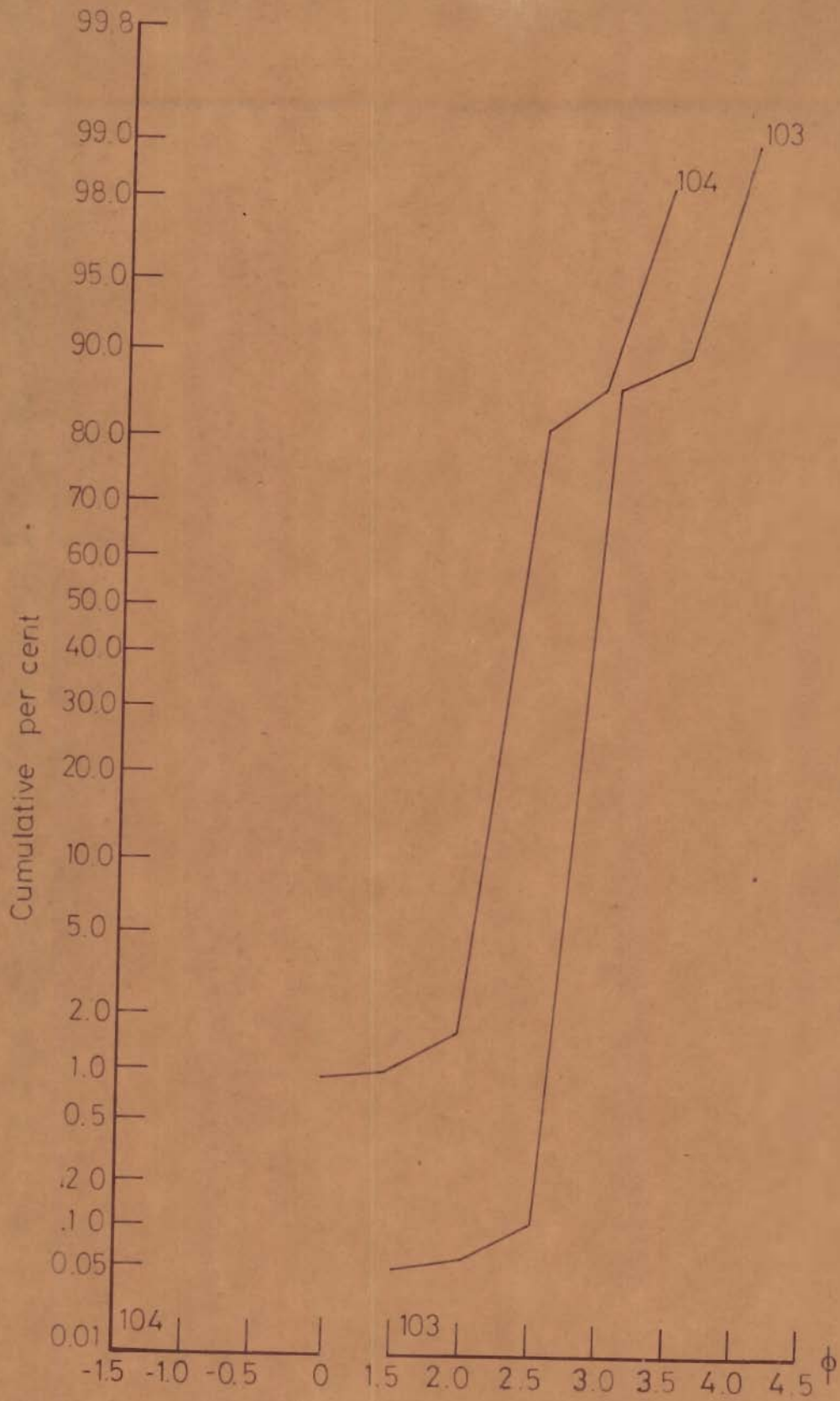


Fig.4.30_Cumulative frequency curves for grain size distributions.

measures have been suggested by different authors and are listed in Table 4.1 along with their efficiencies (McCammon, 1962) in estimating the different grain size parameters. Calculated values of these measures are given in Appendices IV-VII.

Table 4.1 — Formulae for computing graphical grain size parameters after different workers

<u>Mean</u>		<u>Efficiency</u> <u>per cent</u>
Trask (1930)	$Mz1 = \phi 50$	64
Otto (1939), Inman (1952)	$Mz2 = (\phi 16 + \phi 84)/2$	74
Folk and Ward (1957)	$Mz3 = (\phi 16 + \phi 50 + \phi 84)/3$	88
McCammon (1962)	$Mz4 = (\phi 10 + \phi 30 + \phi 50 + \phi 70 + \phi 90)/5$	93
McCammon (1962)	$Mz = (\phi 5 + \phi 15 + \phi 25 \dots \dots + \phi 85 + \phi 95)/10$	97
<u>Sorting</u>		
Trask? Krumbein (1934)	$\sigma_1 = (\phi 75 - \phi 25)/1.35$	37
Otto (1939), Inman (1952)	$\sigma_2 = (\phi 84 - \phi 16)/2$	54
Folk and Ward (1957)	$\sigma_3 = (\phi 84 - \phi 16)/4 + (\phi 95 - \phi 5)/6.6$	79
Calgan 1954 McCammon (1962)	$\sigma_4 = (\phi 85 + \phi 95 - \phi 5 - \phi 15)/5.4$	79
McCammon (1962)	$\sigma = (\phi 70 + \phi 80 + \phi 90 + \phi 97 - \phi 3 - \phi 10 - \phi 20 - \phi 30)/9.1$	87
Tanner 1958 (computer)		

Skewness

Trank

$$\text{Krumbein and Pettijohn (1938)} \quad (Sk_{\phi}) \quad Sk_1 = [\phi 25 + \phi 75 - 2 \phi 50] / 2$$

$$\text{Inman (1952)} \quad (d_{\phi}) \quad Sk_2 = \frac{\phi 16 + \phi 84 - 2 \phi 50}{\phi 84 - \phi 16}$$

$$\text{Inman (1952)} \quad (d_{2\phi}) \quad Sk_3 = \frac{\phi 5 + \phi 95 - 2 \phi 50}{\phi 84 - \phi 16}$$

$$\text{Folk and Ward (1957)} \quad (Sk_1) \quad Sk = \frac{\phi 84 + \phi 16 - 2 \phi 50}{2(\phi 84 - \phi 16)} + \frac{\phi 95 + \phi 5 - 2 \phi 50}{2(\phi 95 - \phi 5)}$$

Kurtosis

Kelley 1924

$$\text{Krumbein and Pettijohn (1938)} \quad (K_{\phi}) \quad Ku_1 = \frac{\phi 75 - \phi 25}{2(\phi 90 - \phi 10)}$$

$$\text{Inman (1952)} \quad (\beta_{\phi}) \quad Ku_2 = \frac{(\phi 95 - \phi 5) - (\phi 84 - \phi 16)}{\phi 84 - \phi 16}$$

$$\text{Folk and Ward (1957)} \quad (K_{\phi}) \quad Ku = \frac{\phi 95 - \phi 5}{2.44(\phi 75 - \phi 25)}$$

4.2.5 Comparison of Graphical Grain Size Parameters

Middleton (1962) suggested that individual grain size parameters from a particular environment can be considered to constitute a homogeneous population. Sahu (1964) also assumed normal distribution for individual grain size parameters in determining discriminatory functions for different environments. Following this line of reasoning, different parameters are considered to constitute samples from normal populations. Histograms depicting distributions of these parameters are shown in Figures 4.31-4.34. Grand means and

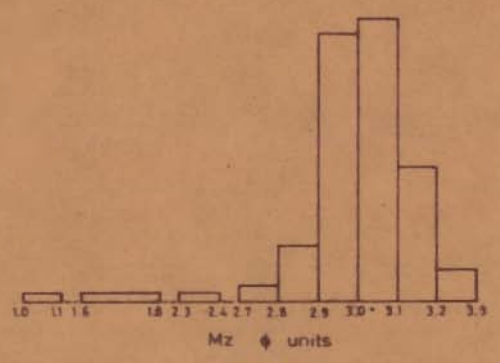
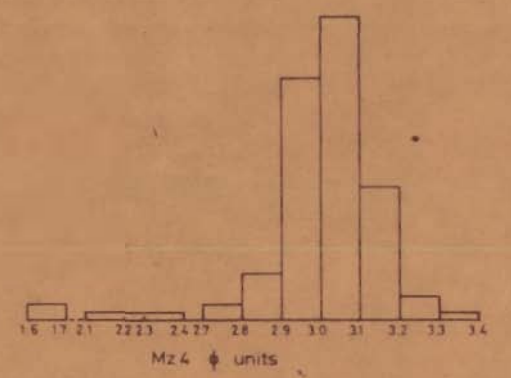
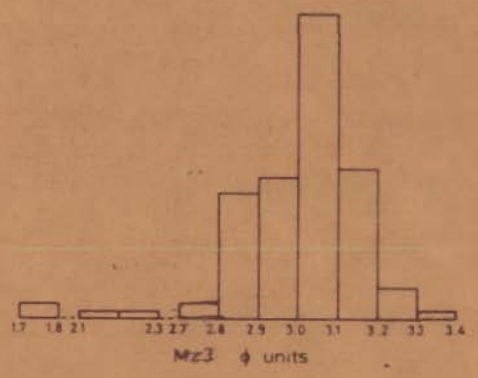
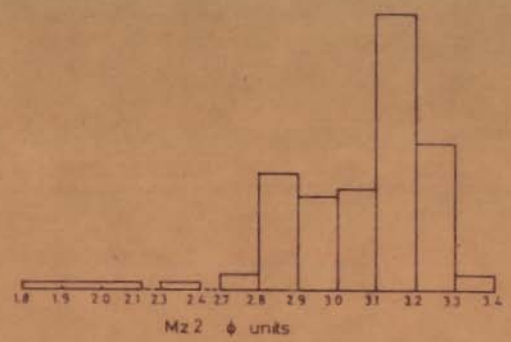


Fig.4.31_Histograms showing distributions of the various measures of mean grain size.

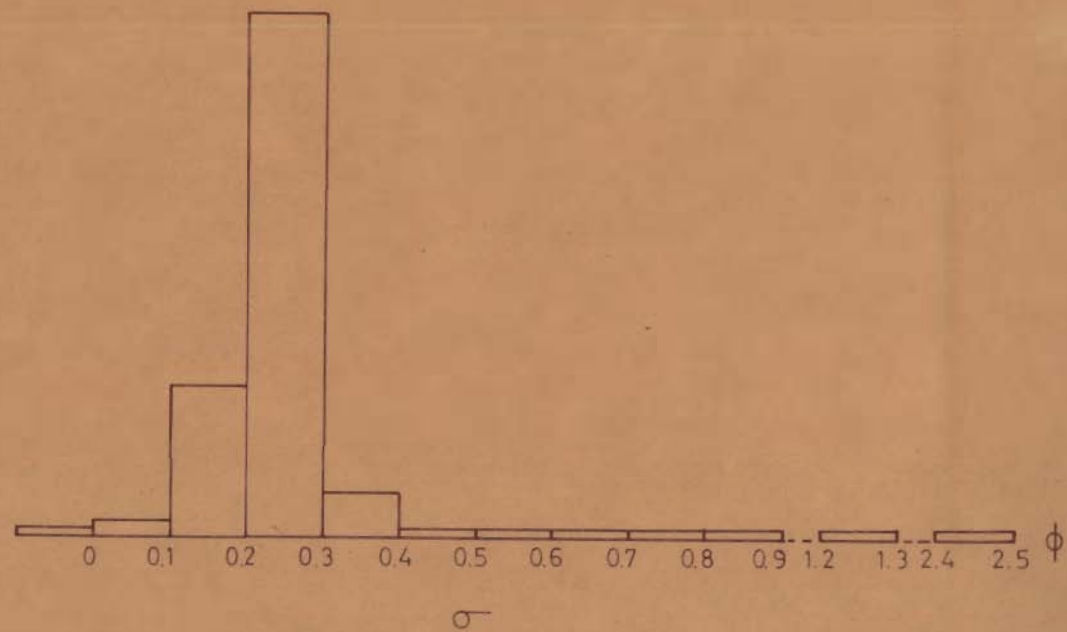
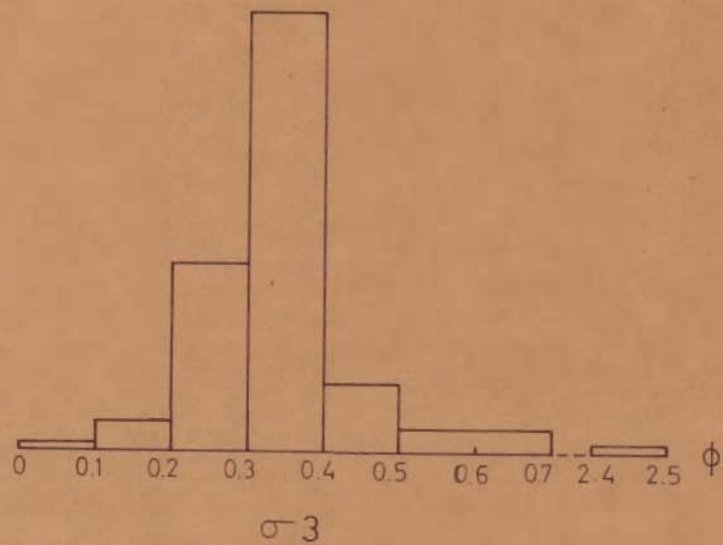
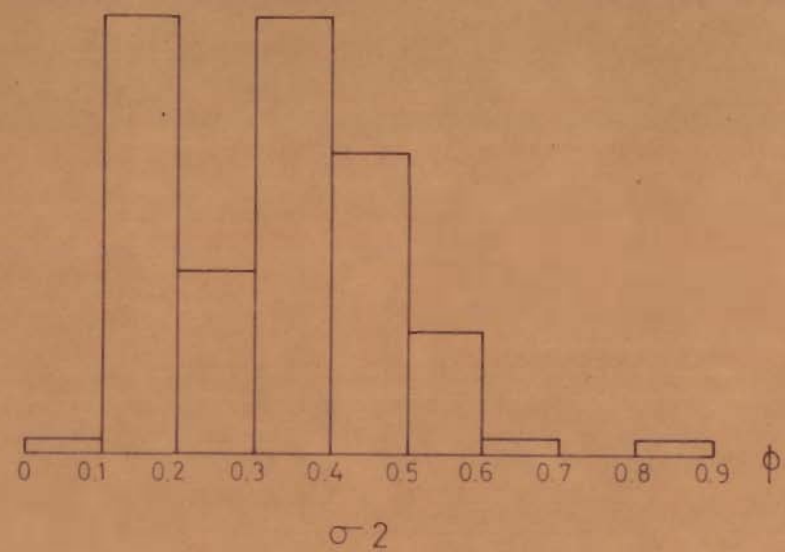
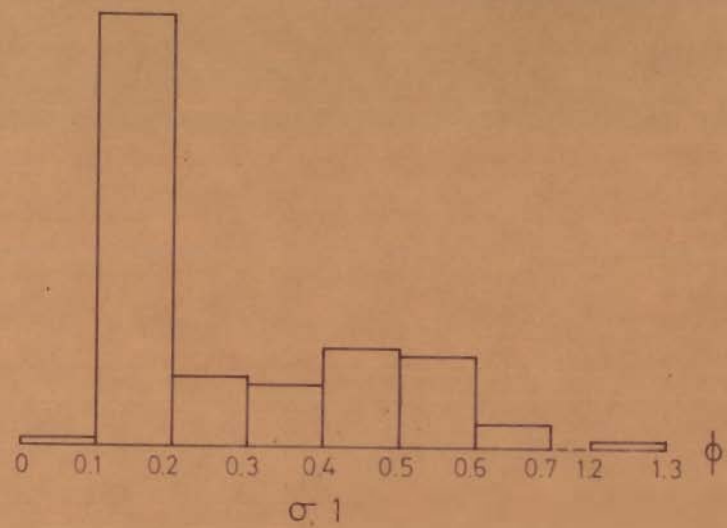


Fig 4.32—Histograms showing distributions of the various measures of sorting.

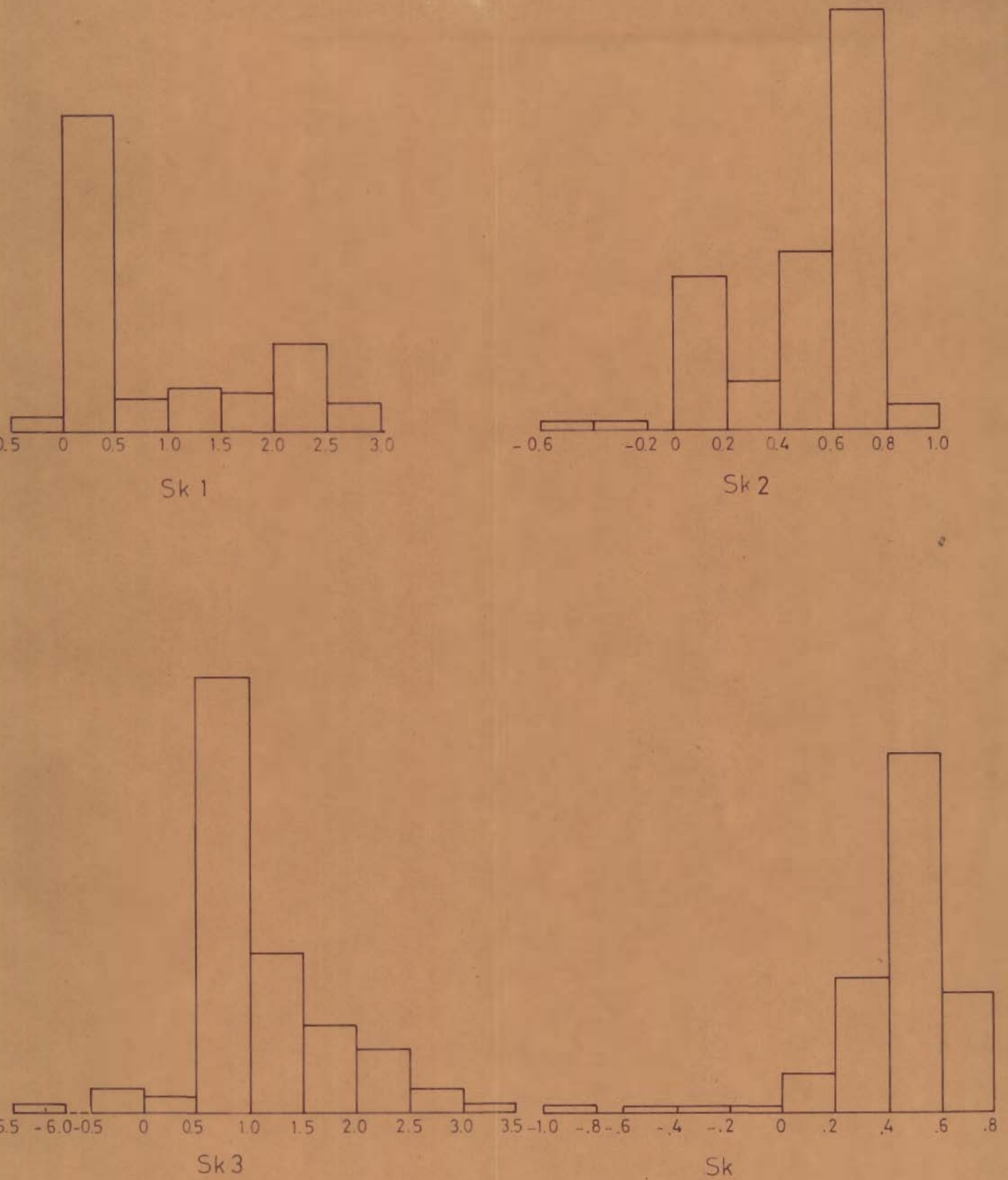
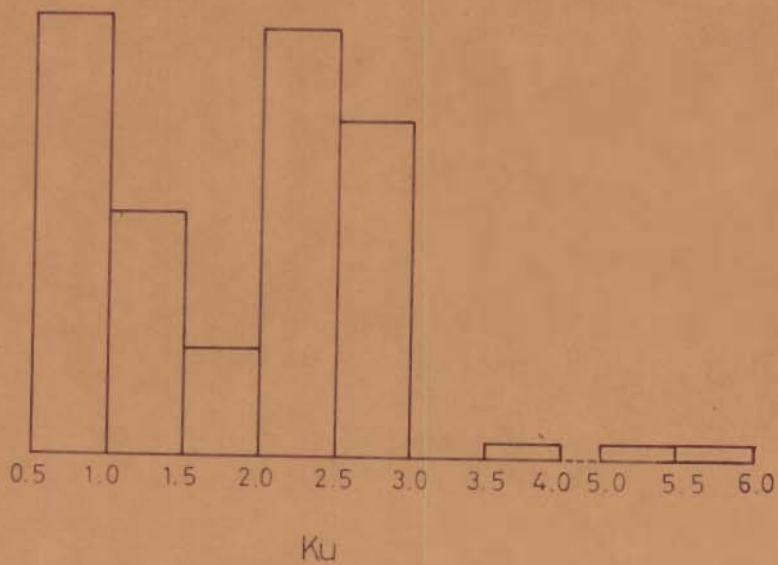
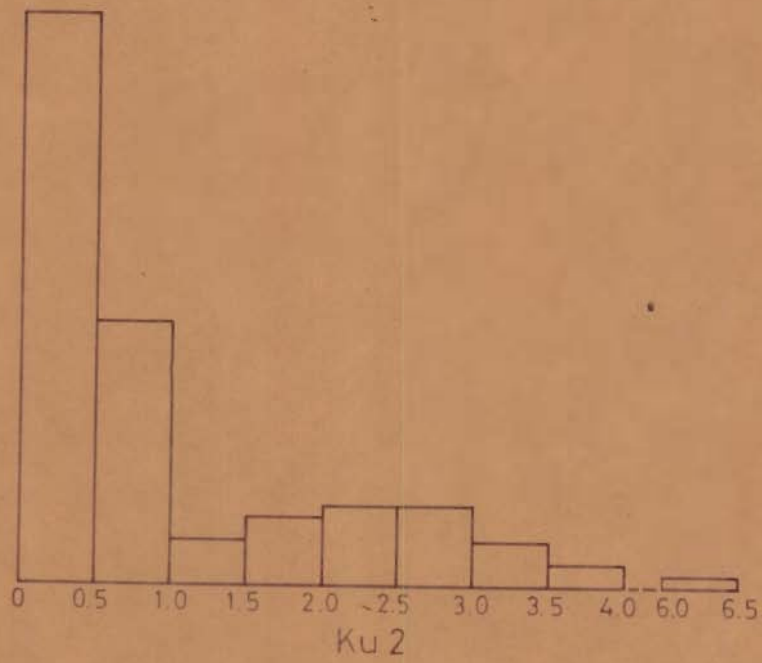
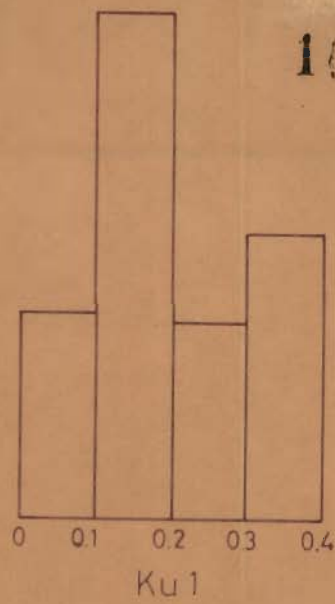


Fig 4.33_ Histograms showing distributions of the various measures of skewness.



g.4.34 - Histograms showing distributions of the various measures of kurtosis.

standard deviations for the various parameters after different authors and 't' values calculated for different pairs of grain size measures are listed in Tables 4.2-4.5.

Table 4.2 — Comparison of graphical measures for mean size.

	Mean	Standard Deviation	't' values			
			Mz1	Mz2	Mz3	Mz4
Mz1	2.868 ϕ	0.330				
Mz2	3.046 ϕ	0.246	1.381			
Mz3	2.987 ϕ	0.232	0.943	0.557		
Mz4	2.974 ϕ	0.246	0.822	0.661	0.123	
Mz	2.968 ϕ	0.290	0.726	0.655	0.182	0.050

Table 4.3— Comparison of graphical measures for standard deviation

	Mean	Standard Deviation	't' values			
			σ_1	σ_2	σ_3	σ_4
σ_1	0.271 ϕ	0.184				
σ_2	0.338 ϕ	0.141	0.923			
σ_3	0.365 ϕ	0.235	1.006	0.315		
σ_4	0.375 ϕ	0.268	1.022	0.390	0.090	
σ	0.366 ϕ	0.385	0.711	0.218	0.007	0.061

Table 4.4 — Comparison of graphical measures for skewness

	Mean	Standard Deviation	't' values		
			Sk1	Sk2	Sk3
Sk1	0.069	0.115			
Sk2	0.464	0.277	4.205 ^x		
Sk3	0.998	0.997	2.956 ^x	1.648	
Sk	0.496	0.222	5.479 ^x	0.288	1.569

x Significant at 5% level of significance.

Table 4.5 — Comparison of graphical measures for kurtosis

	Mean	Standard Deviation	't' values	
			Ku1	Ku2
Ku1	0.192	0.099		
Ku2	1.082	1.065	2.657 ^x	
Ku	1.800	0.865	5.897 ^x	1.671

x Significant at 5% level of significance.

't' values bring out that Sk1 and Ku1 values differ respectively from other measures of skewness and kurtosis significantly (at 5% level of significance) and they are consistently lower than other measures. However, there are no significant differences between different graphic measures estimating all the four parameters viz. mean size, standard deviation, skewness and kurtosis (at 5% significance level) provided Sk1 and Ku1 are not considered. Since formulae for Sk1 and Ku1 take into account very limited portions of the

distributions, these should not be used for estimating skewness and kurtosis. Though any of the graphic measures other than Sk_1 and Ku_1 could be used, yet the most efficient measures designated as Mz , σ , Sk , and Ku are used in further discussions.

4.2.6 Variation of Grain Size Parameters

This section describes variation in grain size parameters of samples analysed in the present study and compares them with similar studies made elsewhere.

To give an idea of dispersion, a term S-range of the parameter is used in the following pages. S-range is the calculated \pm one standard deviation of the parameter and not the counted one, as is done by Folk (1971a).

4.2.6.1 Mean Size

All the samples average about 2.97ϕ (0.13 mm, fine sand) with S-range from 2.78 to 3.26ϕ . Thus, these samples lie within typical dune size range as given by Udden (1898), Alimen (1957), and Chavaillon (1964). However, the Thar desert sands lie on the finer side of the dune range and many samples are even finer than generally described dune range.

Udden (1898) pointed out that dune crest sands tended to evolve towards fine sand size ($2-3\phi$) as this

was the favoured material for saltation load irrespective of the source from which material was available. The comparative finer nature of the sands of the Thar desert could be due to the lower velocities of the prevailing winds which are able to pick up finer material as saltation load. Also finer dust carried by the wind as suspension load may have got deposited and infiltrated to give overall finer nature to these sediments.

4.2.6.2 Sorting

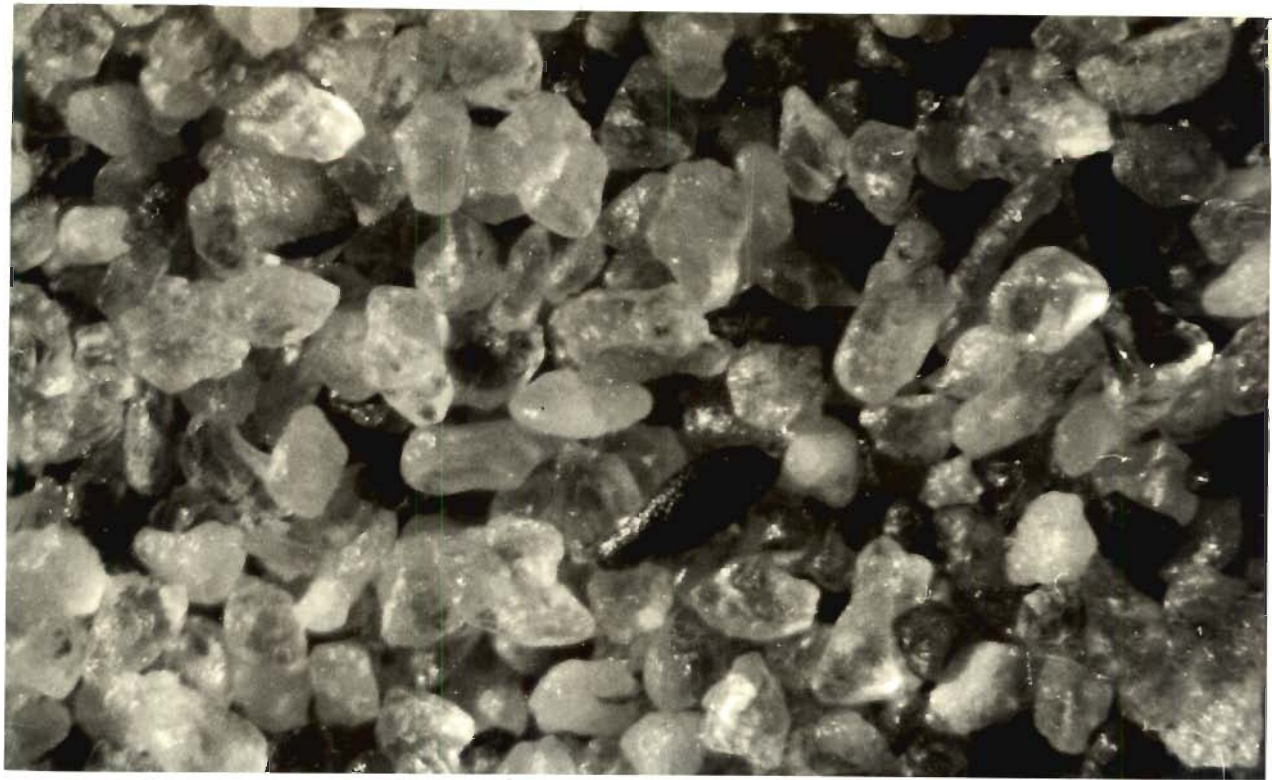
All samples give an overall mean standard deviation of 0.37 ϕ and S-range of 0.00 to 0.76 ϕ , and are classified as well to moderately well sorted. Thus, it is obvious that inland desert dunes are more poorly sorted than the average beach dunes. However, the range of standard deviation is approximately the same, or slightly smaller, than that for beach dunes (Friedman, 1961; Moiola and Weiser, 1968).

A study of the photomicrographs and cumulative frequency curves of typical samples of the area (Figs. 4.35-4.38) shows that sorting seems to be a function of the ratios in which two or more sub-populations are mixed.

4.2.6.3 Skewness

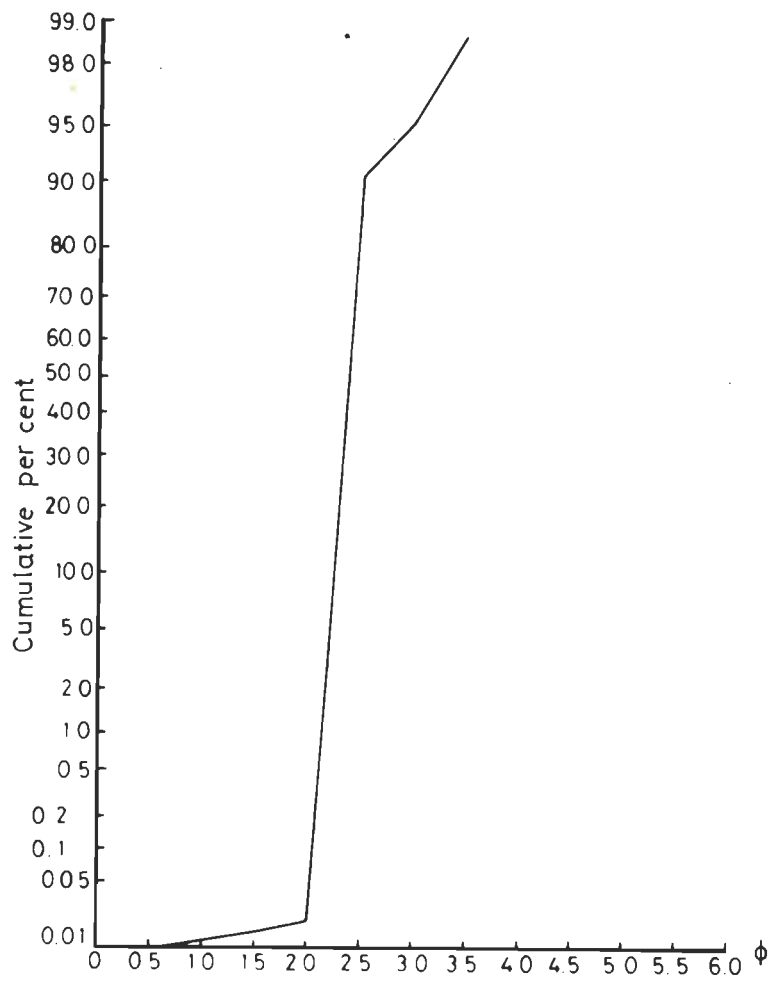
All sand samples except three are positively skewed. The mean value is +0.50 and S-range 0.28 to 0.72. Common skewness range is from 0.05 to 0.7.

Fig. 4:35_Photomicrograph (A) and cumulative frequency curve (B) for sample 63. The sample is from a sand pile. It has a mean size of 2.80ϕ and shows good sorting ($\sigma = 0.170 \phi$).



(A)

Reflected light (X140)



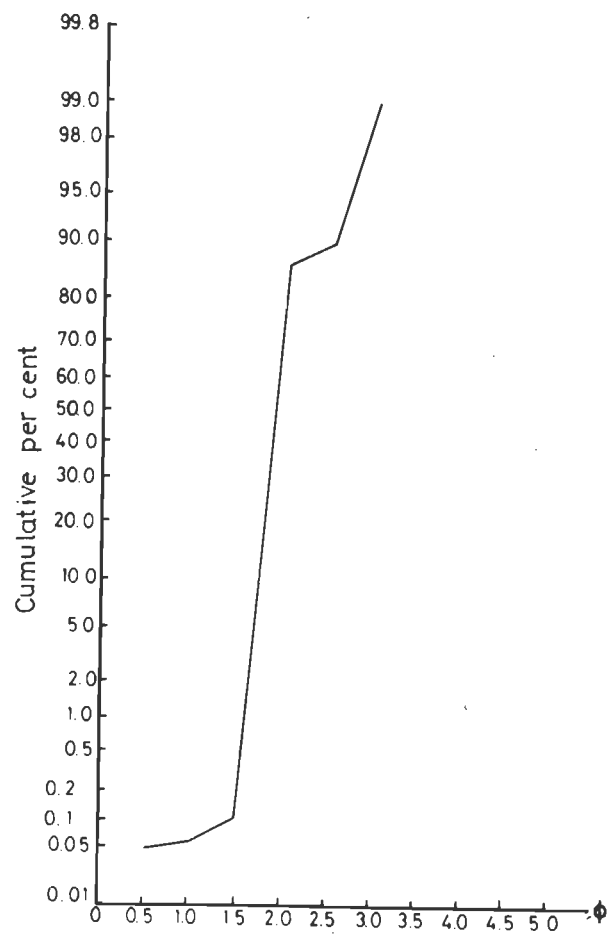
(B)

Fig.4.36_Photomicrograph (A) and cumulative frequency curves (B) of sample 103. The sample is from a barchan having a mean size of 3.00ϕ . It shows good sorting ($\sigma=0.25 \phi$).



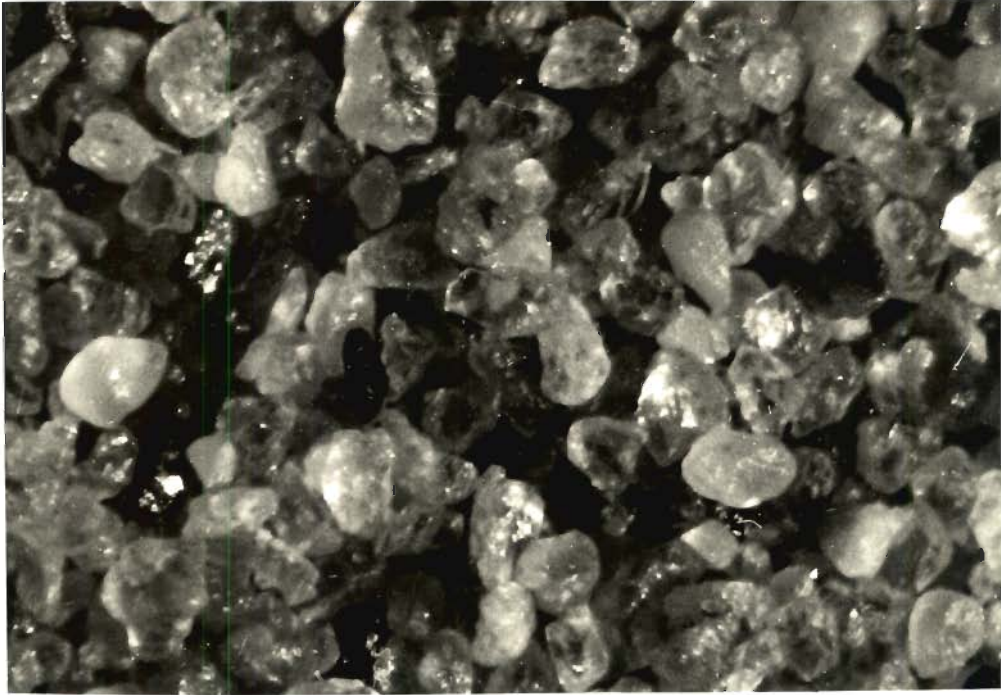
(A)

Reflected light (X140)

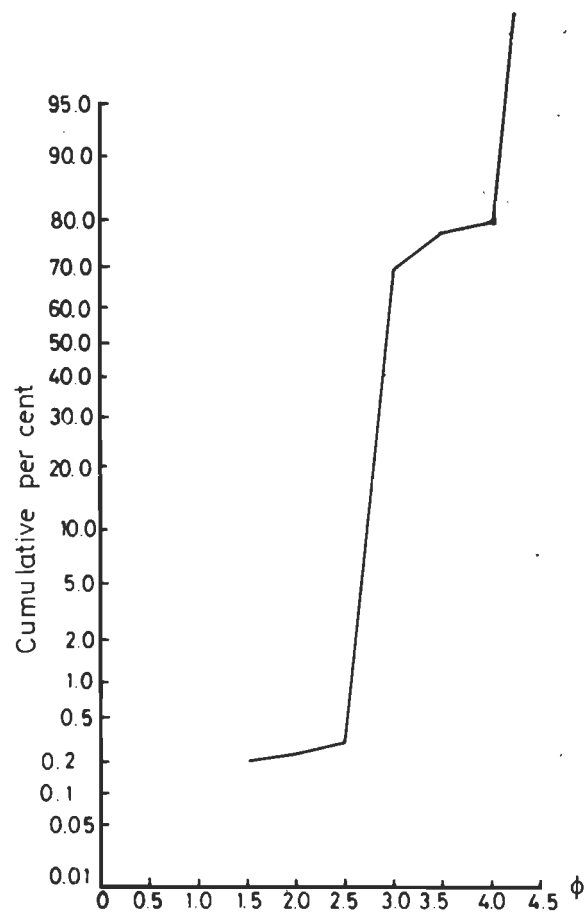


(B)

Fig.4.37_Photomicrograph(A) and cumulative frequency curve(B) of sample 77. The sample is from windward side of a barchan. It has a mean size of 3.12ϕ and shows moderate sorting ($\sigma=0.45 \phi$).

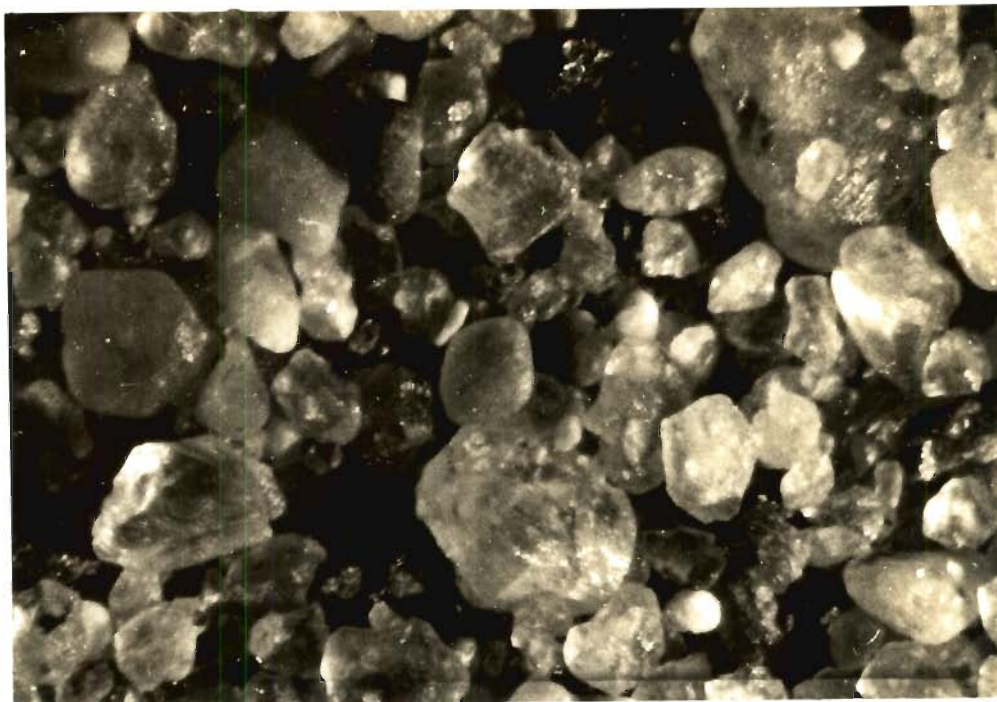


(A) Reflected light (X140)

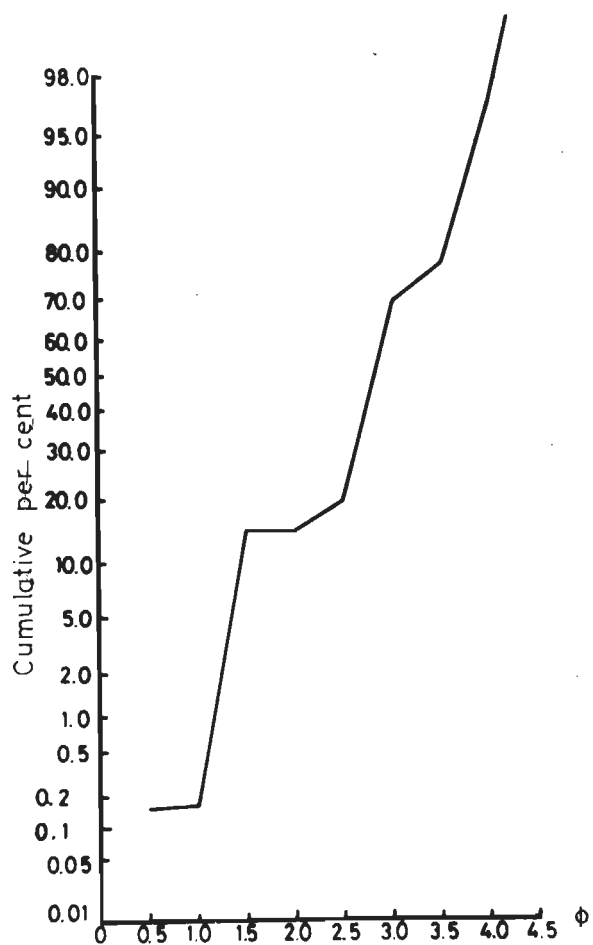


(B)

Fig.4.38_Photomicrograph (A) and cumulative frequency curve (B) of sample 2 collected from the trough of a ripple. It has a mean size of 2.78ϕ and shows poor sorting ($\sigma = 0.71 \phi$).



(A) Reflected light (X140)



(B)

The strong positive skewness of desert dunes is probably produced by the abundance of fines derived from alluvial source. Also it has been emphasized by Friedman (1967) and Folk (1971a) that skewness is a function of the depositing current. In the deposits, where fluid remains in contact with the bed, for example beach sands, the sediments tend to be symmetrical or even negatively skewed. But in those deposits where the current leaves the bed such as leeward side of dunes in streams or deserts, the sediments tend to be positively skewed since they receive fines from suspension which get buried by the advancing avalanche face.

Moiola and Weiser (1968) found that inland dunes had slight negative to positive skewness (-0.3 to +0.35) whereas beach dunes were near symmetrical. Differences of desert sands from beach dune sands can be explained by the fact that the latter are derived from beach sources which are deficient in fine material, a fact consequently reflected in their grain size distribution. On the other hand, inland dunes are usually derived from alluvial sediments which have abundant fine material in the form of levee, flood plain and lake deposits.

4.2.6.4 Kurtosis

The kurtosis values range from 0 to 3.6. There are two groups of samples. One group has values from 1.7 to 2.45 i.e. of very leptokurtic nature suggesting the presence of

coarse and fine tails. The other group has values from 0.0 to 0.8 forming platykurtic distributions. These reflect probably bimodal distributions with two equal and widely separated modes. Usually sand piles are platykurtic and dunes are leptokurtic, though there is a fair overlap of kurtosis values of the two bedforms.

In comparison to the present studies, sands of seifs of Australian Simpson desert were mesokurtic with an average kurtosis of 1.04 (Folk, 1971a). Skocek and Saadallah (1972) found Iraqi desert sands to have kurtosis from 0.58 to 1.62 with a maximum concentration of values between 0.5 to 1.1. Kurtosis values of inland dunes of Moiola and Weiser (1968) were uniformly distributed between 0.8 and 1.45 whereas their coastal dunes had much smaller range i.e. from 0.9 to 1.25.

4.2.7 Parametric Interrelationships

Processes leading to variation of grain size statistical parameters can be best analysed by studying their interrelationships. For this purpose, five scatter plots between the four parameters have been prepared (Figs. 4.39-4.43) and discussed below.

4.2.7.1 Mean Size Versus Sorting

The plot of mean size versus sorting (Fig.4.39) shows a strong correlation between the two parameters. With the decrease of grain size, sorting gets worse. Points lie around

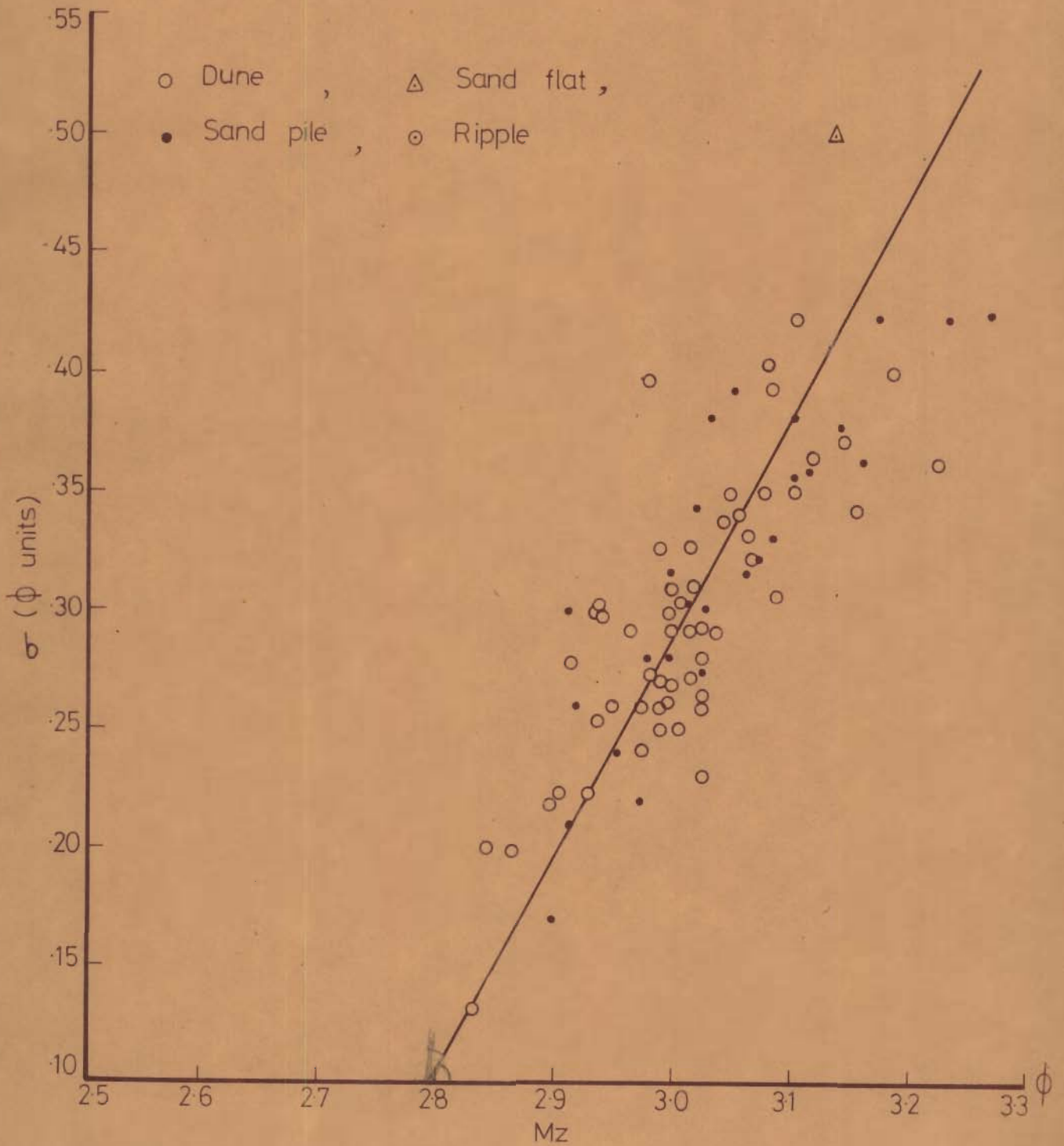


FIG.4.39_ VARIATION OF σ WITH Mz .

a line that makes an angle of about 45° with the mean size axis suggesting that grain size distributions are mixtures of two populations in different proportions (Folk, 1971a).

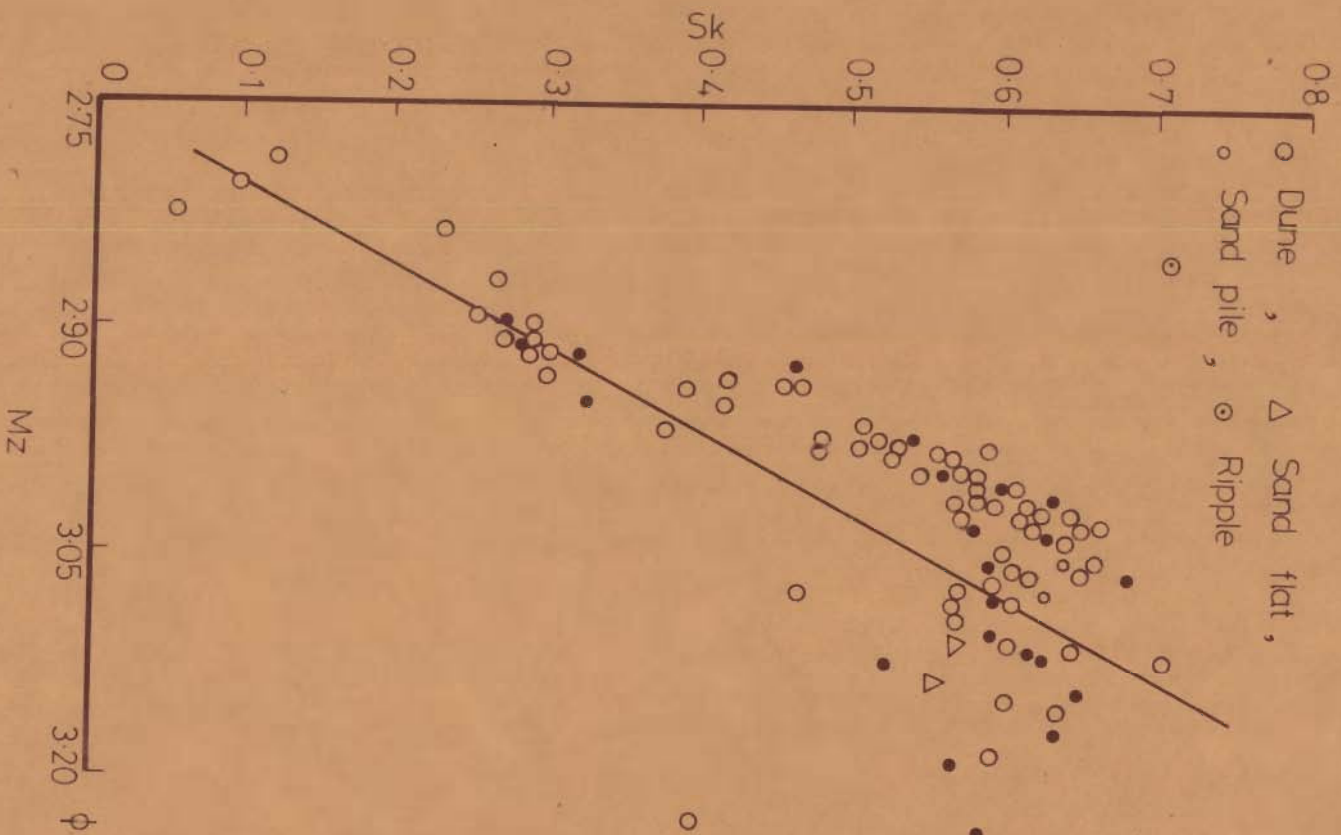
Folk (1971a) found that there is no significant relationship between the mean size and sorting in seif sands of Simpson desert. A similar sorting versus mean size trend has been found for aeolian sandstones in Iraq by Philip et al. (1968) and aeolian sands by Skocek and Saadallah (1972, Fig.5).

Folk and Ward (1957) found a sinusoidal trend in fluvial sediments in plots of mean size versus sorting and concluded that sands were mixtures of three populations with mean sizes in pebbles, fine sand and clay fractions. In the mean size range observed in the present investigation, Folk and Ward (1957) did find a similar relationship between mean size versus sorting.

4.2.7.2 Mean Size Versus Skewness

Covariate plot between mean size and skewness (Fig.4.40) brings out clearly a distinct overall trend in the plotted samples i.e. with a decrease in grain size the samples become more positively skewed thereby suggesting that samples are simply mixtures of two populations. With the addition of finer tail, samples become positively skewed as proposed earlier.

Folk (1971a) found that finest samples were negatively



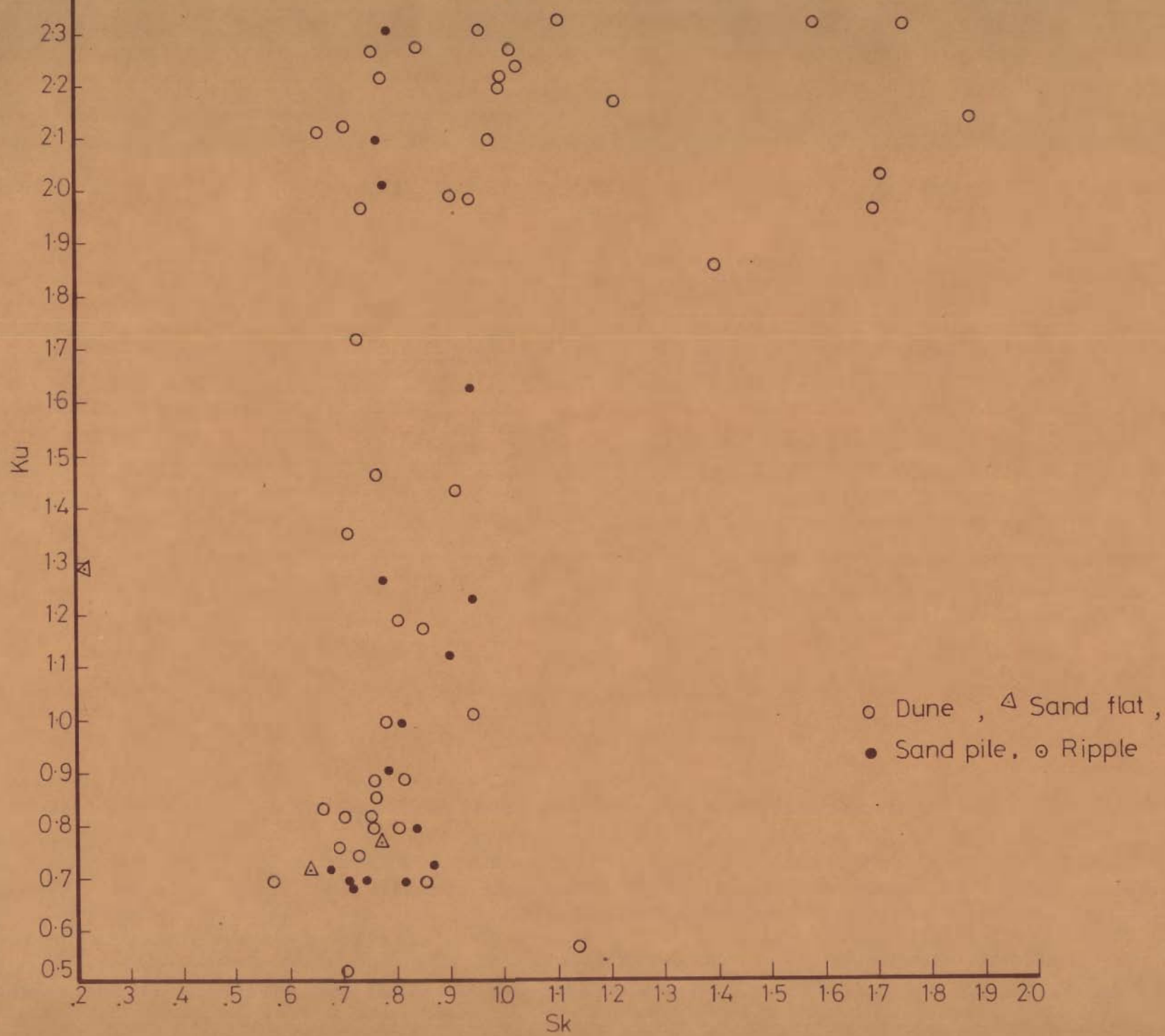
skewed ($Sk \approx -0.15$ at $Mz = 3.1 \phi$) and coarsest being most positively skewed (about $+0.30$ at $Mz = 2.4 \phi$). Samples with mean size of about 2.9ϕ have skewness close to zero. Thus, there are two major differences between the two studies. General trend of increase of skewness value with increase in grain size in Folk's (op.cit.) samples is opposite to that observed in the present investigation. Also, within the observed mean size range of most of the samples (2.6ϕ to 3.2ϕ), we have commonly positive skewness rather than negative or near symmetrical distributions as observed by Folk (1971a).

4.2.7.3 Skewness Versus Kurtosis

Evidently there is no trend in the scatter diagram of skewness versus kurtosis (Fig.4.41), but for the fact that for skewness values between 0.5 and 1.2, kurtosis values show a very wide range i.e. from 0.5 to 2.5 and for skewness values larger than 1.2, kurtosis values have a small range of 1.8 to 2.5.

4.2.7.4 Mean Size Versus Kurtosis

There is a distinct relationship between kurtosis and mean size values (Fig.4.42). Kurtosis values tend to decrease with decrease in grain size. Samples with mean sizes, between 3.0ϕ and 3.05ϕ , are mesokurtic. Grain size distributions with mean size coarser than 3.0ϕ , tend to be more leptokurtic with increase in mean size, though there is



a wide scatter of points around the main trend. Samples with mean size finer than 3.05ϕ tend to become distinctly more platykurtic with decrease in mean size.

4.2.7.5 Sorting Versus Skewness

A definite relationship between standard deviation and skewness in Figure 4.43 is probably a reflection of the fact that both these variables are strongly correlated with mean grain size and values of these parameters increase with decrease in mean grain size.

4.2.8 Variation of Grain Size in Different Bedforms and Sand Flats

Summary statistics i.e. mean and standard deviation of the grain size parameters for the different bedforms and sand flats are listed in Table 4.6. Bar diagrams showing distributions of grain size parameters in relation to bedforms and sand flats are shown in Figures 4.44 and 4.45. Most of the samples are from sand piles and dunes. Number of samples from sand flats and ripples are limited (only 7) for comparison purposes. Comparison of the average values of grain size parameters for different bedforms and sand flats, in conjunction with analysis of their distributions in bar diagrams (Figs. 4.44, 4.45), brings out some interesting results. Ripples are the coarsest grained, worst sorted and have near symmetrical distribution. Sand piles tend to have more often finer size than dunes (Fig. 4.44), though the average

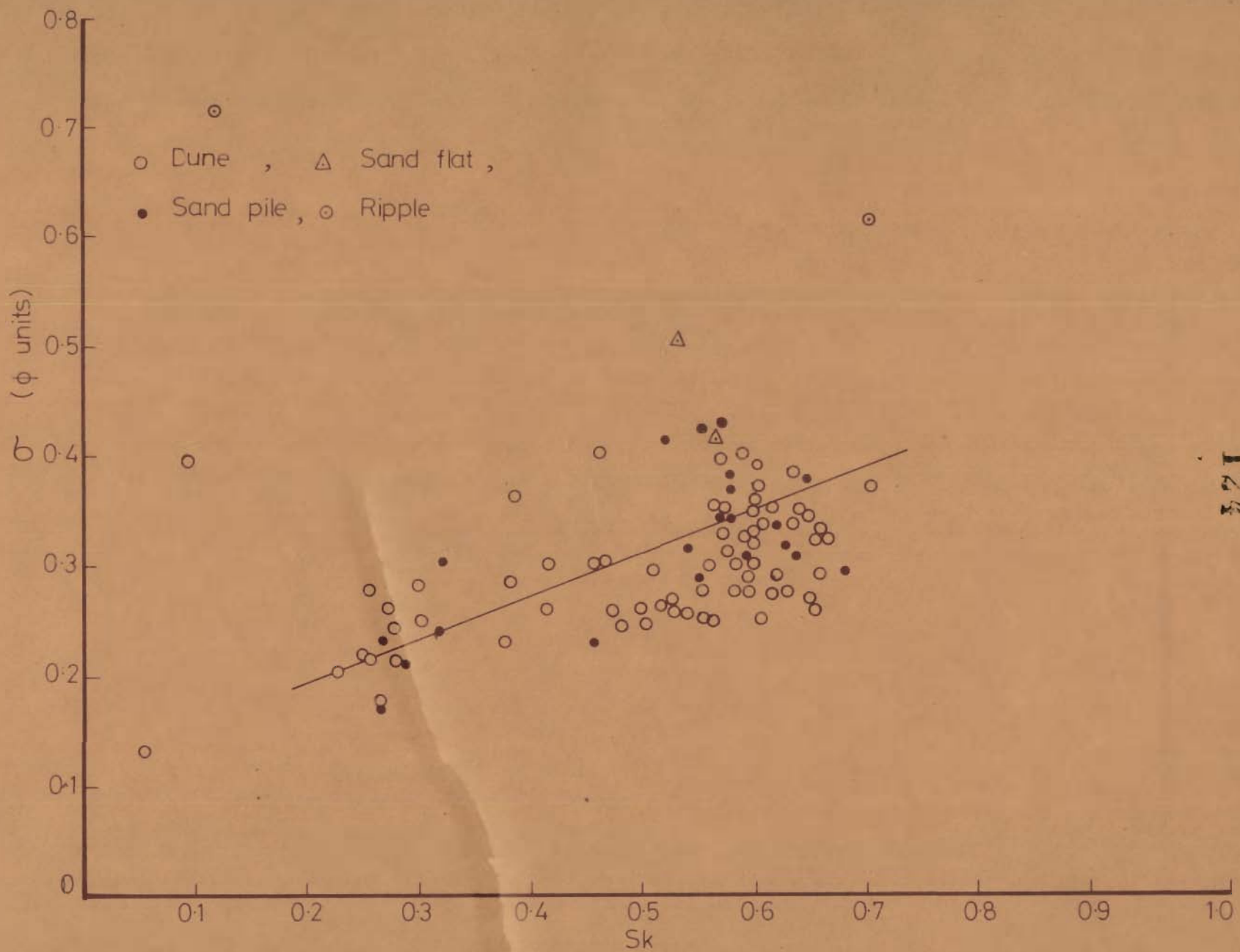


FIG.4.43_VARIATION OF σ WITH Sk .

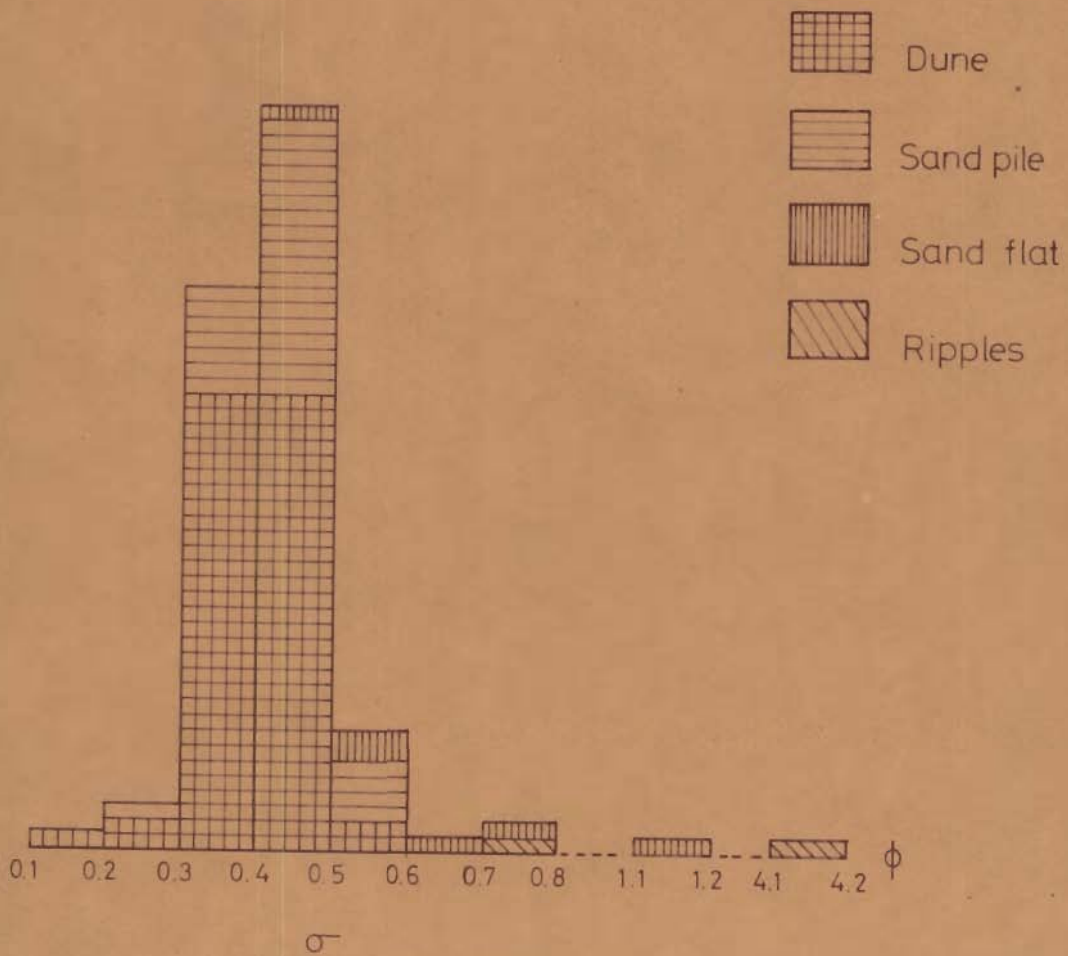
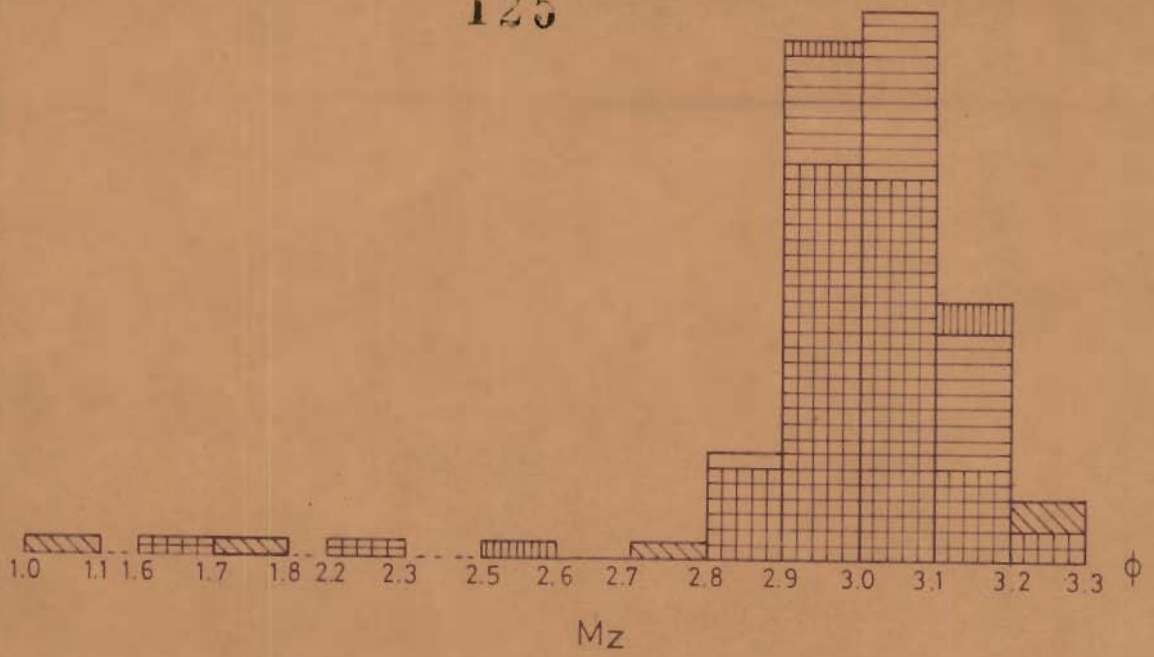
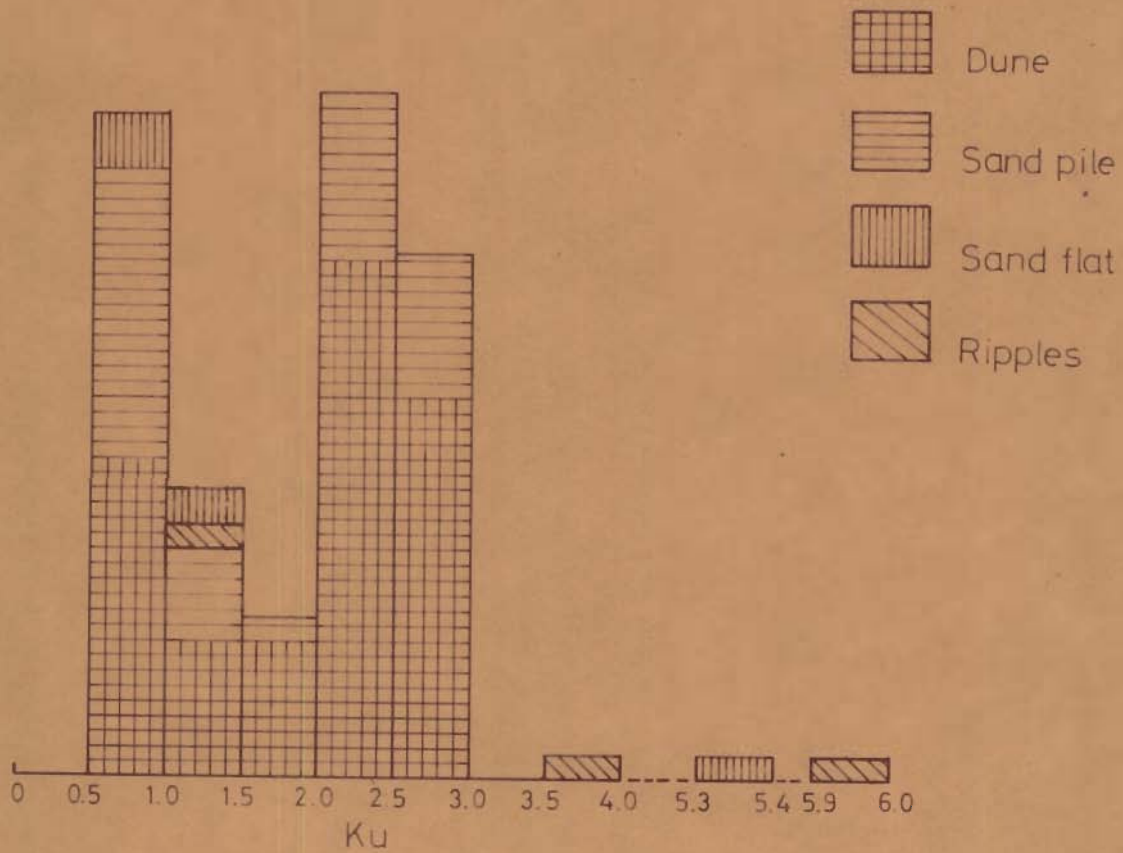
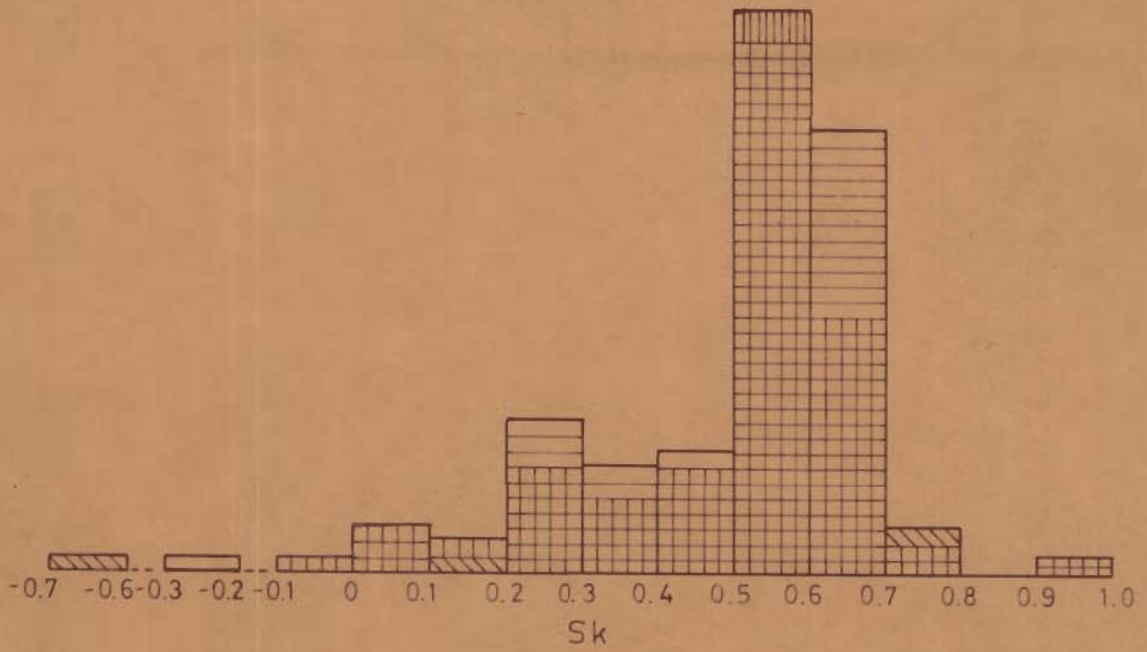


Fig.4.44_ Bar diagrams showing distributions of mean size Mz and standard deviation σ in different bedforms and sand flats.







-  Dune
-  Sand pile
-  Sand flat
-  Ripples

Fig.4.45. Bar diagrams showing distributions of skewness Sk and kurtosis Ku in different bedforms and sand flats.

mean size of sand piles is only slightly finer than that of dunes. Also sand piles tend to have larger standard deviation and skewness values than dunes. Kurtosis values for sand piles are distinctly smaller than those for dunes, though these are leptokurtic in nature for both the bedforms.

Table 4.6 — Variation of grain size parameters in the various bedforms and sand flats

No. of observations	Sand flats		Bedforms					
			Ripples		Sand Piles		Dunes	
	4		3		31		66	
Grain size parameter	Mean	s.d.	Mean	s.d.	Mean	s.d.	Mean	s.d.
Mean size M_z	2.9450	0.255	1.8710	0.874	3.0600	0.096	2.9770	0.203
Standard Deviation σ	0.2920	0.813	0.4990	0.400	0.3310	0.065	0.2990	0.274
Skewness Sk	0.316	0.734	0.098	0.761	0.521	0.187	0.515	0.174
Kurtosis Ku	2.026	2.209	3.591	2.315	1.528	0.815	1.907	0.735

s.d.- Standard deviation.

4.2.9 Variation of Grain Size Parameters within Barchan Dunes

Variation of grain size within barchan dunes has been studied by collecting six or seven samples from each of four representative dunes at Sam and Dhanana. In Figures 4.46-4.49, the various grain size parameters have been plotted against the normalised heights of dunes taking the maximum heights of dunes as units. With the increase in height, there is an increase in mean grain size (Fig.4.46). Also sorting improves

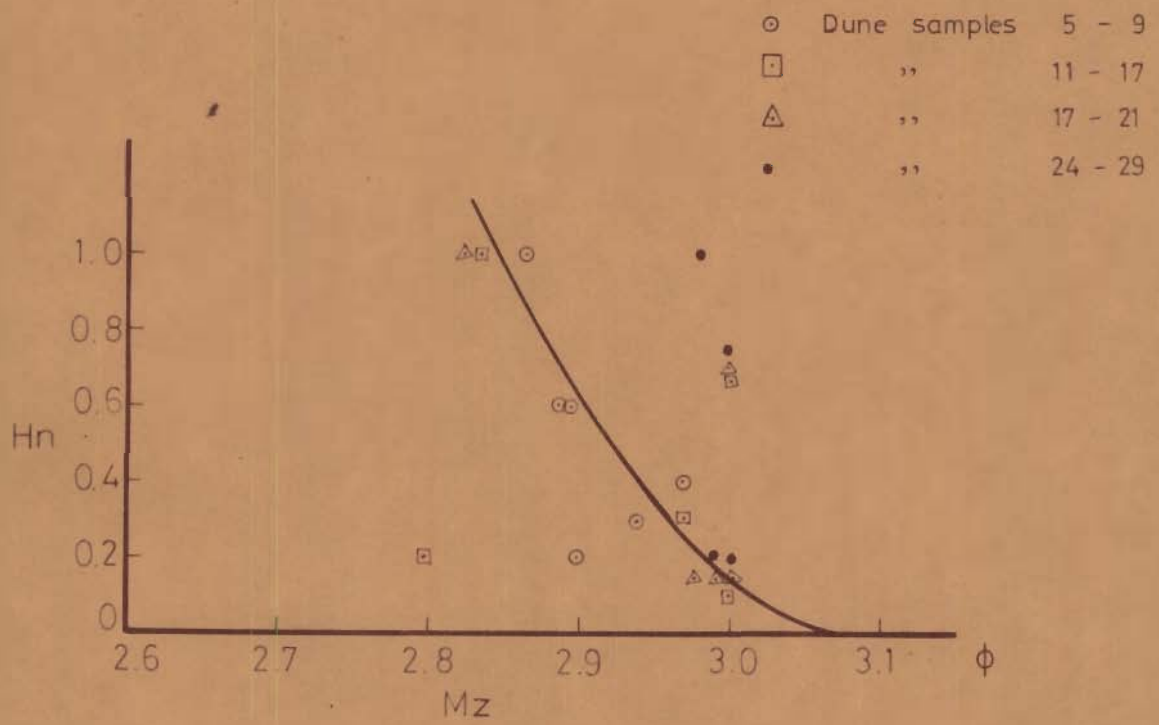


Fig.4.46_Variation of mean size with normalised height in barchans.

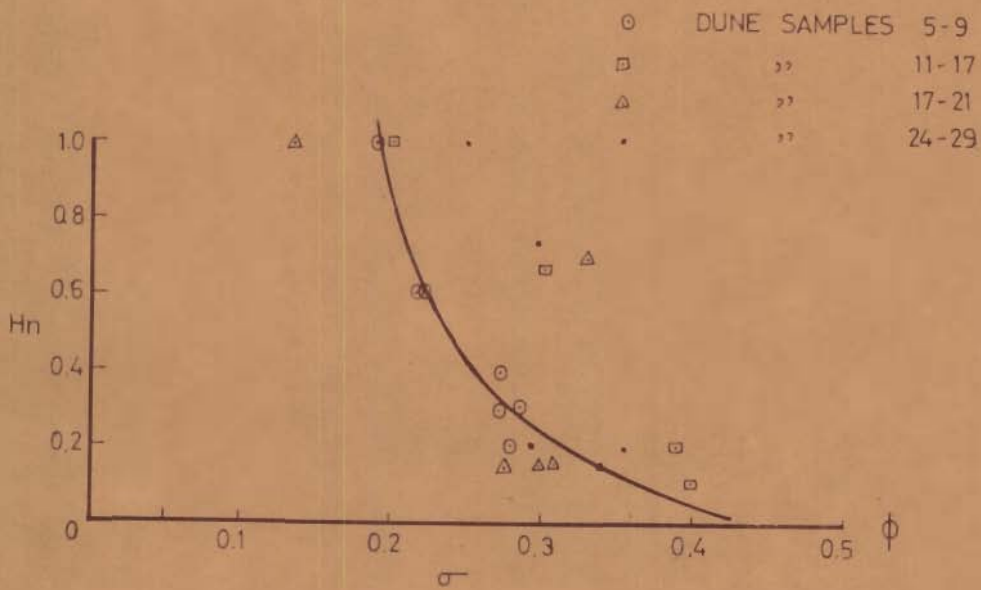


Fig.4.47-Variation of standard deviation with normalised height in barchans.

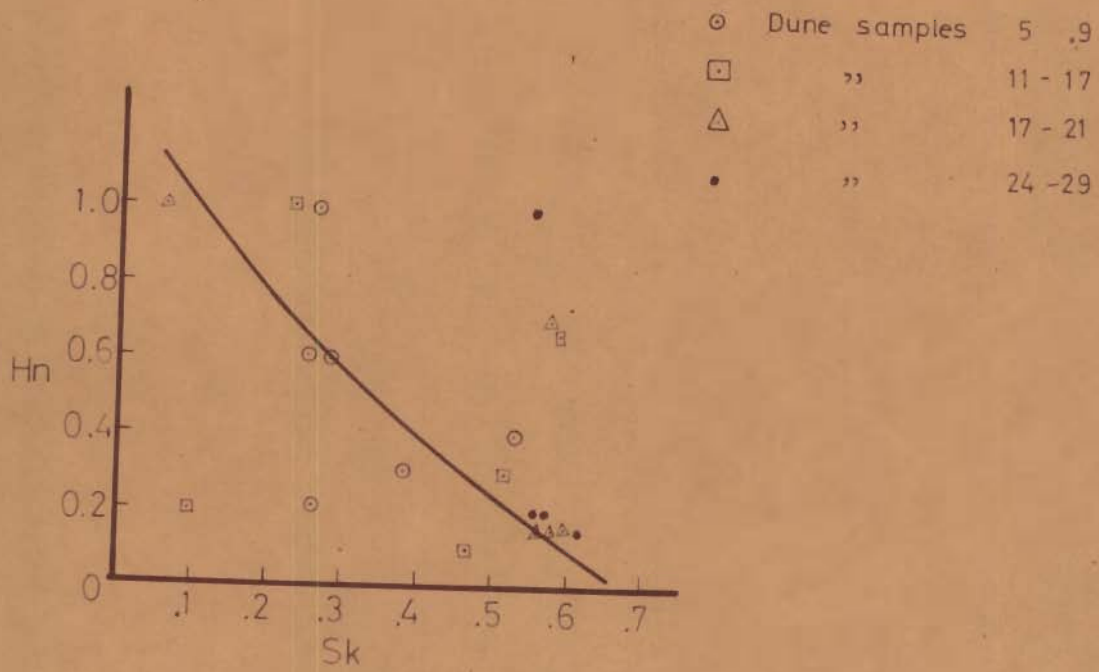


Fig.4.48__ Variation of skewness with normalised height in barchans.

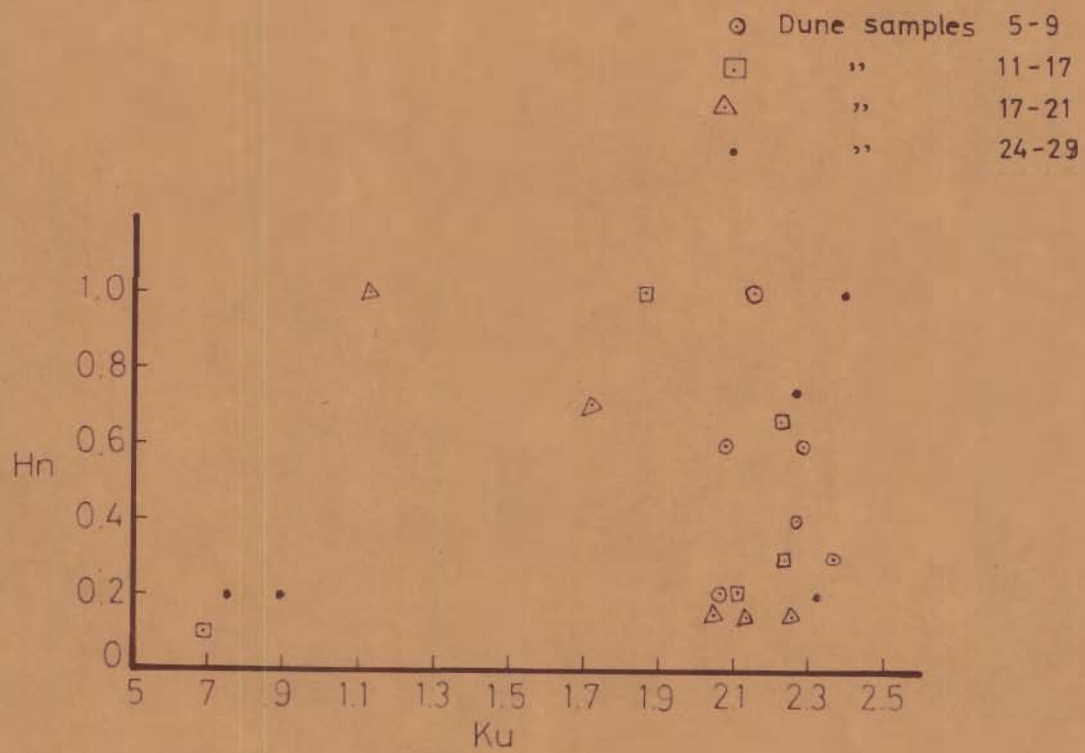


Fig.4.49 - Variation of kurtosis with normalised height in barchans.

with height (Fig.4.47). Sediments are more positively skewed at the foot of the dunes and they get progressively less skewed as one moves towards the crest where they become almost symmetrical (Fig.4.48). Sands show no simple linear relationship between kurtosis and the height of dune (Fig.4.49). Also it has not been possible to detect any significant difference between samples from windward and leeward sides of dunes.

Dunes with crests coarser than the substrata have been described by Alimen (1953), Simonett (1960) and Skocek and Saadallah (1972). However, Richardson (1903, in Folk, 1971a) recorded coarsest size at the toe of leeward side of the dunes as the coarser grains rolled over the finer grains. Wait (1969, in Folk, 1971a) found no difference in mean size of dune crests and interdune flats, but crests were better sorted with positive skewness and more normal kurtosis. Mohan and Puri (1976) have reported that dunes are better sorted than interdune flat areas and also have positive skewness as compared to negatively skewed nature of the flat areas.

4.2.10 Spatial Variation of Grain Size Parameters

Taking the maximum values of grain size parameters of all the samples from barchans and sand piles, the area under investigation was contoured for the different grain size parameters. It may be emphasized that there is a fairly wide variation of grain size parameters within individual bedform and the ideal

procedure for a study of spatial variation of grain size parameters would be to take samples from the same bedform and at similar location on the bedform. However, a particular bedform may not be present in all the areas of interest. To overcome this difficulty, two closely related bedforms i.e. barchans and sand piles were used for study of spatial variation of grain size parameters.

Variation in mean size shows that there are two highs — one near Sam and the other near Lunar (Fig.4.50). The shape of the high near Lunar is circular, whereas, that of one near Sam is elongated in NE-SW direction, which is also the prevailing wind direction.

Sorting and skewness show systematic changes closely related to mean size (Figs.4.50 and 4.52). Standard deviation and skewness increase in value with decrease in grain size.

Kurtosis values decrease from 2.8 from a point near Lunar outwards to a value of 2.0, and there is a probable increase from 0.8 to 1.6 in a contour trough, elongated in the NE-SW direction in the area around Dhanana-Sam road (Fig.4.53).

No similar studies of spatial variation of grain size parameters in deserts are available for comparison, except that a limited study of areal variation of grain size parameters of cover sands of Botswana was made by Baillieul (1975) by taking a few traverses. According to him variation of

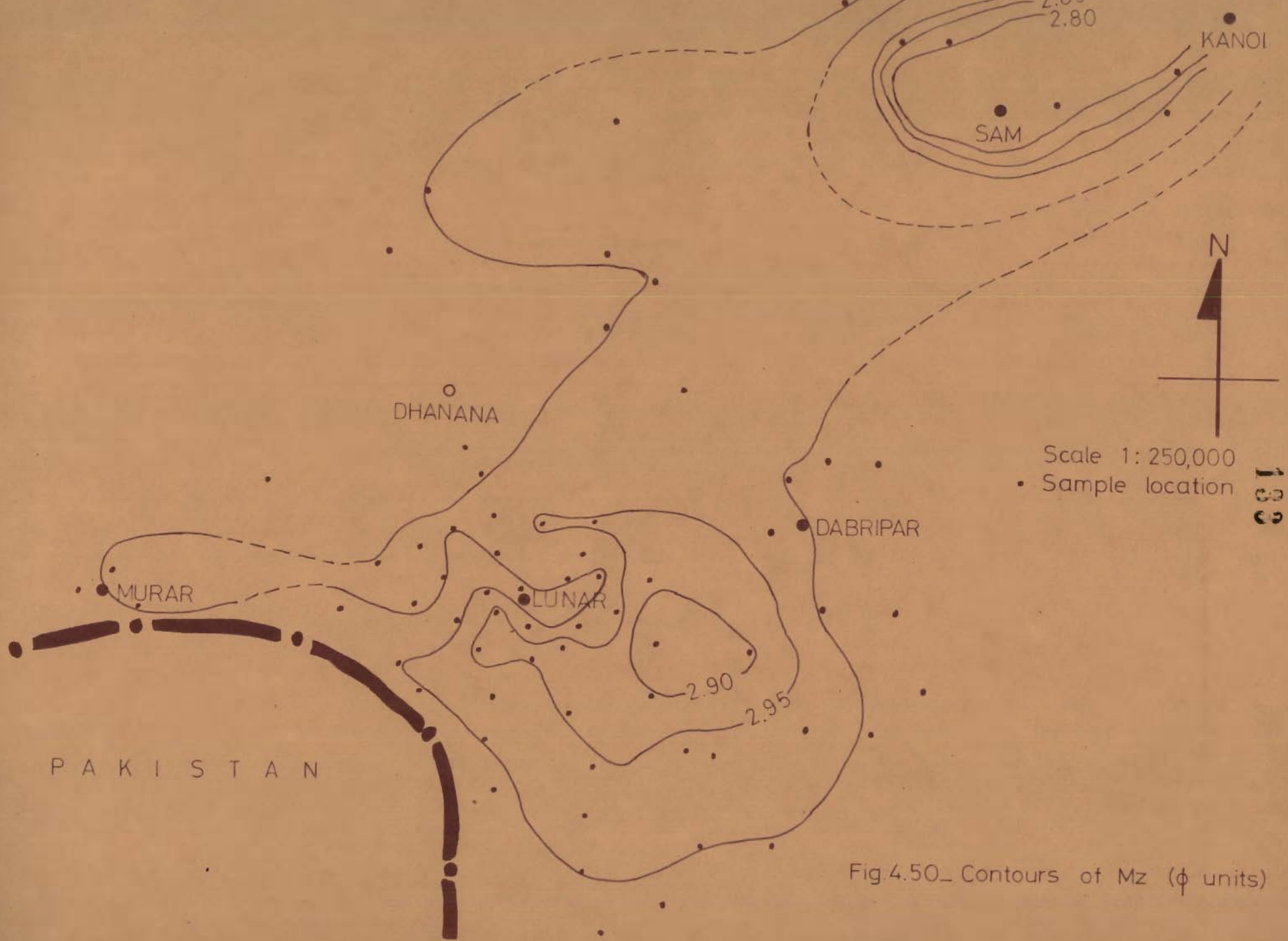


Fig 4.50_ Contours of Mz (ϕ units)

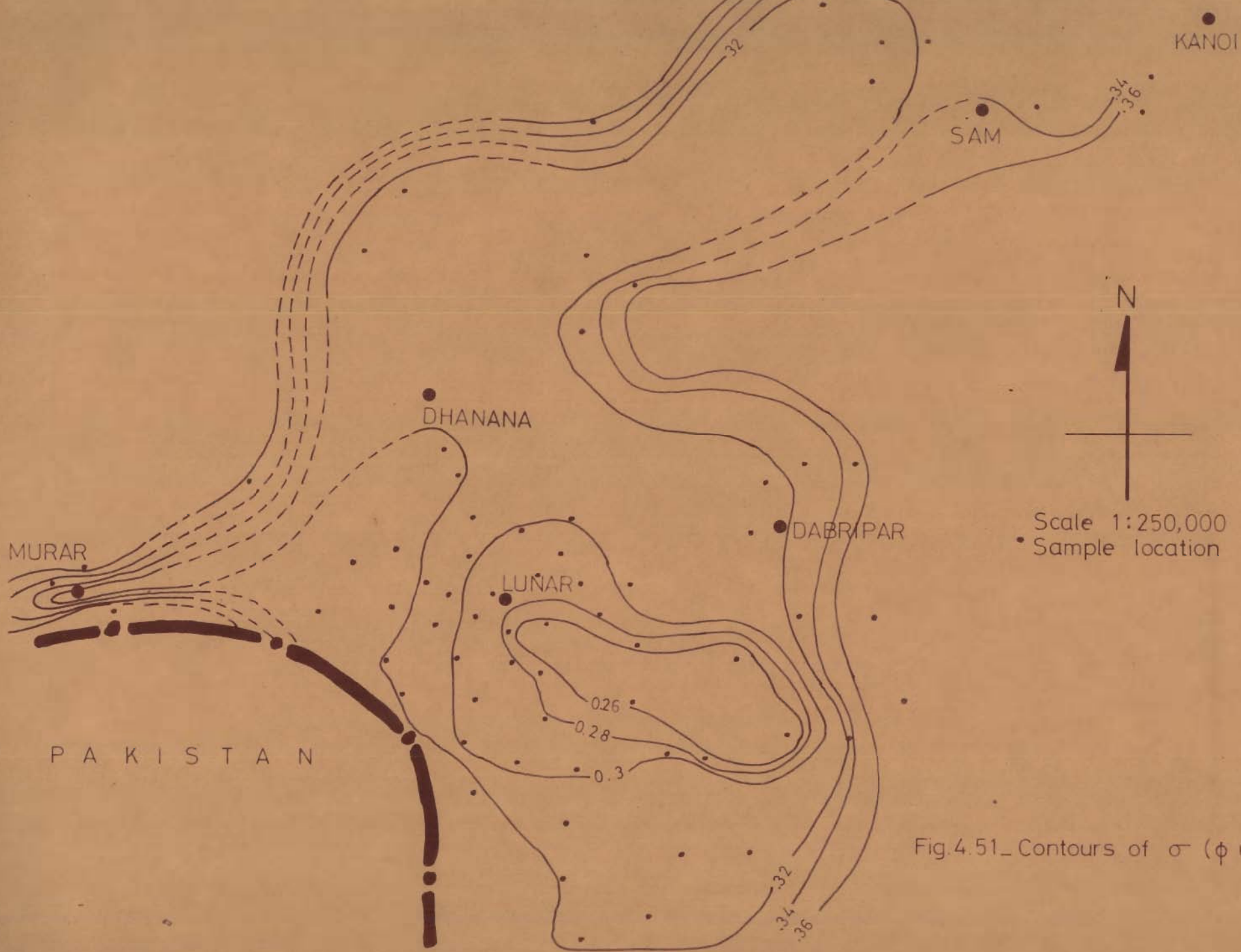


Fig.4.51_ Contours of σ (ϕ units)



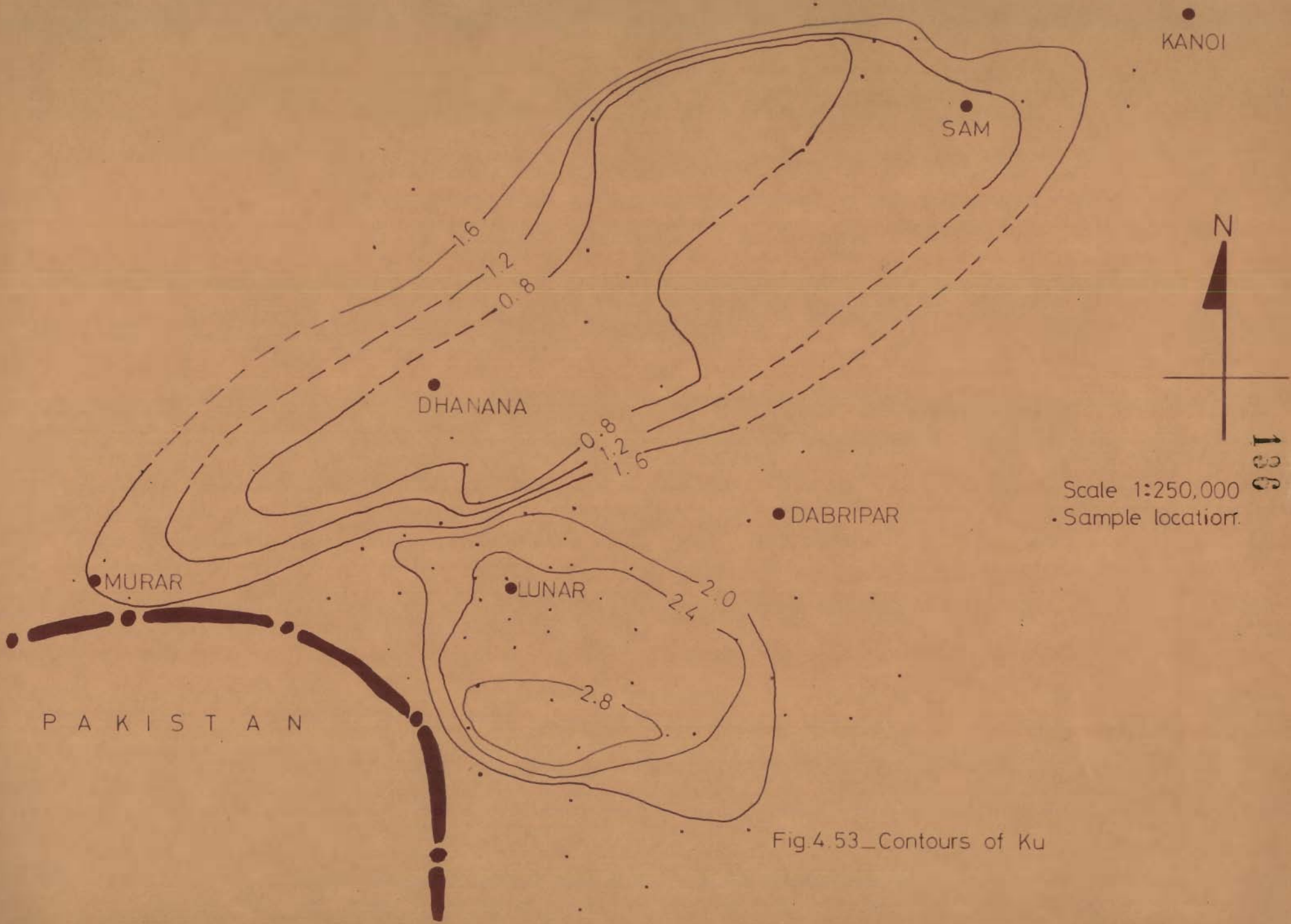


Fig.4.53_Contours of Ku

grain size parameters reflects the nature of local sources of sediments.

Systematic variations of mean size, sorting and skewness are the result of mixing, in different proportions, of saltation and suspension populations of grain sizes carried by the wind as explained in section 4.2.12. However, the presence of highs in mean size near Lunar and Sam are not clearly understood. At Sam, dunes form a large field in a flat area. The presence of the maximum size in the centre probably suggests that recycling of sediments by aeolian transportation has been carried to the highest degree and these have been winnowed out of suspended sediment. In Lunar area, systematic areal variation in grain size parameters, is probably a reflection of areal grain size distribution of the older deposits which have been moulded by the wind into different bedforms.

4.2.11 Evaluation of Grain Size Parameters for the Recognition of Desert Environments

In recent years, many workers have tried to use grain size parameters for characterizing the various depositional environments (Passega, 1957, 1964; Sahu, 1964; Moiola and Weiser, 1968; Friedman, 1961, 1967; Buller and McManus, 1972). In the present study, an attempt is made to evaluate the usefulness of some of these diagrams in characterizing aeolian sediments.

4.2.11.1 Metric Based System of Buller and McManus (1972)

Metric based analysis has been suggested by Buller and McManus (1972) for distinction of aeolian, fluviatile, beach and quiet water deposits. Median-Md (mm) and Trask's quartile skewness 'Ska' were plotted against Trask's quartile deviation 'QDa' on double log papers for the four environments (Figs.4.54-4.56). On each plot, the curves indicate a linear trend. The position and slope of the individual curves are different for different environments. Gradient of each curve was thought to reflect some environmental characteristic relating size to sorting i.e. viscosity and current strength. In the plot of 'QDa' versus Md(mm), there is a decrease of gradient of curves in the sequence aeolian, fluviatile, beach and quiet water deposits and in the plot Ska versus Md(mm), there is a decrease of gradients of the curves in the reverse sequence.

Md, QDa and Ska in mm were determined using the cumulative frequency curves and the values are listed in Appendix VIII.

Plots of samples of the Thar desert in QDa-Md diagram form a very thin almost vertical band (Fig.4.54) indicating that median size range is very narrow in the samples under study, whereas sorting varies fairly widely. Also fairly large number of samples fall outside the aeolian field of Buller and McManus (1972). Plots of samples in Ska-QDa diagram (Fig.4.56) brings out clearly that most of the samples fall outside the aeolian field of Buller and McManus. Gradient of

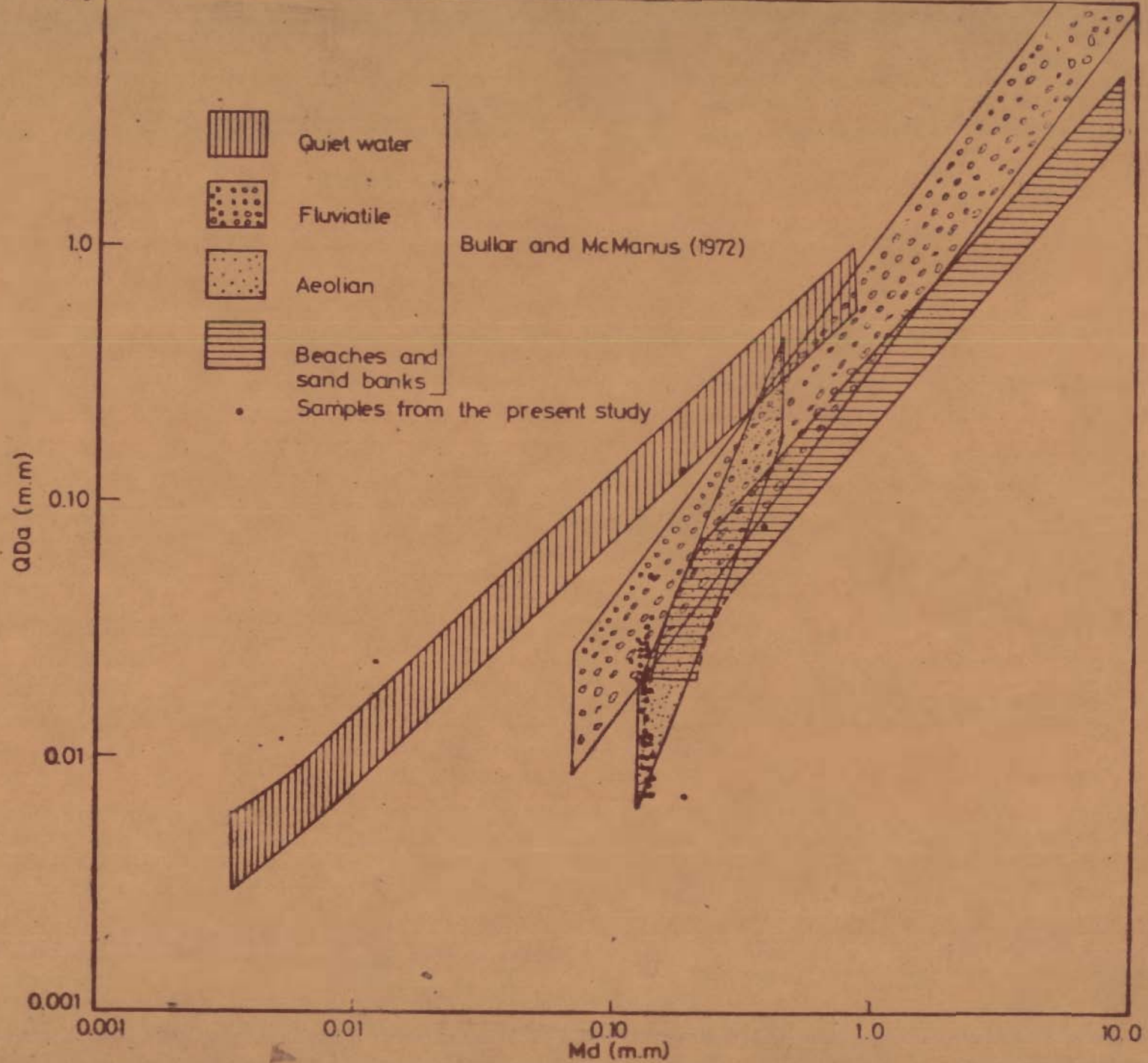


Fig.4.54 - Plot of samples from the present study on Md - QDa diagram of Bullar and McManus (1972)

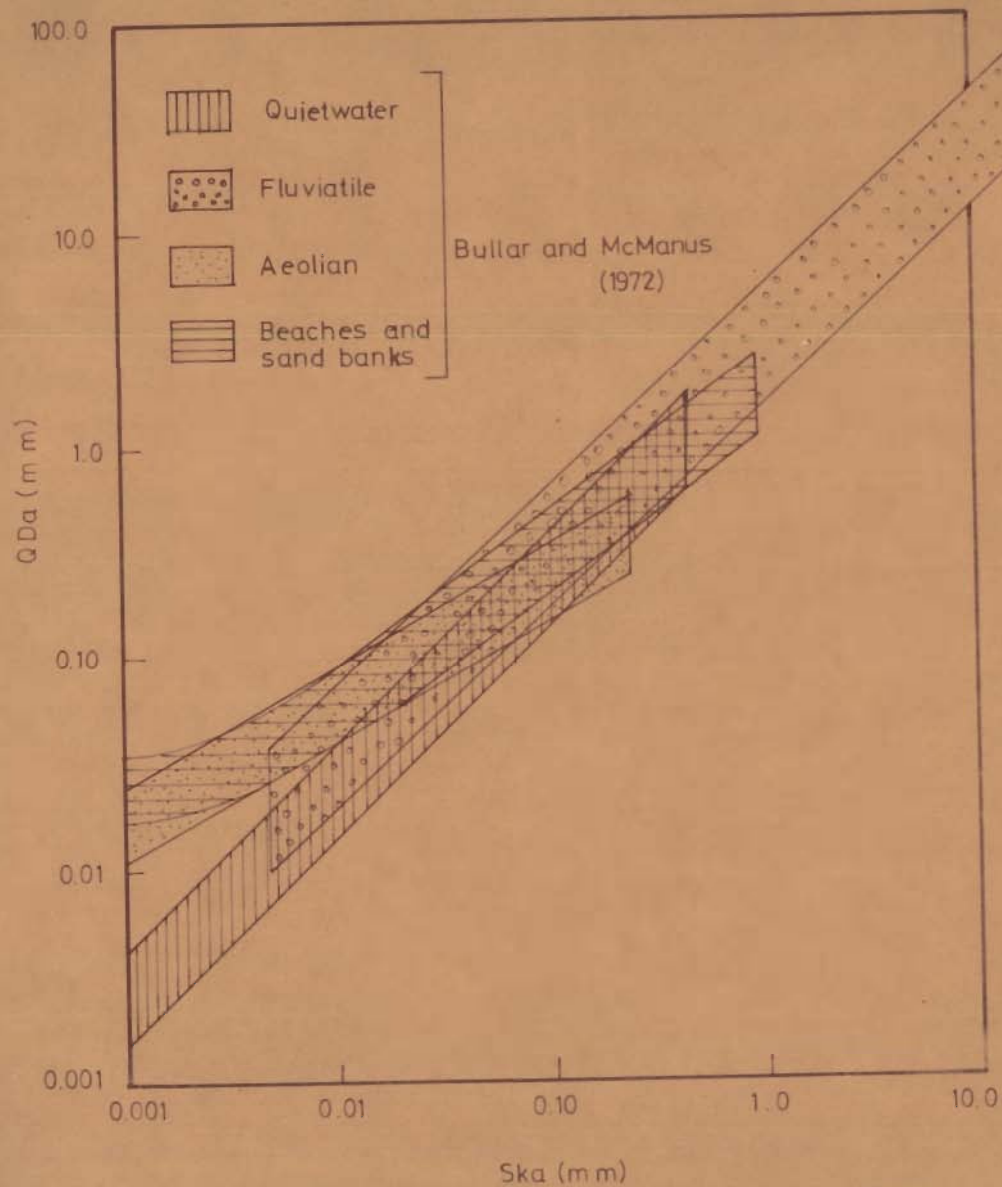


Fig.4.55_Ska_QDa diagram of Bullar and McManus (1972)

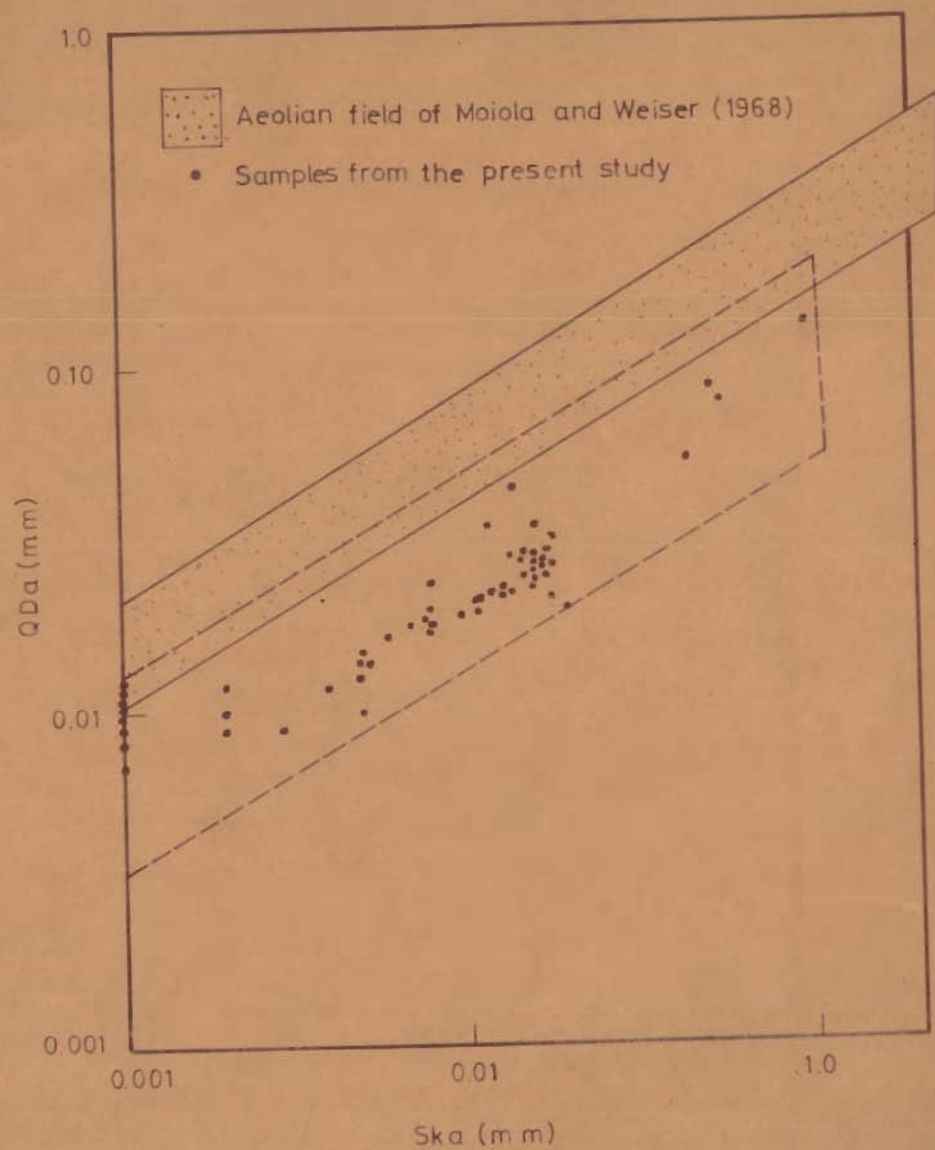


Fig.4.56_Plot of samples from the present study on Ska_QDa diagram. Dotted line marks the boundary of the samples.

the field of samples under investigation is similar to that of Buller and McManus with the difference that we have consistently lower QDa values. Thus the type aeolian field should be widened to accommodate the present samples.

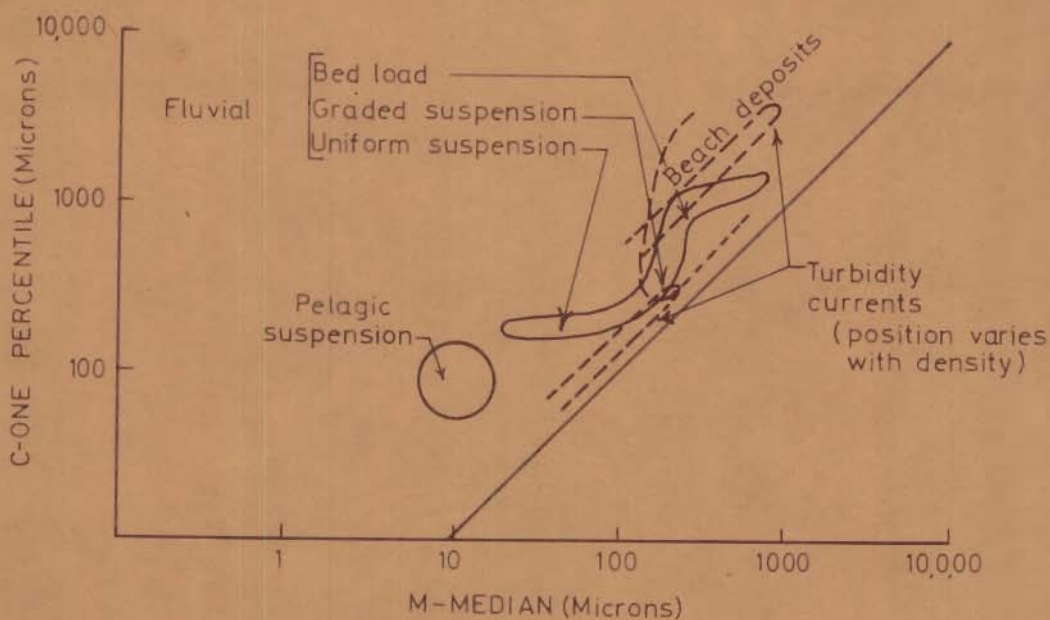
In conclusion, usefulness of the QDa-Md diagram is doubtful, but Ska-QDa diagram may prove quite helpful with minor modification in destinction of aeolian sediments.

4.2.11.2 C-M Pattern

Passega (1957, 1964) used two parameters obtained from grain size distribution curves i.e. C-coarsest one percentile and M - the median grain size. He obtained patterns for deposits of tractive currents, ~~quiet~~ water, beaches and turbidity currents (Fig. 4.57a). These parameters were selected because the coarsest fraction of a sediment is supposed to be more representative of the depositional agent provided that a full range of grain sizes was available for transportation.

It is realized that samples of the Thar desert are not strictly comparable to those studied by Passega (Op.cit) as his samples are from water borne sediments. However, the pattern of these sediments might give some insight into the process of deposition of the present sediments. Plots of samples of the Thar desert are concentrated in a vertical band with a median diameter ranging from 110 to 190 μ and C aranging from 130 to 800 μ suggesting that sand samples

(a)



(b)

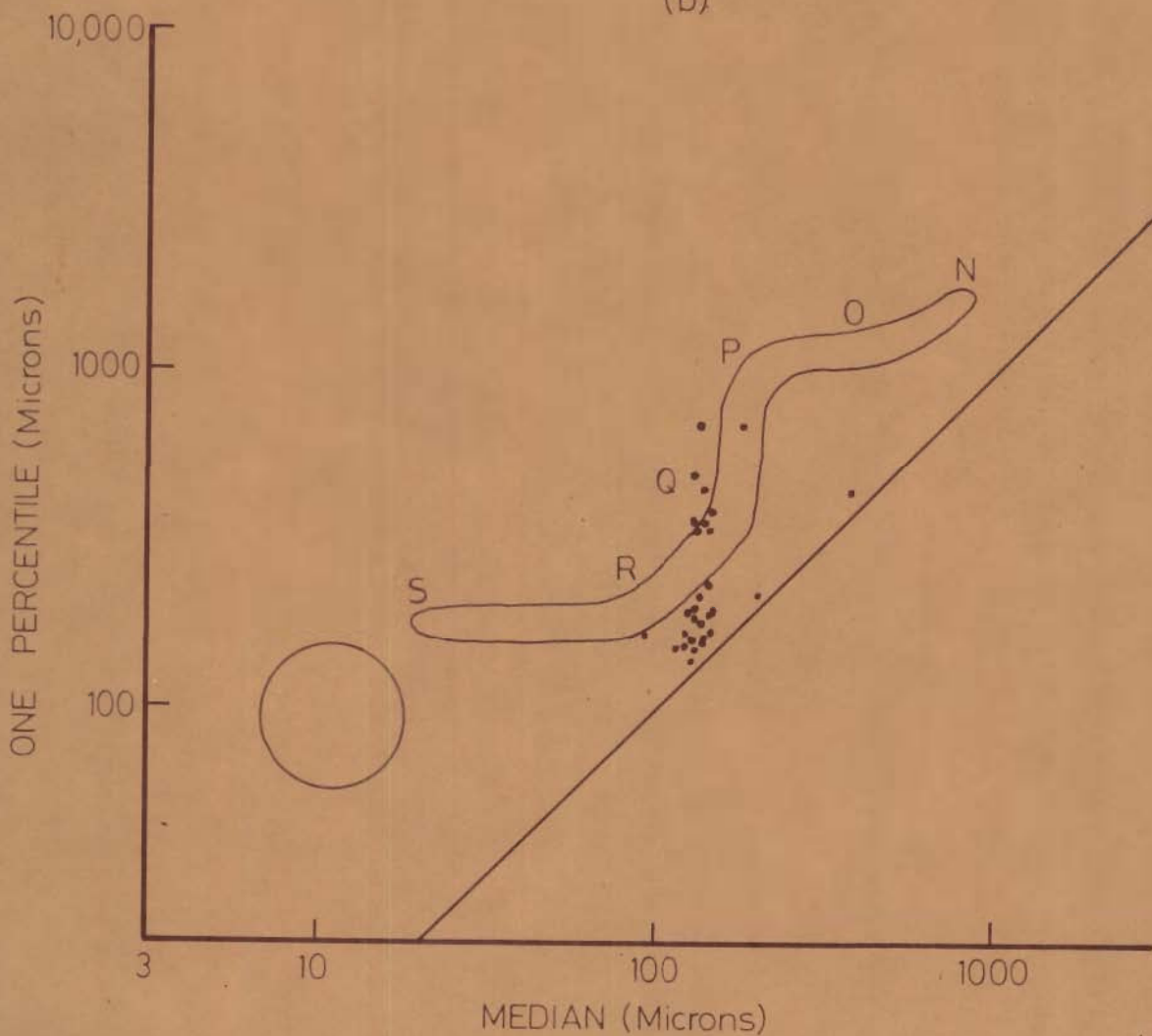


Fig. 4 57_ (a) Passega's (1964) C-M diagram

(b) Plot of samples in C-M diagram

consist mainly of one population with medians in a very small range and perhaps minor additions of coarse material give the observed grain size characteristics and C-M pattern.

4.2.11.3 Mean Size Versus Standard Deviation Diagram of Friedman (1961)

Friedman (1961) delineated fields of river and inland dunes by plotting samples on mean size versus standard deviation (Fig. 4.58). Moiola and Weiser (1968) plotted their samples on this diagram and found that these two textural parameters were not very effective in differentiating between river and inland dune sands. Plots of the samples under study fall in this diagram in a narrow area well inside the aeolian field of Friedman (1961).

4.2.11.4 Skewness Versus Mean Diameter Diagrams of Friedman (1961) and Moiola and Weiser (1968).

Friedman (1961) plotted skewness versus mean size and separated out areas of beach and inland dune sediments using sieves at $1/4 \phi$ interval (Fig. 4.59). However, Moiola and Weiser (1968) had to shift the boundary between the two types of sediments slightly to accommodate their samples. The present samples are comparatively finer and more positively skewed than inland dunes of Moiola and Weiser (1968) and they fall far to one corner of the inland dune sediment field.

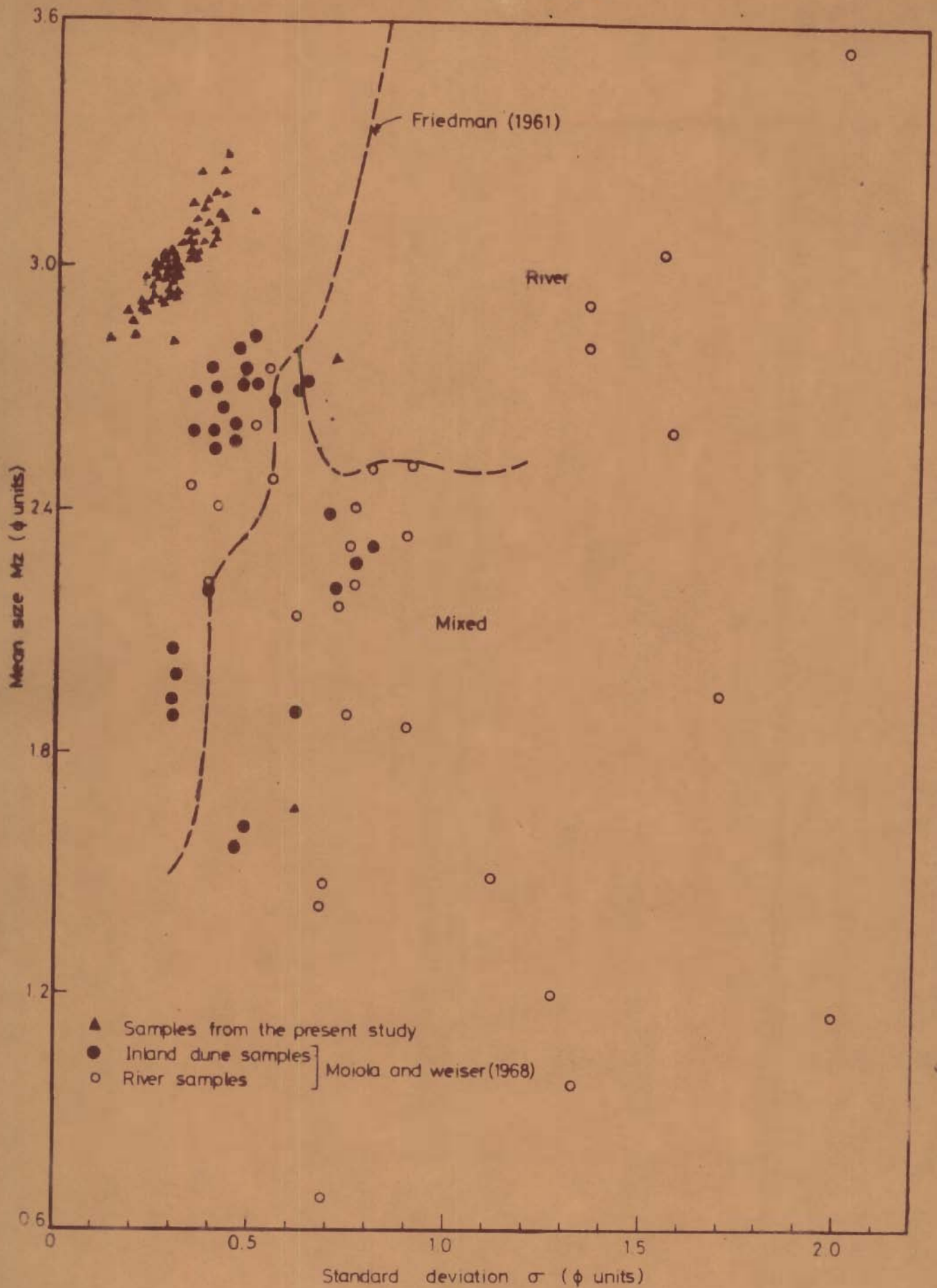


Fig 4.58_Plot of samples from the present study on mean size vs. standard deviation diagram of Friedman (1961) along with Moiola and Weiser (1968) sample points

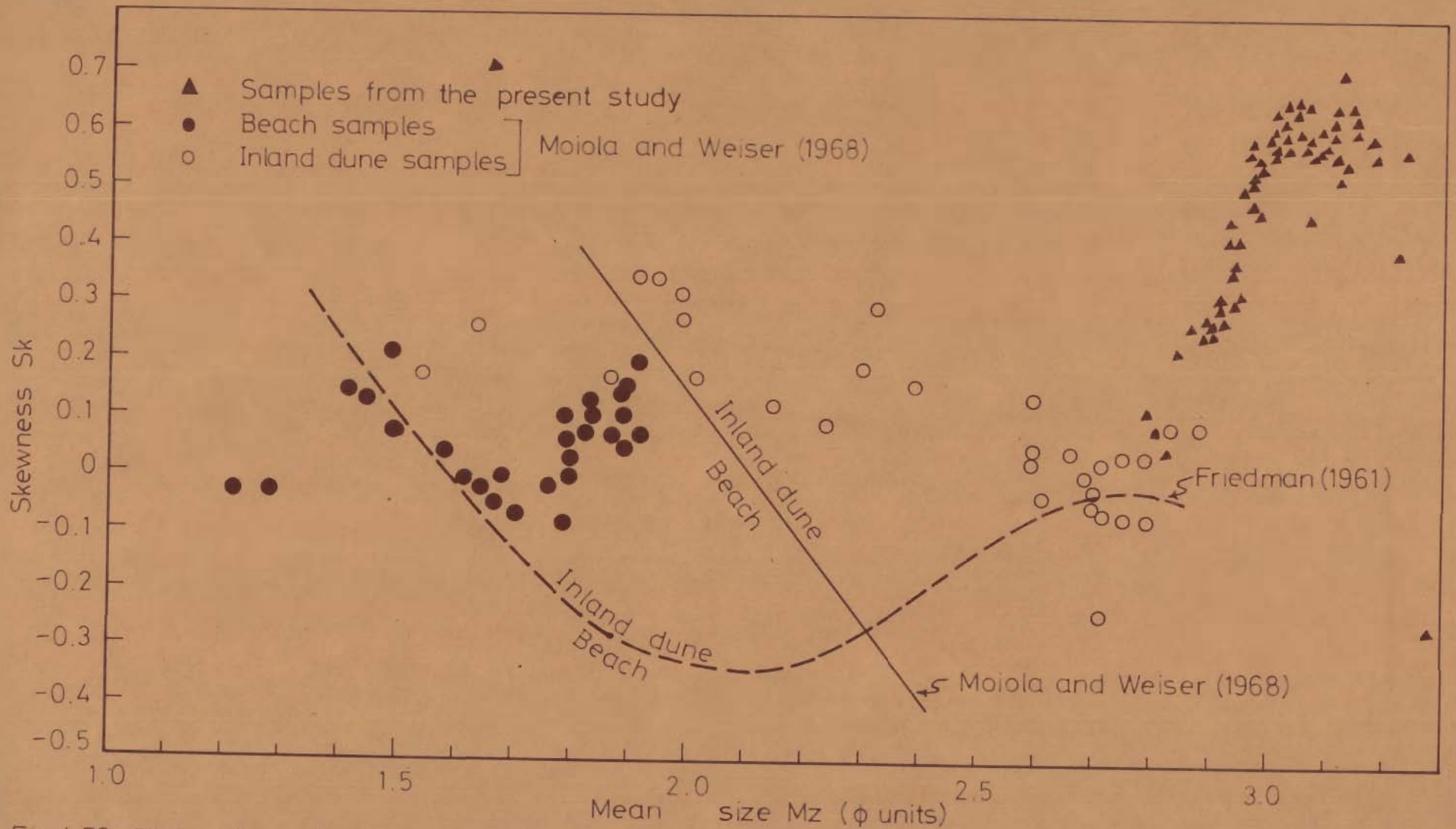


Fig.4.59_Plot of samples from the present study on skewness vs. mean size diagram with superimposed boundaries between beach and inland dune sediments after Friedman (1961) and Moiola and Weiser (1968)

Also, the present samples lie well inside the inland dune sediment field when these are compared with coastal dunes on skewness-mean size plot (Fig. 4.60) of Moiola and Weiser (1968).

4.2.11.5 $\sqrt{\sigma^2}$ versus $\frac{s(Ku)}{s(Mz)} \cdot s(\bar{\sigma}^2)$ plot of Sahu (1964)

Sahu (1964) carried out discriminant analysis of grain size data from different environments. From his study, it became apparent that the standard deviation of the discriminant functions were progressively increasing in the order: aeolian, beach and shallow marine sediments, which suggested that standard deviations of sample statistics might prove helpful in this regard and best results were obtained by plotting $\sqrt{\sigma^2}$ against $s(Ku) / s(Mz) \cdot s(\sigma^2)$ on log-log paper (Fig. 4.61). The general direction of decreasing energy and fluidity for the different environments are also shown in the figure. The lines of demarcation between the processes and environments of deposition have been drawn visually.

The plot of samples under study comes in the right hand corner in the area of low energy (Fig. 4.61). But exclusion of a single sample of ripples with poor sorting shifts the plot to the lower part of the left hand side well inside the aeolian field. Thus, this diagram is very sensitive to slight changes in standard deviation of

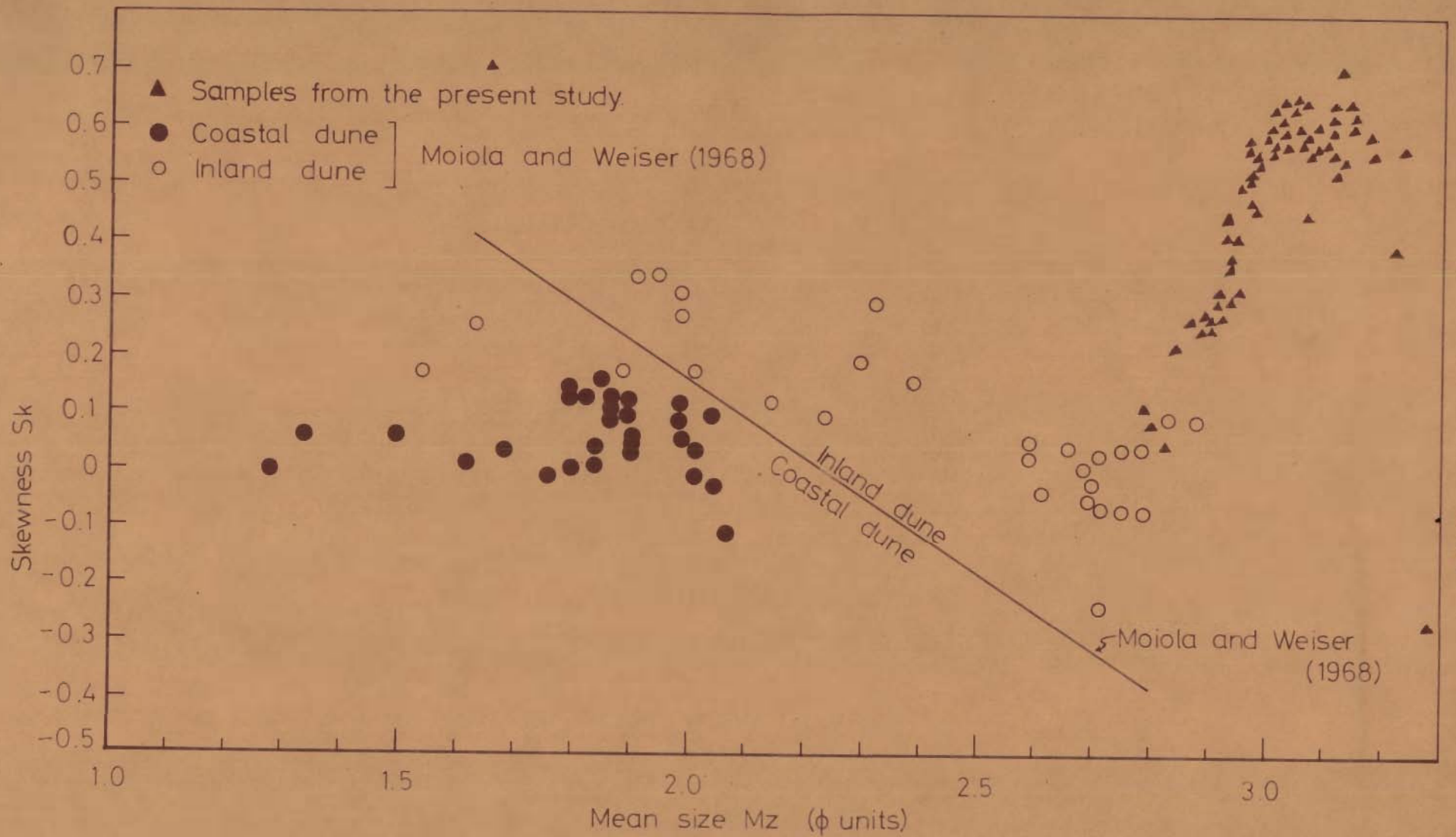


Fig.4.60— Plot of samples from the present study on mean size vs. skewness diagram with superimposed boundary between coastal and inland dunes after Moiola and Weiser, 1968.

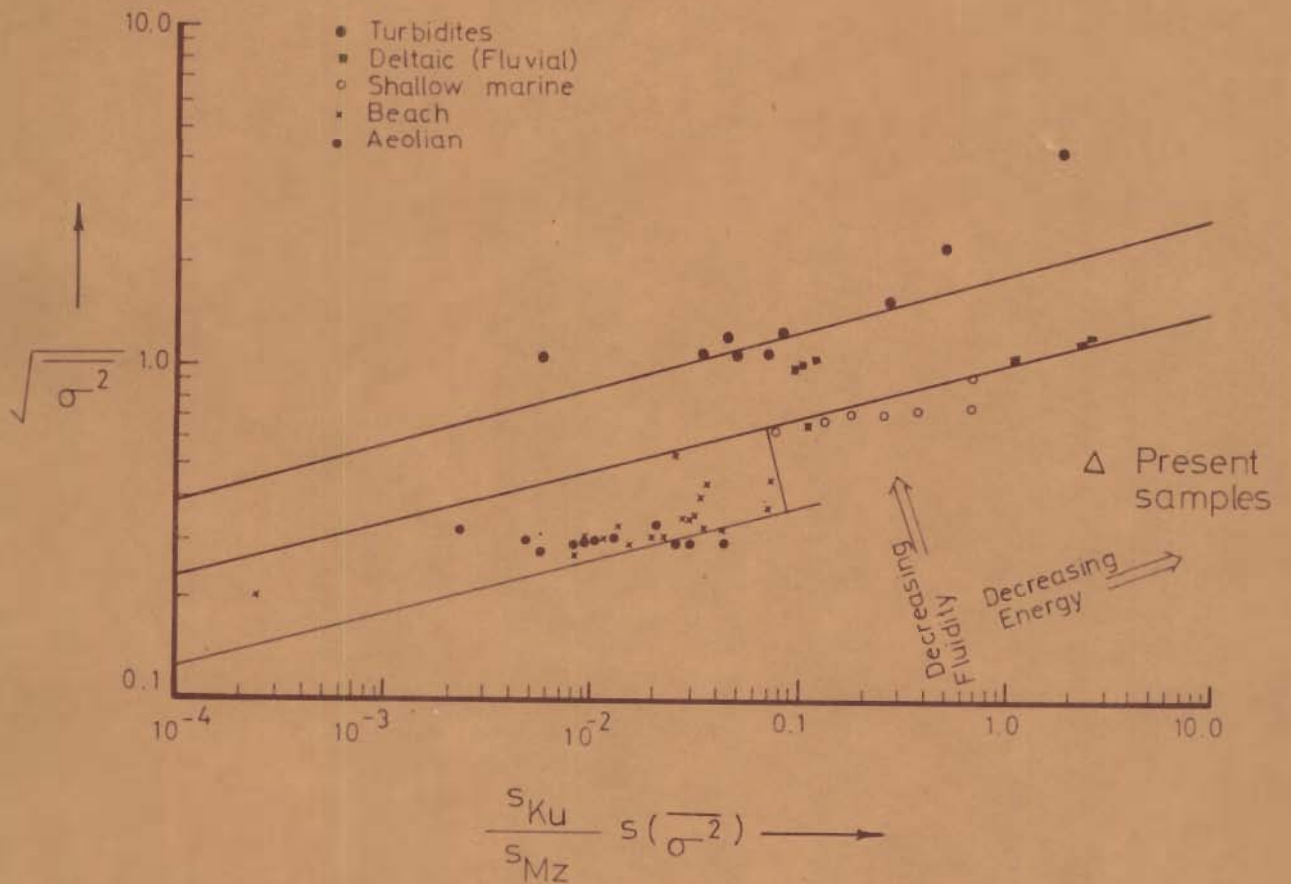


Fig.4.61—Log log plot of $\sqrt{\sigma^2}$ Vs $\frac{s_{Ku}}{s_{Mz}} s(\sigma^2)$ showing the differentiation between the environments of deposition after Sahu (1964) with the plot of present samples

sorting. Inclusion of larger number of samples from sand flats and ^cripples might impair its usefulness for distinguishing aeolian sediments.

4.2.12 Grain Size Populations in Aeolian Sediments

In the present study, an attempt has been made to recognize basic genetic populations on the basis of cumulative curves according to the method suggested by Spencer (1963). In dunes and sand piles, commonly three populations A, B and C can be distinguished. Population A forms usually less than 1% of the samples. **It is** coarser than 2.5 ϕ and is poorly sorted. Population B forms the major portion of the sands, commonly constituting 60% to 90% of the samples and lying mainly between 2.5 ϕ and 3.25 ϕ . Its sorting is excellent. Population C forms 10% to 40% of the samples and is finer than 3.25 ϕ . Its sorting is excellent to good. Distributions of amounts of A and C populations in dunes and sand piles are shown in the form of histograms in Figure 4.62a. Histograms bring out the fact that amounts of population A are approximately log-normally distributed, whereas percentages of population C are approximately normally distributed.

In the case of sand flats, population A constitutes 2 to 10% of samples and its mixing with population B is extremely poor. Population B forms 30-60% of the samples and its mixing with population C is good. Except that population A may contain

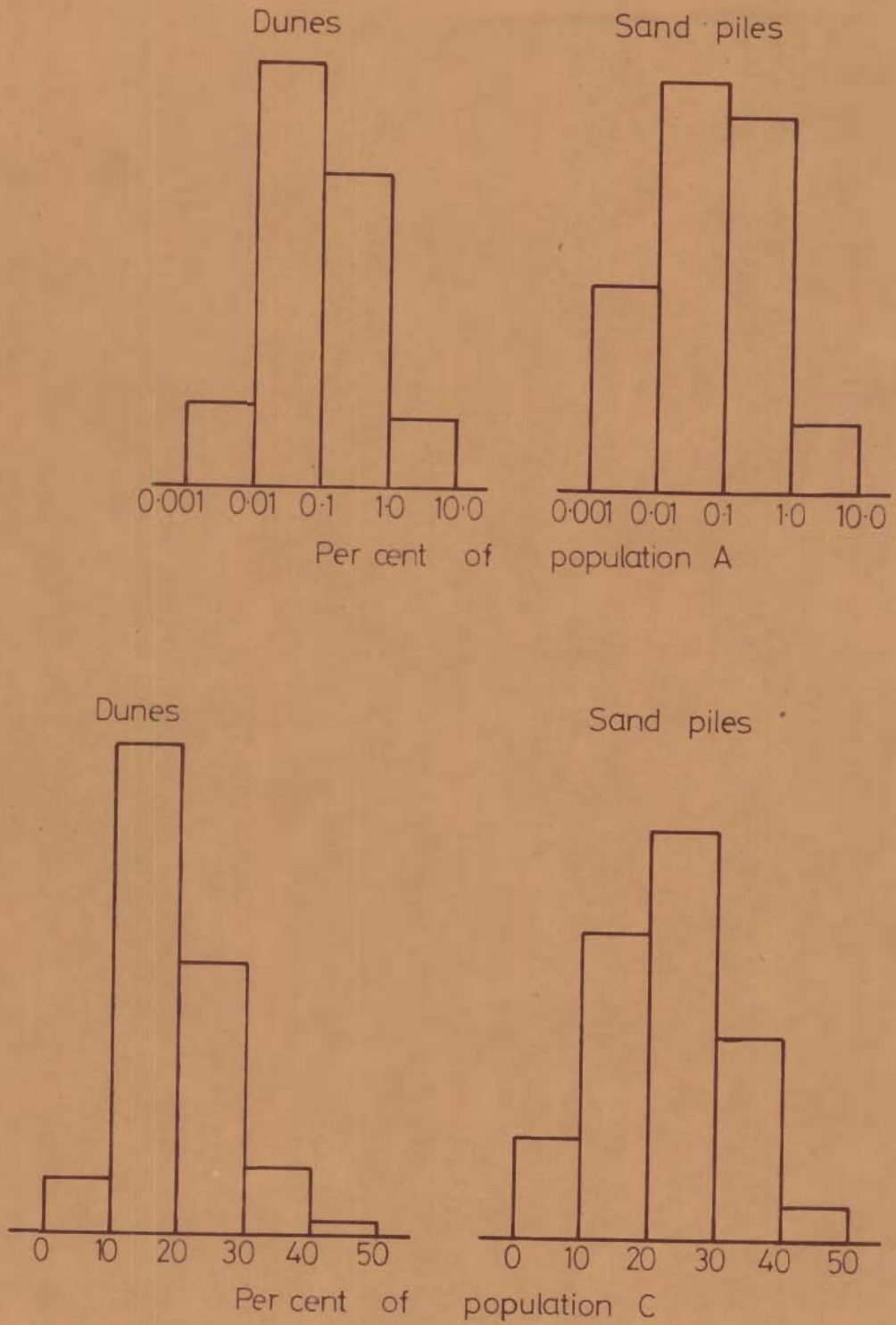


Fig.4.62(a)_Histograms showing distributions of amounts of populations A and C in dunes and sand piles.

particles of quite coarse size, the size limits of the different populations are similar to those of dunes and sand piles. Sand flats differ from dunes and sand piles essentially in possessing less amounts of population B and correspondingly higher amounts of populations A and C.

Ripples have population A in the range 1.0-1.5 ϕ and distinction between populations B and C is difficult.

Bagnold (1937, 1941) and Sharp (1963) recognized three basic genetic types of populations i.e. (a) surface creep, (b) saltation population and (c) suspension populations in aeolian sediments. Populations A, B and C of the present study can obviously be taken as surface creep, saltation and suspension populations, though their maximum and minimum limits have a smaller range than hitherto reported.

Folk (1971 a) dissected the frequency curves of grain size distributions of samples from Simpson desert, Australia. He found that dune sediments consisted mainly of saltation population with mean size range of 1.5 ϕ to 4.0 ϕ . Also the sediments had different quanta or sub-populations with a standard deviation of 0.25-0.50 ϕ . Each quantum is carried by a separate puff of wind and deposited in a particular microlocality as a laminae or a patch of grains.

Using an analysis similar to that of (Folk, 1971 a) for sand piles and dunes, it can be seen that these sediments consist mainly of two populations in different proportions i.e. saltation population with a mean size of 2.75ϕ and standard deviation of about 0.2ϕ and another suspension population with a mean size of 3.75ϕ and a standard deviation of about 0.25ϕ . When these sediments consist mainly of saltation population with minor additions from suspension, sediment is well sorted with nearly symmetrical distribution and leptokurtic. With larger additions of suspension population to saltation population so that the two populations become subequal, composite frequency curve for the sample becomes poorly sorted, positively skewed and platykurtic (Fig. 4.62 b). This explains the observed interrelationship of the grain size parameters, their variation within dunes and their spatial variation.

Essential bimodal nature of the sand piles and dunes is obvious from the above discussion. Skocek and Saadallah (1971) summarized the various suggested causes of bimodality as follows:

- (a) Repeated reworking of a unimodal sand and thus transportation by saltation and suspension may produce bimodality of the aeolian sediments. This process is called 'rectification' by Wood (1970).

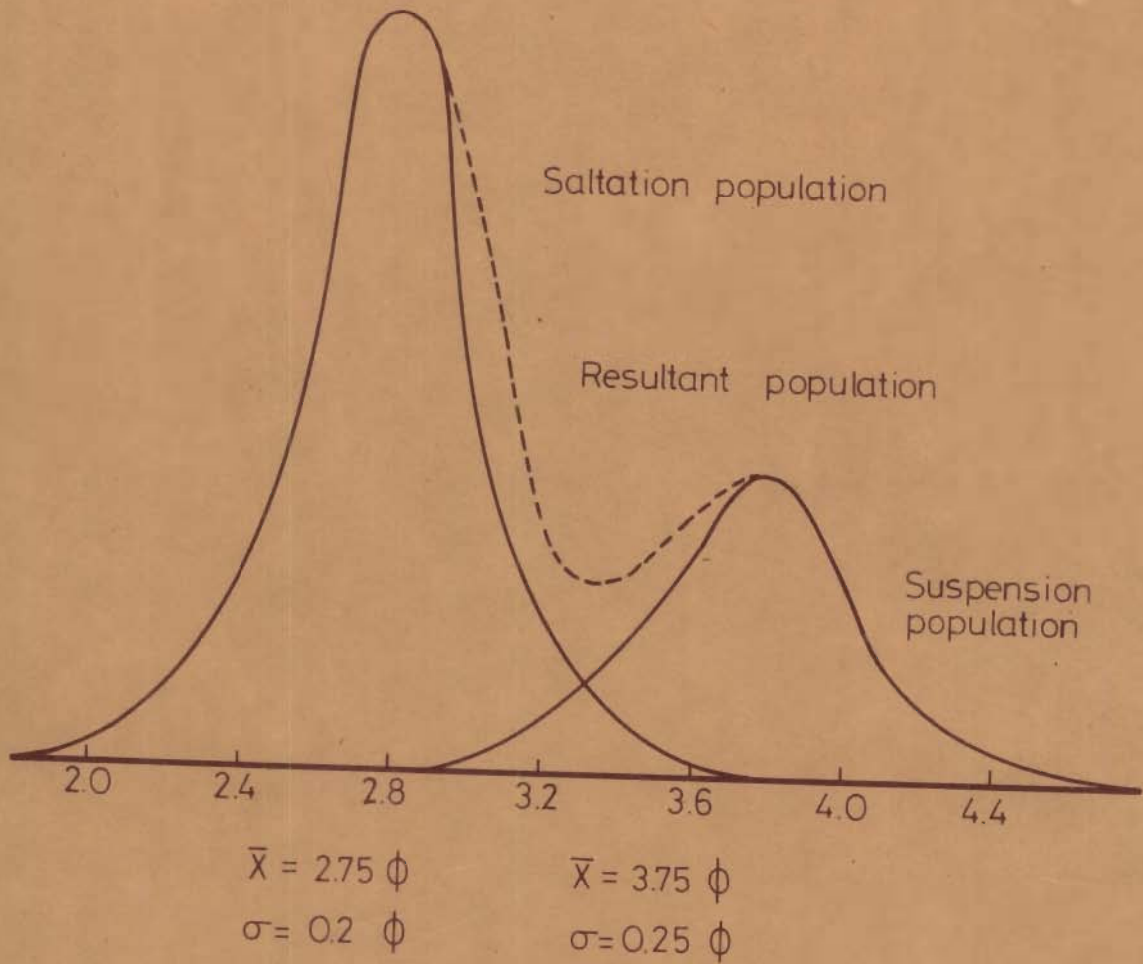


Fig.4.62(b)– Diagrammatic representation to explain the observed grain size characteristics of samples studied by mixing of two distinct populations with $\bar{X}=2.75 \phi$, $\sigma=0.2 \phi$ and $\bar{X}=3.75 \phi$, $\sigma=0.25 \phi$ respectively.

- (b) Lack of grains in the range 3.0ϕ to 3.5ϕ in the source sediments could produce bimodality of the sediments under study.
- (c) Decomposition of unstable grains due to weathering may destroy certain grain size fractions of the source material.
- (d) Deposition of different 'quanta' of sediment sizes in various distinct layers with changing velocity of wind (Stokes, 1964; McKee and Tibbitts, 1964; Folk, 1971 a) may also explain bimodality of aeolian sands.
- (e) A large amount of fine material during slackening of dust storm may infiltrate down the sand.

Skocek and Saadallah (1971) favoured the infiltration hypothesis as mentioned above. In the present area also, such an explanation seems to be plausible. Fine materials, in the form of dust storms, could be transported from the flood plains of the Indus River in the upwind direction. There are plenty of fine materials along levees, flood basin and abandoned channels of the Indus rivers. Also fine sediment could be derived locally from the parent materials which were essentially fluvial sediments with plenty of fines and deposited by tributaries of the Indus, as mentioned elsewhere.

Differences in grain size distributions of sand piles and dunes can be explained by the fact that piles are essentially stationary bedforms and fines, deposited by slackening dust storms, infiltrate down and with time their amount increases. However, barchan dunes travel under the influence of wind which transports sand grains along the stoss side on to the crest and across with occasional avalanching of the sand along the slip face. This process is repeated continuously, whereby, fines may be picked up by the strong wind and removed from the dunes leaving dune sediments better sorted than sand piles.

4.3 STUDY OF ROUNDNESS

4.3.1 Procedure

Wadell (1932) first described a quantitative procedure for determination of roundness of particles and defined the 'degree of curvature' as the ratio of average radius of curvature of the different corners or edges to the radius of curvature of the maximum inscribed sphere or to the nominal radius of the fragment.

Using Wadell's scale of roundness, Russel and Taylor (1937) set up five roundness classes with irregular intervals. Pettijohn (1949) redefined the class limits in such a manner that the middle points of classes form a geometric pattern. Folk (1955) defined six roundness classes such

that the ratio of upper class limit to the lower limit of each class is 0.7 and called his scale as ρ (rho) scale.

It is tedious and cumbersome to determine the radius of curvature of corners and radius of the largest inscribed circle of a fragment and calculate the roundness value. In the present study, roundness values of individual grains were obtained by comparison with Folk's (1955) roundness images that are convenient to use because of the logarithmic nature of the scale. All the $1/2 \phi$ size fractions of eleven samples were examined for their roundness using grain-mount slides and by studying one hundred clear quartz grains from each slide.

4.3.2 Operator Experiment

An operator experiment was performed to determine two factors (i) operator consistency and (ii) operator error resulting from variation from person to person. Four slides were selected randomly from the whole lot. These slides were analysed by two operators by the above described method. The experiment was repeated after two days by the same operators. The results are shown in Table 4.7.

Table 4.7 - Values of \bar{X}_ρ for different slides and operators

Slide No.	Operator No.1		Operator No.2	
	First attempt	Second attempt	First attempt	Second attempt
90/45	2.91	2.81	2.73	2.73
55/ F	2.04	2.14	1.94	2.30
55/45	2.54	2.48	2.61	2.76
10/230	2.36	2.32	2.31	2.57

A Two Way Analysis of Variance model with replication (Miller and Kahn, 1962, p. 171) has been used to analyse the data. The calculations are done assuming that slides and operators are random samples from larger populations of thin sections and operators respectively. Results of ANOVA are given in Table 4.8.

Table 4.8 - Operator experiment data subjected to Analysis of Variance.

Source of Variation	Degrees of freedom	Sum of squares	Mean squares	Variance Ratio F
Variation between operators	1	0.0076	0.0076	1.90 NS
Variation between slides	3	1.0459	0.3486	87.15 ^X
Interaction	4	0.1422	0.0355	
Replication	7	0.0280	0.0040	
Total	15	1.2237		

NS - Not significant at $\alpha = 0.05$

X - Significant at $\alpha = 0.05$

Analysis of Variance (Table 4.8) brings out the following important features:

- (i) Replication error is very small (mean square = 0.004).
- (ii) Operator error due to personal bias of operators is not significant statistically.

- (iii) Differences between mean roundness of slides are significant.

It is observed that differences between roundness values of different slides are small, but these can be detected by the present method.

Thus, it seems that the present method of determining roundness is quite satisfactory.

4.3.3. Results of Roundness Study

Mean and standard deviation of roundness for different slides are listed in Table 4.9. Mean roundness for different slides has a very limited range of 2.02 to 2.91 ρ suggesting thereby, that different sized quartz grains are mainly subangular in nature. Standard deviation of roundness of the different slides also has a limited range of 0.30 to 0.67 ρ indicating that all the grains in a certain size fraction are rounded approximately to the same degree.

Variation of roundness with grain size is shown in Figure 4.63. It seems that there is extremely small, but distinct decrease in roundness value with decrease in grain size. Also, Figure 4.63 brings out the fact that quartz grains smaller than 120 mesh (0.125 mm) have roughly the same roundness value, whereas, particles larger than 120 mesh show higher roundness values, thereby suggesting that wind is an effective rounding agent

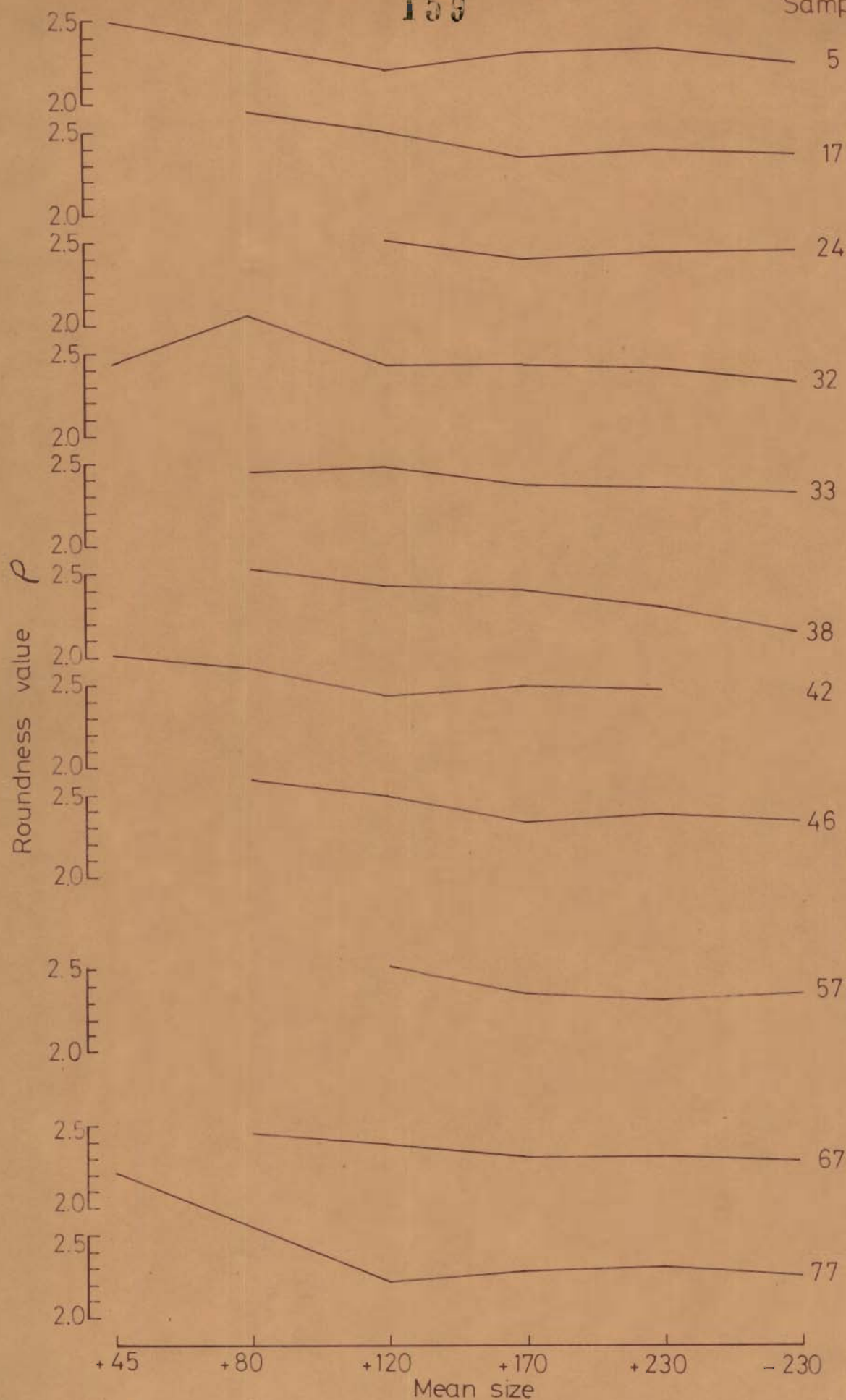


Fig.4.63_Variation of mean roundness of quartz grains with grain size in different samples.

for particles carried in saltation and traction.

Table 4.9 - Mean and standard deviation of roundness values of quartz grains of the various fractions of different samples

Sample No.	17		24		32	
	\bar{x}_p	s_p	\bar{x}_p	s_p	\bar{x}_p	s_p
+45 Mesh					2.43	0.42
+80 Mesh	2.62	0.43			2.72	0.55
+120 Mesh	2.50	0.35	2.51	0.41	2.42	0.47
+170 Mesh	2.36	0.46	2.39	0.48	2.41	0.37
+230 Mesh	2.39	0.45	2.42	0.50	2.39	0.42
-230 Mesh	2.36	0.45	2.43	0.37	2.30	0.46

Sample No.	33		38		42	
	\bar{x}_p	s_p	\bar{x}_p	s_p	\bar{x}_p	s_p
+45 Mesh					2.68	0.52
+80 Mesh	2.44	0.42	2.52	0.34	2.59	0.51
+120 Mesh	2.47	0.40	2.42	0.30	2.42	0.41
+170 Mesh	2.37	0.45	2.38	0.48	2.48	0.44
+230 Mesh	2.34	0.48	2.29	0.48	2.45	0.33
-230 Mesh	2.31	0.51	2.13	0.58		

Sample No.	46		62		57	
	\bar{x}_p	s_p	\bar{x}_p	s_p	\bar{x}_p	s_p
+45 Mesh	2.54	0.41				
+80 Mesh	2.53	0.52	2.57	0.50		
+120 Mesh	2.40	0.43	2.28	0.52	2.52	0.45
+170 Mesh	2.24	0.49	2.22	0.48	2.33	0.51
+230 Mesh	2.04	0.67	2.10	0.51	2.30	0.47
-230 Mesh	2.02	0.59	1.79	0.56	2.33	0.45

Sample No.	67		77		5	
+45 Mesh			2.91	0.54	2.50	0.51
+80 Mesh	2.47	0.45			2.47	0.50
+120 Mesh	2.40	0.45	2.20	0.54	2.51	0.44
+170 Mesh	2.32	0.49	2.30	0.42	2.56	0.41
+230 Mesh	2.32	0.42	2.32	0.38	2.36	0.53
-230 Mesh	2.29	0.46	2.27	0.42	2.43	0.51

4.4 STUDY OF SPHERICITY OF QUARTZ GRAINS

4.4.1 Introduction

Russel and Taylor (1937) observed that both experimental and petrographic studies of natural sands suggested that sphericity of quartz sand grains was not significantly modified by abrasion, but was inherited from the parent rock. Krynine (1940) found that clastic quartz of metamorphic origin tended to be more elongated than that of igneous rocks. Pettijohn (1957, p.66, 119) also emphasized that the end shape of a sand grain depends upon its original shape. Thus there could be some quantitative distinction between quartz grains of different origins.

Sphericity (ψ) of quartz grains has been commonly studied by measuring axial ratio i.e. short axis/long axis after Bokman (1952) who claimed that there existed significant differences in axial ratios of quartz grains from

schistose and granitic sources. Numerous observations of axial ratios of quartz grains in thin sections show that the average axial ratio of quartz grains ranges only from 0.61 to 0.73 (Griffiths, 1967, p.123). Bokman (1957) too endorsed it subsequently.

Mukherjea (1975) has restudied data of Bokman (1952) and claims that a major inflection point exists at elongation quotient (inverse of axial ratio) at 1.2 and a minor one around 2.0. He found that the various transformations do not help in normalisation of data. Also he suggests a triangular diagram for possible identification of schistose and plutonic sources.

Sahu and Patro (1970) indicated that $\log(\psi/1 - \psi)$ transformation normalized the sphericity distributions. Sahu (1973) attempted to relate sphericity distributions with environments.

In the present study, sphericity of quartz grains has been studied with a view to determine their possible ultimate source and the effect of aeolian action on the mean sphericity and type of distribution.

4.4.2 Procedure of Study

Five sand samples studied for roundness from widely separated localities were selected. Slide mounts of all the $1/2 \phi$ size fractions were examined for axial ratios of

quartz grains. The maximum number of grains available in the slide or grains observed in four fields of view (>100 grains) were studied.

Distributions of sphericity values of quartz grains are depicted in the form of cumulative frequency curves on arithmetic-probability paper in Figures 4.64 - 4.68. Mean and standard deviation for sphericity of each slide are calculated and are listed in Table 4.10.

4.4.3 Distribution of Sphericity Values

Nature of distribution of sphericity values has been examined by studying the shape of cumulative frequency curves in Figures 4.64 - 4.68. These curves can be grouped into polymodal, normal, positively skewed and negatively skewed classes. All the curves except that for slide 5/230 lend themselves to this type of visual examination. The curve for slide 5/230 is positively skewed in the lower part and negatively skewed in the upper part and as such has been grouped in polymodal class. This analysis gives the following results for different curves: normal - 11, polymodal - 6, positively skewed - 4 and negatively skewed - 4. Thus it seems that there is no need for any transformation of the sphericity data. Deviations from normality probably reflect the degree of abrasion, distance from the source and mixing of sediments from different sources.

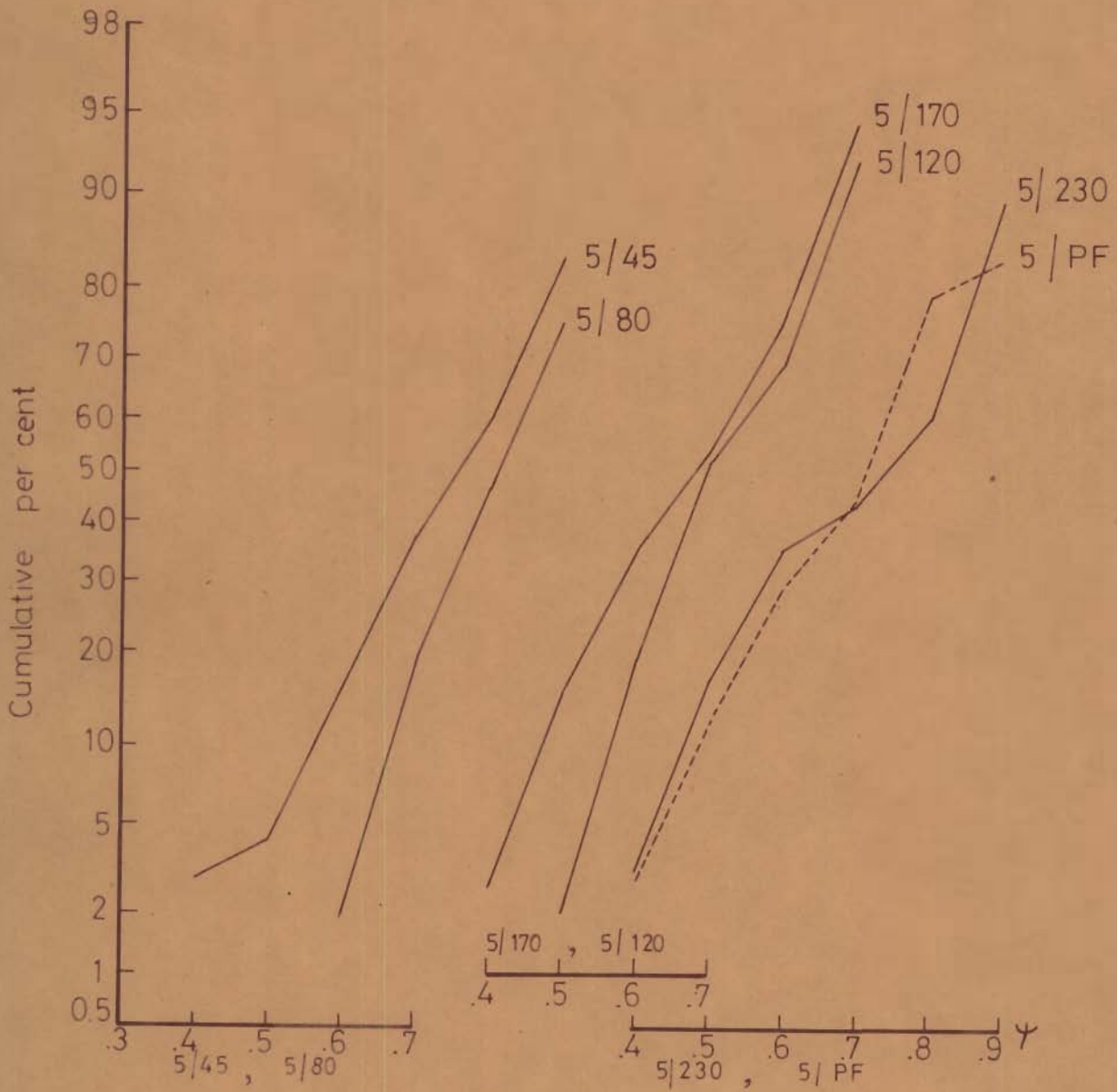


Fig.4.64 - Cumulative per cent frequency curves for sphericity values of quartz grains of different fractions of sample 5.

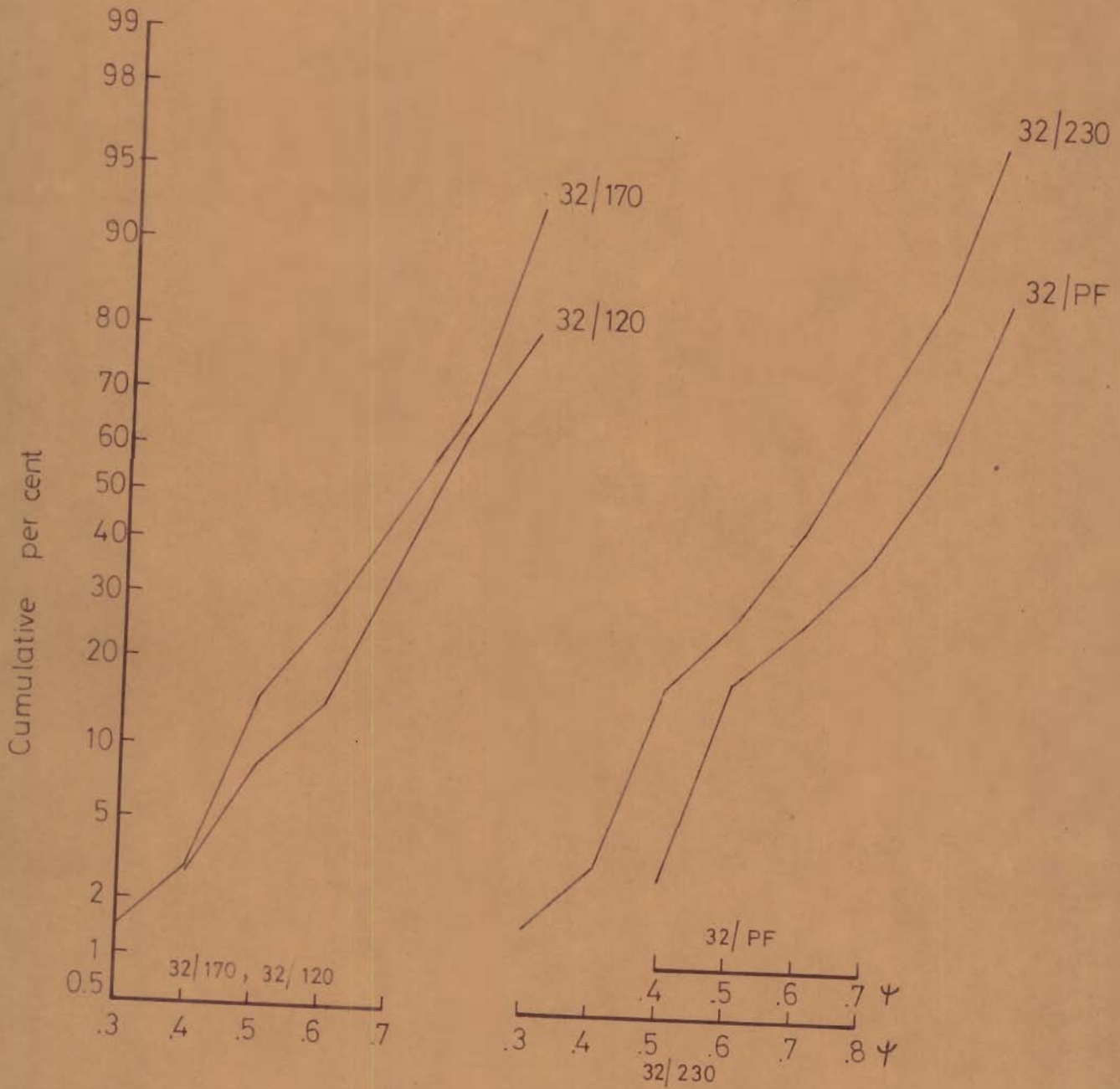


Fig. 4.65. Cumulative per cent frequency curves for sphericity values of quartz grains of different size fractions of sample 32.

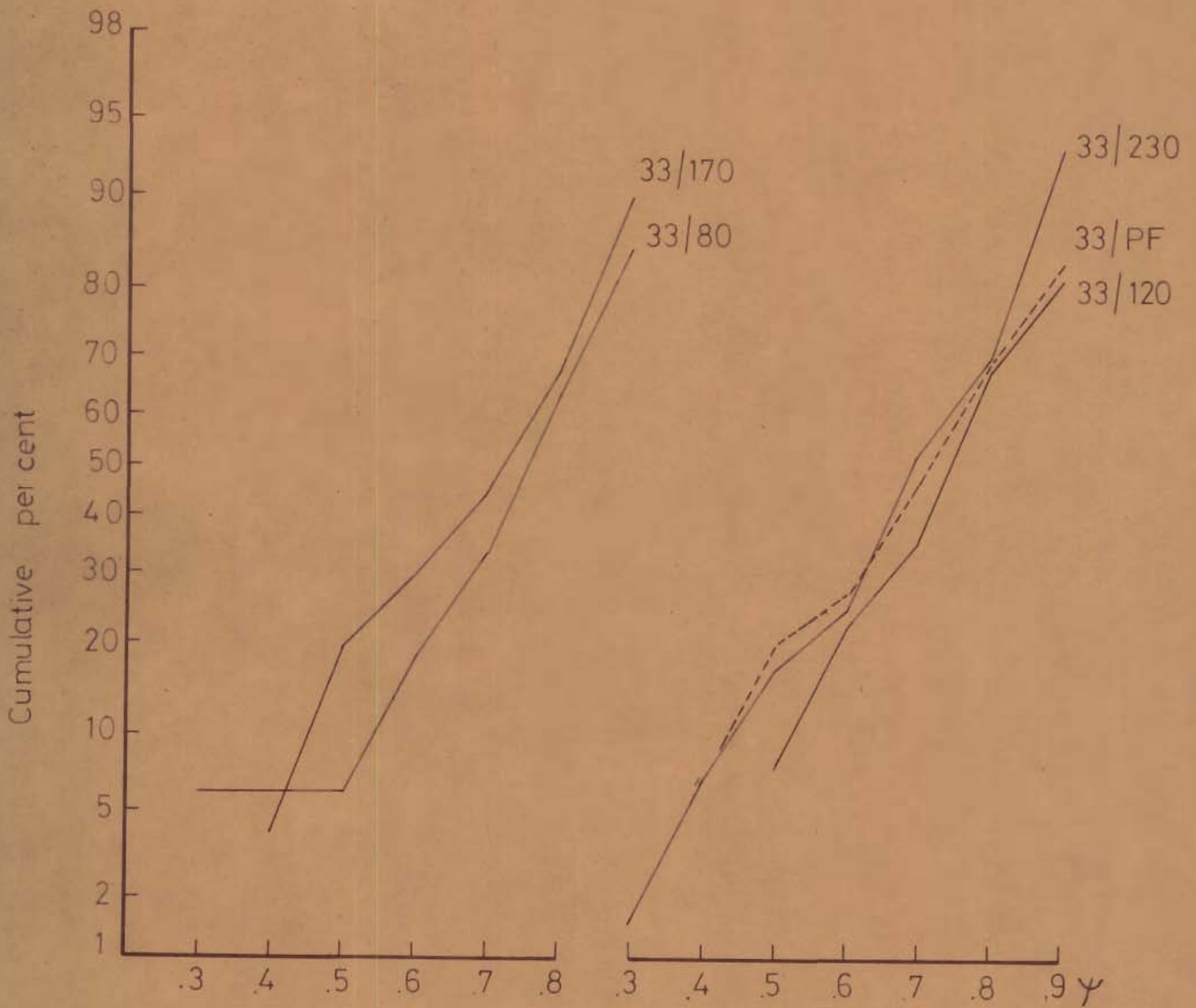


Fig.4.66—Cumulative per cent frequency curves for sphericity values of quartz grains of different size fractions of sample 33.

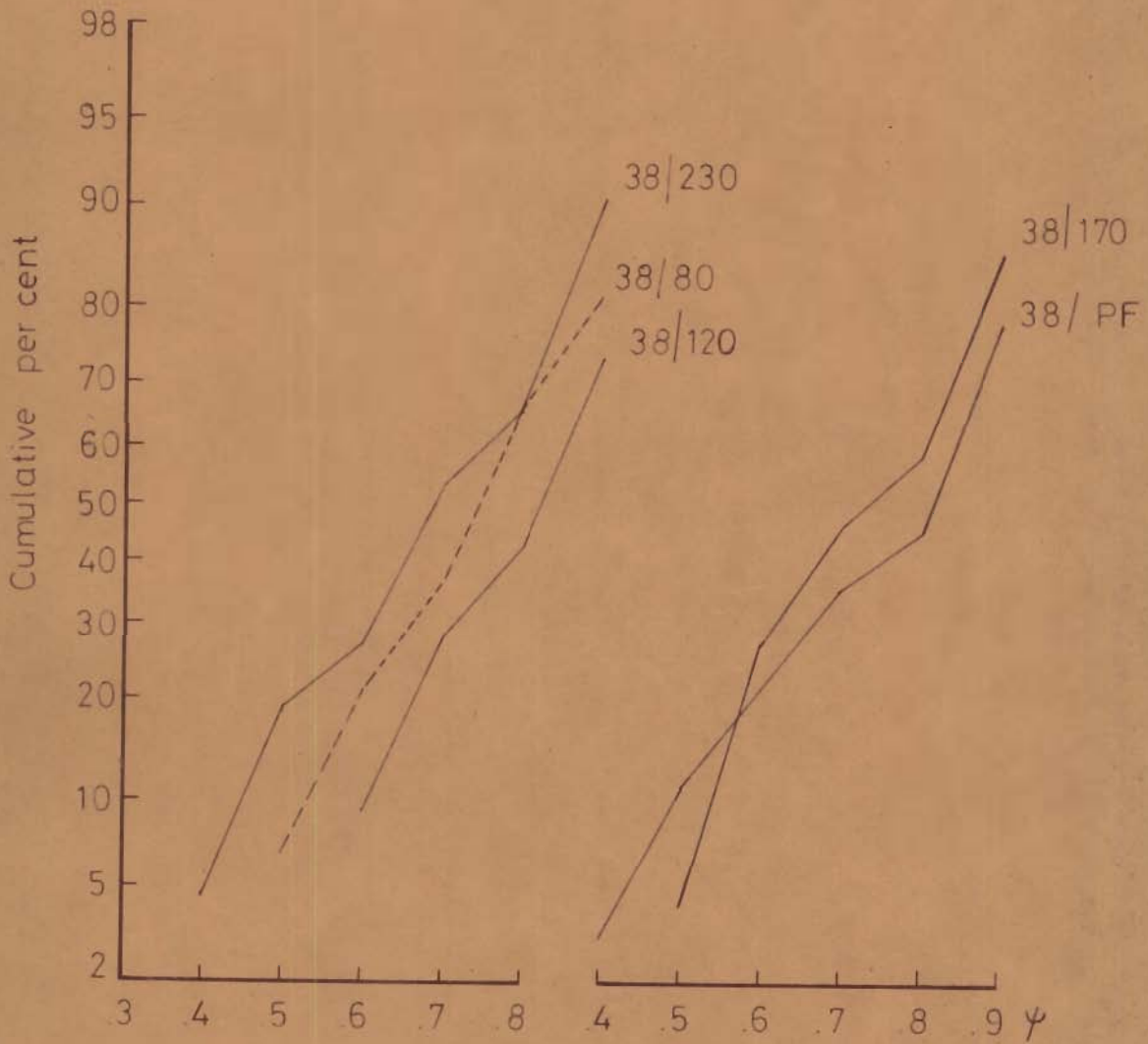


Fig.4.67_ Cumulative per cent frequency curves for sphericity values of quartz grains of different size fractions of sample 38.

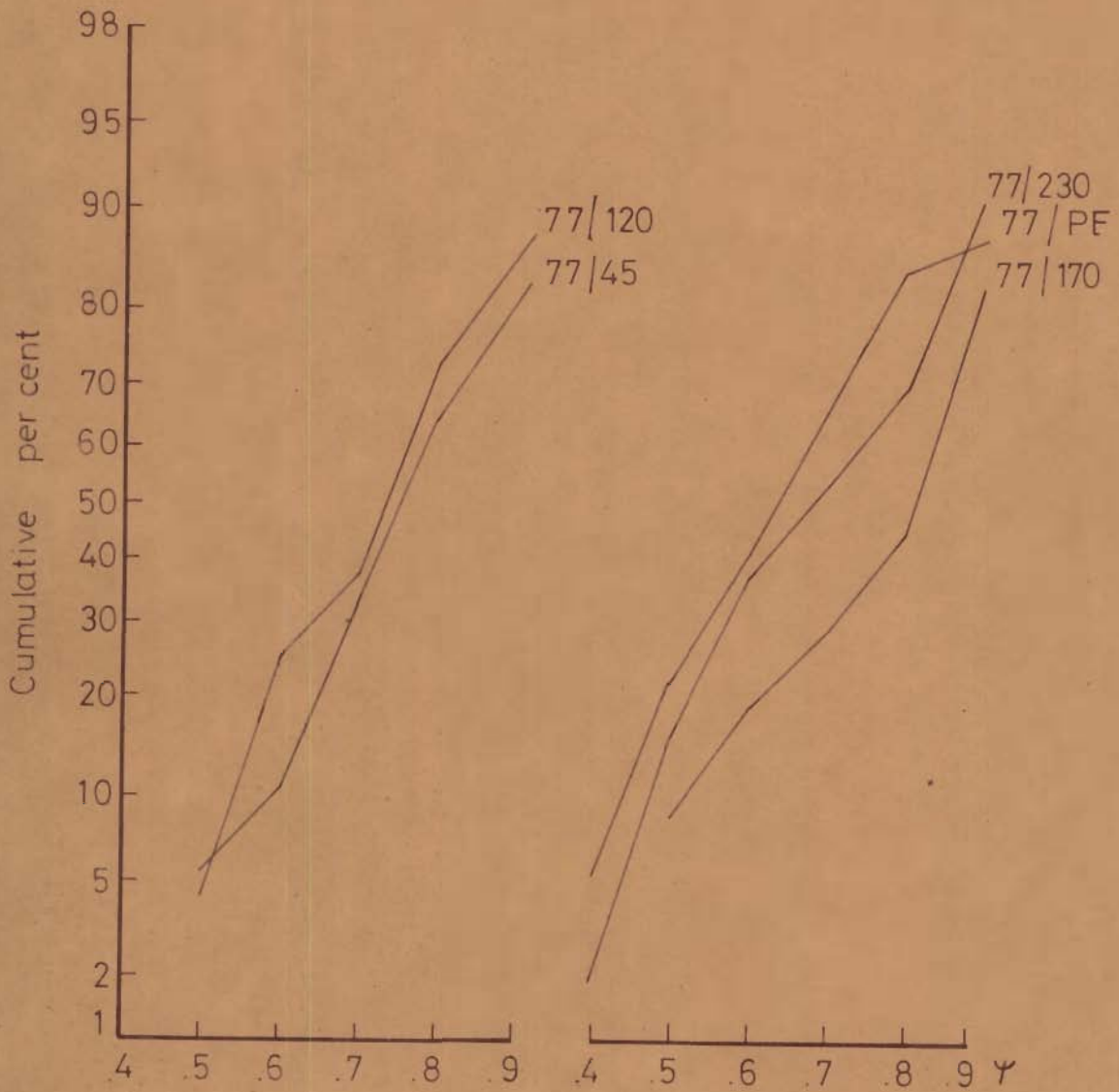


Fig.4.68 - Cumulative per cent frequency curves for sphericity values of quartz grains of different size fractions of sample 77.

4.4.4 Mean and Standard Deviation of Sphericity Values

Mean value of sphericity for the different slides ranges from 0.56 to 0.81 \downarrow However, for most of slides it lies between 0.6 and 0.78 \downarrow (Table 4.10). Also, there seems to be little evidence of change of mean sphericity with grain size (Fig. 4.69). All fractions of sample no. 38 show consistently low sphericity values.

Standard deviation of sphericity values for the four samples with numbers 5, 24, 33 and 77 ranges from 0.11 to 0.20 \downarrow but for the sample number 38 from Rangarh area, it varies from 0.39 to 0.54 \downarrow and these are much higher than those reported from other areas (Griffiths, 1967, p.123). In the vicinity of Rangarh, there are exposures of Jurassic and Eocene sandstones and limestones. It seems probable that quartz grains of all size fractions under consideration with lower sphericity value are contributed from these rocks resulting in slightly lower mean and high standard deviation for sphericity values.

Release of low sphericity quartz grains from the Jurassic and Eocene sediments suggests that perhaps these sediments are also first cycle ones which did not suffer much transport before deposition.

Synthesis of the present observations and those of others (Griffiths, 1967, p.123) suggests that slight

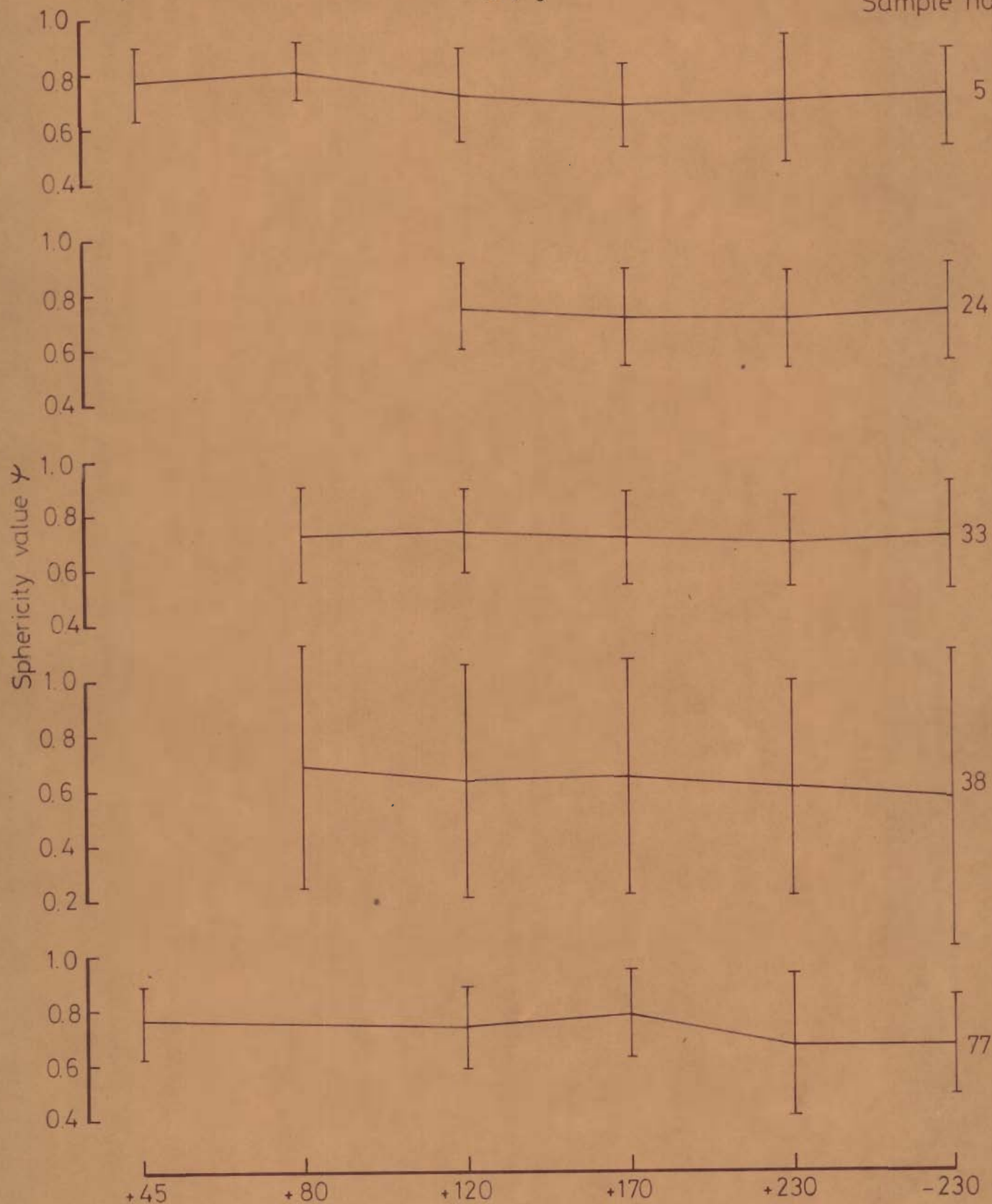


Fig.4.69_Variation of mean sphericity values with grain size in different samples.

± One standard deviation range is shown by vertical lines.

Table 4.10- Mean, standard deviation and type of distribution of sphericity values

Mesh size	Sample No. 5			Sample No.24			Sample No. 33		
	Mean	s.d.	type of distribution	Mean	s.d.	type of distribution	Mean	s.d.	type of distribution
+45	0.769	0.135	N						
+80	0.814	0.103	N				0.730	0.170	N
+120	0.719	0.172	SP	0.755	0.158	N	0.737	0.149	N
+170	0.680	0.153	N	0.714	0.173	SN	0.710	0.172	N
+230	0.702	0.226	P	0.706	0.177	SN	0.694	0.162	P
-230	0.708	0.176	P	0.727	0.177	SN	0.713	0.196	P

	Sample No.38			Sample No.77		
+45				0.759	0.135	N
+80	0.689	0.444	P			
+120	0.636	0.422	N	0.735	0.145	P
+170	0.639	0.428	SP	0.785	0.160	SN
+230	0.602	0.392	N	0.666	0.253	SP
-230	0.562	0.538	SP	0.666	0.180	N

N- Normal.
P- Polymodal.
SN- Negatively skewed.
SP- Positively skewed.

abrasion gives mean sphericity values of 0.6 to 0.8 ψ , so that away from the source, axial ratios can hardly be of any significance regarding their provenance. However, if the sediments have not travelled far from a metamorphic source, the provenance may be reflected in slightly lower sphericity and higher variance than as commonly observed.

CHAPTER - 5

PETROGRAPHIC STUDIES5.1 INTRODUCTION

A preliminary study of the petrography of the aeolian sands has been made to determine variation in light and heavy minerals with grain size, regional variation in petrographic composition and to find out provenance of these sands.

5.2 LIGHT MINERALS5.2.1 Method of Study

Light minerals have been studied under a polarizing microscope by mounting grains on slides with Canada balsam. Maximum number of grains available or about 170 grains are counted. All the half phi size fractions of three samples with number 5,24 and 77 have been analysed for light mineral composition. Modal composition data for different fractions of these samples are utilized to recalculate nodal composition of the whole samples. In addition, +120 mesh fractions of five other samples have been analysed for light mineral composition. Modal analysis data are listed in Table 5.1 and histograms depicting distributions of the different nodes of the various slides are shown in Figures 5.1 - 5.2.

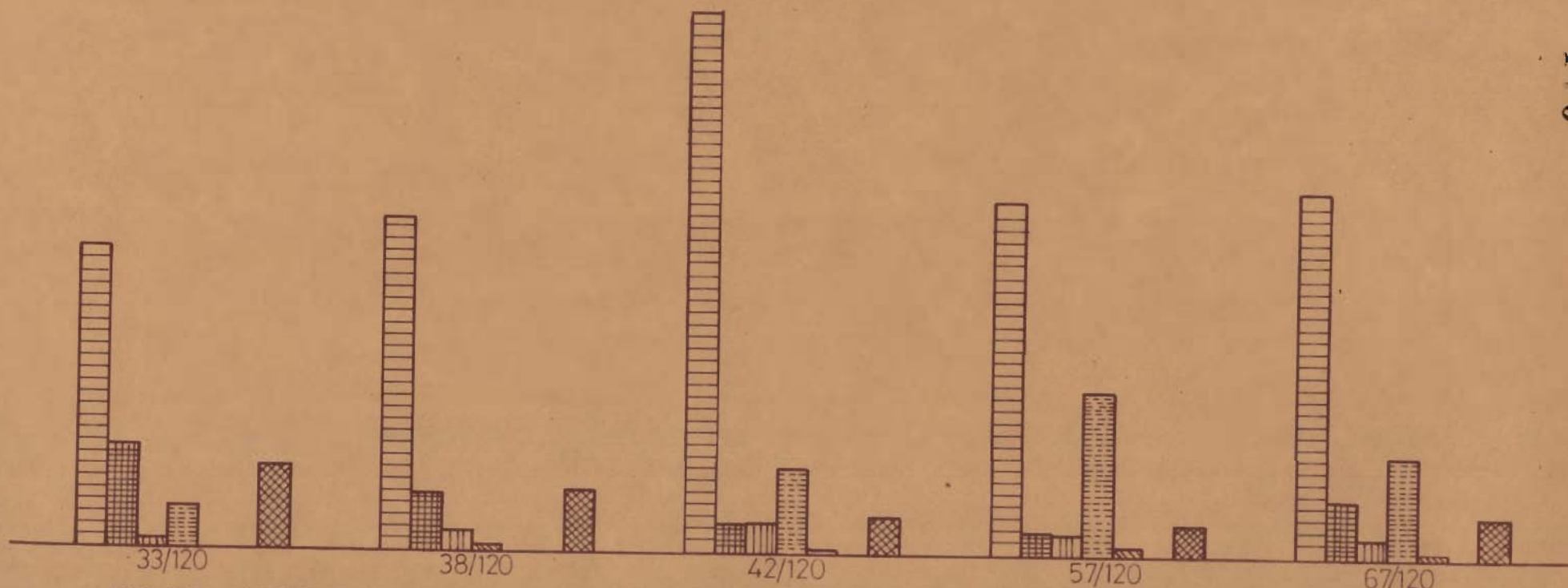
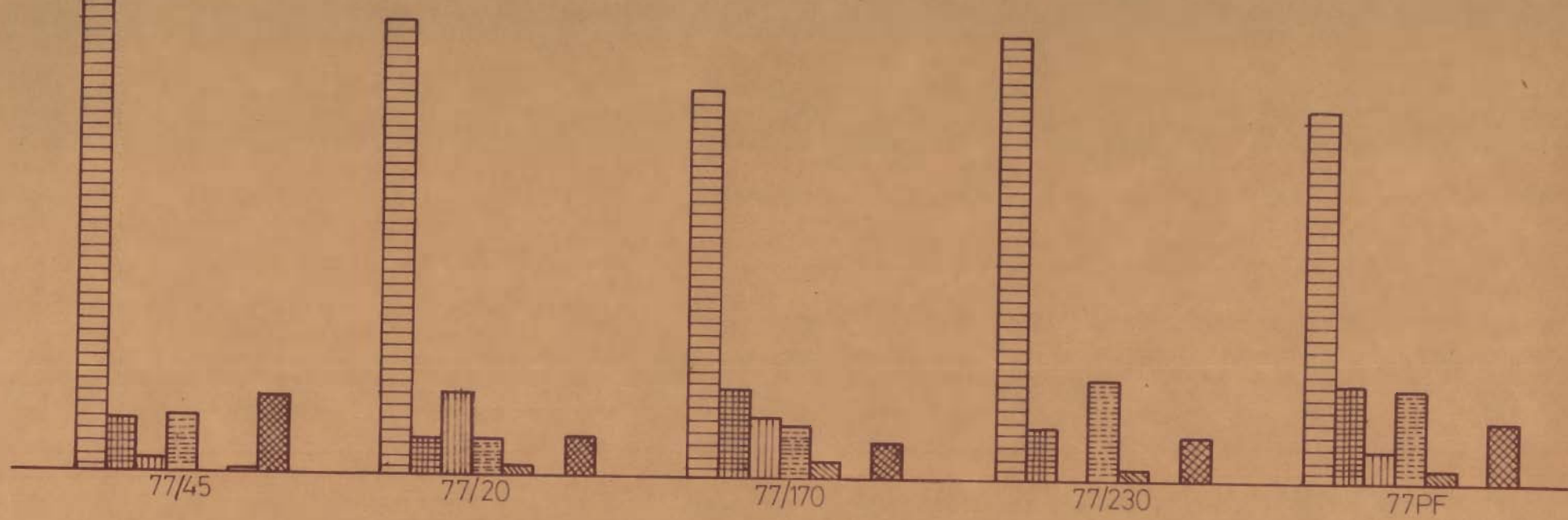


FIG. 5-2 - HISTOGRAMS SHOWING DISTRIBUTIONS OF LIGHT MINERALS IN DIFFERENT SLIDES. SYMBOLS ARE THE SAME AS IN FIGURE 5.1.

Mainly six modes i.e. quartz, chert, K-feldspar, plagioclase, calcite and aragonite are recognized. Heavy minerals and opaques are grouped in 'others' category.

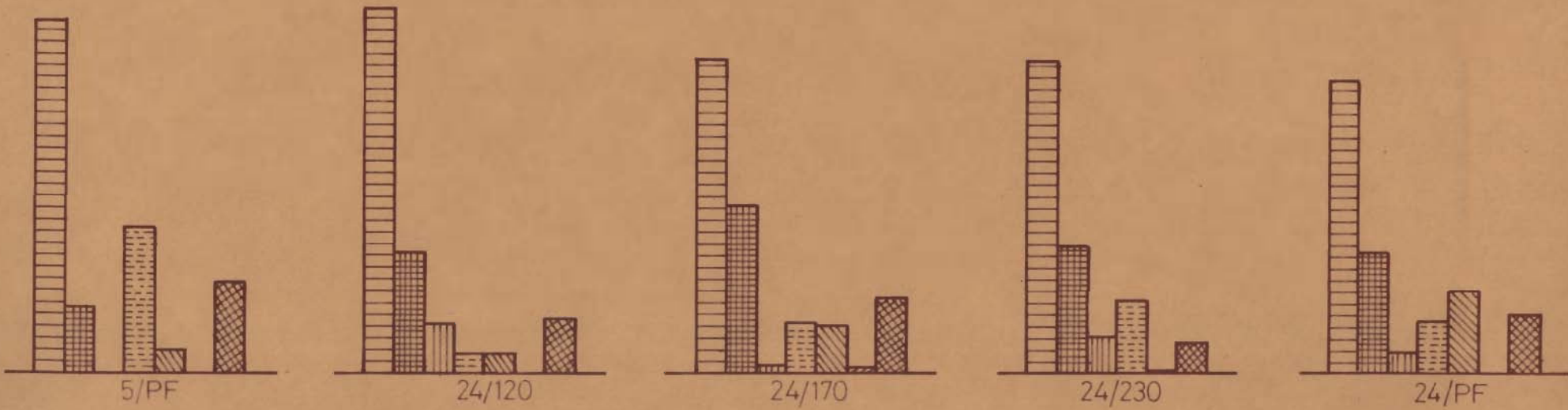
5.2.2 Description of Light Mineral Constituents

A brief description of light mineral modes and their significance is given below.

5.2.2.1 Quartz

The percentage of quartz varies from 45 to 71 for different slides, though its amount ranges from 51.4 to 55.9% for complete sand samples. Its shape varies considerably — from angular to rounded. Many grains are pitted and exhibit grounded surfaces. Striations on grain surfaces are not uncommon. Inclusions of tourmaline crystals are observed in a few grains. Tourmaline inclusions are sharp, well defined prismatic needles randomly distributed in the grain. Some grains have tiny inclusions of iron oxide, which are distributed randomly or arranged in straight lines. Quartz grains show often straight or uneven fractures. Many grains are stained by iron oxide which often penetrates the fractures of the grains. Quartz grains are distinguished from feldspar by low relief and fresh appearance.

1 [horizontal lines] 2 [grid] 3 [vertical lines] 4 [diagonal lines /] 5 [diagonal lines \] 6 [cross-hatch] 7 [dots]



174

FIG. 5-1_ HISTOGRAMS SHOWING DISTRIBUTIONS OF LIGHT MINERALS IN DIFFERENT SLIDES. 1_ QUARTZ, 2_ CHERT, 3_ K-FELDSPAR, 4_ PLAGIOCLASE, 5_ CALCITE, 6_ ARAGONITE, AND 7. OTHERS.

The use of undulosity in detrital monocrystalline quartz for provenance interpretation declined significantly since Blatt and Christie (1963) suggested that broad overlap in character of undulosity of plutonic and metamorphic quartz makes determination of undulosity of quartz of little value in source identification. Also these workers observed that flat stage microscopic measurements of undulosity lack validity because they bear no simple relation to the true values which are measurable on a universal stage. However, Blatt, Middleton and Murray (1972, p. 272 - 274) observed that number of crystal units in sand sized grains of polycrystalline quartz varies depending on the source rock of quartz.

More recently Basu et al. (1975) suggested that the distinction among quartz grains from different sources remains valid even when a flat stage microscope is used for determination of undulosity. Also determination of undulosity of monocrystalline quartz, percentage of polycrystalline quartz and number of crystal units per grain leads to a striking discrimination of source rocks such as plutonic, and low, medium and high rank metamorphic rocks.

Following Basu et al. (1975), four types of detrital quartz were recognized i.e.,

- (i) quartz with single crystal unit, having $\leq 5^\circ$ undulosity, called as monocrystalline, non-undulatory quartz,

- (ii) quartz with a single crystal unit, having $>5^{\circ}$ undulosity named monocrystalline undulatory quartz,
- (iii) polycrystalline quartz with 2-3 crystal units per grain and
- (iv) polycrystalline quartz with more than 3 crystal units per grain.

Percentages of different types of quartz are also listed in Table 5.1. Different slides and the whole sand samples are represented in the diagram of Basu et al. (1975) (Fig. 5.3). All slides and samples fall in the low to high rank metamorphic provenance zones of the diagram.

5.2.2.2 Chert

Chert grains constitute 3 to 25% of different slides and 8.0 to 11.7% of whole sand samples. These grains show turbid appearance with low relief. Some grains show a slight fibrous nature and exhibit anomalous optical properties. These also show surficial fractures.

5.2.2.3 K-feldspars

The K-feldspars constitute upto 12.5% of detrital grains of different slides, but form 8 to 11.7% of whole sand samples. Many grains show twinning according to

Table 5.1- Modal analysis of different slides and samples

Slide/sample No.	Non undulose quartz	Undulose quartz	Polycrystalline quartz		Chert	K-feldspar	Plagioclase	Calcite	Aragonite	Others
			2-3 grains	> 3 grains						
5/45	18.84	11.54	8.33	15.73	18.84	3.14	6.80	1.05	0.52	15.20
5/80	20.49	16.40	7.17	17.42	8.54	3.98	14.23	1.14	0.57	10.05
5/120	12.29	30.73	4.92	14.75	12.05	1.45	13.50	0.96	-	9.34
5/170	8.39	28.29	4.19	16.76	6.63	-	19.38	3.06	1.02	12.28
5/230	5.56	27.79	16.67	6.67	12.30	1.07	12.30	0.54	0.54	16.57
5/PF	10.99	28.39	0.92	10.07	9.65	-	20.90	3.21	-	15.87
24/120	14.41	24.02	6.73	12.48	18.51	7.93	3.17	3.17	-	9.57
24/170	8.43	22.76	6.74	8.43	24.92	1.16	7.53	6.95	0.58	12.50
24/230	6.19	27.40	7.96	7.96	20.42	6.18	11.76	4.95	0.62	6.54
24/PF	10.54	21.08	4.87	8.11	21.39	3.05	7.94	12.83	-	10.18
77/45	30.11	9.26	6.95	22.00	7.70	1.92	8.66	-	0.48	12.92
77/120	23.33	14.73	11.05	19.64	5.62	12.50	5.62	1.25	-	6.25
77/170	28.37	15.89	10.21	5.68	14.12	9.41	7.85	2.61	-	5.84
77/230	25.85	14.96	17.69	9.52	7.82	-	15.05	1.81	-	7.30
77/PF	33.77	5.28	10.55	5.28	14.18	5.03	13.74	1.82	-	10.36
33/120	32.69	5.45	5.45	15.26	17.71	1.71	7.43	-	-	14.29
38/120	29.92	8.55	6.41	10.68	9.66	3.86	19.81	0.48	-	10.63
42/120	45.52	10.12	5.06	10.11	4.97	3.11	14.29	0.62	-	6.21
57/120	26.60	9.26	9.26	13.87	2.25	3.93	27.53	1.69	-	5.62
67/120	23.13	8.41	13.67	15.77	9.76	3.66	17.07	0.61	-	7.93
5	11.16	30.11	6.36	13.82	11.67	1.30	13.80	1.06	0.14	10.53
24	12.98	24.98	6.89	11.62	19.08	7.32	4.58	3.64	0.11	9.29
77	25.79	13.01	10.99	15.59	7.98	10.57	7.52	1.48	-	7.04

179

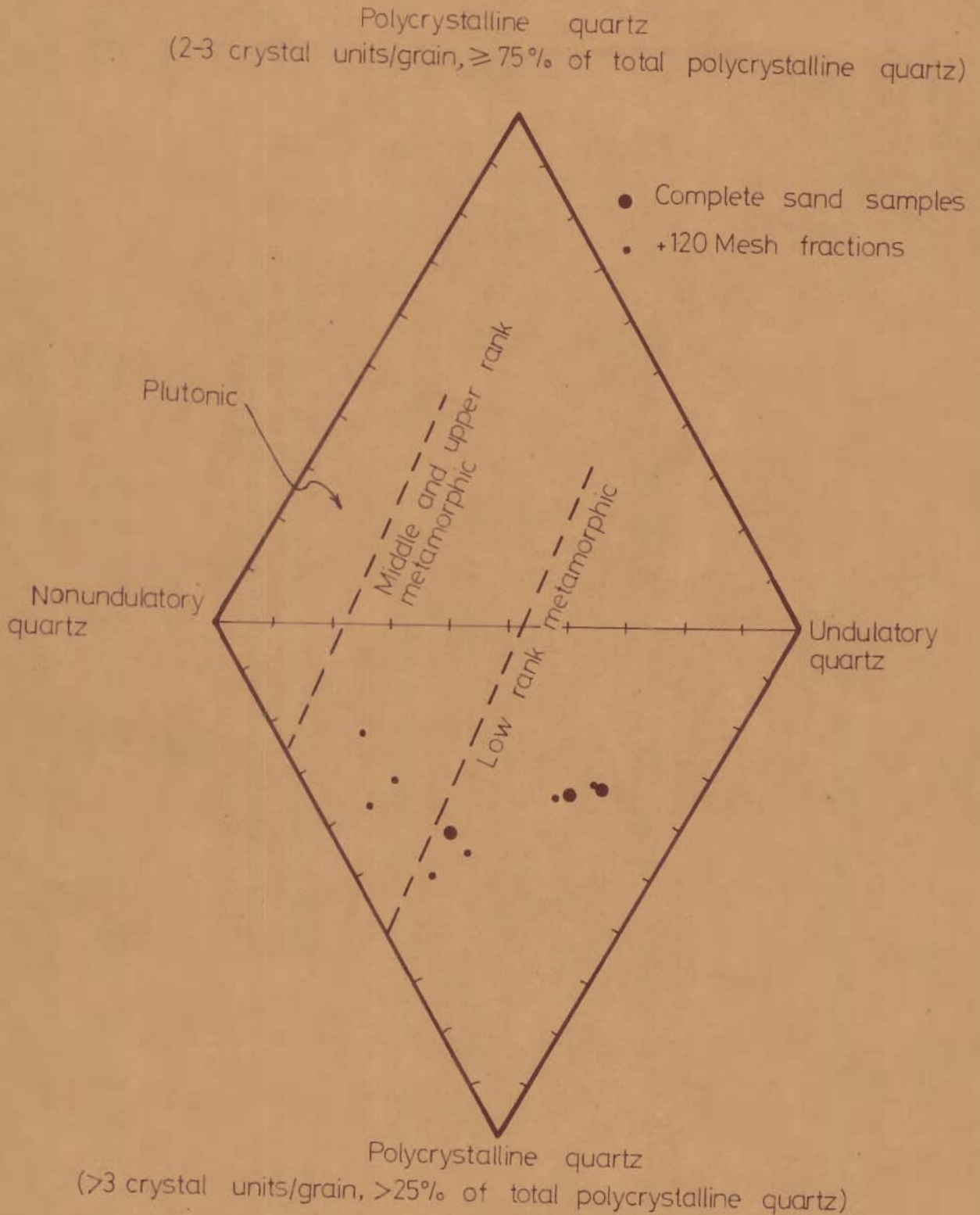


FIG.53_PLOT OF DIFFERENT +120 MESH FRACTIONS AND SAMPLES IN THE DIAMOND DIAGRAM OF BASU ET AL. (1975) FOR PROVENANCE DETERMINATION.

carlsbad law or cross-hatched twinning typical of microcline. The feldspar grains are angular to rounded in shape. On the whole, they show higher degree of roundness than quartz grains. Often feldspar grains are weathered along cleavage or twin planes which are altered to clay minerals imparting them cloudiness — a fact which helps in their diagnosis. Feldspars show all degrees of alteration from completely unaltered to almost fully altered nature. Inclusions of quartz and iron oxide are seen in a few grains.

5.2.2.4 Plagioclase Feldspars

The percentage of plagioclase feldspars shows a fair degree of variation i.e. 3 to 28% for different slides. Compositionally they are albite to oligoclase in nature. These are recognised by their well marked cleavage and albite law twin lamellae. They also show higher roundness as compared to quartz grains. A few very angular grains are also observed. These feldspars show higher degree of weathering than K-feldspars. Most of the grains show rigours of weathering and some are rendered almost opaque due to alteration to clay minerals. Alteration of feldspars is often along the twin lamellae, cleavage or fractures. A few unweathered grains are observed from -230 mesh fractions, occasionally containing inclusions of iron oxide.

5.2.2.5 Calcite

Calcite forms upto 7% grains of different slides. It occurs as well rounded grains showing pitted appearance often resulting in general grounding of the grain surface which masks its typical sheen. A few grains show clear sparry calcitic nature. Coloured spectrum bands are seen even under polarized light with characteristic sheen in some grains.

5.2.2.6 Aragonite

A few aragonite chips with woody appearance are seen. These show parallel striations. Ornamentations on some of these fragments suggest the possibility of their being chips of some shells.

5.2.3 Variation of Modal Composition with Grain Size

An examination of Table 5.1 reveals significant trends in variation of amount of different modes with grain size. The percentages of quartz and K-feldspar tend to decrease with decrease in grain size, whereas plagioclase feldspars and calcite tend to occur in higher proportions in smaller sizes. The amount of chert varies irregularly with grain size.

5.2.4 Areal Variation of Constituent Modes

The samples selected for petrographic study are from widely separated localities. These samples can thus be

analyzed to see the homogeneity of composition of sands in the area under investigation. For this purpose +120 mesh fractions of all the samples have been compared using χ^2 (chi) test. Five modal classes i.e. quartz, chert, K-feldspar and plagioclase and 'others' are recognized for this purpose. The mean of all the samples is taken as the expected value for each of the modal classes. The statistic χ^2 is then calculated as

$$\chi^2 = \sum_{i=1}^n \frac{(O_i - E_i)^2}{E_i}$$

where O_i and E_i are observed and expected frequencies of a particular modal class i , and n is the total number of modal classes. For details of χ^2 -test, Dixon and Massey (1957, p.221) may be referred.

χ^2 values for different samples (Table 5.2) indicate that four samples differ from the average modal composition significantly and the other four samples seem to come from a population with the average modal composition at 95%

confidence level. Also an examination of the contribution of the various nodes to total χ^2 for individual

samples (Table 5.2) shows that the minimum variation is shown by quartz amount and the maximum variation is shown by plagioclase amount.

A valuable property of χ^2 is that the sum of n sample values is itself distinguished as chi square with n

Table 5.2- Comparison of light mineral constituents in +120 mesh fractions to determine whether they are all from the same population.

Slide No.	Light Mineral Constituents					
	Quartz	Chert	K-felds- par	Plagio- clase	Others	
(a) Observed Frequencies						
5/120	62.69	12.05	1.45	13.50	10.3	
24/120	57.64	18.51	7.93	3.17	12.74	
33/120	58.85	17.71	1.71	7.43	14.29	
38/120	55.56	9.66	3.86	19.81	11.11	
42/120	70.81	4.97	3.11	14.29	6.83	
57/120	58.99	2.25	3.93	27.53	7.31	
67/120	60.98	9.76	3.66	17.07	8.54	
77/120	68.75	5.62	12.50	5.62	7.50	
Total	494.17	80.53	38.15	108.42	78.62	
Mean/ Expected	61.77	10.07	4.77	13.55	9.83	
(b) Contributions to Criterion $(O_i - E_i)^2 / E_i = \chi^2$						
						Total χ^2
5/120	0.01	0.39	2.31	0.00	0.02	2.73NS
24/120	0.28	7.07	2.09	7.95	0.86	18.25x
33/120	0.05	5.80	1.96	2.76	2.02	12.59x
38/120	0.10	0.02	0.17	2.89	0.17	3.35x
42/120	0.15	2.58	0.58	0.04	0.92	4.27NS
57/120	0.50	6.07	0.15	14.44	0.64	21.80x
67/120	0.01	0.01	0.26	0.91	0.17	1.36NS
77/120	0.11	1.97	12.53	4.64	0.55	19.80x
						84.15

NS- Not significant at $\alpha = 0.05$

x- Significant at $\alpha = 0.05$

$\chi^2_{4, 0.95} = 9.49$

$\chi^2_{8, 0.95} = 15.51$

degrees of freedom (Snedecor, 1956, p.213). Thus χ^2 values of different samples can be added and tested for 'homogeneity'. Cumulative χ^2 for all the samples is also significant at 5% significance level, suggesting that the samples belong to a 'heterogeneous' population.

Large scale transport of sand by wind over long distances should tend to result in a certain amount of uniformity of mineral composition of the sediments especially in the saltation loads. However, highly significant differences in the composition of saltation load of sediments (+120 mesh fraction) from different localities suggest that the wind is reworking the local sediments and cumulative sediment transport by wind is very small. Of course, it is realized that slight changes in composition of sediments could be introduced due to abrasion effects of wind. Incidentally, it should be interesting to determine the distances over which wind is able to bring about uniformity of sediment composition and thus to determine the distance of sediment transport.

5.2.5 Classification of Sands

Folk's (1968b, in Blatt et al. 1972, p.311) triangle for classifying sandstones (Fig. 5.4) on the basis of detrital modes with slight modification is used here for categorizing the sands under study. The three end-members Q, F and L representing the three ends of the triangle

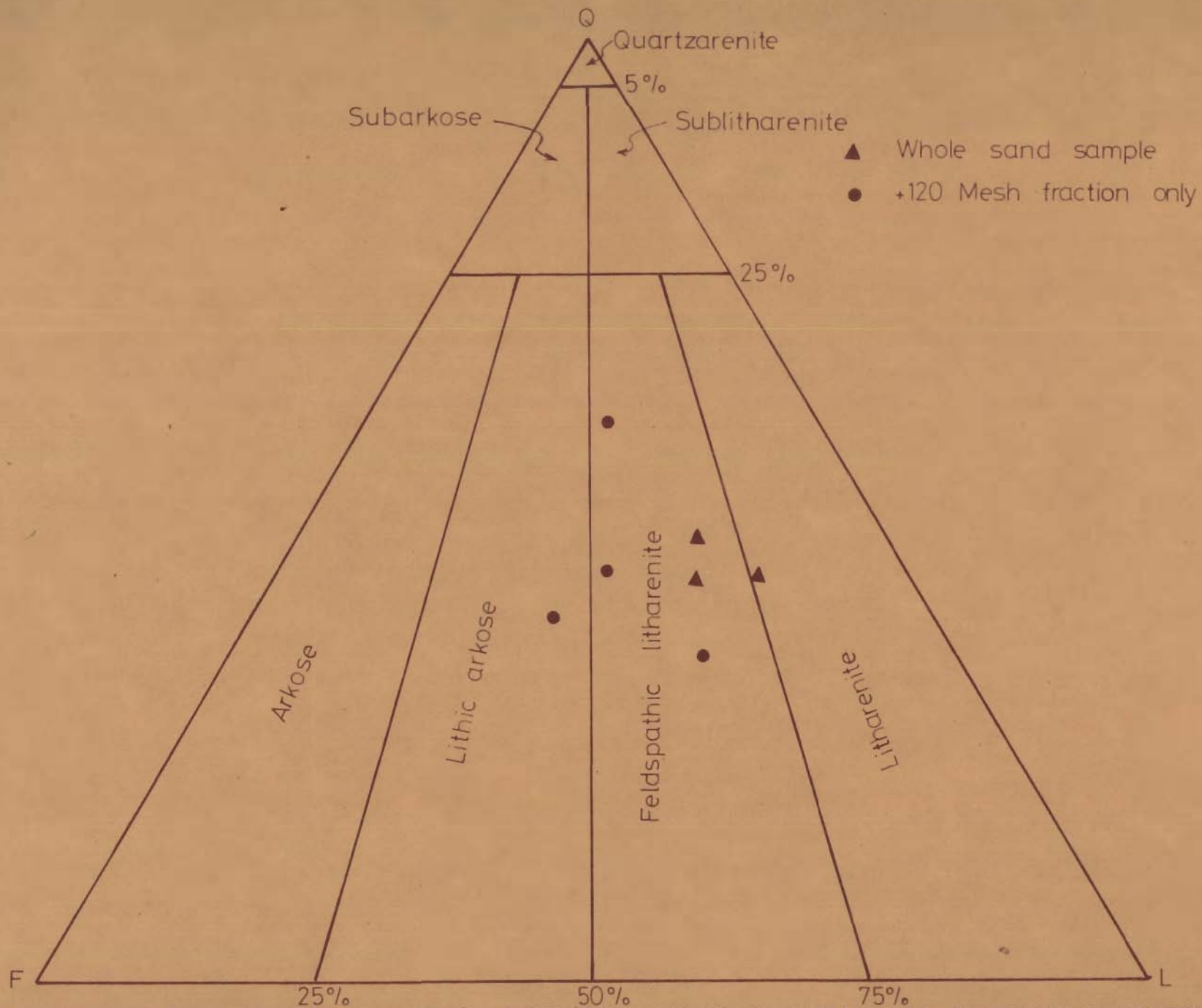


FIG. 5-4. PLOT OF SAMPLES ON FOLK'S (1968b) TRIANGULAR DIAGRAM FOR CLASSIFYING SANDSTONES.

are Q-monocrystalline quartz, F-feldspars and L-rock fragments, chert and polycrystalline quartz. Following Dickinson (1970), chert and polycrystalline quartz are included with rock fragments instead of combining with Q as suggested by Folk (1968b) so as to emphasize the aspects of provenance. According to this classification most of the whole sand samples and +120 mesh fractions fall in feldspathic-litharenite class suggesting the importance of plutonic and metamorphic rocks with preponderance of the latter as provenance of these sands.

5.3 HEAVY MINERALS

5.3.1 Method of Study

Since sands are coated with ferruginous material, the desired grain size fraction of the sands are first boiled with dilute hydrochloric acid. Then heavy mineral fraction is separated using bromoform in a separating funnel. The heavy minerals are mounted on slides with Canada balsam and about 200 grains are counted to determine the relative abundance of different minerals by studying all the minerals in four or five fields of view.

Four fractions i.e. +120, +170, +230 mesh and pan fractions of two samples with numbers 24 and 77 and +230 mesh fractions of other six with numbers 32, 33, 38, 42, 46 and 57, are studied in the manner described above. The

data are given in Table 5.3 and are represented in the form of histograms in Figures 5.5 - 5.6.

5.3.2 Description of Heavy Minerals

Hornblende, zircon, staurolite, kyanite, sphene, sillimanite and andalusite are the major nonopaque heavy minerals. Monazite is observed only in sample 24. A brief description of these minerals is attempted below.

5.3.2.1 Hornblende

Hornblende is the most abundant heavy mineral and its percentage varies from 22.8 to 43.7. Most of the grains are subrounded but some elongated fragments are also noticed. Many grains show development of schiller structure. Some grains are pitted and have fractures.

The body colour of hornblende is green, but some samples contain a few brown hornblende grains. Also green hornblende grains show uneven colour distribution, deepest in the centre becoming paler towards the peripheries. Green hornblende is strongly pleochroic, from bottle green to pale yellow colour. Brown hornblende is also strongly pleochroic and the colour varies from golden yellow to brown.

Extinction angles, when measured with crystal boundaries (cleavage being indistinct) for green hornblende range from 5° to 15° . Brown hornblende shows higher extinction angles of 20° to 22° .

Table 5.3 - Percentages of different minerals in heavy mineral fractions

Sample No.	Hornblende	Kyanite	Staurolite	Sillimanite and andalusite	Zircon	Tourmaline	Rutile	Sphene	Monazite	Opagues
24/120	30.8	0.5	-	-	22.1	-	8.1	2.2	4.3	31.9
24/170	22.8	3.5	-	-	23.7	-	14.1	3.0	6.1	21.7
24/230	36.7	1.7	3.3	-	13.9	-	11.1	2.8	6.1	24.4
24/PF	50.6	2.4	1.8	0.6	16.5	-	2.9	3.5	2.9	18.8
77/120	26.7	1.6	11.2	-	9.6	0.5	6.4	7.0	-	36.9
77/170	27.4	1.6	15.6	-	18.3	-	9.1	2.7	-	25.3
77/230	37.6	2.1	3.1	1.5	10.8	1.0	4.1	10.8	-	28.9
77/PF	42.9	1.1	14.3	0.6	14.9	-	5.1	7.4	-	13.7
32/230	42.3	1.2	9.5	1.2	13.7	-	5.4	4.8	-	22.0
33/230	34.7	2.3	2.3	9.2	10.4	-	4.0	16.8	-	19.7
38/230	26.4	1.9	1.9	6.9	12.6	1.3	5.0	15.1	-	30.2
42/230	41.3	4.2	8.4	1.2	12.0	-	4.8	8.4	-	19.8
46/230	34.8	1.7	1.1	6.1	9.9	0.6	6.1	13.3	-	26.5
57/230	43.7	3.2	10.3	2.2	11.3	-	9.2	4.9	-	15.1

601

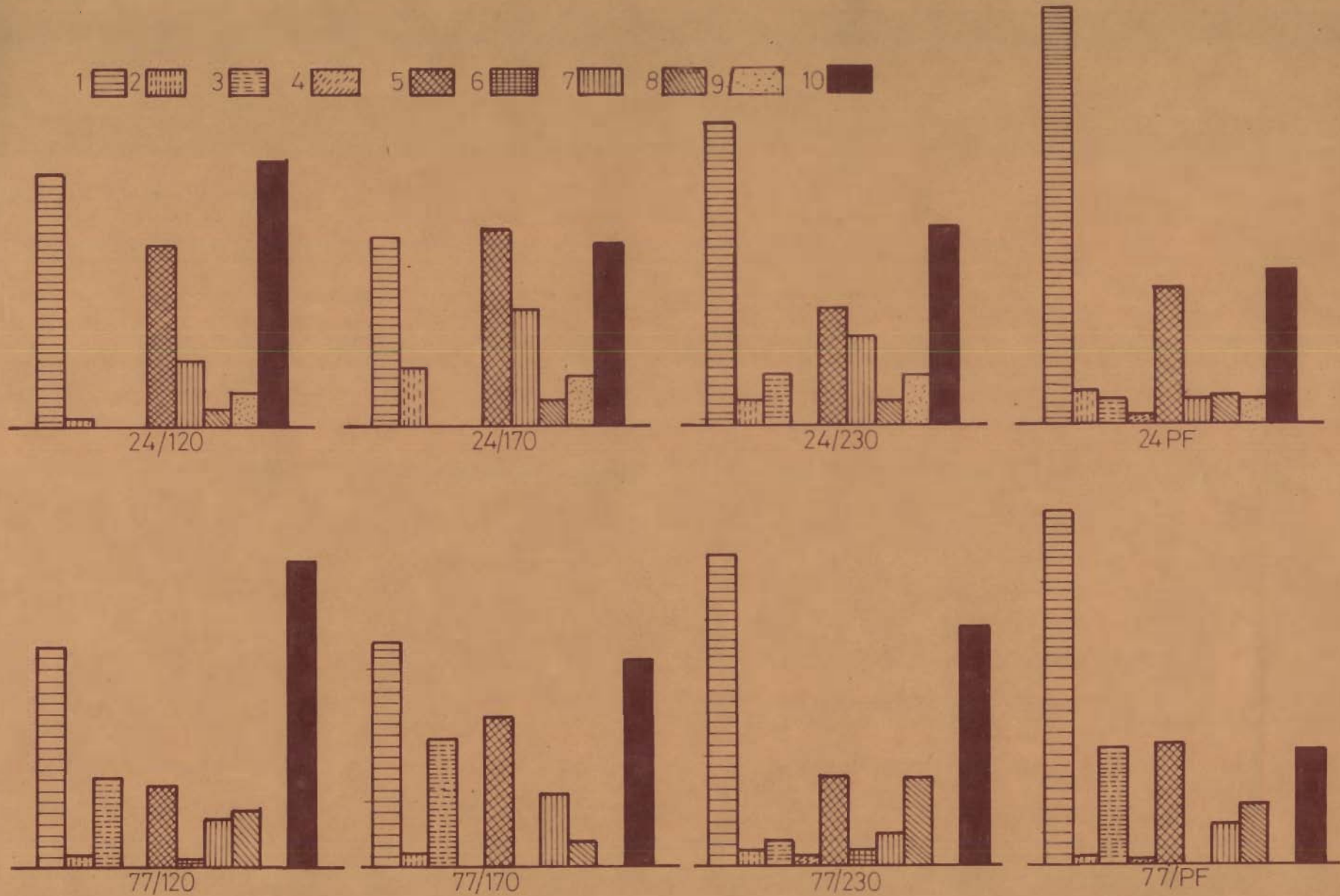


FIG. 5.5_ HISTOGRAMS SHOWING DISTRIBUTIONS OF HEAVY MINERALS IN DIFFERENT SIZE FRACTIONS OF SAMPLES 24 AND 77. 1-HORNBLENDE, 2-KYANITE, 3-STAUROLITE, 4-SILLIMANITE & ANDALUSITE, 5-ZIRCON, 6-TOURMALINE, 7-RUTILE, 8-SPHENE, 9-MONAZITE, AND 10-OPAQUES.

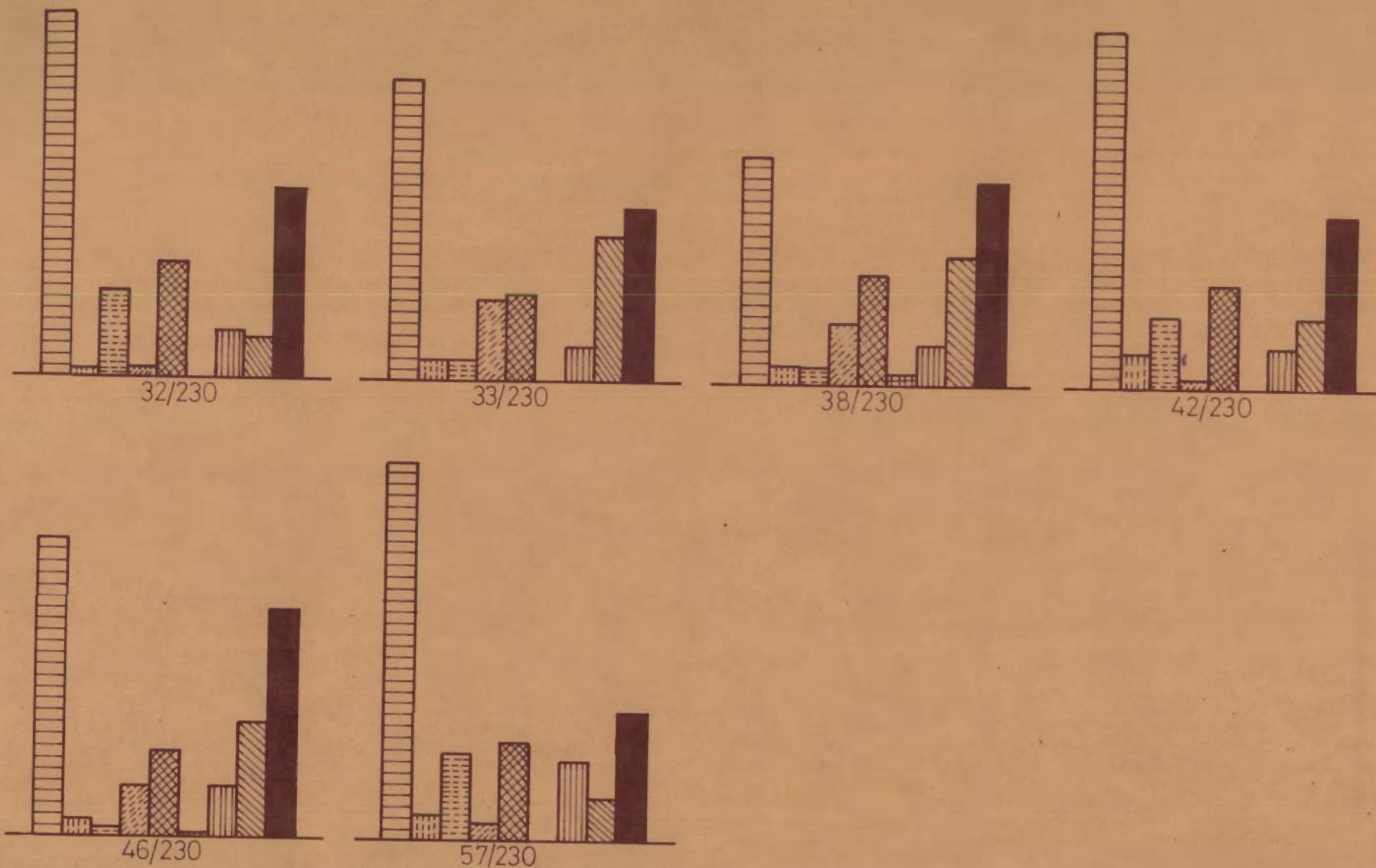


FIG 5-6_ HISTRGRAMS SHOWING DISTRIBUTIONS OF HEAVY MINERALS IN SAMPLES FROM DIFFERENT LOCATIONS. SYMBOLS ARE THE SAME AS IN FIGURE 5-5.

Many grains show alteration to iron oxides especially along cleavage planes or fractures. Some grains show sharp edges probably due to splitting. Inclusions of iron oxides and apatite are not uncommon.

5.3.2.2 Kyanite

Kyanite grains show uneven surface due to flaking. It has a very high refractive index. Extinction angle is low and varies from 5° to 8° . One grain shows inclusions of rutile. Grains show partings which are at right angles to the grain elongation.

5.3.2.3 Staurolite

Amount of staurolite varies from 1.1 to 15.6% . Staurolite shows considerable variation in form and habit. Most of the grains are short and stumpy and others exhibit irregular platy forms with distinct cleavage and fractures. It has pleochroic colours from pale yellow to golden yellow.

5.3.2.4 Sphene

A few grains of sphene are always present in all the slides. It occurs as irregular or slightly rounded grains, whereas a few euhedral, diamond shaped grains are also noticed in some slides showing brown to brownish yellow colour with very high index of refraction under cross nicols. It never shows complete extinction

due to high dispersion. Some grains are marked by a network of fractures which criss-cross the grain.

5.3.2.5 Rutile

Rutile occurs as either euhedral, slightly rounded or even anhedral prismatic grains with characteristic foxy red or reddish brown colour. It shows strong pleochroism from weak brown to reddish brown colour. Grains are often fractured. In case of many prismatic grains, parallel striations which run more or less obliquely to the prism boundary are observed.

5.3.2.6 Other Minerals

Grains of nonopaque minerals such as actinolite, sillimanite, andalusite and tourmaline are also noticed. These occur in very subordinate amounts. Also a fairly large amount of opaque minerals are recorded.

Similar heavy mineral assemblage has been reported from the aeolian sands of Barner district by Rao (1962).

5.3.3 Areal Variation of Heavy Mineral Frequencies

Heavy mineral frequencies of +230 mesh fractions of different samples are compared with the values for the mean of all these samples, using χ^2 test as described earlier. Seven classes i.e. hornblende, staurolite,

Kyanite, sillimanite, zircon, rutile, sphene and 'others' are recognized for this purpose. Calculations are shown in Table 5.4.

The analysis brings out the fact that the maximum variation is shown by staurolite, sphene and rutile frequencies. Five samples are not different from the average value whereas other three are considerably different from the average value at 5% significance level suggesting that there is probably higher uniformity in heavy mineral frequencies of samples than light mineral frequencies. These samples belong to a "heterogeneous" population as indicated by sum of χ^2 for all the slides. Only sample 33 shows strong deviations from average values for both light and heavy minerals. Other slides showing significant difference from the average heavy mineral frequencies are 24/230 and 57/230, but these samples show similar light mineral composition as the average of +120 mesh fractions of all the samples analysed. Significance of this observation is not obvious at this stage.

5.4 PROVENANCE OF THE AEOLIAN SANDS

The presence of heavy minerals like spherical and elongated hornblendes and zircons and staurolite, sillimanite, kyanite, andalusite and monazite suggest a dominant low to high rank metamorphic rocks and a minor plutonic rock source for these sands. Light mineral composition and relative abundance of different types of quartz give a similar provenance.

Table 5.4- Comparison of heavy mineral frequencies in +230 mesh fractions to determine whether they are all from the same population

Slide No.	Hornblende	Staurolite	Kyanite + Sillimanite + Andalusite	Zircon	Rutile	Sphene	Others
-----------	------------	------------	------------------------------------	--------	--------	--------	--------

(a) Observed Frequencies

24/230	36.7	3.3	1.7	13.9	11.1	2.8	30.5
32/230	42.3	9.5	2.4	13.7	5.4	4.8	22.0
33/230	34.7	2.3	11.5	10.4	4.0	16.8	19.7
38/230	26.4	1.9	8.8	12.6	5.0	15.1	31.3
42/230	41.3	8.4	5.4	12.0	4.8	8.4	19.8
46/230	34.8	1.1	7.8	9.9	6.1	13.3	27.1
57/230	43.7	10.3	5.4	11.3	9.2	4.9	15.1
77/230	37.6	3.1	3.6	10.8	4.1	10.8	29.9
Total	297.5	39.9	46.6	94.6	49.7	76.9	195.6
Mean	37.2	5.0	5.8	11.8	6.2	9.6	24.5

(b) Contributions to Criterion $(O_i - E_i)^2 / E_i = \chi^2$

								Total χ^2
24/230	0.01	0.58	2.90	0.37	3.87	4.82	17.47	14.02x
32/230	0.70	4.05	1.99	0.31	0.10	2.40	0.26	9.80NS
33/230	0.17	1.46	5.60	0.17	0.78	5.40	0.94	14.52x
38/230	3.14	1.92	1.55	0.05	0.23	3.15	1.89	11.93NS
42/230	0.45	2.31	0.03	0.00	0.32	0.15	0.90	4.16NS
46/230	0.15	3.04	0.69	0.31	0.00	1.43	0.28	5.90NS
57/230	1.14	5.62	0.03	0.02	1.45	2.30	3.61	14.17x
77/230	0.00	0.72	0.83	0.08	0.71	0.15	1.19	3.68NS

78.19

x Significant at $\alpha = 0.05$
 NS Not significant $\alpha = 0.05$

χ^2 6, 0.95 = 12.59

χ^2 8, 0.95 = 15.51

The presence of chert, however; points to some contribution from sedimentary rocks also.

Comparison of light minerals of +120 mesh fractions and heavy minerals of +230 mesh fractions of samples from different areas using χ^2 test suggest that samples have significantly different composition from each other and they belong to a 'heterogeneous' population. Thus it seems that probably the older deposits with areally varying composition are being reworked by the wind and as such are not transported over long distances. Regarding the desert expansion, it may be said here that it occurs either due to alteration of climatic conditions, massive transport of sediments engulfing the bordering fertile lands or due to reworking of older deposits under the influence of excessive deforestation and land use. Since there is no appreciable change in the climatic conditions of the Thar desert and its bordering regions, nor there is large scale sediment transport, there should not be any cause of alarm of desert expansion particularly so when the conservation of forests and proper land use methods are adopted.

Gupta (1958) considers that sands of the Thar desert are probably derived from the beaches of pre-existing seas in the area. Wadia (1966, p.53) also finds that these sands are indistinguishable from sands of the seashore and remarks that these have been derived mostly from the Rann of Kutch and partly from the basin of the lower Indus. Ghosh's (1964) investigations reveal that most of the desert sands have

roundness similar to that of the sands of old flood plains having more rounded quartz grains than the piedmont apron sediments. He maintains that the origin of the sands of the western Rajasthan is mainly due to reworking by aeolian cycle of earlier alluvial deposits.

Usually the shoreline sediments are poor in fines, whereas the flood plains of rivers contain plenty of them along levees, in the flood basin and in ox-bow lakes. The presence of high percentage of fines in the Thar desert sediments as mentioned in section 4.2.12 and significant changes in their composition from place to place suggest their derivation from earlier alluvial deposits after reworking by the wind. In fact, sediments of most of the large deserts in the world have been considered to be derived from the loose alluvial deposits of the Pleistocene times (Madigan, 1946; Holm, 1960; Alimen, 1965; Smith, 1965).

CHAPTER-6

ENGINEERING PROPERTIES6.1 INTRODUCTION

The use of soil as an engineering material and its behaviour towards various civil engineering structures forms an interesting field of study which demands a detailed investigation of its various engineering properties such as shear strength, permeability, compaction and mortar making property.

The area of the Thar desert under study is a virgin area and has much potential for future development, particularly from defence and traction points of view due to its strategic location near the international border. Therefore, the importance of such geotechnical investigations is self-evident. Also, there is a need to classify the desert soils according to their engineering properties.

These studies may be of use in the following civil engineering construction works:

- (i) Foundation design of various structures like buildings, bridges, tunnels, canals etc,
- (ii) Flexible or rigid pavement design and the suitability of the soil as construction material for building highways, airports, railways, earthfills or cuts etc *and*
- (iii) The design of subterranean and earth retaining

structures such as underground buildings, drainage structures, pipe lines, anchored bulk-head, coffer dams etc.

6.2 LABORATORY INVESTIGATIONS

The sands of the area have been subjected to laboratory investigations to determine the following engineering properties:

- (i) Mortar Compressive Strength,
- (ii) Compaction,
- (iii) Shear Strength and
- (iv) Permeability.

6.2.1 Mortar Compressive Strength

The compressive strength of sand cement mortar is one of the most important properties to determine the suitability of sand for use as one of the constituents in the structural concrete - both reinforced and plain. Six representative sand samples from San (sample 20), Dhanana (samples 25 and 32), Murar (sample 34), Ramgarh (sample 38) and Lunar (sample 77) are used to determine the mortar compressive strength using ordinary ACC Portland Cement with the properties given in Table 6.1.

The cement sand cubes were prepared by mixing the two in the proportions of 1:3. The water cement ratio has been kept as 0.4. Five cubes of 2.54 cm size were prepared from each sand sample. The cube moulds are filled with mortar in

two layers and each layer was compacted thoroughly by hand.

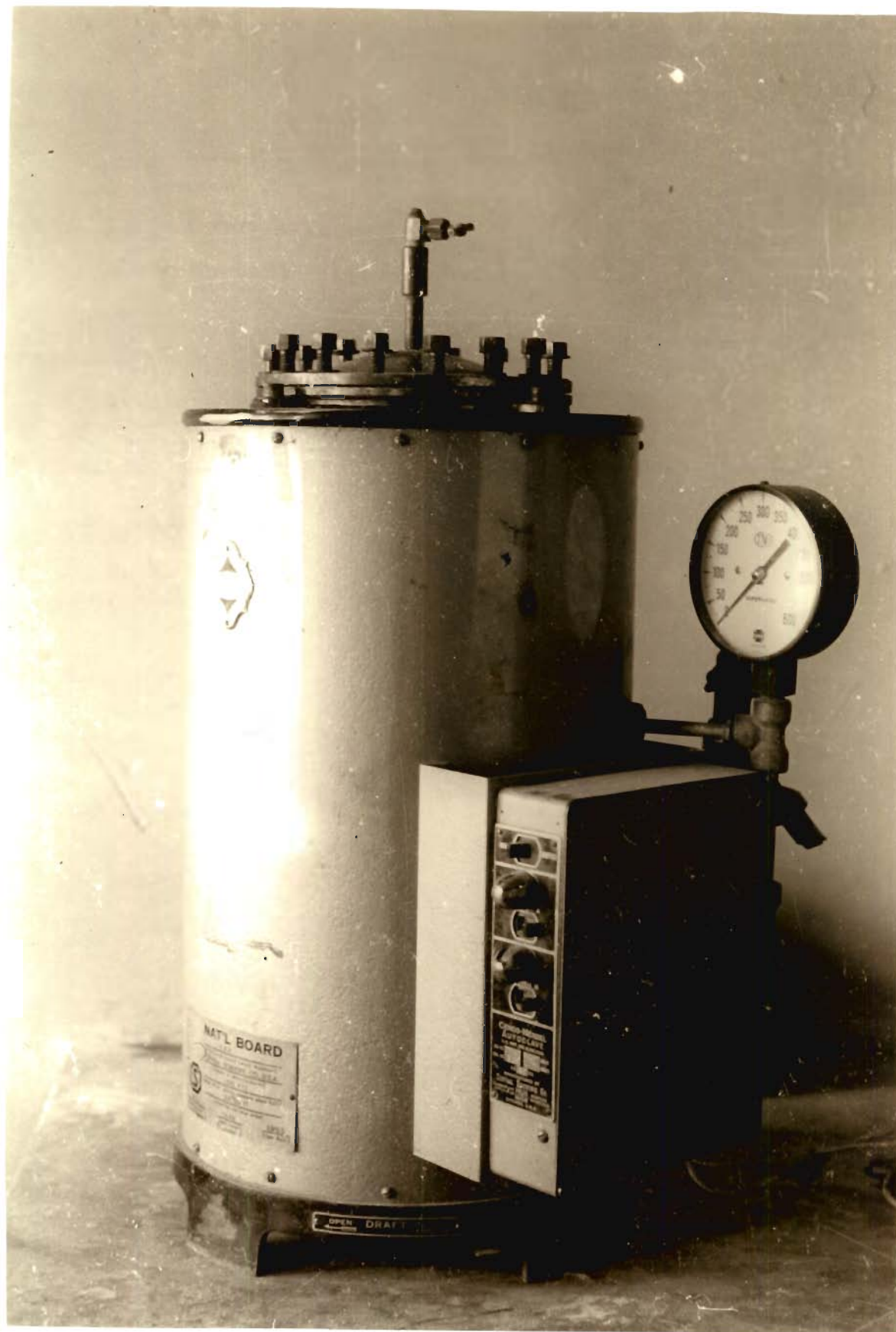
Table 6.1- Properties of ACC Portland Cement

Normal consistency-water in per cent of cement by weight.			Values specified by Indian Standard (Anon., 1967)
	26%.		
Setting time in mts	Initial	90	✗ 30
	Final	300	✗ 600
Compressive strength in kg/cm ² of 1:3 cement sand mortar (with single sized sand)	at 3 days	200	✗ 115
	at 7 days	300	✗ 175

These moulds were then kept in the constant temperature and humidity chamber for 24 hours. The temperature of the chamber was controlled at $(27 \pm 2) ^\circ\text{C}$ and relative humidity at $(90 \pm 5)\%$. The curing of concrete products can be accelerated easily by placing them in a chamber at elevated temperatures. It is, however, essential that the atmosphere should be damp to prevent drying of the product. Therefore, steam heating is a convenient way of curing. High pressure steam curing has an additional advantage of giving very high strength in a considerably short time.

The cubes were demoulded and kept in the autoclave (Fig.6.1) for high pressure steam curing. The autoclave temperature was raised to boiling point. After keeping it boiling for a few minutes to allow for the escape of air, the escape valve is closed and the pressure allowed to rise to

Fig. 6.1_ Autoclave for high pressure
steam curing.



8.44 kg/cm² (120 psi gauge) which was maintained for 12 hours. This curing time gives strength corresponding to one year's strength of normal curing at standard conditions of temperature and humidity. After this the contents were cooled slowly in four hours and were taken out of the autoclave. These cubes were then tested in the Universal Testing Machine of 5 tonne capacity. The compressive strength data so obtained has been correlated with grain size parameters M_z , σ , Sk and Ku as shown in Figure 6.2.

The compressive strength increases from 99 to 174 kg/cm² as M_z increases from 3.0 ϕ to 3.15 ϕ (Fig.6.2a). This may be due to increase in the surface area of the particles. Similarly the variation in the sorting coefficient σ also has significant effect on the compressive strength. As is evident from the curve (Fig.6.2b), compressive strength increases from 99 to 168 kg/cm² with the increase of σ from 0.25 to 0.44 ϕ .

The effect of variation in skewness on compressive strength is somewhat different than that of M_z and σ . It can be noted from Figure 6.2c that as skewness increases from 0.57 to 0.64 the compressive strength also increases from 106 to 166 kg/cm². With further increase in the skewness from 0.64 to 0.71 the compressive strength decreases gradually from 166 to 150 kg/cm². Kurtosis too has similar effect on the compressive strength as seen in Figure 6.2d. The compressive strength increases from 118

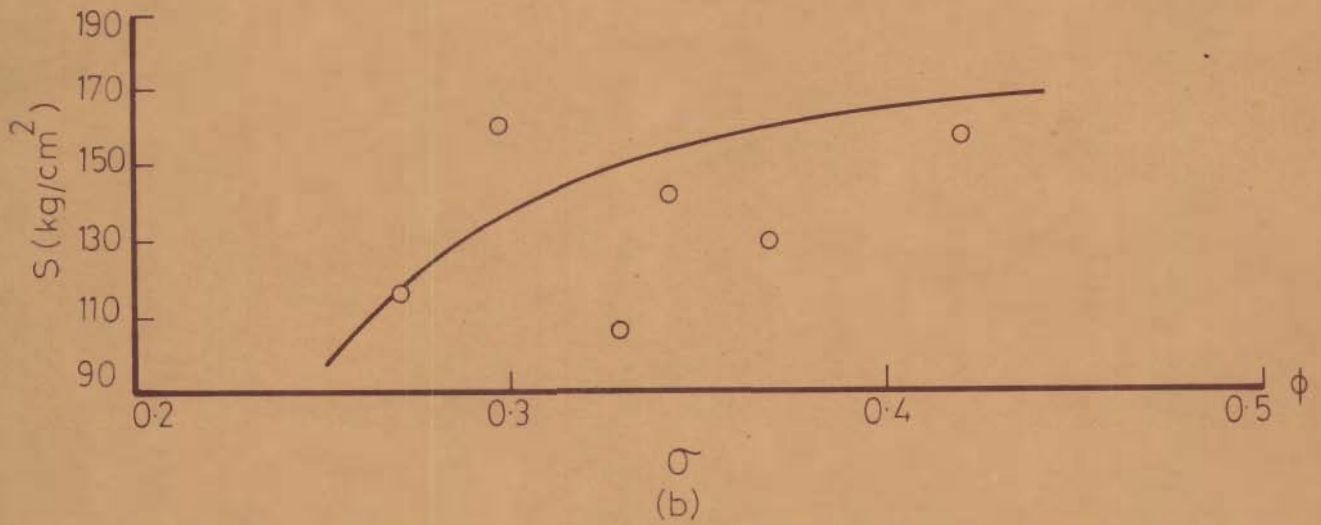
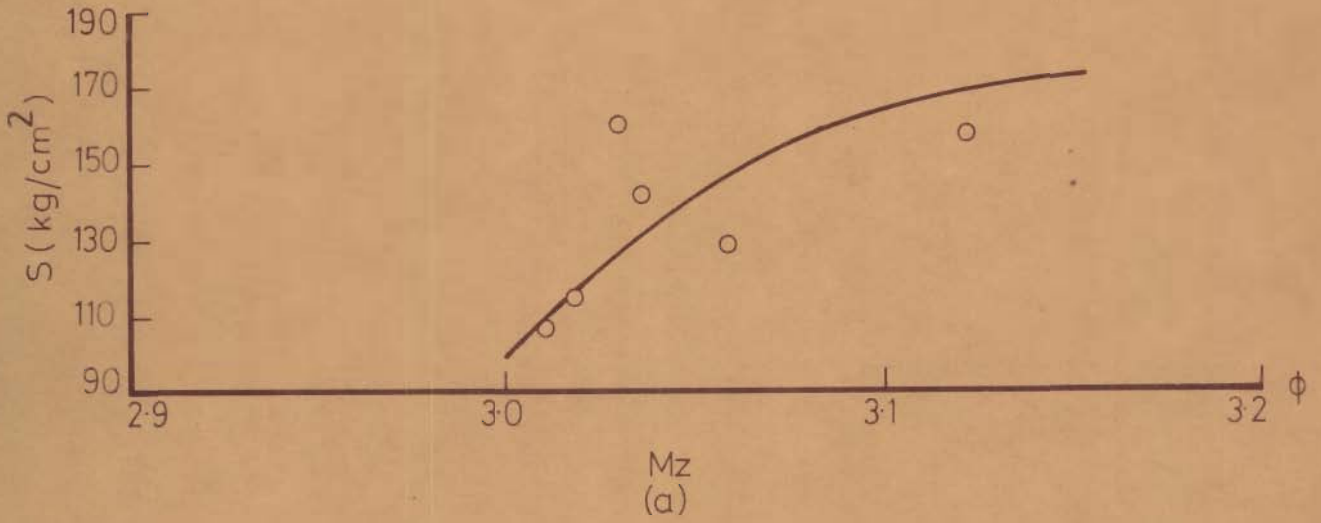


FIG.6.2 - VARIATION OF COMPRESSIVE STRENGTH WITH GRAIN SIZE PARAMETERS.

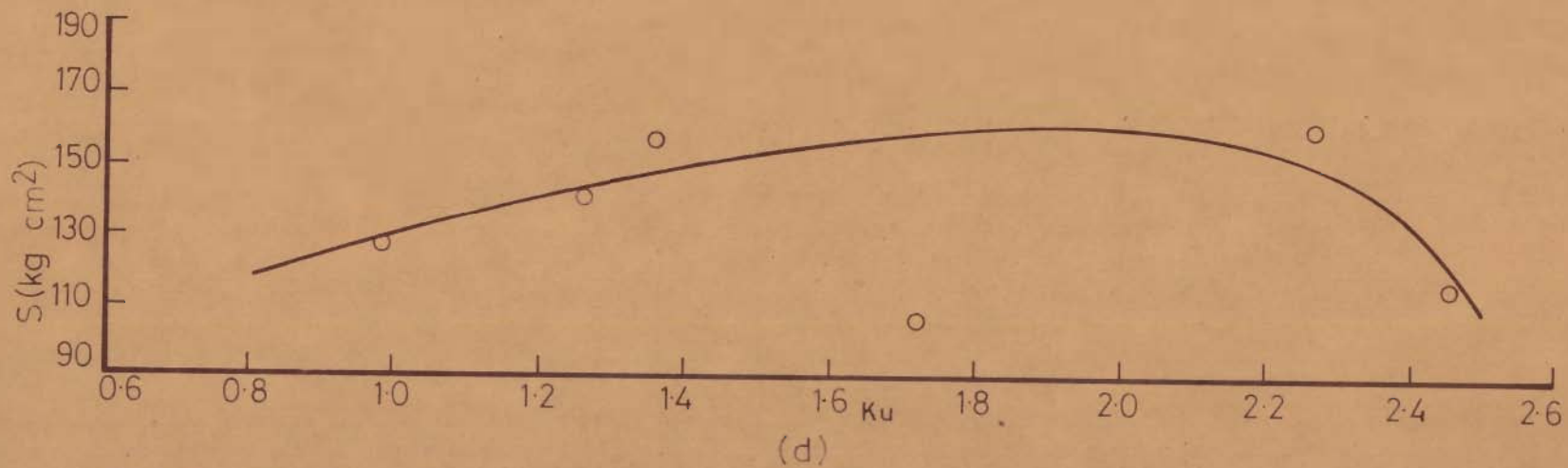
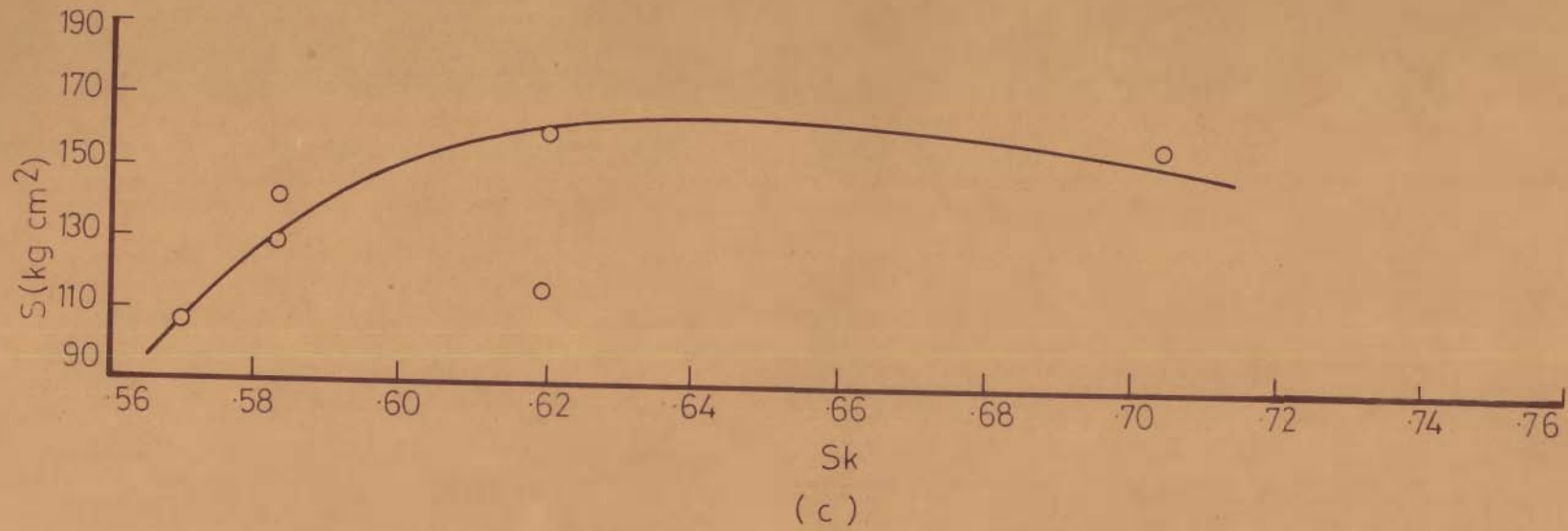


FIG.6-2_ VARIATION OF COMPRESSIVE STRENGTH WITH GRAIN SIZE PARAMETERS.

to 160 kg/cm² with the increase of kurtosis from 0.8 to 2.0. Thereafter, any increase in K_u causes a decrease in the compressive strength. As evident from the curve there is a fall in compressive strength from 160 to 110 kg/cm² with an increase in K_u from 2.0 to 2.5.

With a view to compare these results with the findings of other investigators, the mortar strength literature has been surveyed. Unfortunately, it appears that no worker has correlated mortar strength with grain size parameters employed in this study. Therefore, no comparison could be made.

6.2.2 Compaction

The compaction of soil can be defined as the process of packing soil particles closely together by mechanical treatment thereby increasing the dry density of soil. In the present investigation the standard Proctor test has been used to study the compaction which is measured quantitatively in terms of dry density to which a soil sample can be compacted. The dry density γ_d for the compacted soil is calculated from the following equation,

$$\gamma_d = \frac{W}{V(1+w)} \quad \dots (6.1)$$

where W is the weight of wet compacted specimen, w the water content and V the volume of the mould.

The test is repeated on soil samples with increasing water contents (12%, 15%, 18% and 21%) and corresponding

dry densities γ_d obtained. A compaction curve is plotted between the water content as abscissa and dry density as ordinate.

The standard Proctor test has been carried out on representative samples collected from six localities of the area namely, Dabri (sample A), San (sample B), Murar (sample C), Dhanana (sample D), Lunar (sample E) and Rangarh (sample F). The compaction curves for the above samples are discussed below.

(i) Dabri - Near Dabri (Fig.6.3a), the maximum dry density obtained is 1.64 gm/cm^3 at an optimum water content of 13.1%. The dry density at 6.3% water content is 1.63 gm/cm^3 while at 19% the dry density decreases to a low value of 1.52 gm/cm^3 .

(ii) San - In the San area (Fig.6.3b), the dry density increases from 1.63 gm/cm^3 at 6% water content to maximum dry density of 1.67 gm/cm^3 at the optimum water content of 14.4%. With further increase in water content the dry density rapidly declines to a value of 1.57 gm/cm^3 at water content of 20.25%.

(iii) Murar - At Murar (Fig.6.4a), the maximum dry density obtained is 1.61 gm/cm^3 at 9.8% water content, which is comparatively lower than those of above mentioned areas. The dry density is 1.59 gm/cm^3 at 5% water content and it decreases to 1.55 gm/cm^3 at 21% water content.

(iv) Dhanana - At Dhanana (Fig.6.4b), the dry density varies from 1.58 gm/cm^3 at 5% water content to a peak value of

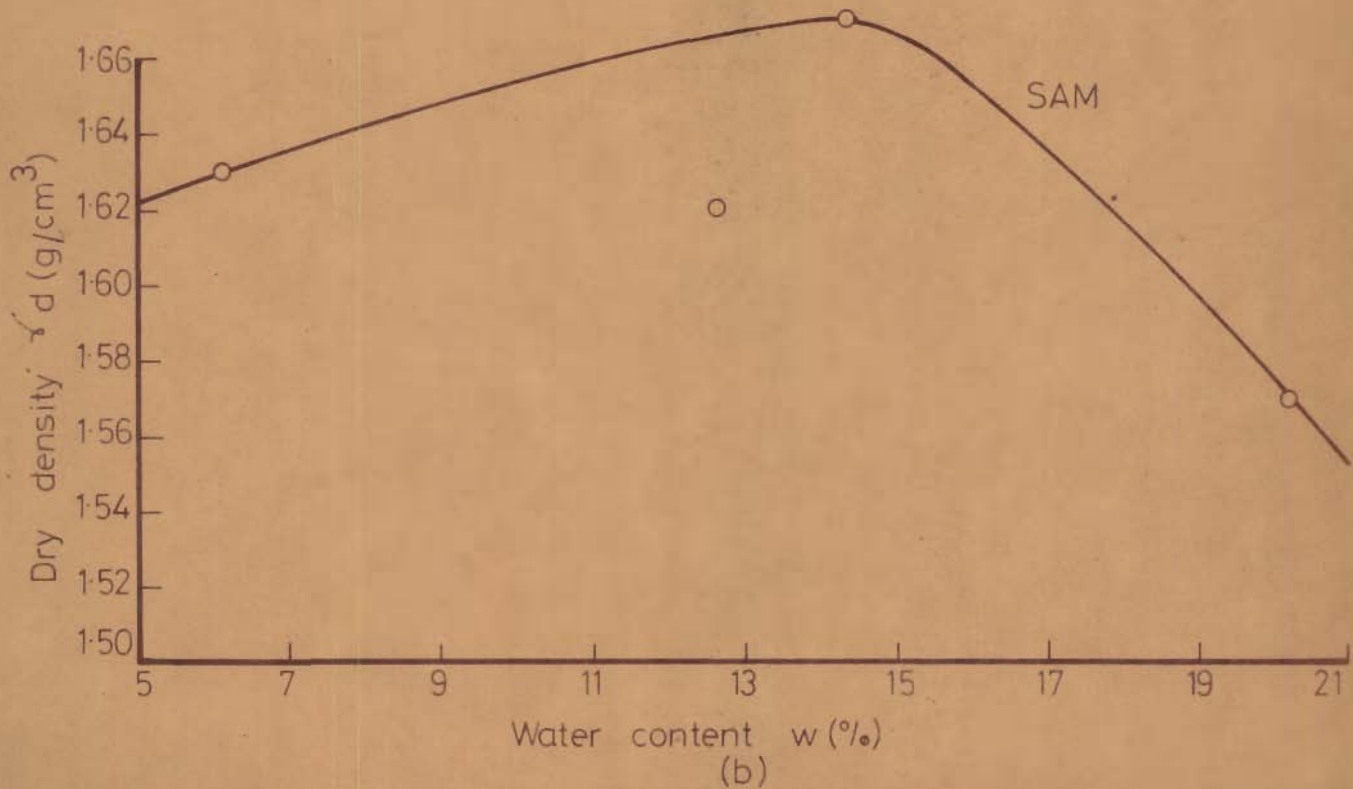
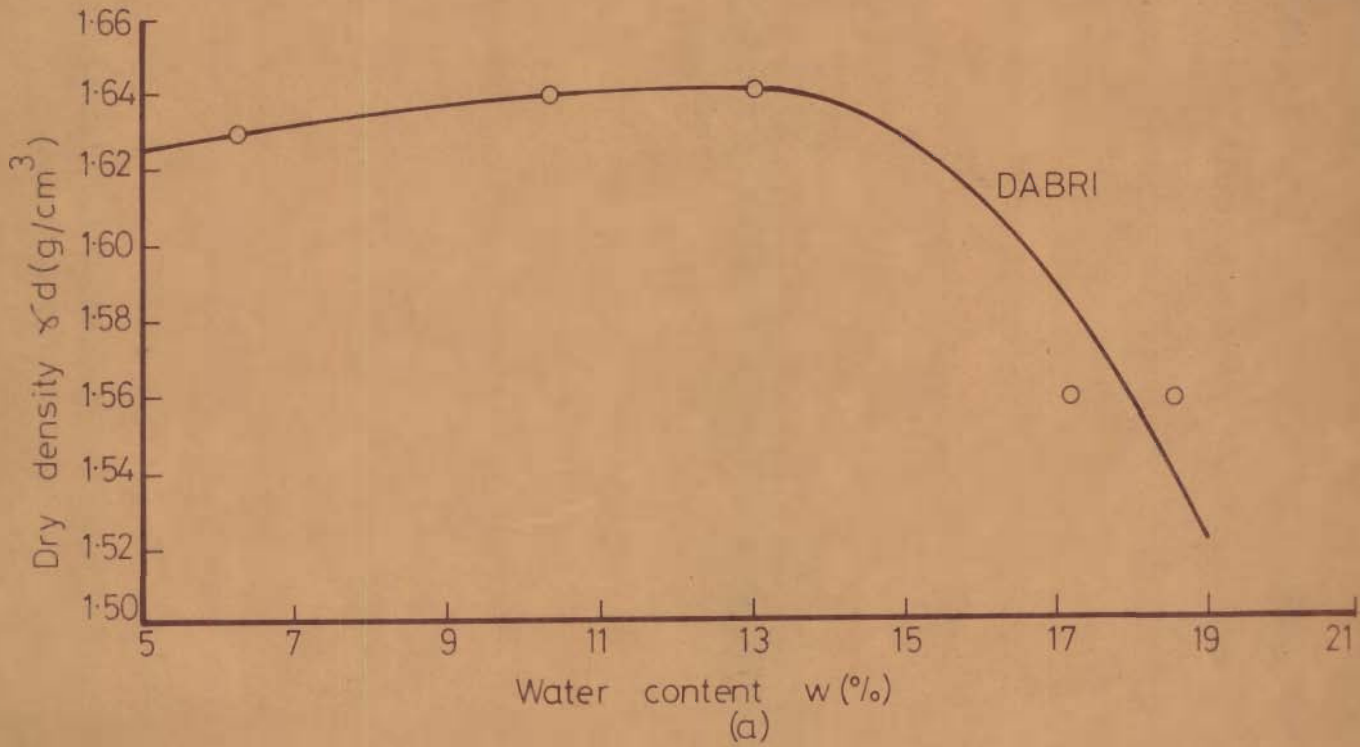


FIG.6.3_VARIATION OF DRY DENSITY WITH WATER CONTENT.

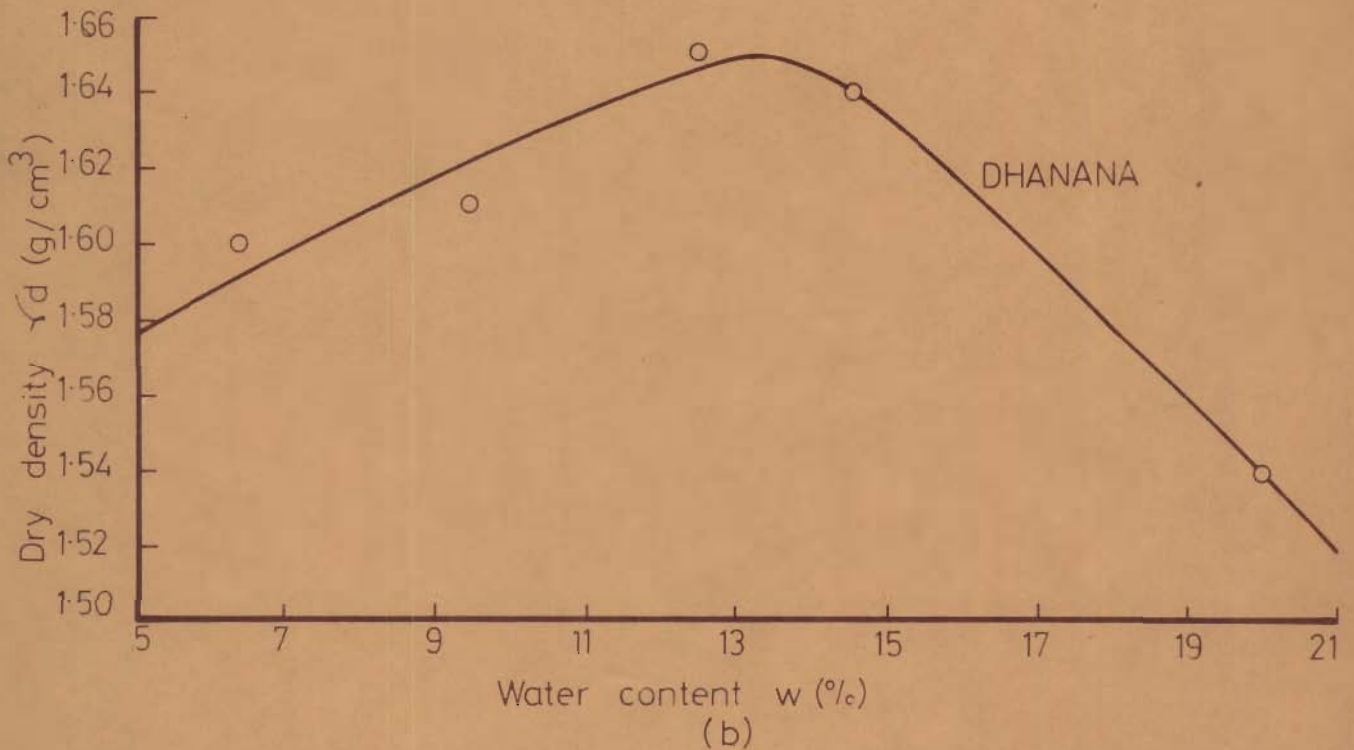
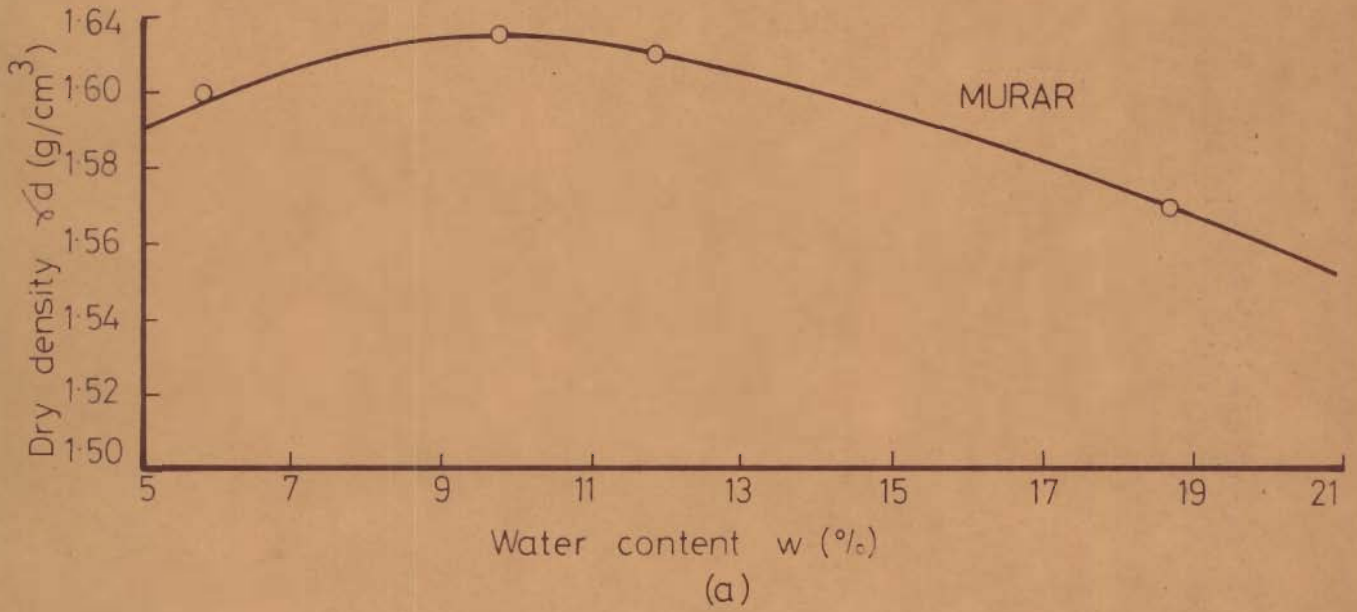
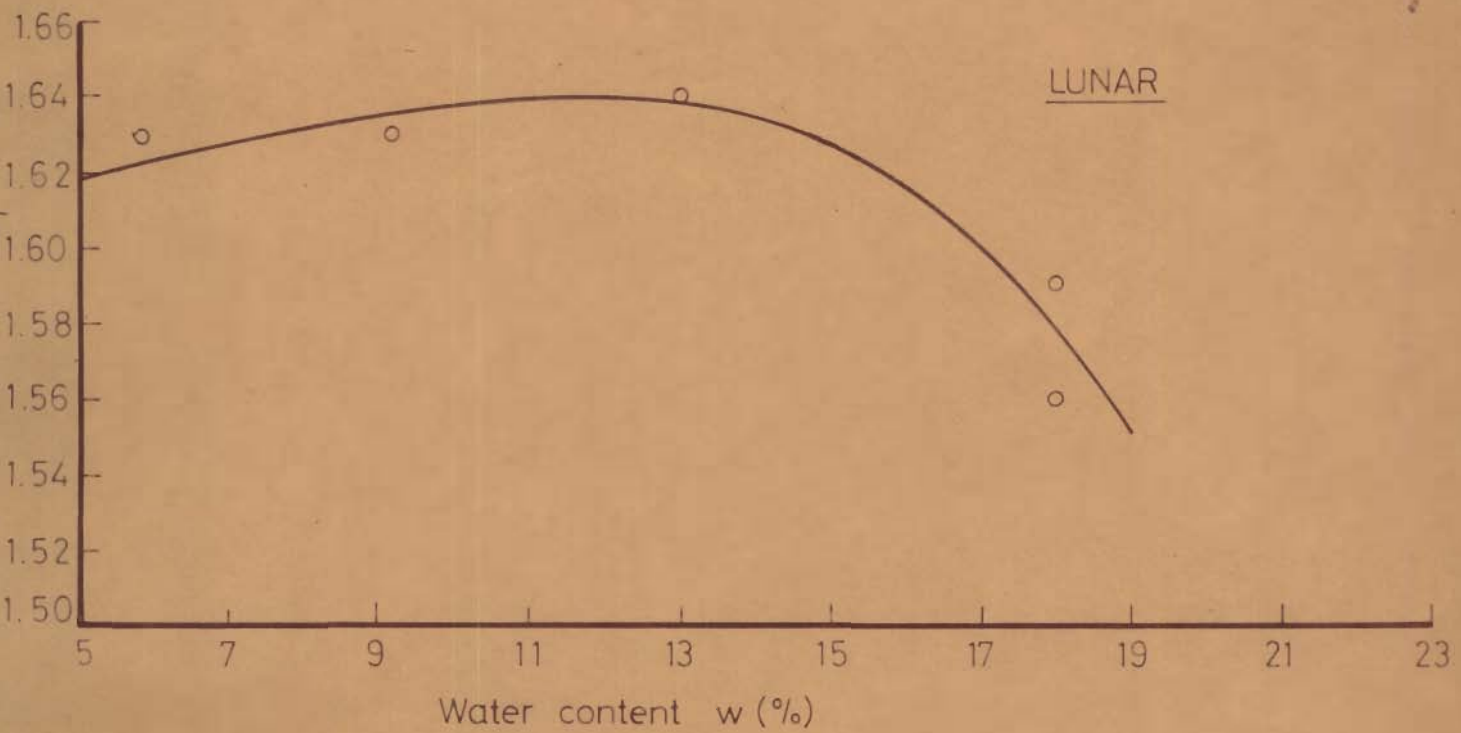
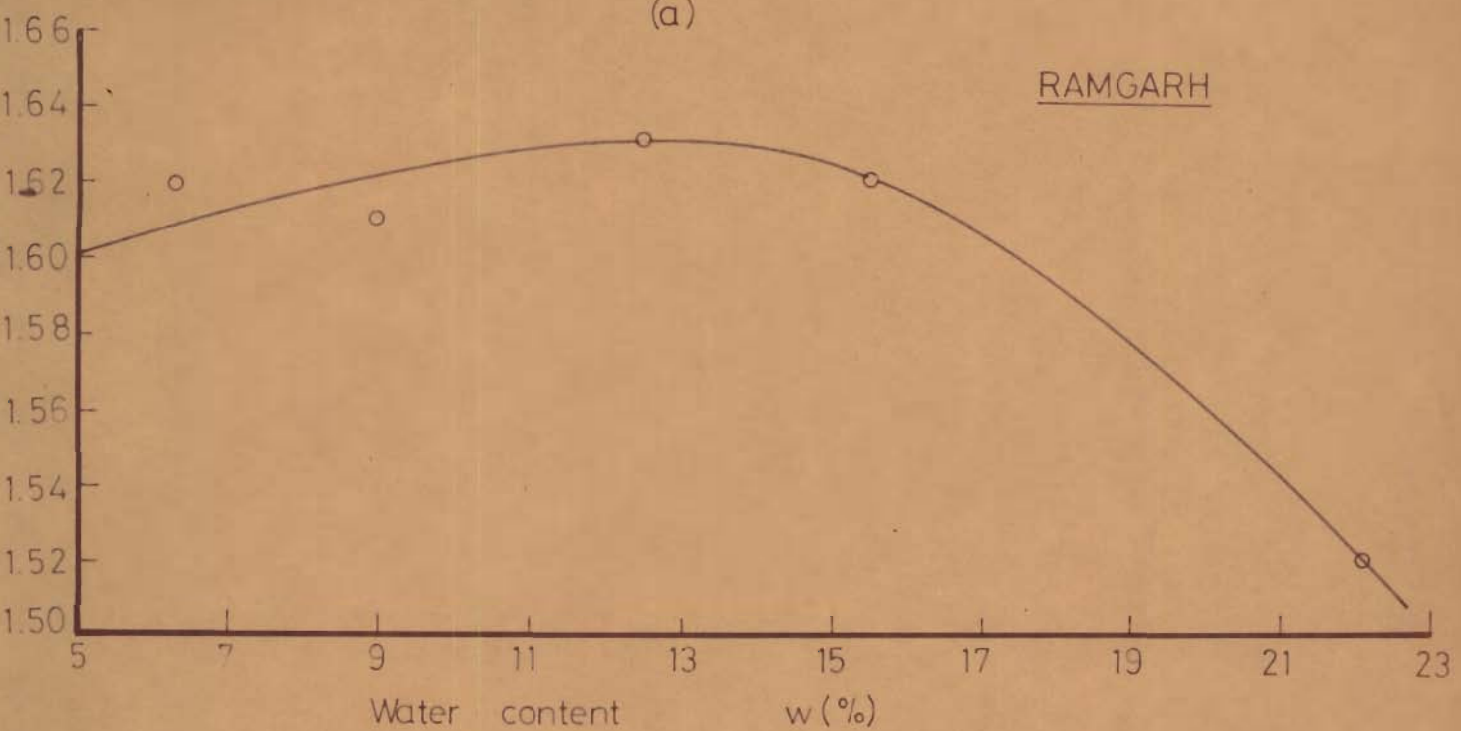


FIG.6-4_ VARIATION OF DRY DENSITY WITH WATER CONTENT.



(a)



(b)

FIG.6.5 VARIATION OF DRY DENSITY WITH WATER CONTENT.

1.65 gm/cm³ at 12% water content. It declines to 1.52 gm/cm³ at 21% water content.

(v) Lunar - At Lunar (Fig.6.5a), the dry density is 1.62 gm/cm³ at 5% water content and attains a maximum value of 1.64 gm/cm³ at 12% water content. It decreases to 1.55 gm/cm³ at 19% of water content.

(vi) Ramgarh - Figure 6.5b is a curve representing variation of dry density near Ramgarh area. Here the dry density is 1.60 gm/cm³ at 5% water content and attains a maximum value of 1.63 gm/cm³ at 13% water content which falls to a low value of 1.52 gm/cm³ at 22% of water content.

Table 6.2 summarises the values of maximum dry density ($\gamma_{d \max}$), the optimum moisture content (OMC) and the relevant grain size parameters. The variation of $\gamma_{d \max}$ has been correlated with the grain size variations of the samples from the six localities in Figure 6.6. It may be noted from Figure 6.6a that as M_z decreases from 2.89 to 3.1 ϕ the value of $\gamma_{d \max}$ continuously decreases. Therefore, it is clearly indicated that larger the grain size the smaller the $\gamma_{d \max}$. Similarly, Figure 6.6b shows the variation in $\gamma_{d \max}$ with standard deviation σ of grain size. It may be observed that as σ value increases from 0.24 to 0.36 ϕ the value of $\gamma_{d \max}$ decreases from 1.67 to 1.61 gm/cm³. This clearly indicates that poorer the sorting, lesser is the $\gamma_{d \max}$.

The range of $\gamma_{d \max}$ and OMC values of the sand samples

Table 6.2 - Bulk sample data

Sample No.	Location	Grain Size Parameter		Compaction		Permeability K (cm/sec)
		Mz (ϕ)	σ (ϕ)	γ_d max (gm/cm ³)	OMC (%)	
A	Dabri	3.10	0.37	1.64	13.1	0.33×10^{-3}
B	Sam	2.89	0.24	1.67	14.4	0.86×10^{-3}
C	Murar	3.03	0.36	1.61	12.0	0.31×10^{-3}
D	Dhanana	3.05	0.32	1.65	12.0	0.55×10^{-3}
E	Lunar	3.02	0.33	1.64	13.0	0.92×10^{-3}
F	Bangarh	2.06	0.34	1.63	12.5	0.76×10^{-3}

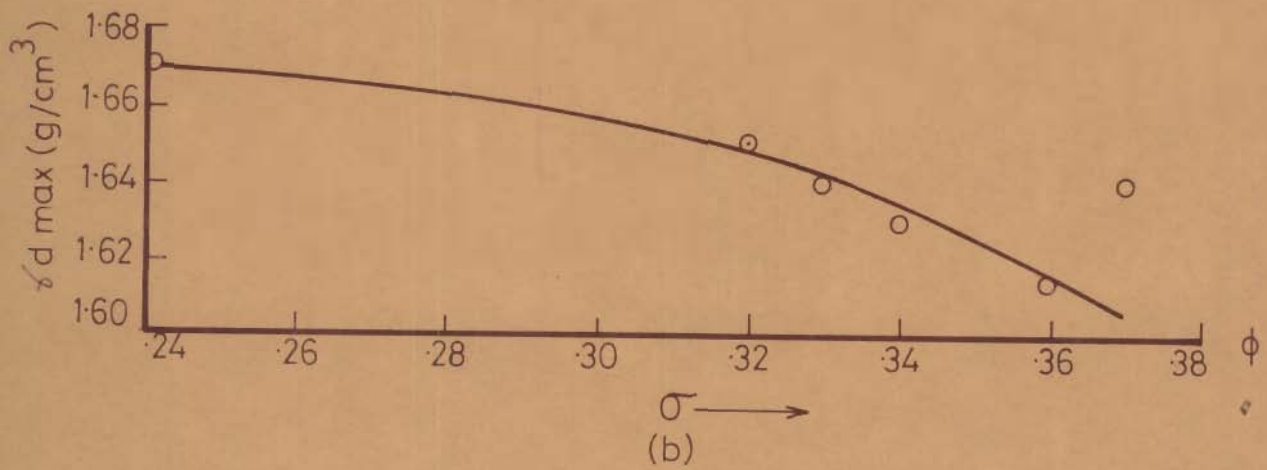
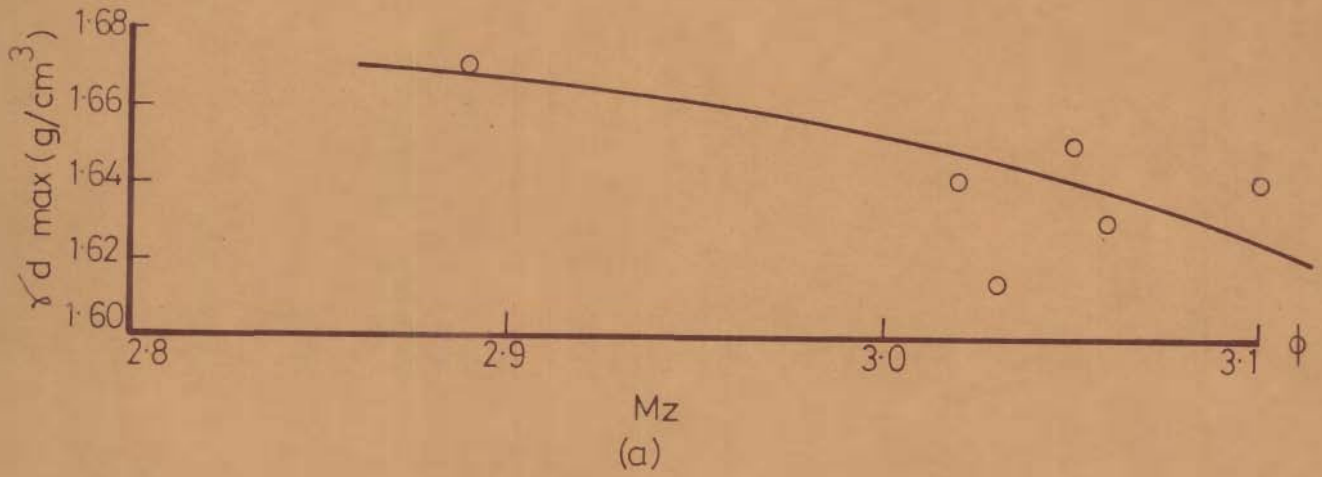


FIG.6.6_VARIATION OF MAXIMUM DRY DENSITY WITH GRAIN SIZE PARAMETERS.

investigated fall almost in SW and SP groups of soil according to Unified Soil Classification System (Anon., 1962). To the awareness of the author, no investigation has been reported which correlates $\gamma_d \text{ max.}$ and OMC with grain size parameters employed in this study.

6.2.3 Shear Strength

The shear strength of the soil is its maximum resistance to shearing stresses. It is taken to be equal to the shear stress at failure on the failure surface. It consists of (i) internal friction, or the resistance due to interlocking of particles and friction between individual particles at their contact points, (ii) cohesion, or the resistance due to interparticle forces which tend to hold the particles together in a soil mass.

The shear strength τ of soil can be represented by Coulomb's equation:

$$\tau = C + \sigma_n \tan \phi_i \quad \dots (6.2)$$

where σ_n is the normal stress on the failure plane, C the cohesion and ϕ_i the angle of internal friction.

The shear strength of the desert soil under consideration was determined by direct shear test in which the plane of shear failure is predetermined.

A graph is plotted between the normal stress σ_n as abscissa and shear strength τ as ordinate. The inclination to the horizontal of the strength envelope so obtained is the

angle of shearing resistance and the intercept on the ordinate is taken as cohesion.

Sand samples from Sam (samples 6 and 21), Dhanana (sample 31) and Lunar (sample 78) have been tested for shear strength. The results of these tests, in the form of τ vs. σ_n plots, are shown in Figures 6.7 and 6.8. The shear strength plot for sample 21 from Sam (Fig.6.7) shows that it has zero cohesion thereby indicating that clay content is almost absent. The equation of the plot comes out as $\tau = 0.606 \sigma_n$.

The sample 78 from Lunar (Fig.6.7) exhibits a cohesion of 0.145 kg/cm^2 thereby, indicating the presence of fines (-75μ) in the sand sample. The equation of the τ vs. σ_n graph for Lunar sample comes out as $\tau = 0.110 + 0.450 \sigma_n$.

The sample 31 from Dhanana (Fig.6.8) again exhibits almost cohesionless nature of the sand. The equation of the graph is found as $\tau = 0.706 \sigma_n$.

The curve of the sample 6 from Sam (Fig.6.8) has the following relation:

$$\tau = 0.055 + 0.706 \sigma_n .$$

The $\tan \phi_i$ values for the sand samples agree well with the range of values for SP and SW soil groups of Unified Soil Classification System (Anon., 1962).

6.2.4 Permeability

Permeability is defined as the property of a porous

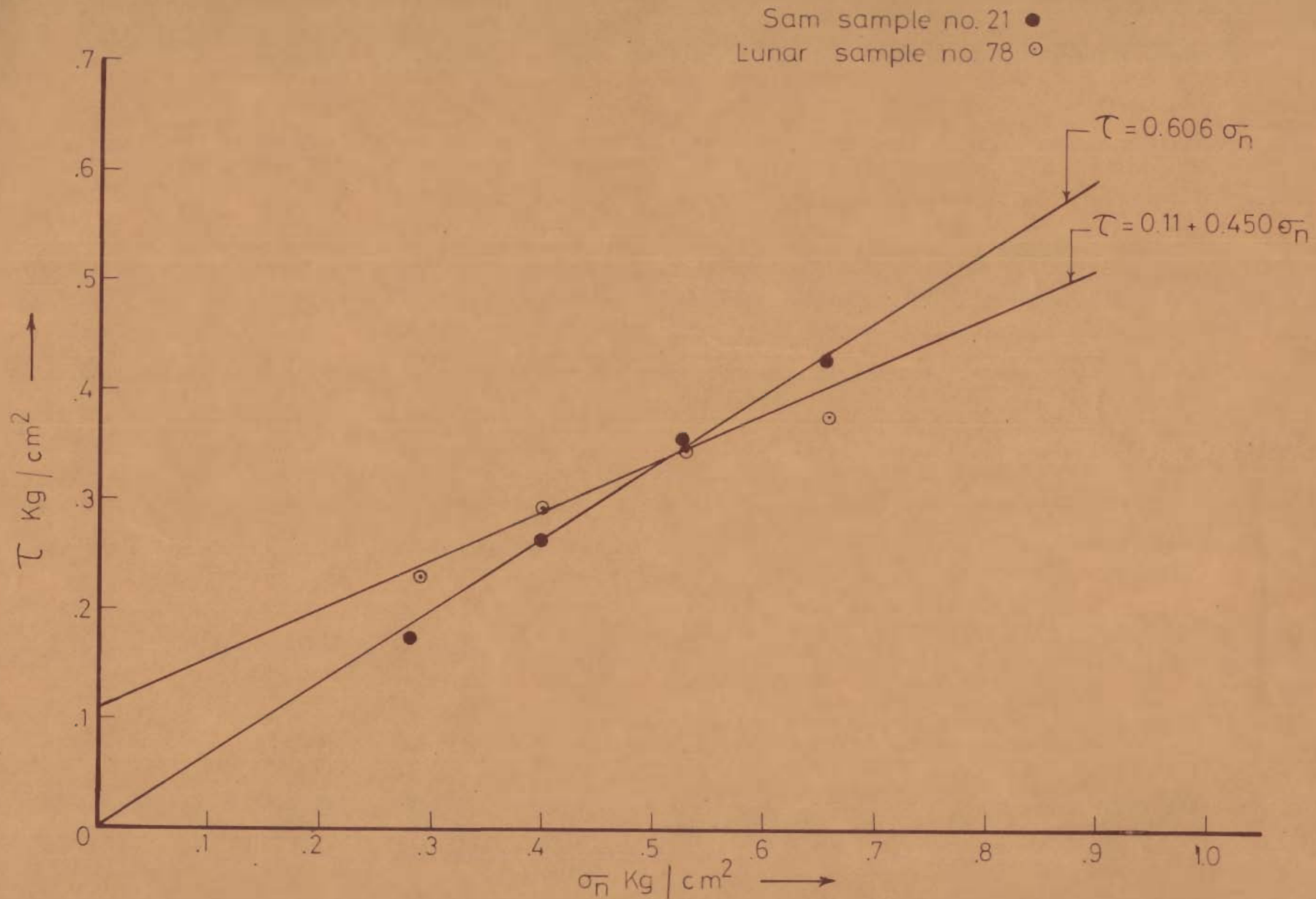


FIG.6.7_VARIATION OF SHEAR STRESS WITH NORMAL STRESS.

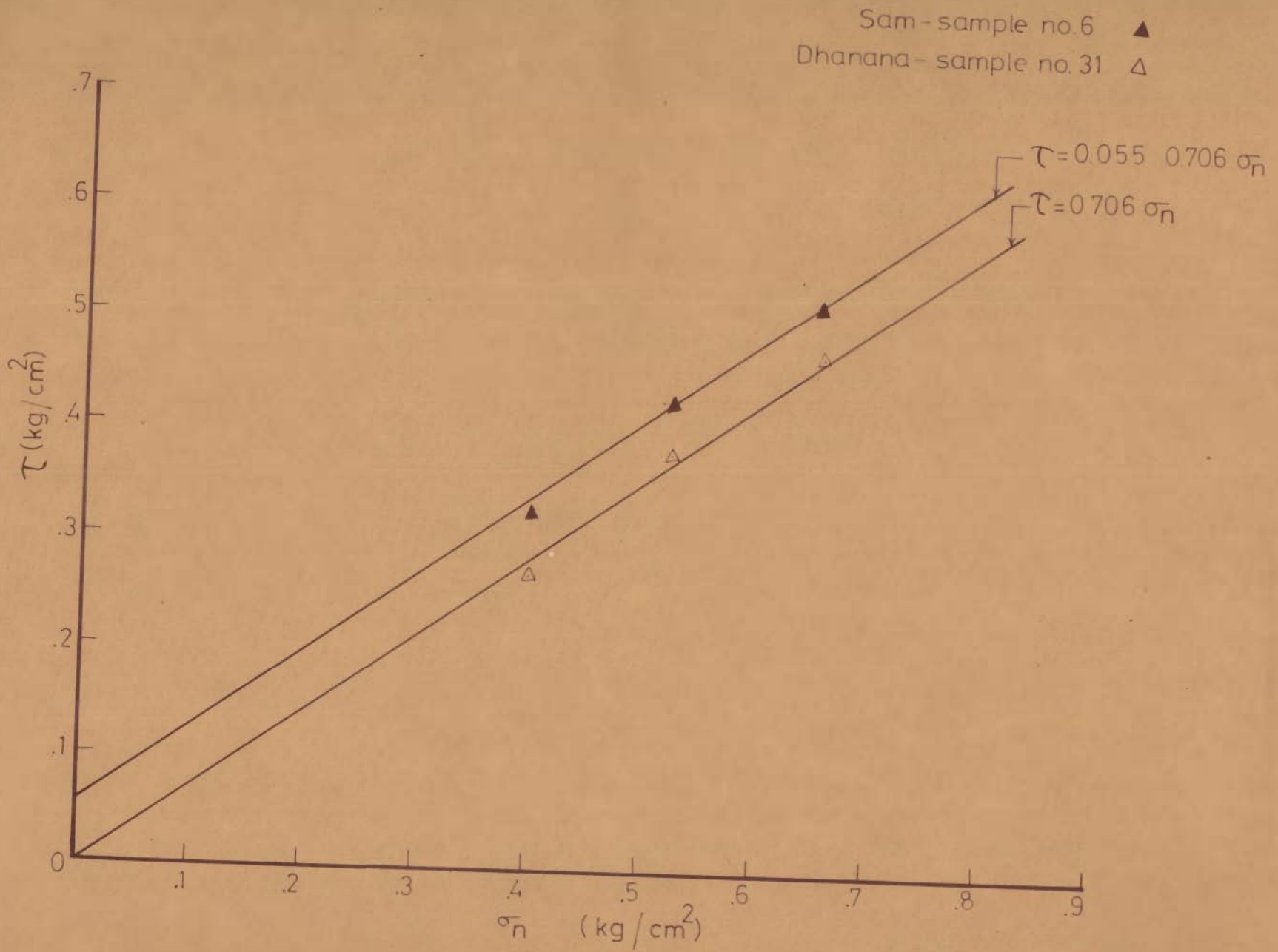


FIG.6.8 - VARIATION OF SHEAR STRESS WITH NORMAL STRESS.

material which permits the seepage of water (or other fluids) through its interconnecting voids. A material having continuous voids is called permeable.

The study of seepage of water through soil is important for many engineering problems, for example, determination of rate of settlement, calculation of seepage through the body of earth dams and stability of slope, calculation of uplift pressure under the hydraulic structures and their safety against piping, ground water flow towards wells and drainage of soils etc.

The coefficient of permeability can be determined by constant head and falling head permeability tests in the laboratory, and by pumping-out and pumping-in tests in the field. For the permeability investigations of the sand samples of the present area falling head permeability test has been performed. In this test the water is allowed to flow through the soil sample and the time 't' taken for the water level to fall from a height h_1 to h_2 is noted.

If A is the cross-sectional area of the soil sample, 'a' the cross-sectional area of the stand pipe and L the length of the soil sample, then the permeability of the soil sample is given by the expression.

$$K = 2.303 \frac{a \cdot L}{A \cdot t} \log_{10} \left(\frac{h_1}{h_2} \right) \quad \dots (6.3)$$

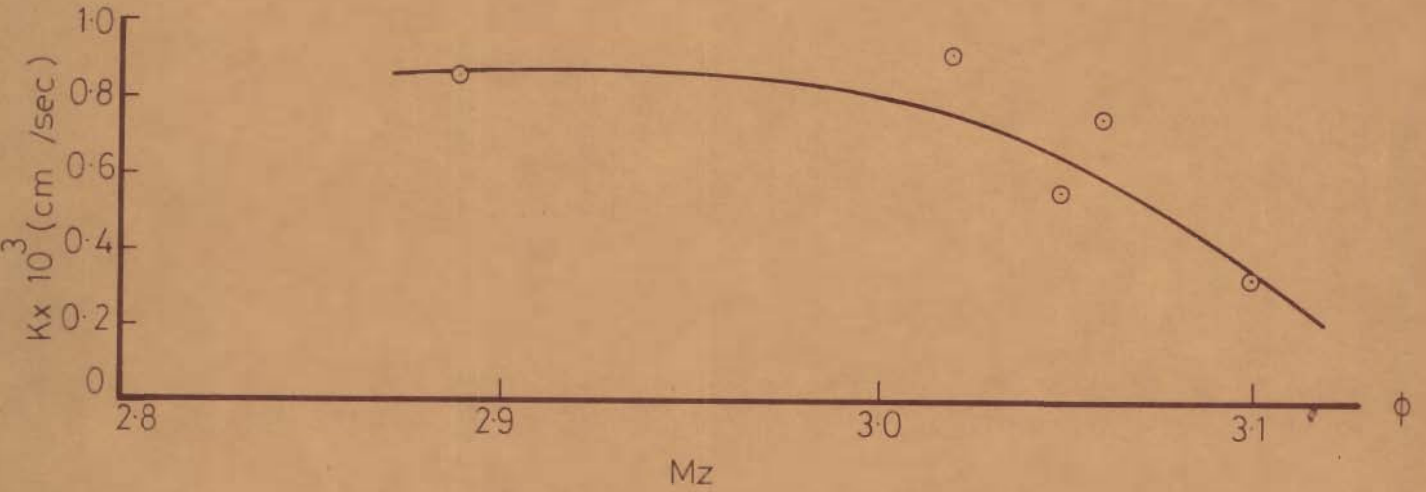
For the permeability determination, representative sand samples were collected from five localities of the area.

namely, Dabri (sample A), Sam (sample B), Murar (sample C), Dhanana (sample D) and Lunar (sample E). Table 6.2 also includes the permeability results of these samples. The variation of permeability has been correlated with grain size parameters like M_z and sorting coefficient σ . It has been found (Fig. 6.9a) that permeability decreases from a value of 0.86×10^{-3} to 0.33×10^{-3} cm/sec as M_z increases from 2.89 to 3.10. Thus, it is evident that larger grain size supports larger interstitial spaces resulting in higher permeability. From Figure 6.9b it is clearly seen that permeability is the function of sorting, as indicated by a decrease in its value from 0.9×10^{-3} to 0.33×10^{-3} cm/sec with an increase of σ from 0.33 to 0.370.

The above trends of decreasing permeability with increasing M_z and σ agree with the findings of Krumbein and Monk (1943) and Masch and Denny (1966). The values of permeability obtained correspond to the values of the soil group SP of the Unified Soil Classification (Anon., 1962).

A permeability traverse has also been prepared from the permeability test data as shown in Figure 6.10. As one proceeds from Sam to Dabri, the permeability decreases from 0.86×10^{-3} to 0.33×10^{-3} cm/sec while it again increases from Dabri to Lunar from 0.33×10^{-3} to 0.92×10^{-3} cm/sec. From Lunar to Dhanana, there is a continuous decrease in permeability from 0.92×10^{-3} to 0.55×10^{-3} cm/sec. Further, towards Murar the permeability decreases gradually from 0.55×10^{-3} to 0.31×10^{-3} cm/sec.

(a)



(b)

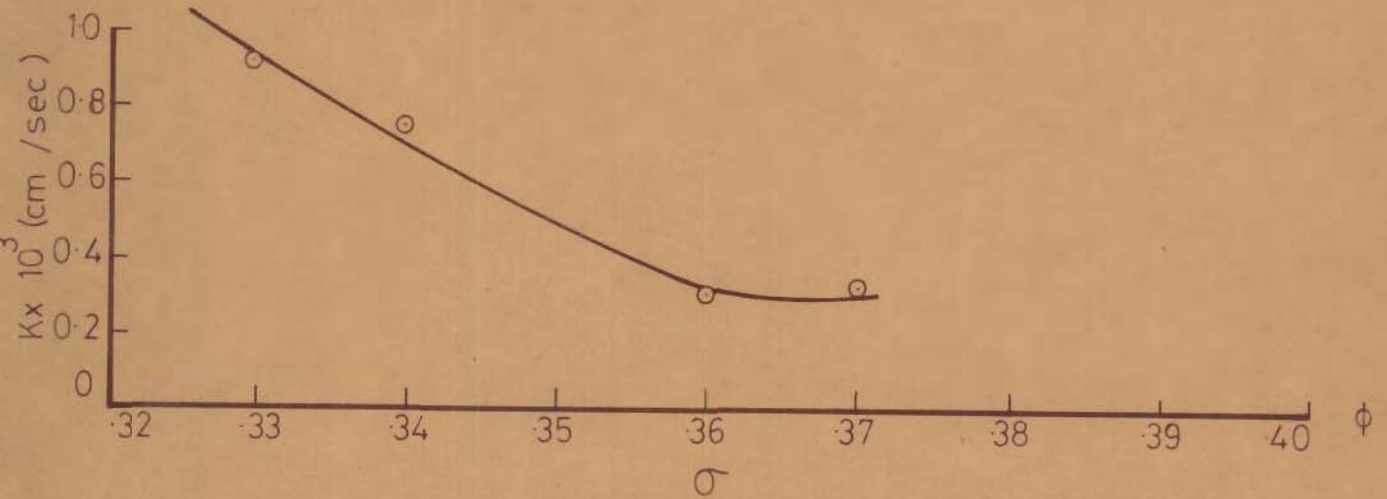


FIG.6-9_VARIATION OF PERMEABILITY WITH GRAIN SIZE PARAMETERS.

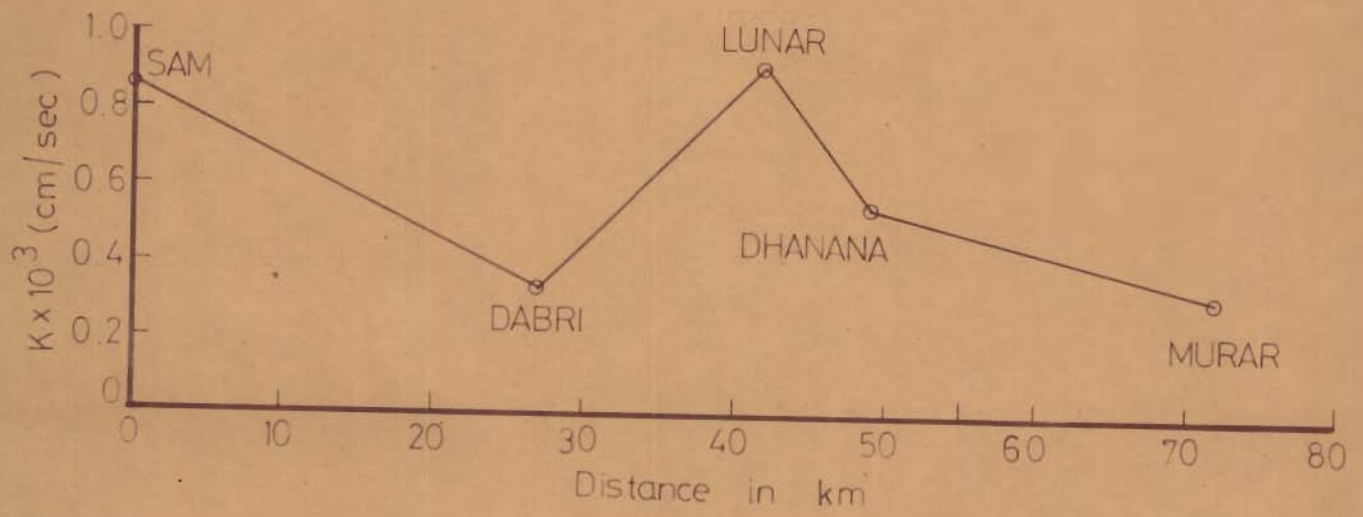


FIG 6.10_VARIATION OF PERMEABILITY, WITH DISTANCE

CHAPTER-7

SUMMARY AND CONCLUSIONS7.1 SUMMARY

The Thar desert has remained neglected geologically perhaps due to the inhospitable terrain and the extreme climatic conditions. But lately the desert has come to prominence due to its strategic location and future potential for development, particularly with the advance of work on the Rajasthan canal. Considering this, together with the author's interest in the deserts, a type area, falling in latitudes $26^{\circ}30'$ to $26^{\circ}52'$ and longitudes $70^{\circ}0'$ to $70^{\circ}33'$, in district Jaisalmer has been selected for investigations. The present study embodies fairly exhaustive and systematic sedimentological and geotechnical investigations of the sands of the area.

Climatically, the Thar desert can be referred to as a hot desert characterised by an annual rainfall of 25 cm or less and a mean diurnal range of temperature of 13.5°C or more. The relative humidity ranges between 50 to 60% in the morning hours and 25 to 35% in the afternoon hours whereas, summer relative humidity for the corresponding hours ranges between 35 to 60% and 10 to 30% respectively.

Regarding physiography, in a general way, the various features have largely been controlled by climate typical of a wind governed terrain. The sand cover may be a few meters thick, thin or absent altogether to bare the rocky

surface. There appears to be a tendency of the sand cover to thicken in the west and southwest of the area where it is occupied by longitudinal dunes separated by more or less flat and comparatively firm interdune areas. The marginal fringe of the desert where the thickness of the sand is less, barchan dunes predominate.

A review of the literature indicates that mainly climatic conditions are responsible for the initiation, growth and maintenance of the world deserts. Arid conditions of the Thar desert are attributed to the location of the Himalayan, the Kirthar and the Suleiman mountain ranges including Tibetan plateau which induce low pressures over western India and central part of Pakistan. Atmospheric dust, recent tectonic movements resulting in change of river courses and global climatic changes also might be additional causes of aridity of the region.

Regarding the age of the Thar desert, it is suggested that it came into existence about 10,000 years back, when mainly longitudinal dunes and sand piles were formed. These were stabilised during the relatively humid and warm period of 10,000 to 3,000 years B.P. The area has been subjected to wind action again since 3,000 years B.P. with the advent of arid conditions to form active barchans, transverse dunes and some sand piles. Thus the present scenario of the area is a product of the superposition of the present wind regime over the fossil longitudinal dunes and sand piles.

Three distinct types of bedforms are recognised in the area, namely, ripples, dunes and sand piles. Ripples are mostly asymmetrical, developed transverse to the dominant wind direction. Usually they are straight and parallel but at many places they show wavy strikes. Well developed branching of ripple is observed. When they branch, it is the crest line that bifurcates. Arcuate ripples tend to straighten out until they become more or less transverse to the dominant wind direction. Crests are composed of comparatively coarser grains than the troughs. Rarely, ripples of different wavelengths occur in juxtaposition, if the modality of the sand alters. Ripples are well developed on finer sands than on coarse ones.

Plots between the different ripple parameters show that ripple amplitude is proportional to the wavelength. The ripple index (λ/H) varies from 5 to 40 with a mean value of 20.1. Ripple index is minimum for a critical range of amplitude (0.45 to 0.55 cm) and it starts increasing with either increase or decrease of amplitude. Also, ripple index increases with the wavelength.

Three varieties of dunes, namely, barchans, transverse dunes and seifs are found in the area. Two families comprising active and stabilized barchans are noticed. Two morphologically distinct active barchans have been recognised. One, having a perfect crescentic shape and the other, which is reported for the first time, resembles a hat-shape. Both of

these types have similar lee slopes but they differ in their windward slopes since the latter has a narrow trench which opens on both the flanks some distance down the crest line.

Mechanism of formation of barchans has been visualized to occur in three stages such as initiation or nucleation stage, youth stage and the old stage.

The occurrence of narrow (0.5 to 1 m wide) high angle band at the toe of the lee slope and the narrow trench on the windward slope of hat-shape barchan is attributed to lee eddies and the newly reported windward eddies respectively.

Transverse dunes which are normal to the dominant wind direction, seem to originate by the lateral conjugation of two or more barchans, though their independent origin is not ruled out.

Longitudinal dunes are long, parallel, linear structures which are the dominant feature in the desert interior where sufficient sand supply is available. Their mean length is 8.8 km when measured between extreme ends. Many of them have 'Y' shaped bifurcations facing the wind direction. Their origin is attributed to the complex helicoidal wind circulations.

Sand piles may be thought as low stabilized longitudinal dunes which may be difficult to recognize in the field as linear structures.

Orientation of different bedforms indicates N 25°E to N 30°E direction of net sediment transport. Both the stabilised and active dunes give similar sediment transport directions suggesting that the same wind regime has been prevailing since the formation of stabilised dune system. The 15°N divergence of net sediment transport direction from the resultant wind direction is attributed to the 'Ekman spiral' effect.

More than one hundred samples have been collected from the various bedforms and sand flats situated in different parts of the area. Samples are analysed using ASTM sieves at half phi intervals. Two instruments - sample splitter and transfer funnel-~~were~~ designed and fabricated for quick analysis of samples. Sieve data are analyzed using IBM-1620 computer. Normal curves are fitted between the two adjacent points. Grain size parameters according to different workers are calculated.

A comparison of grain size parameters according to different workers shows that formulae of Krumbein and Pettijohn (1938) for skewness and kurtosis give very different results from those of others and these formulae should not be used for these sediments. But other formulae for the different grain size parameters give similar results. For detailed discussion, formulae of McCammon (1962) for mean and standard deviation and those of Folk and Ward (1957) for skewness and kurtosis are taken into consideration.

The average mean size for all the samples is 2.97ϕ (0.13 mm) with a S-range (\pm one standard deviation) of 2.78 to 3.26ϕ . Thus the Thar desert sediments lie on the finer side of dune sands reported earlier. The average standard deviation of all the samples is 0.37ϕ with a S-range of 0.00 to 0.76ϕ . A comparison of photomicrographs and cumulative frequency curves of typical samples brings out clearly that sorting in the present samples is a function of the ratio of mainly two populations.

Most of the samples studied are positively skewed with an average skewness of $+0.50$ and a S-range of 0.28 to 0.78 . Samples can be roughly divided into two groups with different kurtosis values. One group is very leptokurtic with kurtosis values between 1.7 and 2.45 . The other group has platykurtic character with kurtosis values lying mainly between 0.0 and 0.8 .

Study of interrelationship of the different grain size parameters brings out some interesting features. There is a significant relationship between the mean size and standard deviation and points fall around a line making an angle of about 45° with each of the axes. Standard deviation increases with decrease in mean size. Sediments become more positively skewed with decrease in mean size. These observations lead to a significant relationship between sorting and skewness. Kurtosis values tend to decrease with decrease in mean size but they seem to be independent of skewness.

Comparison of the average size parameters between the various bedforms indicates that ripples are *quite* coarse grained, poorly sorted and nearly symmetrical in nature. Sand piles and dunes are distinguished by small but distinct differences in grain size parameters. The former are fine grained, poorly sorted and more positively skewed than the latter. Further, sand piles commonly tend to fall in platykurtic group whereas dunes, in general, tend to have leptokurtic nature.

Plots of normalized heights versus grain size parameters indicate that there is an increase in grain size, improvement in sorting and change from near symmetrical nature to higher positive skewness from the foot to the crest of the dune. No significant differences between samples from windward and leeward sides of barchans are observed.

Using values of grain size parameters from sand piles and dunes, contours are drawn to study their spatial variability. There is a mean grain size 'high' in an area southeast of Lunar. The same general area forms a 'low' for skewness and standard deviation values and a 'high' for kurtosis values. A 'high' for mean grain size and similar related changes in other parameters are seen near Sam. The variation in grain size parameters in the Lunar area is thought to reflect areal grain size distribution of an older deposit which has been reworked by the wind. Changes in grain size parameters near Sam are probably a result of repeated

reworking of sand flats around Sam and piling of sediments into large mounds covered with dunes.

Evaluation of the various diagrams by different workers for discrimination of desert deposits from other types of deposits brings out that QDa-Md diagram of Buller and McManus (1972) is not particularly useful, whereas desert sediment field, delineated on Ska-QDa diagram of these workers should be widened to include samples of the Thar desert. Mean size versus standard deviation diagram of Friedman (1961) for distinction between desert and fluvial sediments and skewness versus mean size diagrams of Friedman (1961) and Mpiola and Weiser (1958) for discriminating between beach, coastal dunes and inland dunes seem to be useful. Sahu's (1964) plot of $\sqrt{\sigma^2}$ vs. $\frac{s_{Ku}}{s_{Mz}} \cdot s(\sigma^2)$ is very sensitive to the presence of extreme values of standard deviation and should be used with care for recognition of desert sediments.

The shape of cumulative curves, photomicrographs of the typical samples from the area and interrelationships of the grain size parameters suggest that sediments of the Thar desert consist mainly of two populations of grains mixed in different proportions, namely, a saltation population and a suspension population. The saltation population has a mean size of about 2.75 ϕ and a standard deviation of 0.20 ϕ and the suspension population has a mean size of about 3.75 ϕ and a standard deviation of about 0.25 ϕ . The saltation

population constitutes 60-90% and the suspension population forms 10-40% of the samples. A minor amount of a traction population with grains coarser than 2.5ϕ may constitute less than 1% of the samples. When the sediments consist chiefly of the saltation population with minor additions of the suspension population, they are well sorted, nearly symmetrical and leptokurtic. With larger additions of the suspension population, the composite samples become more poorly sorted, positively skewed and platykurtic. This also explains the variation of grain size parameters spatially and within barchans.

Strong winds transport saltation population in large amount and heap them in the form of various bedforms. Slackening winds deposit suspension population which percolates down with time. Consequently, the stabilized sands contain higher proportions of suspension population.

Roundness of desert sediments has been studied by determining roundness of one hundred quartz grains from each $1/2 \phi$ fraction of five samples from different areas. Roundness is determined by comparison with photographic chart on ρ (rho) scale of Folk (1955). Operator experiment has been run to find the accuracy and consistency of the method. Different grain size fractions have a roundness of 1.79 to 2.91 ρ . Quartz grains of the saltation population (larger than 0.125 mm) show small increase in roundness with increase in grain size, but quartz grains of the suspension

population (smaller than 0.125 mm) are comparatively less rounded than the saltation population grains and have similar roundness irrespective of grain size.

Sphericity of the aeolian sediments is studied by mounting grains from each of 1/2 ϕ fractions of samples in Canada balsam on glass slides and by measuring axial ratios of more than 100 quartz grains from each slide. About half of the slides show normal distribution of sphericity values and other slides are roughly equally distributed in positively skewed, negatively skewed and polymodal groups indicating that there is no need for transformation of sphericity values for their normalization as suggested by earlier workers. Mean sphericity for different slides lies between 0.56 and 0.81. One of the samples shows exceptionally low mean sphericity and high standard deviation values, reflecting probably an ultimate metamorphic source. Sphericity values are independent of grain size.

The aeolian sands have been studied for their light as well ^{as} heavy mineral contents. Light minerals are studied by mounting grains of all the 1/2 ϕ fractions of three samples and +120 mesh fractions of other five samples in Canada balsam on glass slides. Dominant light minerals are quartz, K-feldspar, plagioclase, chert, calcite and aragonite. The whole sand samples fall in feldspathic litharenitic sand class of Folk's (1968b) classification of sandstones indicating their mineralogically immature nature. Heavy minerals are

separated using gravity separation method mainly from +230 mesh fractions of samples, in which these are abundant. Major non-opaque heavy minerals met with are hornblende, zircon, staurolite, kyanite, sillimanite and andalusite. Comparison of light minerals of +120 mesh fractions and heavy minerals of +230 mesh fractions using χ^2 test suggests that the samples differ from one another significantly and they belong to a 'heterogeneous' population.

The presence of spherical and elongated zircon and hornblende, staurolite, kyanite, sillimanite, and andalusite and relative abundance of the different types of quartz indicate mainly low to high rank metamorphic provenance with a minor contribution from plutonic source. Some contribution from sedimentary source is indicated by chert. Spatial inhomogeneities in light and heavy mineral composition of sands suggest that probably older deposits are being reworked by the wind and sediments are not transported over long distances. Thus no significant expansion of the desert is contemplated due to transportation of sand.

Considering the strategic location of the area and the future development potential it holds, engineering properties of the sands of the area have been studied. These include mortar making properties, compaction, shear strength and permeability.

Mortar strength test of the autoclaved cement sand cubes

reveals that strength increases with increase of M_z and σ . Further, the strength increases with increase in S_k and K_u and after critical values of S_k and K_u there is appreciable fall in strength.

Compaction test indicates that the maximum dry density decreases with increase in M_z and σ .

The determination of shear strength indicates that the soil is almost noncohesive.

The correlation of permeability with grain size parameters indicates that K decreases with increase in M_z and σ .

On the basis of these tests it can be concluded that the sands of the area belong to SW and SP soil groups of the Unified Soil Classification System (Anon., 1962).

7.2 CONCLUSIONS

Following are the salient conclusions:

- i. The Thar desert probably came into existence 10,000 years B.P. The present scenario is the product of superposition of the prevailing wind regime over the fossil longitudinal dunes and sand piles.
- ii. Three types of bedforms, namely, ripples, dunes (barchans, transverse and longitudinal) and

sand piles are recognised in the area of study.

- iii. Ripples invariably ornament the skins of dunes and sand piles. Barchans show a preferential tendency to develop in the marginal areas whereas longitudinal dunes, in general, are restricted to the desert interior.
- iv. Ripples of different wavelengths and amplitudes may occur in juxtaposition due to change in the modality of sands. Ripple index varies from 5 to 40 with a mean value of 20.1.
- v. Hat-shape barchan dunes are reported for the first time. A narrow trench scooped on its windward slope is attributed to the existence of a windward eddy.
- vi. Three stage mechanism for the formation of barchans is suggested.
- vii. Transverse dunes may originate due to lateral conjugation of two or more barchans.
- viii. The net sediment transport direction, as indicated by different dunes, deviates 15° N from the resultant wind direction. This is attributed to 'Ekman spiral' effect.
- ix. The wind regime has remained essentially unchanged since the fossil bedforms formed around 10,000 years B.P.

- x. The Thar desert sediments lie on the finer side of the dune sands reported earlier.
- xi. Sorting appears to be a function of intermixing of mainly two populations in different proportions.
- xii. Most of the sand samples are positively skewed.
- xiii. Sand samples fall in either very leptokurtic or platykurtic groups.
- xiv. Correlations of grain size parameters indicate that σ and Sk increase with increase in Mz whereas Ku decreases with increase in Mz .
- xv. Ripples are coarse grained, poorly sorted and have symmetrical grain size distribution, whereas sand piles and dunes, in general, have platykurtic and leptokurtic natures respectively.
- xvi. Mz , σ and Sk decrease as one moves from the foot to the crest of the barchans.
- xvii. Spatial variation as indicated in the contour maps of the various grain size parameters is thought to reflect areal variability of the grain size distribution of the original deposits being reworked or the degree of reworking by wind.
- xviii. The Thar desert sediments consist chiefly of two populations, namely, a saltation population (60-90% with $Mz = 2.75 \phi$ and $\sigma = 0.20 \phi$) and a

suspension population (10-40% with $Mz = 3.75 \phi$ and $\sigma = 0.25 \phi$). Interrelationships of the various grain size parameters and their spatial variation may be explained in terms of intermixing of these two populations in different proportions.

- xix. Roundness of quartz grains ranges from 1.79 to 2.91 ρ . Saltation population is more rounded and the roundness increases with increase of grain size whereas suspension population is less rounded and roundness is independent of grain size.
- xx. Sphericity of the quartz grains varies from 0.56 to 0.81 and is independent of grain size.
- xxi. The present sands fall in the feldspathic litharinitic class of Folk's (1968b) triangular diagram indicating their mineralogical immaturity. Variations of light and heavy minerals suggest that samples belong to a 'heterogeneous' population. This further indicates that sands are not being transported over long distances and no significant expansion of the desert is taking place by transportation of sand.
- xxii. The mineralogical assemblage suggests low to high rank metamorphic provenance with minor contributions from the plutonic and sedimentary sources.
- xxiii. There is a significant effect of variation in

the grain size parameters on the mortar strength of cement sand cubes.

- xxiv. The maximum dry density and permeability decrease with increase in M_z and σ .
- xxv. The sand is almost noncohesive and falls in SW and SP soil groups of the Unified Soil Classification System.

7.3 SUGGESTIONS FOR FURTHER STUDY

- i. Dynamics of dune formation and rate of their migration in relation to the prevailing wind regime may be investigated in the field. It may provide clues for controlling their migration.
- ii. Ages of the stabilized dunes may be determined accurately by analyzing their pollen contents and by carbon dating method.
- iii. Internal structures of the various bedforms may be studied by trenching.
- iv. Exhaustive study of the variation of grain size distribution within the various bedforms needs to be undertaken.
- v. Regional variation of the thickness of sand cover, its permeability and detection of the buried channels, faults etc. in relation to the occurrence of groundwater should be carried out.

- vi. Geotechnical investigations of the desert sands reported in the dissertation need to be supplemented with further studies.

REFERENCES

- Ahmad, E., 1969, Origin and geomorphology of the Thar desert. Ann. Arid Zone, vol.8, p.171-180.
- Ahmad, F., 1975, The origin of the Rajasthan desert-a geological approach. Workshop on Problems of the Deserts in India, Jaipur (Preprint).
- Alimen, H., 1953, Variations granulométriques du sable le long de profils dunaires au Sahara occidental. Coll. Intern. Cent. Natl. Rech. Sci. (Alger), vol.35, p.219-235
- Alimen, H., 1965, The Quarternary Era in the northwest Sahara. Geol. Soc. Am. Spec. Paper 84, p.273-291.
- Anonymous, 1952, First Five Year Plan, Govt. of Ind. Plan. Comm., New Delhi.
- Anonymous, 1953, Climatological Tables of Observations in India Govt. Cent. Press, Bombay, 508p.
- Anonymous, 1962, Unified Soil Classification System for Roads, Airfields, Embankments and Foundations. Military Standard, MIL-STD-619A, U.S. Deptt. of Defence, Washington.
- Anonymous, 1967, Ordinary, Rapid-hardening and Low-heat Portland Cement, IS-269, Indian Standards Institution, New Delhi.
- Axelrod, D.I., 1950, Studies in late Tertiary paleobotany. Publ. Carnegie Inst., vol.590.
- Axelrod, D.I. and Ting, W.S., 1960, Late Pliocene floras east of the Sierra Nevada. Univ. Calif. Publs. Bull. Dept. Geol., vol.39.
- Babu, P.V.L.P. and Rao, V.P., 1974, A note on geomorphology of the Jaisalmer desert, West Rajasthan. Ind. Jour. Earth Sci., vol.1, p.214-217.
- Bagnold, R.A., 1931, Journeys in the Libyan desert, 1929 and 1930. Geogr. Jour., vol.78, p.13-39, 524-533.
- Bagnold, R.A., 1933, A further journey through the Libyan desert. Geogr. Jour. vol.82, p.103-129, 211-235.
- Bagnold, R.A., 1937, The size grading of sand by wind. Proceed. Roy. Soc. London, Ser.A., vol.163, p.250-264.

- Bagnold, R.A., 1941, The Physics of Blown Sand and Desert Dunes. Methuen, London, 265p.
- Bagnold, R.A., 1953, The surface movement of blown sand in relation to meteorology. in Desert Research. Unesco, Jerusalem, p.89-96.
- Bagnold, R.A., 1954, Experiments on a gravity-free dispersion of large solid spheres in a Newtonian fluid under shear. Proceed. Roy. Soc. London, Ser.A., vol.225, p.49-63.
- Baillieul, T.A., 1975, A reconnaissance survey of the cover sands in the Republic of Botswana. Jour. Sediment. Petrol., vol.45, p.494-503.
- Ball, J., 1927, Problems of the Libyan desert. Geogr. Jour., vol.70, p.21-38, 105-128, 209-224.
- Banerji, S.K., 1952, Weather factors in the creation and maintenance of the Rajputana desert. in Symp. on Rajputana Desert, Bull. Natn. Inst. Sci. Ind., vol.1.
- Basu, A., Young, S.W., Suttner, L.J., James, W.C., and Mack, G.H., 1975, Re-evaluation of the use of undulatory extinction and polycrystallinity in detrital quartz for provenance interpretation. Jour. Sediment. Petrol., vol.45, p.873-882.
- Bhattacharya, N., 1956, The nature and origin of the sand dunes on the western side of the Mount Abu. Nat. Geogr. Jour. Ind., vol.11, p.91-96.
- Blanford, W.T., 1876, On the physical geography of the Great Indian desert with special reference to the former existence of the sea in the Indus valley, and on the origin and mode of formation of sand hills. Jour. Asiatic Soc. Bengal, vol.45, p.86-103.
- Blatt, H., and Christie, J.M., 1963, Undulatory extinction in quartz of igneous and metamorphic rocks and its significance in provenance studies of sedimentary rocks. Jour. Sediment. Petrol., vol.33, p.559-579.
- Blatt, H., Middleton, G.V. and Murray, R., 1972, Origin of Sedimentary Rocks. Prentice Hall, Englewood Cliffs, N.J., 634p.
- Bokman, J., 1952, Clastic quartz particles as indices of provenance. Jour. Sediment. Petrol., vol.22, p.17-24.

- ✓ Bokman, J., 1957, Comparison of two and three dimensional sphericity of sand grains. Bull. Geol. Soc. Am., vol.68, p.1689-1692.
- Bryson, A.R. and Baerreis, A.D., 1967, Possibilities of major climatic modification and their implications: Northwest India, a case for study. Bull. Am. Meteorological Soc., vol.48, p.136-142.
- ✓ Buller, A.T. and McManus, J.C., 1972, Simple metric sedimentary statistics used to recognize different environments. Sedimentology, vol.18, p.1-21.
- Chakrabarti, A., 1968, Polymodal character in dune sediments. Quart. Jour. Geol. Mining Met. Soc. Ind., vol.40, p.51-54.
- Chavaillon, J., 1964, Les formations Quarternaires du Sahara nord-occidental (Colomb-Bechra-Reggane). Centre Natl. Rech. Sci. - Publ. Centre Rech. Zones Arides Ser Geol., vol.5, 393p.
- Clos-Arceuduc, A., 1967, La direction des dunes et ses rapports avec celle due vent. C.R. de la Acad. des Sci., Ser D., vol.264, p.1393-1396.
- Cooper, W.S., 1958, Coastal sand dunes of Oregon and Washington. Geol. Soc. Am. Mem., vol.72.
- Cornish, V., 1897, On the formation of sand dunes. Geogr. Jour., vol.9, p.278-302.
- Cornish, V., 1914, Waves of Sand and Snow. Fisher-Unwin, London, 383p.
- Das Gupta, S.K., 1973, Hydrocarbon accumulation in the shelf sediments of Rajasthan. Proceed. Indo-Soviet Symp., Delhi (in press).
- Das Gupta, S.K., Gupta, P.K. and Chandra, M., 1974, Tectonic elements of the West Rajasthan shelf and their stratigraphy. Proceed. Golden Jubilee Symp. Geol. Min. Met. Soc. Ind. Calcutta (in press).
- Das Gupta, S.K., 1975a, A revision of the Mesozoic-Tertiary stratigraphy of the Jaisalmer Basin, Rajasthan. Ind. Jour. Earth Sci., vol.2, no.1, p.77-79.
- Das Gupta, S.K., 1975b, Stratigraphy of the West Rajasthan. Proceed. IV Coll. Ind. Micropal. and Strat., p.219-233.

- Dickinson, W.R., 1970, Interpreting detrital modes of graywacke and arkose. Jour. Sediment. Petrol., vol.40, p.695-707.
- Dixon, W.J., and Massey, F.J. Jr., 1957, Introduction to Statistical Analysis, 2nd Ed., McGraw Hill. New York, 488p.
- Durand de Corbiac, H., 1958, Autant en emporte le vent ou l'erosion et l'accumulation autour du Tibesti. Bull. d'Information, Assoc. Ing. Geographes, vol.4, p.147-156.
- Enquist, F., 1932, The relation between dune-form and wind direction. Geol. Stockholm Fook, vol.54, p.19-59.
- Finkel, H.J., 1959, The barchans of southern Peru. Jour. Geol., vol.67, p.614-647.
- Fisher, R.L., Scalater, J.G., and Mckenzie, D.P., 1971, Evolution of the Central Indian Ridge, Western Indian Ocean. Geol. Soc. Am. Bull., vol.82, p.553-562.
- ✓ Folk, R.L., 1955, Student operator error in determination of roundness, sphericity and grain size. Jour. Sediment. Petrol., vol.25, p.297-843.
- ✓ Folk, R.L., and Ward, W.C., 1957, Brazos River bar, a study in the significance of grain size parameters. Jour. Sediment. Petrol., vol.27, p.3-27.
- Folk, R.L., 1966, Sands of the Simpson desert, Maryvale Station, Northern Territory, Australia: Contribution to the problem of Paleozoic bimodal-superature quartz arenites. Geol. Soc. Am. Ann. Meeting, Atlantic City (Abs.).
- Folk, R.L., 1968a, Bimodal superature sandstone: Product of the desert floor. Intern. Geol. Cong. 23rd Session, vol.8, p.9-32.
- Folk, R.L., 1968b, Petrology of Sedimentary Rocks. Austin, Texas.
- Folk, R.L., 1971a, Longitudinal dunes of the nrthwestern edge of the Simpson desert, Northern Territory, Australia, 1, Geomorphology and grain size relationships. Sedimentology, vol.16, p.5-54.

- Folk, R.L., 1971b, Genesis of longitudinal and oghurd dunes elucidated by rolling upon grease. Geol. Soc. Am. Bull., vol.82, p.3461-3468.
- Frere, H.B.E., 1870, Notes on the Rann of Cutch. Jour. Roy. Geogr. Soc., vol.40, p.181-207.
- ✓ Friedman, G.R., 1961, Distinction between dune, beach and river sands from their textural characteristics. Jour. Sediment. Petrol., vol.31, p.514-529.
- ✓ Friedman, G.M., 1967, Dynamic processes and statistical parameters compared for size-frequency distribution of beach and river sands. Jour. Sediment Petrol., vol.37, p.327-354.
- Geological Survey of India, 1962, Geological Map of India, 6th Ed., Calcutta
- ✓ Ghosh, A., 1952, The Rajputana Desert, its Archaeological aspect. Proceed. Nat. Inst. Soc. Ind., p.37-42.
- Ghose, B., 1964, Geomorphological aspects of the formation of salt basins in Western Rajasthan. Proceed. Symp. on Problems Ind. Arid Zone, Jodhpur, p.79-83.
- Ghose, B., 1965, Genesis of desert plains in central Luni basin of Western Rajasthan, Jour. Ind. Soc. Soil sci., vol.13, p.123-126.
- Ghose, B., Pandey, S., Singh, S. and Lal, G., 1966, Geomorphology of Central Luni basin, western Rajasthan. Ann. Arid Zone, vol.5, p.10-25.
- Ghosh, R.N., 1975, The Luni-a case history of application of photogeomorphological techniques. Workshop on Problems of Deserts in India. (Preprint).
- ✓ Glennie, K.W., 1970, Desert sedimentary Environments Developments in Sedimentology, vol.14, Amsterdam, Elsevier, 222p.
- Godbole, N.N., 1952, Does Sambhar lake owe its salt to the Rann of Kutch. Ind. Sci. Congr., p.1-57.
- Goudie, A.S., Allchin, B. and Hedge, K.T.M., 1973, The former extension of the great Indian sand desert. Geogr. Jour., vol.139, p.244-257.
- Griffiths, I.C., 1967, Scientific Method in Analysis of Sediments. McGraw Hill, New York. 508p.

- Grove, A.T., 1960, Geomorphology of the Tibesti region. Geogr. Jour., vol.126, p.18-31.
- ✓ Gupta, R.S., 1958, Investigation on the desert of Rajasthan-Fertility and Mineralogical studies. Jour. Ind. Soc. Soil Sci. vol.6, p.115-122.
- Gupta, R.K., and Prakash, I., 1975, Environmental Analysis of the Thar Desert. English Book Depot., 484p.
- Hastenrath, S.L., 1967, The barchans of the Arguipa region, Southern Peru. Z.f.Geomorph., vol.11, p.300-331.
- Holland, T.H. and Christie, W.A.K., 1909, The origin of the salt deposits in Rajputana, Rec. Geol. Surv. Ind., vol.38, p.154-186.
- Holm, D.A., 1960, Recent geomorphology in the Arabian Peninsula. Sci., vol.132, p.1369-1379.
- Hoyt, J.H., 1966, Air and sand movements to the lee of dunes. Sedimentology, vol.7, p.137-143.
- ✓ Inman, D.L., 1952, Measures for describing the size distribution of sediments. Jour. Sediment. Petrol., vol.22, p.125-145.
- Kadar, L., 1934, A study of the sand sea in the Libyan desert. Geogr. Jour., vol.83, p.470-478.
- Kendrew, W.G., 1961, The Climate of the Continent Clarendon Press, Oxford.
- King, D., 1956, The Quarternary stratigraphic record at Lake Eyre north and the evolution of existing topographic forms. Trans. Roy. Soc. S. Australia, vol.79, p.93-103.
- King, D., 1960, The sand ridge deserts of South Australia and related aeolian landforms of the Quarternary arid cycles. Trans. Roy. Soc. S. Australia, vol.93, p.99-108.
- Krishnan, A., 1968, Distribution of arid areas in India in Symp. on Arid Zone, Intern. Geogr. Uni., Jodhpur.
- Krishnan, M.S., 1968, Geology of India and Burma, Higginbothams, Madras, 536p.
- ✓ Krumbein, W.C., 1934, Size frequency distribution of sediments. Jour. Sediment. Petrol. vol.4, p.65-77.

- Krumbein, W.C. and Pettijohn, F.J., 1938, Manual of Sedimentary Petrology. Appleton-Century-Crofts, New York, 549p.
- Krumbein, W.C. and Monk, G.D., 1943, Permeability as a function of the size parameters of unconsolidated sands. Trans. Am. Inst. Min. Met. Engrs., vol.151, p.153-163.
- Krynine, P.D., 1940, Petrology and genesis of the Third Bradford Sand. Penn. State Coll. Min. Ind. Expt. Sta. Bull., vol.29, p.13-20.
- ✓ Laughton, A.S., McKenzie, D.P. and Sclater, J.G., 1972, The structure and evolution of the Indian Ocean. Proceed. 24th Intern. Geol. Congr., p.65-73.
- Long, J.T. and Sharp, R.P., 1964, Barchan dune movement in Imperial Valley, California. Geol. Soc. Am. Bull., vol.78, p.1039-1044.
- Lukose, N.G., 1972, Palynological evidences of the age of the Lathi formation, west Rajasthan, India. Proceed. Sem. Paleopalynol. and Ind. Strat., Calcutta Univ. Publ., p.155-159.
- Lukose, N.G., 1974, Palynology of the subsurface sediments of the Manhera Tibba structure, Jaisalmer, West Rajasthan, India. Ind. Paleobotanist, vol. 21, p.283-297.
- Lukose, N.G. and Misra, C.M., 1974, Palynological evidence on the age of the Bap Boulder Bed, Rajasthan and Palynology and age of the Badhaura Formation Rajasthan, India. IV Coll. Ind. Micropal. and Strat., Dohradun. (Abstract)
- Madigan, C.T., 1930, An aerial reconnaissance into the southeastern portion of the Central Australia. Proceed. Roy. Geogr. Soc. Australia, Sess. 1928-29, vol.30, p.83-108.
- Madigan, C.T., 1936, The Australian sand-ridge deserts, Geogr. Rev., vol.26, p.205-227.
- Madigan, C.T., 1938, The Simpson desert and its borders. Jour. Proceed. Roy. Soc. N.S. Wales, vol.71, p.503, 535.
- Madigan, C.T., 1946, The Simpson Desert Expedition, 1939. Trans. Roy. Soc. S. Australia, vol.70, p.45-63.

- Masch, F.D. and Denny, K.J., 1966, Grain size distribution and its effect on the permeability of unconsolidated sediments. Water Resources Res., vol.2, p.665-677.
- ✓ McBride, E.F., 1971, Mathematical treatment of size distribution data. in Carver, R.E. (Ed.), Procedures in Sedimentary Petrology, Wiley, New York, 653p.
- ✓ McCammon, R.B., 1962, Efficiencies of percentile measures for describing the mean size and sorting of sedimentary particles. Jour. Geol., vol.70, p.453-465.
- McKee, E.D. and Tibbitts, G.C., Jr., 1964, Primary structures of a seif dune and associated deposits in Libya. Jour. Sediment Petrol., vol.34, p.5-17.
- McKenzie, D. and Sclater, J.G., 1971, The evolution of the Indian Ocean since the Late Cretaceous. Geophys. Jour. Res. Astro. Soc., vol.25, p.437-528.
- Melton, F.A., 1940, A tentative classification of sand dunes - its application to dune history in the southern high plains. Jour. Geol., vol.48, p.113-174.
- ✓ Middleton, G.V., 1962, On sorting, sorting coefficients, and the lognormality of grain-size distributions of sandstones - a discussion. Jour. Geol., vol.70, p.754-756.
- Miller, R.L. and Kahn, J.S., 1962, Statistical Analysis in the Geological Sciences. Wiley, New York, 461p.
- Mohan, P.C. and Puri, N., 1976, Spatial variation of grain size in a barchan. Trans. Ind. Soc. Desert Techn. and Univ. Cent. Desert Studies, vol.1, p.135-138.
- ✓ Moiola, R.J. and Weiser, D., 1968, Textural parameters: an evaluation. Jour. Sediment. Petrol., vol.38, p.45-53.
- Mukherjca, A., 1975, Length-breadth ratio of quartz grains as indicators of provenance - A reappraisal in Banerjee et al. (Eds.), Symp on Sediment, Sedimentation and Sediment Environ., Delhi, p.169-176.
- Narayanan, K., 1964, Stratigraphy of the Rajasthan shelf. in Symp. on Problems of Indian Arid Zone, Jodhpur.

- Otto, G.H., 1939, A modified logarithmic probability graph for the interpretation of mechanical analyses of sediments. Jour. Sediment. Petrol., vol.9, p.62-76.
- Pandey, S., Singh S. and Ghose, B., 1964, Orientation, distribution and origin of sand dunes in the central Luni Basin. Symp. Problems Ind. Arid Zone. Jodhpur.
- Pandey, S. and Chatterji, P.C., 1970, Genesis of 'Mitha Ranns', 'Kharia Rann' and 'Kanodwala Ranns' in the Great Indian desert. Ann. Arid Zone., vol.9, p.175-180.
- ✓ Pandey, S., Ghose, B. and Singh, S., 1972, Meandering behaviour and erosion characteristics of stream channels in semi-arid environment of western Rajasthan. Proceed. Ist Ind. Geogr. Congr., New Delhi.
- Pareek, H.S., 1975, Geological configuration of north western Rajasthan. Workshop on Problems on the Deserts in India, Jaipur (Abstract)
- ✓ Passega, R., 1957, Texture as characteristic of clastic deposition. Bull. Am. Assoc. Petrol. Geologists, vol.41, p.1952-1984.
- ✓ Passega, R., 1964, Grain size representation by CM patterns as a geological tool. Jour. Sediment Petrol., vol.34, p.830-847.
- Pettijohn, F.J., 1949, Sedimentary Rocks, 1st ed., Harper, 526p.
- Pettijohn, F.J., 1957, Sedimentary Rocks, 2nd Ed., Harper, 718p.
- Philip, G., Saadalla, A., and Ajina, T., 1968, Mechanical analysis and mineral composition of the Middle Triassic Ga'ara Sandstone (Iraq). Sediment Geol., vol.2, p.51-76.
- Pramanik, S.K., 1952, Hydrology of Rajasthan desert rainfall, humidity, and evaporation in Symp. on Rajputana Desert, Bull. Natn. Inst. Sci. Ind., vol.1.
- Ramadurai, S., and Gupta, S.K., 1975, Drainage analysis of part of Banganga internal drainage basin, Rajasthan. Workshop on the Problems of the Desert in India, Jaipur (Preprint).
- Ramanathan, K.R., 1952, Atmospheric conditions over the Rajasthan Desert. in Proc. Symp. Rajasthan Desert Bull. Natn. Inst. Sci. Ind., vol.1, p.179-182

- Rao, K.N., 1961, Climatic changes in India in Changes of Climate Proceed. Rome Symp., Unesco.
- ✓ Rao, A.D.P., 1962, Heavy minerals of desert sands of Barmer. Ind. Min., vol.1, p.65.
- Richardson, H., 1903, Sea sand. Rept. Yorkshire Phil. Soc., 1902, p.43-58.
- ✓ Russell, R.D. and Taylor, R.E., 1937, Roundness and shape of Mississippi River sands. Jour. Geol. vol.45, p.225-267.
- Roy, B.B. and Pandey, S., 1970, Expansion or Contraction of the great Indian desert. Proceed. Ind. Natn. Sci. Aca., vol.36B, p.331-344.
- Rozycki, S.S., 1967, Le sens de rent portant la poussiere de loess, a la lumiere de l' analyse des formes d'accumulation en Bulgarie et Europe Central. Rev. Geomorph. Dyn., vol.17, p.7-9.
- ✓ Sahu, B.K., 1964, Depositional mechanisms from the size analysis of clastic sediments Jour. Sediment. Petrol., vol.34, p.73-83.
- ✓ Sahu, B.K. and Patro, B.C., 1970, Treatment of sphericity and roundness data of quartz grains of clastic sediments. Sedimentology, vol.14, p.51-66.
- Sajanani, P.P., 1964, Is Indian desert a continuation of Sahara? in Symp. on Problems of Indian Arid Zone, Jodhpur.
- Sclater, J.G. and Harrison, C.G.A., 1971, Elevation of Mid ocean ridges and the evolution of the South-western Indian ridge. Nature, vol.230, p.75-77.
- ✓ Sharp, R.P., 1963, wind ripples. Jour. Geol., vol.71, p.617-636.
- Simonett, D.S., 1960, Development and grading of dunes in western Kansas. Assoc. Am. Geogr. Ann., vol.50, p.216-241.
- Singh, S., 1969-70, The application of aerial photo-interpretation in geographical research. Univ. studies in Geogr., vol.2, p.46-60.

- Singh, S., Ghose, B., Wasi, U. and Kaith, D.S., 1969-71, Interpretation of aerial photographs of quantitative geomorphic characteristics of drainage basins in sub-humid to humid environment. Ind. Jour. Geogr., vol.4-6, p.1-11.
- Singh, S.S., Pandey, B. and Ghoshe, B., 1971, Geomorphology of the middle Luni basin of W. Rajasthan. Ann. Arid. Zone, vol.10, p.1-14.
- Singh, S. and Ghose, B., 1973, Interrelationships between quantitative geomorphic characteristics of the drainage basins in subhumid to humid environment of Rajasthan. Ann. Arid Zone, vol.12, p.62-79.
- ✓ Singh, G., Joshi, R.D., Chopra, S.K. and Singh, A.B., 1974, Late Quarternary history of vegetation and climate of the Rajasthan desert, India. Phil. Trans. Roy. Soc., London, vol.267, p.467-501.
- Singh, S., Vats, P.C. and Kaith, D.S., 1975, Some aspects of desert geomorphology of Bikaner district, western Rajasthan. Workshop on the Problems of the Desert in India, Jaipur, (Pre-print).
- Skocek, V. and Saadallah, A.A., 1972, Grain size distribution, carbonate content and heavy minerals in eolian sands, southern Desert, Iraq. Sediment Geol., vol.8, p.29-46.
- Smith, H.T.U., 1965, Dune morphology and chronology in central and western Nebraska. Jour. Geol., vol.73, p.557-578.
- Snedecor, G.W., 1956, Statistical Methods-Applied to Experiments in Agriculture and Biology, Fifth Ed., Iowa State Univ. Press, Ames (U.S.A.), 534p.
- ✓ Spencer, D.W., 1963, The interpretation of grain size distribution curves of clastic sediments. Jour. Sediment. Petrol., vol.33, p.180-190.
- Stokes, W.L., 1964, Eolian varving in the Colorado Plateau. Jour. Sediment. Petrol., vol.34, p.34, p.34, p.429-433.
- Striem, H.L., 1954, The seifs on the Israel- Sinai border and the correlation of their alignment. Res. Council Israel Bull., vol.4, p.195-198.

- Trask, P.D., 1930, Mechanical analysis of sediments by centrifuge. Econ. Geol., vol.25, p. 581-599.
- ✓ Udden, J.A., 1898, Mechanical composition of wind deposits. Augustana Library Publ. vol.1, 69p.
- Veevers, J.J. and Wells, A.T., 1961, The geology of the Canning Basin, western Australia. Commonwealth Australia Bur. Mineral Resources Geo. Geophys. Bull., vol.60, 323p.
- Verlaque, C., 1958, Les dunes d'In Salah. Travaux de l'Institute Rech. Sahariennes, vol. 42, p.506-515.
- Verma, K.K., 1975, The fossil and environment of desert areas of western India. Workshop on Problems of the Deserts in India, Jaipur (Abstract).
- Verstappen, H., Th., Ghose, B., Pandey, S., 1969, Landforms and Resources in Central Rajasthan (India). Results of Jalore Pilot Survey. Intern. Inst. Aerial Surv. Earth. Sci. Publ., B51, p.1-20.
- ✓ Wadell, H., 1932, Volume, shape, and roundness of rock particles. Jour. Geol., vol.40, p.443-451.
- Wadia, D.N., 1955, Deserts of Asia-their origin and growth in the late Pleistocene time. 2nd Sir Albert C. Seward. Mem. Lect.-1954. B. Sahn Inst. Paleobot.
- Wadia, D.N., 1959, Evolution of the desert of Asia. Jour. Geol. Soc. Ind., vol.1, p.6-9.
- Wadia, D.N., 1960, The post-glacial desiccation of central Asia: Evolution of the arid zone of Asia. Nat. Inst. Sci. Ind. Monograph, p.1-25.
- Wadia, D.N., 1966, Geology of India, 4th Ed., Eng. Lang. Book Soc. and McMillan, London, 536p.
- Waite, M.B.C., 1969, Desert dunes of the Karmit Sandhills, Winkler, Country, Texas. Thesis Univ. Texas, 90 p. (unpublished).
- Warren, A., 1976, Dune trend and Ekman Spiral. Nature, vol.259, p.653-654.
- Wilson, I.G., 1971, Desert sandflows, basins and a model for the origin of ergs. Geogr. Jour., vol.137, p.180-199.

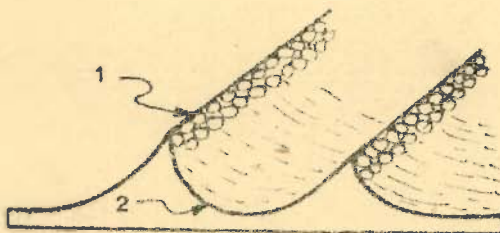
- ✓ Wilson, I.G., 1972, Aeolian bedforms-their development and origins. Sedimentology, vol.19, p.173-210.
- Wilson, I.G., 1973, Ergs. Sedimentary Geol., vol.10, p.77-106.
- Wingate, O., 1934, In search of Zerzeua. Geogr. Rev., vol.83, p.281-308.
- Wood, W.H., 1970, Rectification of wind-blown sand. Jour. Sediment. Petrol, vol.40, p.29-37.

APPENDIX I

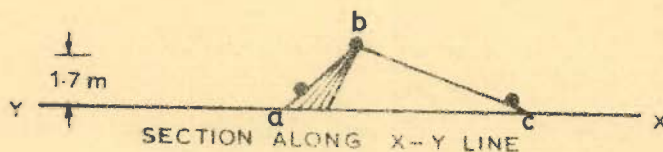
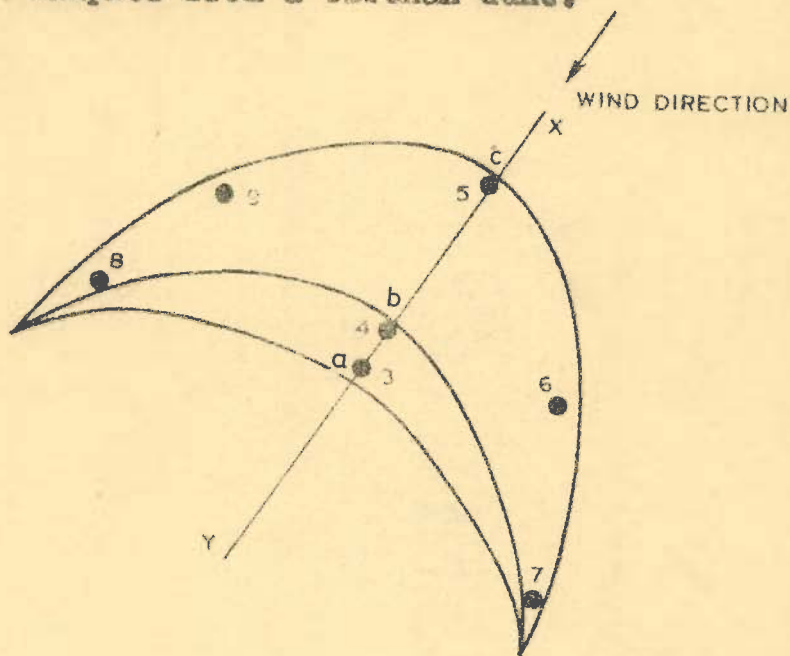
DESCRIPTION OF SAMPLE LOCATIONS
(Refer Figure 1.3)

Sample No.	Sample location
------------	-----------------

- | | |
|---|---|
| 1 | Sample from the crest of a ripple. |
| 2 | Sample from the trough of the above ripple. |



3 to 9 Samples from a barchan dune.

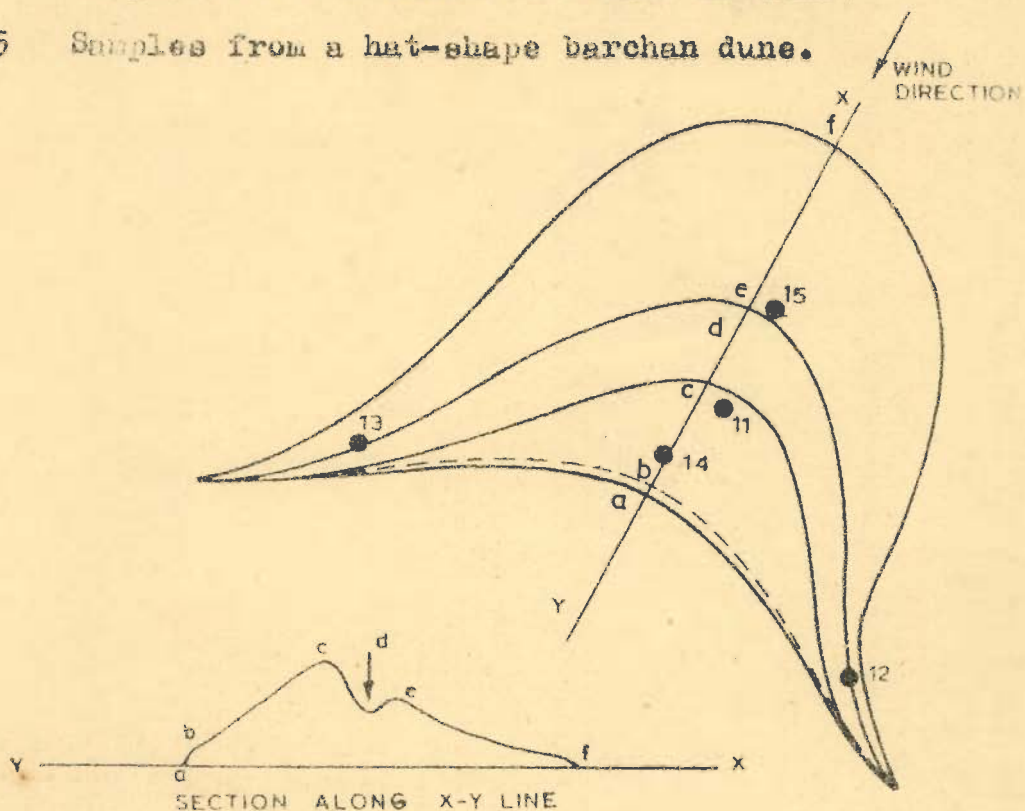


Sample No.

Sample location

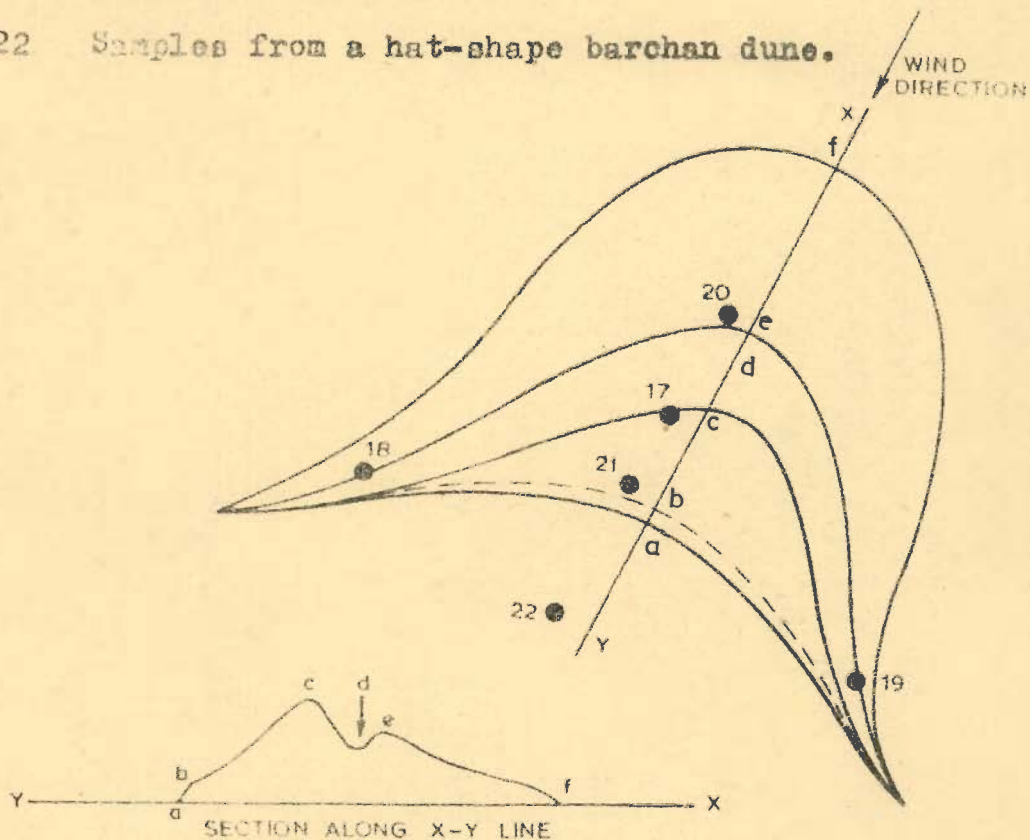
10 Sample from the crest of a barchan dune.

11 to 15 Samples from a hat-shape barchan dune.



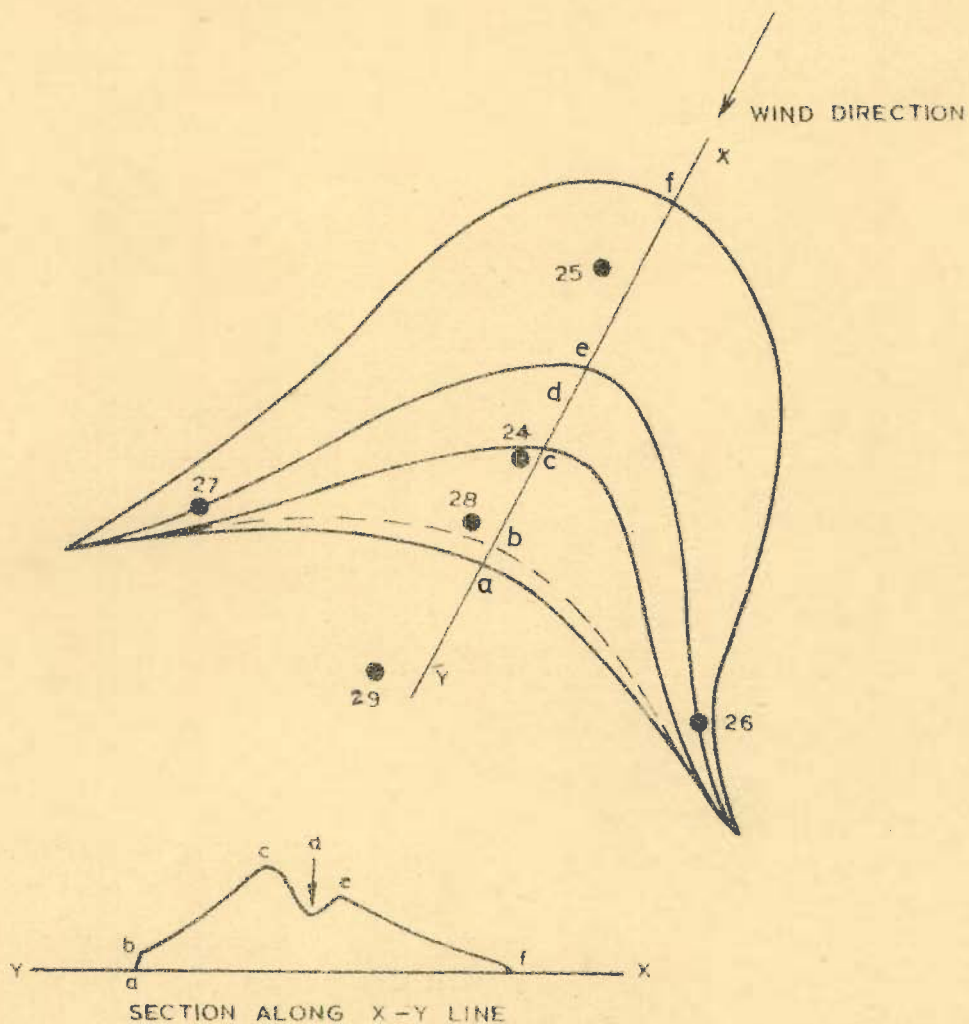
16 Sample from a sand pile.

17 to 22 Samples from a hat-shape barchan dune.



Appendix I - continued

Sample No.	Sample location
23	Sample from a sand flat (from the ripple crest)
24 to 29	Samples from a hat-shape barchan dune.



30

Sample from a sand pile.

Appendix I- continued

Sample No.	Sample location
31	Sample from the windward side of a barchan dune.
32	Sample from the windward side of a barchan dune.
33	Sample from the southeastern flank of a longitudinal dune.
34 to 36	Samples from different sand piles.
37 to 40	Samples from different sand piles near Ramgarh ($27^{\circ}23'$: $70^{\circ}30'$). Locations not shown in Figure 1.3.
41 and 42	Samples from a sand pile near Ludharwa ($26^{\circ}25'0''$: $70^{\circ}48'30''$).
43	Sample from leeward side of a barchan dune.
44	Sample from windward side of the above barchan.
45	Sample from a sand pile.
46	Sample from windward side of a barchan dune.
47	Sample from leeward side of the above barchan.
48	Sample from windward side of a barchan dune.
49	Sample from leeward side of the above barchan.
50	Sample from leeward side of a barchan dune.

Appendix I- continued

Sample No.	Sample location
51	Sample from windward side of the above barchan.
52 to 54	Samples from different sand piles.
55	Sample from a sand flat.
56	Sample from a sand pile.
57	Sample from leeward side of a barchan dune.
58	Sample from windward side of the above barchan.
59	Sample from a sand pile.
60	Sample from a sand pile.
61	Sample from a sand flat.
62 to 65	Samples from different sand piles.
66	Sample from windward side of a barchan dune.
67	Sample from windward side of a barchan dune.
68	Sample from leeward side of a barchan dune.
69	Sample from leeward side of a barchan dune.
70 to 74	Samples from different sand piles.
75	Sample from windward side of a barchan dune.
76	Sample from leeward side of the above barchan.
77	Sample from windward side of a barchan dune.
78	Sample from leeward side of the above barchan.
79 to 104	Samples from the crests of different barchan dunes.

Appendix II- Percentages of weight retained
on different sieves

Sample Number	Mesh Number								
	25	35	45	60	80	120	170	230	PF
1	2.05	.03	71.31	0.00					
2	.16	.01	14.87	0.00	6.27	14.21	2.42	3.07	.60
3	0.00	0.00	.06	0.00	.22	53.21	7.75	20.69	3.50
4	.01	0.00	.10	.01	.36	85.84	6.04	7.10	.57
5	0.00	0.00	.07	0.00	.47	91.89	2.47	4.47	.56
6	0.00	0.00	.14	0.00	.29	79.02	6.95	12.88	.77
7	0.00	0.00	.15	0.00	.25	88.21	3.59	7.16	.62
8	0.00	0.00	.23	0.00	.60	82.60	3.86	11.31	1.45
9	0.00	0.00	.09	0.00	1.35	82.64	4.52	10.71	.52
10	0.00	0.00	.09	0.00	.48	86.56	4.12	8.72	0.00
11	0.00	0.00	.46	.01	.15	84.42	5.52	9.39	.39
12	0.00	0.00	1.20	.05	.91	91.95	1.99	3.30	1.34
13	0.00	0.00	3.27	.04	1.07	60.69	11.32	24.73	.89
14	0.00	0.00	.26	.06	4.94	77.97	4.92	8.45	.37
15	0.00	0.00	.19	.02	.10	79.85	6.03	13.01	.65
16	0.00	0.00	.13	0.00	.10	75.33	7.24	16.37	.70
17	0.00	0.00	.09	0.00	.10	74.97	6.77	17.11	.88
18	0.00	0.00	.13	0.00	.22	93.42	5.50	.28	.46
19	0.00	0.00	.16	0.00	.44	81.56	1.63	15.74	.46
20	0.00	0.00	.03	.02	.11	74.32	6.86	18.05	.45
21	0.00	0.00	.45	0.00	.48	73.72	6.23	18.82	.68
22	3.24	0.00	3.86	.04	.23	76.88	5.66	16.20	.55
23	6.45	.08	2.47	.01	.11	56.76	5.23	24.30	6.42
24	0.00	.03	0.00	.05	.95	38.51	42.68	8.19	.63
25	0.00	.01	.06	0.00	0.00	80.79	5.02	13.69	.38
26	.02	0.00	.17	0.00	0.00	74.65	7.80	16.47	.98
27	0.00	0.00	.05	0.00	.09	65.90	9.95	22.97	.85
28	0.00	0.00	.03	0.00	.35	78.93	5.91	13.60	1.12
29	.36	0.00	.42	0.00	.07	67.50	10.47	20.61	1.30
30	0.00	0.00	.16	0.00	.29	63.68	8.61	22.35	4.24
31	.00	.00	.00	.00	.42	43.69	6.95	47.16	1.59
32	.00	.00	.01	.00	.04	72.96	8.17	17.45	1.36
33	0.00	0.00	0.00	0.00	.01	76.39	7.80	15.19	.54
34	.00	.00	.11	.09	0.00	77.48	6.39	15.33	.76
35	0.00	0.00	.55	0.00	.57	69.53	6.92	19.94	2.59
					1.21	76.69	5.67	14.51	1.34

Appendix II- continued

Sample Number	Mesh Number								
	25	35	45	60	80	120	170	230	PF
36	.01	0.00	.53	.06	.48	71.44	5.10	17.14	5.19
37	0.00	0.00	.05	0.00	.24	64.56	8.39	25.18	1.55
38	0.00	0.00	.08	0.00	.37	72.09	6.73	19.46	1.23
39	0.00	0.00	.03	0.00	.02	65.79	8.93	23.68	1.52
40	0.00	0.00	.05	0.00	.36	80.14	4.65	13.35	1.40
41	0.00	0.00	.07	0.00	.31	56.46	9.55	30.97	2.62
42	0.00	0.00	.07	0.00	.15	50.65	9.91	35.65	3.54
43	0.00	0.00	.07	0.00	.42	72.44	8.27	17.57	1.20
44	0.00	0.00	.08	0.00	.25	66.85	10.85	20.58	1.36
45	0.00	0.00	.37	0.00	.57	59.10	11.68	26.25	2.00
46	0.00	0.00	.07	0.00	.12	70.37	9.29	18.08	2.03
47	0.00	0.00	.02	0.00	.06	55.14	12.15	30.48	2.11
48	0.00	0.00	0.00	0.00	0.00	56.51	18.35	23.99	1.12
49	0.00	0.00	0.00	0.00	0.00	45.38	21.21	32.12	1.25
50	0.00	0.00	0.00	0.00	.05	58.65	14.58	24.96	1.72
51	0.00	0.00	0.00	0.00	.08	63.24	13.38	21.42	1.83
52	.01	0.00	.02	0.00	0.00	62.68	13.94	21.59	1.73
53	0.00	0.00	.01	.01	.03	65.62	13.75	19.72	.82
54	0.00	0.00	0.00	0.00	0.00	73.74	11.10	14.02	1.11
55	.99	0.00	.34	.42	1.14	60.34	7.23	18.05	11.46
56	.04	0.00	0.00	.02	.01	68.77	12.59	15.70	2.84
57	0.00	0.00	0.00	0.00	0.00	53.02	16.64	28.73	1.58
58	0.00	0.00	0.00	0.00	.02	59.66	15.81	20.26	4.24
59	0.00	0.00	0.00	0.00	0.00	82.28	7.36	9.68	.65
60	0.00	0.00	0.00	0.00	0.00	72.56	9.47	16.05	1.88
* 61	1.94	0.00	.06	.08	.01	65.53	8.56	9.34	3.44
62	0.00	0.00	.01	.01	.11	88.53	4.48	5.32	1.49
63	0.00	0.00	.01	0.00	0.00	91.63	3.72	3.32	1.29
64	0.00	0.00	0.00	.01	.16	80.89	6.45	11.80	.67
65	0.00	0.00	0.00	.01	.72	84.00	5.85	8.15	1.23
66	0.00	0.00	.01	0.00	.05	75.94	10.07	11.66	2.23
67	0.00	0.00	.02	0.00	.10	81.42	4.86	12.67	.88
68	0.00	0.00	.01	0.00	0.00	83.59	5.25	10.20	.92
69	0.00	0.00	0.00	0.00	0.00	79.56	5.05	13.33	2.02
70	0.00	0.00	.08	0.00	.01	81.90	4.22	10.36	3.40

* Sample 61 contains coarse fractions for which additional sieves were used as given below:

Mesh No.	7	10	14	18
Wt. retained	1.00	3.50	6.20	9.30

Appendix II- continued

Sample Number	Mesh Number								
	25	35	45	60	80	120	170	230	PF
71	0.00	0.00	0.00	0.00	0.00	85.37	4.44	8.56	1.60
72	0.00	0.00	.01	.07	.26	78.48	4.28	13.22	3.65
73	0.00	0.00	0.00	0.00	.01	58.90	10.42	28.70	1.94
74	0.00	0.00	.08	0.00	2.00	84.27	4.15	1.13	8.33
75	.07	0.00	.20	0.00	.02	82.76	4.15	12.20	.55
76	.01	0.00	.02	0.00	0.00	77.93	7.25	12.51	2.25
77	0.00	0.00	.20	0.00	.01	70.86	8.03	1.76	19.10
78	0.00	0.00	.16	0.00	.02	74.70	5.69	15.45	3.94
79	0.00	0.00	.53	0.00	.23	76.29	5.52	16.15	1.25
80	0.00	0.00	.06	0.00	.14	70.03	6.31	22.71	.72
81	.02	0.00	.08	0.00	.30	72.12	5.63	19.91	1.90
82	0.00	0.00	.01	0.00	0.00	72.65	6.95	18.49	1.87
83	0.00	0.00	0.00	0.00	0.00	82.27	4.56	10.58	2.54
84	0.00	0.00	.02	0.00	0.00	82.35	5.77	10.89	.94
85	0.00	0.00	.15	0.00	.02	77.73	7.67	11.00	3.39
86	0.00	0.00	0.00	0.00	.01	67.53	7.14	23.64	1.64
87	0.00	0.00	0.00	0.00	0.00	77.48	6.39	15.33	.76
88	0.00	0.00	.86	0.00	2.04	78.26	4.52	13.44	.85
89	0.00	0.00	.37	.02	.14	85.61	3.89	7.35	2.58
90	0.00	0.00	1.37	.12	1.37	78.08	5.57	12.79	.91
91	.02	0.00	.23	0.00	.21	81.26	3.59	11.40	3.25
92	.10	0.00	.92	0.00	.37	68.32	4.46	22.55	3.24
93	0.00	0.00	.02	0.00	.01	82.36	4.52	12.33	.72
94	0.00	0.00	0.00	0.00	.04	74.02	6.73	16.05	3.13
95	0.00	0.00	0.00	0.00	.02	74.10	6.98	15.76	3.11
96	0.00	0.00	.13	.01	.03	80.44	4.68	12.84	1.83
97	0.00	0.00	.01	0.00	.01	78.74	4.53	14.01	2.66
98	0.00	0.00	.05	0.00	.02	75.32	6.79	17.17	.61
99	0.00	0.00	0.00	0.00	.01	83.01	4.12	11.14	1.68
100	0.00	0.00	1.28	.03	.65	80.81	3.78	11.90	1.51
101	0.00	0.00	.04	.01	.03	71.61	5.83	21.57	.86
102	0.00	0.00	.05	0.00	.04	85.84	3.13	9.99	.91
103	0.00	0.00	.03	0.00	.01	80.64	4.24	14.30	.75
104	2.05	.03	72.42	0.00	6.27	14.21	1.31	3.07	.60

Appendix III- Interpolated percentile values
in phi units

Sample Number	Percentile							
	P-1	P-3	P-5	P-10	P-15	P-16	P-20	P-25
1	1.100	1.160	1.200	1.230	1.270	1.280	1.300	1.320
2	1.155	1.273	1.336	1.433	1.499	2.516	2.566	2.622
3	2.540	2.600	2.631	2.680	2.713	2.719	2.739	2.762
4	2.523	2.579	2.609	2.655	2.686	2.692	2.711	2.732
5	2.550	2.614	2.648	2.700	2.735	2.741	2.762	2.786
6	2.542	2.599	2.630	2.677	2.709	2.714	2.734	2.756
7	2.514	2.580	2.614	2.668	2.704	2.710	2.733	2.757
8	2.366	2.542	2.579	2.637	2.676	2.682	2.707	2.733
9	2.526	2.587	2.619	2.669	2.703	2.708	2.729	2.752
10	2.560	2.618	2.649	2.697	2.729	2.735	2.755	2.777
11	2.333	2.542	2.574	2.623	2.656	2.662	2.683	2.705
12	1.476	2.523	2.574	2.652	2.705	2.714	2.747	2.783
13	1.381	1.490	2.212	2.521	2.570	2.579	2.610	2.643
14	2.542	2.606	2.640	2.692	2.728	2.734	2.756	2.780
15	2.556	2.622	2.656	2.710	2.746	2.752	2.774	2.799
16	2.569	2.633	2.666	2.719	2.754	2.760	2.782	2.805
17	2.547	2.599	2.627	2.669	2.698	2.703	2.721	2.741
18	2.527	2.592	2.626	2.679	2.715	2.721	2.743	2.767
19	2.563	2.628	2.662	2.715	2.751	2.757	2.780	2.804
20	2.534	2.604	2.641	2.698	2.736	2.743	2.766	2.793
21	2.520	2.589	2.626	2.683	2.721	2.727	2.751	2.777
22	.500	.500	1.266	2.547	2.615	2.627	2.669	2.715
23	.500	1.000	1.010	1.077	1.159	1.173	1.225	1.281
24	2.595	2.651	2.681	2.727	2.758	2.763	2.783	2.804
25	2.608	2.666	2.697	2.744	2.777	2.782	2.802	2.824
26	2.566	2.636	2.674	2.731	2.770	2.776	2.801	2.827
27	2.545	2.609	2.643	2.696	2.731	2.737	2.759	2.784
28	2.605	2.668	2.701	2.753	2.788	2.794	2.815	2.839
29	2.350	2.576	2.620	2.689	2.734	2.742	2.771	2.802
30	2.541	2.634	2.684	2.760	2.812	2.821	2.853	2.888
31	2.630	2.700	2.730	2.760	2.790	2.800	2.810	2.830
32	2.158	2.193	2.211	2.239	2.258	2.262	2.274	2.287
33	2.649	2.708	2.739	2.787	2.820	2.825	2.845	2.868
34	2.519	2.594	2.633	2.694	2.735	2.742	2.768	2.796
35	2.243	2.538	2.579	2.642	2.684	2.691	2.718	2.747

Appendix III- continued

Sample Number	Percentile							
	P-1	P-3	P-5	P-10	P-15	P-16	P-20	P-25
36	2.413	2.570	2.611	2.674	2.716	2.724	2.750	2.779
37	2.565	2.637	2.675	2.733	2.772	2.779	2.804	2.830
33	2.542	2.612	2.649	2.705	2.744	2.750	2.774	2.800
39	2.623	2.684	2.717	2.767	2.801	2.806	2.827	2.851
40	2.543	2.607	2.640	2.693	2.728	2.734	2.756	2.780
41	2.558	2.637	2.679	2.743	2.786	2.794	2.821	2.850
42	2.588	2.666	2.707	2.771	2.814	2.821	2.848	2.877
43	2.539	2.609	2.646	2.703	2.741	2.748	2.772	2.798
44	2.559	2.630	2.667	2.725	2.764	2.771	2.795	2.822
45	2.503	2.589	2.634	2.704	2.751	2.759	2.789	2.821
46	2.579	2.645	2.679	2.732	2.768	2.775	2.797	2.821
47	2.618	2.687	2.724	2.780	2.818	2.825	2.849	2.874
48	2.690	2.746	2.775	2.820	2.850	2.856	2.875	2.895
49	2.686	2.749	2.782	2.834	2.869	2.875	2.896	2.920
50	2.630	2.694	2.729	2.781	2.817	2.823	2.845	2.870
51	2.611	2.676	2.710	2.763	2.799	2.805	2.827	2.852
52	2.636	2.697	2.729	2.779	2.813	2.819	2.840	2.863
53	2.618	2.680	2.713	2.764	2.798	2.804	2.826	2.849
54	2.653	2.705	2.733	2.775	2.804	2.809	2.827	2.846
55	1.001	2.503	2.556	2.637	2.692	2.701	2.735	2.773
56	2.614	2.675	2.707	2.757	2.791	2.796	2.817	2.840
57	2.999	2.999	2.999	2.999	2.999	2.999	2.999	2.999
58	2.815	2.847	2.864	2.890	2.907	2.910	2.921	2.933
59	2.651	2.699	2.724	2.763	2.789	2.794	2.810	2.828
60	2.636	2.691	2.720	2.765	2.796	2.801	2.820	2.841
61	-1.700	-1.200	-0.950	-0.550	2.500	2.520	2.560	2.600
62	2.575	2.628	2.657	2.700	2.730	2.735	2.753	2.773
63	2.619	2.665	2.689	2.726	2.752	2.756	2.772	2.789
64	2.600	2.660	2.690	2.720	2.760	2.770	2.790	2.800
65	2.515	2.580	2.614	2.666	2.702	2.708	2.730	2.754
66	2.608	2.666	2.696	2.743	2.775	2.780	2.800	2.821
67	2.583	2.641	2.671	2.718	2.750	2.755	2.775	2.796
68	2.660	2.700	2.730	2.770	2.800	2.820	2.820	2.830
69	2.637	2.688	2.715	2.757	2.785	2.790	2.808	2.827
70	2.594	2.650	2.680	2.725	2.756	2.761	2.780	2.801

Appendix III- continued

Sample Number	Percentile							
	P-1	P-3	P-5	P-10	P-15	P-16	P-20	P-25
71	2.637	2.685	2.710	2.749	2.775	2.780	2.796	2.814
72	2.552	2.616	2.650	2.702	2.737	2.743	2.765	2.789
73	2.654	2.714	2.746	2.796	2.829	2.834	2.855	2.878
74	2.365	2.524	2.562	2.620	2.659	2.666	2.690	2.717
75	2.554	2.614	2.646	2.695	2.729	2.734	2.755	2.778
76	2.623	2.678	2.706	2.750	2.780	2.785	2.804	2.824
77	2.575	2.640	2.675	2.729	2.765	2.771	2.794	2.818
78	2.578	2.640	2.674	2.725	2.759	2.765	2.787	2.810
79	2.514	2.584	2.622	2.679	2.718	2.725	2.749	2.775
80	2.578	2.644	2.678	2.732	2.768	2.774	2.797	2.822
81	2.548	2.617	2.653	2.709	2.747	2.753	2.777	2.803
82	2.635	2.691	2.720	2.765	2.796	2.801	2.820	2.841
83	2.633	2.683	2.709	2.750	2.778	2.783	2.800	2.819
84	2.624	2.676	2.703	2.745	2.773	2.778	2.795	2.815
85	2.577	2.637	2.670	2.719	2.753	2.759	2.779	2.802
86	2.643	2.700	2.731	2.777	2.809	2.814	2.833	2.855
87	2.650	2.701	2.728	2.769	2.797	2.801	2.819	2.838
88	2.055	2.502	2.544	2.610	2.654	2.662	2.689	2.719
89	2.530	2.591	2.623	2.673	2.707	2.713	2.734	2.757
90	1.467	2.510	2.552	2.617	2.660	2.668	2.695	2.725
91	2.538	2.601	2.635	2.687	2.722	2.728	2.750	2.774
92	1.494	2.558	2.601	2.668	2.713	2.721	2.749	2.780
93	2.616	2.669	2.696	2.739	2.768	2.773	2.791	2.811
94	2.622	2.678	2.708	2.755	2.786	2.791	2.811	2.832
95	2.630	2.686	2.715	2.760	2.790	2.796	2.815	2.835
96	2.577	2.636	2.667	2.716	2.748	2.754	2.774	2.796
97	2.626	2.679	2.707	2.751	2.780	2.785	2.803	2.823
98	2.605	2.663	2.694	2.742	2.774	2.780	2.800	2.821
99	2.624	2.675	2.702	2.744	2.772	2.776	2.794	2.813
100	1.467	2.529	2.568	2.629	2.670	2.677	2.702	2.730
101	2.604	2.665	2.697	2.746	2.780	2.786	2.806	2.829
102	2.587	2.641	2.670	2.714	2.743	2.748	2.767	2.787
103	2.615	2.668	2.697	2.740	2.770	2.775	2.794	2.814
104	1.050	1.120	1.170	1.220	1.260	1.270	1.300	1.320

Appendix III- continued

Sample Number	Percentile							
	P-30	P-35	P-45	P-50	P-55	P-65	P-70	P-75
1	1.350	1.360	1.400	1.410	1.420	1.460	1.490	1.120
2	2.671	2.717	2.803	2.845	2.886	2.972	3.119	3.444
3	2.782	2.801	2.836	2.853	2.869	2.904	2.923	2.943
4	2.751	2.769	2.802	2.817	2.833	2.866	2.884	2.903
5	2.808	2.828	2.865	2.882	2.900	2.937	2.957	2.979
6	2.775	2.793	2.827	2.843	2.859	2.893	2.911	2.931
7	2.780	2.800	2.838	2.857	2.875	2.913	2.934	2.956
8	2.757	2.779	2.820	2.840	2.860	2.901	2.923	2.947
9	2.773	2.792	2.827	2.844	2.862	2.897	2.916	2.937
10	2.797	2.815	2.849	2.865	2.882	2.916	2.934	2.954
11	2.726	2.744	2.779	2.796	2.813	2.848	2.867	2.888
12	2.815	2.845	2.901	2.928	2.955	3.081	3.297	3.505
13	2.674	2.702	2.754	2.779	2.805	2.857	2.885	2.915
14	2.801	2.821	2.859	2.877	2.895	2.932	2.952	2.974
15	2.821	2.841	2.879	2.898	2.916	2.954	2.974	2.996
16	2.827	2.847	2.884	2.902	2.920	2.957	2.977	2.998
17	2.758	2.775	2.805	2.820	2.834	2.865	2.881	2.899
18	2.789	2.809	2.847	2.865	2.884	2.921	2.942	2.964
19	2.826	2.846	2.884	2.903	2.921	2.959	2.979	3.025
20	2.816	2.838	2.878	2.898	2.917	2.958	2.980	3.055
21	2.800	2.822	2.862	2.882	2.901	2.942	2.963	2.987
22	2.756	2.795	2.866	2.901	2.935	3.089	3.510	3.584
23	1.332	1.378	1.466	2.500	2.552	2.660	2.718	2.781
24	2.823	2.840	2.873	2.889	2.905	2.938	2.955	2.974
25	2.844	2.862	2.896	2.912	2.929	2.963	2.981	3.015
26	2.851	2.873	2.914	2.933	2.953	2.994	3.180	3.436
27	2.805	2.826	2.863	2.881	2.899	2.937	2.957	2.979
28	2.860	2.880	2.917	2.935	2.953	2.989	3.106	3.342
29	2.830	2.856	2.905	2.929	2.952	3.011	3.294	3.522
30	2.920	2.949	3.052	3.411	3.522	3.583	3.616	3.652
31	2.860	2.870	2.900	2.920	2.930	2.970	2.990	3.120
32	2.298	2.309	2.329	2.339	2.349	2.369	2.380	2.391
33	2.887	2.906	2.940	2.957	2.973	3.106	3.349	3.524
34	2.821	2.845	2.888	2.909	2.930	2.974	2.997	3.314
35	2.773	2.797	2.842	2.863	2.885	2.930	2.954	2.980

Appendix III- continued

Sample Number	Percentile							
	P-30	P-35	P-45	P-50	P-55	P-65	P-70	P-75
36	2.805	2.829	2.874	2.896	2.918	2.962	2.987	3.233
37	2.854	2.877	2.918	2.938	2.958	3.007	3.298	3.517
38	2.824	2.846	2.886	2.906	2.925	2.966	2.988	3.172
39	2.871	2.890	2.926	2.943	2.961	2.996	3.223	3.502
40	2.801	2.821	2.858	2.876	2.894	2.931	2.951	2.973
41	2.877	2.901	2.947	2.969	2.991	3.423	3.533	3.582
42	2.904	2.928	2.974	2.996	3.205	3.536	3.581	3.630
43	2.822	2.843	2.884	2.904	2.923	2.964	2.986	3.115
44	2.845	2.868	2.909	2.929	2.949	2.990	3.120	3.348
45	2.850	2.877	2.926	2.951	2.975	3.203	3.420	3.533
46	2.843	2.864	2.902	2.920	2.939	2.977	2.997	3.225
47	2.898	2.919	2.960	2.979	2.999	3.396	3.523	3.570
48	2.914	2.931	2.964	2.979	2.995	3.218	3.355	3.501
49	2.941	2.961	2.998	3.105	3.221	3.459	3.526	3.567
50	2.891	2.912	2.949	2.968	2.986	3.205	3.378	3.517
51	2.874	2.894	2.932	2.950	2.968	3.056	3.235	3.428
52	2.883	2.902	2.938	2.955	2.972	3.075	3.247	3.433
53	2.870	2.889	2.926	2.943	2.961	2.997	3.143	3.323
54	2.864	2.880	2.910	2.925	2.940	2.970	2.986	3.048
55	2.807	2.838	2.896	2.924	2.952	3.117	3.464	3.602
56	2.861	2.880	2.915	2.932	2.949	2.985	3.040	3.227
57	2.999	2.999	2.999	2.999	3.056	3.352	3.502	3.548
58	2.944	2.954	2.973	2.982	2.991	3.157	3.313	3.482
59	2.844	2.859	2.887	2.900	2.914	2.942	2.956	2.972
60	2.860	2.877	2.909	2.925	2.940	2.973	2.990	3.116
61	2.650	2.680	2.700	2.800	2.810	2.870	2.920	2.970
62	2.791	2.808	2.839	2.854	2.869	2.900	2.917	2.935
63	2.804	2.818	2.845	2.858	2.871	2.897	2.912	2.927
64	2.850	2.850	2.870	2.890	2.910	2.930	2.960	2.980
65	2.776	2.796	2.833	2.851	2.869	2.907	2.927	2.949
66	2.841	2.859	2.892	2.908	2.924	2.958	2.976	2.995
67	2.816	2.834	2.867	2.883	2.900	2.933	2.951	2.970
68	2.850	2.870	2.900	2.900	2.910	2.940	2.910	2.970
69	2.844	2.860	2.890	2.904	2.919	2.949	2.965	2.982
70	2.820	2.837	2.869	2.885	2.901	2.933	2.951	2.969

Appendix III- continued

Sample Number	Percentile							
	P-30	P-35	P-45	P-50	P-55	P-65	P-70	P-75
71	2.830	2.845	2.873	2.887	2.900	2.928	2.943	2.959
72	2.810	2.830	2.867	2.885	2.903	2.940	2.960	2.981
73	2.898	2.917	2.952	2.969	2.986	3.284	3.505	3.554
74	2.741	2.763	2.804	2.824	2.844	2.886	2.908	2.932
75	2.798	2.817	2.852	2.870	2.887	2.922	2.941	2.961
76	2.842	2.859	2.891	2.906	2.921	2.953	2.970	2.988
77	2.840	2.861	2.899	2.918	2.936	2.974	2.995	3.232
78	2.831	2.851	2.887	2.905	2.923	2.959	2.979	3.007
79	2.799	2.821	2.862	2.882	2.902	2.943	2.965	2.989
80	2.844	2.864	2.903	2.921	2.940	2.978	2.998	3.370
81	2.826	2.848	2.888	2.907	2.926	2.966	2.988	3.210
82	2.859	2.877	2.909	2.925	2.940	2.972	2.990	3.157
83	2.836	2.852	2.881	2.895	2.909	2.938	2.954	2.971
84	2.832	2.848	2.878	2.892	2.907	2.937	2.953	2.970
85	2.823	2.842	2.877	2.894	2.912	2.947	2.966	2.987
86	2.874	2.892	2.925	2.941	2.957	2.991	3.164	3.503
87	2.855	2.870	2.900	2.914	2.928	2.958	2.973	2.990
88	2.746	2.771	2.818	2.840	2.863	2.910	2.935	2.962
89	2.778	2.797	2.833	2.850	2.867	2.903	2.922	2.943
90	2.752	2.776	2.823	2.845	2.867	2.914	2.938	2.965
91	2.795	2.815	2.852	2.870	2.888	2.925	2.945	2.966
92	2.808	2.833	2.881	2.904	2.927	2.975	3.029	3.510
93	2.828	2.845	2.875	2.890	2.905	2.935	2.952	2.969
94	2.851	2.869	2.902	2.917	2.933	2.966	2.984	3.064
95	2.854	2.871	2.904	2.919	2.935	2.967	2.984	3.056
96	2.816	2.834	2.869	2.885	2.902	2.936	2.955	2.974
97	2.841	2.858	2.889	2.904	2.919	2.950	2.967	2.985
98	2.841	2.859	2.893	2.910	2.926	2.960	2.978	2.998
99	2.830	2.846	2.876	2.890	2.905	2.934	2.950	2.967
100	2.755	2.778	2.821	2.842	2.863	2.906	2.929	2.954
101	2.850	2.869	2.904	2.921	2.938	2.974	2.993	3.273
102	2.805	2.822	2.854	2.869	2.884	2.915	2.932	2.951
103	2.832	2.849	2.880	2.895	2.910	2.941	2.958	2.976
104	1.340	1.380	1.410	1.420	1.440	1.480	1.490	2.350

Appendix III- continued

Sample Number	Percentile						
	P-80	P-84	P-85	P-90	P-95	P-97	P-99
1	2.810	3.050	3.100	3.300	3.800	4.210	4.670
2	3.563	3.632	3.651	3.761	3.924	4.005	4.037
3	2.966	2.986	2.992	3.282	3.599	3.706	3.909
4	2.924	2.943	2.949	2.980	3.501	3.634	3.884
5	3.038	3.316	3.392	3.569	3.706	3.795	3.963
6	2.952	2.972	2.977	3.176	3.604	3.713	3.920
7	2.981	3.076	3.200	3.568	3.742	3.855	4.011
8	2.974	2.998	3.076	3.525	3.659	3.747	3.912
9	2.960	2.980	2.986	3.330	3.537	3.568	3.626
10	2.976	2.996	3.024	3.477	3.629	3.716	3.880
11	2.910	2.931	2.936	2.970	3.400	3.687	4.009
12	3.554	3.599	3.611	3.683	3.789	3.858	3.988
13	2.949	2.980	2.988	3.365	3.610	3.699	3.867
14	2.998	3.292	3.379	3.567	3.698	3.783	3.944
15	3.285	3.514	3.528	3.610	3.731	3.809	3.957
16	3.342	3.527	3.541	3.625	3.750	3.831	3.984
17	2.918	2.936	2.941	2.970	3.061	3.193	3.441
18	2.988	3.502	3.515	3.591	3.703	3.776	3.914
19	3.383	3.528	3.541	3.612	3.719	3.788	3.918
20	3.457	3.542	3.555	3.631	3.744	3.818	3.957
21	3.203	3.509	3.523	3.600	3.716	3.791	3.932
22	3.666	3.741	3.762	3.882	4.008	4.024	4.054
23	2.850	2.914	2.931	3.269	3.628	3.731	3.927
24	2.995	3.297	3.400	3.564	3.679	3.753	3.893
25	3.324	3.520	3.535	3.623	3.754	3.838	3.998
26	3.538	3.584	3.597	3.670	3.779	3.849	3.983
27	3.049	3.383	3.474	3.594	3.742	3.837	4.003
28	3.523	3.575	3.590	3.674	3.800	3.881	4.008
29	3.598	3.668	3.687	3.799	3.964	4.011	4.043
30	3.691	3.727	3.737	3.795	3.881	3.937	4.014
31	3.420	3.550	3.600	3.750	4.020	4.230	4.630
32	2.404	2.416	2.419	2.439	2.467	2.485	2.741
33	3.587	3.644	3.660	3.752	3.888	3.977	4.029
34	3.536	3.601	3.618	3.721	3.874	3.973	4.029
35	3.126	3.486	3.514	3.616	3.765	3.863	4.009

Appendix III- continued

Sample Number	Percentile						
	P-80	P-84	P-85	P-90	P-95	P-97	P-99
36	3.546	3.635	3.659	3.801	4.001	4.017	4.049
37	3.571	3.621	3.635	3.715	3.833	3.910	4.014
38	3.508	3.562	3.576	3.662	3.789	3.872	4.006
39	3.558	3.609	3.623	3.705	3.826	3.905	4.013
40	2.997	3.358	3.472	3.602	3.760	3.863	4.010
41	3.637	3.688	3.702	3.783	3.903	3.980	4.029
42	3.685	3.735	3.748	3.828	3.947	4.005	4.038
43	3.419	3.539	3.554	3.644	3.777	3.863	4.005
44	3.523	3.577	3.591	3.677	3.804	3.886	4.010
45	3.590	3.642	3.656	3.739	3.862	3.942	4.021
46	3.501	3.564	3.582	3.683	3.833	3.931	4.022
47	3.623	3.672	3.685	3.763	3.878	3.952	4.023
48	3.553	3.600	3.613	3.689	3.802	3.875	4.003
49	3.613	3.656	3.667	3.735	3.835	3.900	4.007
50	3.573	3.624	3.638	3.720	3.842	3.921	4.017
51	3.541	3.597	3.612	3.703	3.836	3.923	4.019
52	3.541	3.596	3.611	3.699	3.831	3.916	4.017
53	3.506	3.554	3.567	3.645	3.761	3.835	3.977
54	3.260	3.454	3.502	3.600	3.744	3.839	4.003
55	3.728	3.843	3.875	4.004	4.027	4.042	4.070
56	3.434	3.549	3.570	3.691	3.871	3.988	4.032
57	3.600	3.646	3.659	3.734	3.846	3.918	4.014
58	3.573	3.647	3.667	3.786	3.962	4.011	4.043
59	2.990	3.101	3.163	3.507	3.656	3.753	3.936
60	3.379	3.532	3.551	3.656	3.813	3.914	4.019
61	3.550	3.700	3.760	3.580	3.850	4.050	4.400
62	2.955	2.974	2.979	3.127	3.614	3.787	4.012
63	2.944	2.960	2.964	2.989	3.436	3.682	4.008
64	3.000	3.210	3.300	3.540	3.700	3.770	3.940
65	2.973	2.995	3.017	3.438	3.676	3.803	4.006
66	3.178	3.380	3.436	3.606	3.803	3.931	4.024
67	2.999	2.999	2.999	2.999	3.056	3.352	3.502
68	2.000	3.050	3.130	3.530	3.700	3.800	4.000
69	3.037	3.431	3.507	3.626	3.803	3.917	4.021
70	2.990	3.225	3.345	3.630	3.877	4.004	4.037

Appendix III- continued

Sample Number	Percentile						
	P-80	P-84	P-85	P-90	P-95	P-97	P-99
71	2.977	2.993	2.998	3.505	3.713	3.849	4.014
72	3.128	3.521	3.546	3.693	3.911	4.006	4.039
73	3.607	3.656	3.670	3.748	3.865	3.940	4.020
74	2.959	2.983	2.990	3.429	4.017	4.032	4.061
75	2.984	3.102	3.218	3.551	3.681	3.765	3.924
76	3.127	3.405	3.481	3.622	3.812	3.935	4.025
77	3.743	4.006	4.009	4.023	4.044	4.058	4.083
78	3.443	3.573	3.596	3.734	3.937	4.008	4.041
79	3.254	3.521	3.537	3.631	3.771	3.861	4.007
80	3.534	3.578	3.590	3.661	3.767	3.835	3.965
81	3.524	3.583	3.599	3.694	3.834	3.925	4.020
82	3.505	3.566	3.582	3.680	3.825	3.920	4.019
83	2.990	3.175	3.283	3.597	3.815	3.957	4.028
84	2.989	3.127	3.209	3.542	3.698	3.799	3.991
85	3.123	3.383	3.455	3.643	3.881	4.004	4.037
86	3.560	3.612	3.626	3.710	3.833	3.914	4.015
87	3.183	3.501	3.516	3.601	3.728	3.810	3.966
88	2.992	3.301	3.416	3.581	3.719	3.809	3.978
89	2.966	2.987	2.992	3.491	3.772	3.950	4.029
90	2.995	3.280	3.373	3.574	3.717	3.810	3.986
91	2.990	3.305	3.449	3.645	3.874	4.002	4.035
92	3.580	3.644	3.661	3.764	3.916	4.002	4.035
93	2.989	3.164	3.273	3.559	3.697	3.786	3.954
94	3.435	3.562	3.583	3.707	3.891	4.001	4.034
95	3.412	3.557	3.578	3.703	3.888	4.001	4.034
96	2.997	3.350	3.463	3.611	3.786	3.899	4.019
97	3.127	3.514	3.536	3.663	3.851	3.973	4.030
98	3.326	3.522	3.535	3.613	3.728	3.803	3.944
99	2.986	3.107	3.225	3.574	3.757	3.877	4.016
100	2.982	3.151	3.281	3.582	3.754	3.865	4.013
101	3.526	3.573	3.586	3.661	3.773	3.846	3.983
102	2.971	2.989	2.994	3.522	3.683	3.788	3.985
103	2.996	3.381	3.500	3.588	3.718	3.802	3.962
104	2.520	2.630	2.680	2.860	3.200	3.460	4.900

Appendix IV- Mean grain size values (phi units) as estimated by different formulae

Sample Number	Mz1	Mz2	Mz3	Mz4	Mz
1	1.4100	2.1650	1.9133	1.7560	1.7830
2	2.8450	3.0743	2.9978	2.7663	2.7859
3	2.8530	2.8530	2.8530	2.9045	2.9055
4	2.8179	2.8179	2.8179	2.8179	2.8655
5	2.8829	3.0285	2.9800	2.9838	2.9780
6	2.8436	2.8436	2.8436	2.8769	2.8984
7	2.8572	2.8934	2.8813	2.9618	2.9406
8	2.8406	2.8406	2.8406	2.9368	2.9036
9	2.8449	2.8449	2.8449	2.9069	2.8917
10	2.8657	2.8657	2.8657	2.9545	2.9228
11	2.7969	2.7969	2.7969	2.7969	2.8350
12	2.9283	3.1567	3.0806	3.0753	3.0752
13	2.7798	2.7798	2.7798	2.8453	2.8062
14	2.8773	3.0135	2.9681	2.9784	2.9710
15	2.8980	3.1333	3.0549	3.0028	3.0050
16	2.9024	3.1436	3.0632	3.0104	3.0127
17	2.8202	2.8202	2.8202	2.8202	2.8251
18	2.8659	3.1119	3.0299	2.9737	2.9756
19	2.9032	3.1434	3.0633	3.0077	3.0118
20	2.8983	3.1425	3.0611	3.0049	3.0119
21	2.8822	3.1187	3.0399	2.9861	2.9880
22	2.9010	3.1842	3.0898	3.1197	2.9637
23	2.5002	2.0442	2.1962	2.1795	1.0437
24	2.8895	3.0305	2.9835	2.9921	2.9857
25	2.9127	3.1517	3.0720	3.0214	3.0255
26	2.9339	3.1807	3.0984	3.0736	3.0820
27	2.8816	3.0605	3.0009	2.9872	2.9882
28	2.9352	3.1850	3.1017	3.0661	3.0803
29	2.9290	3.2055	3.1133	3.1085	3.1059
30	3.4114	3.2744	3.3201	3.3009	3.2763
31	2.9200	3.1750	3.0900	3.0560	3.0760
32	2.3394	2.3394	2.3394	2.3394	2.3394
33	2.9571	3.2351	3.1424	3.1470	3.1428
34	2.9096	3.1720	3.0845	3.0290	3.0612
35	2.8637	3.0889	3.0138	2.9698	2.9726

Appendix IV- continued

Sample Number	Mz1	Mz2	Mz3	Mz4	Mz
36	2.8963	3.1796	3.0852	3.0329	3.0587
37	2.9388	3.2006	3.1133	3.1081	3.1027
38	2.9063	3.1565	3.0731	3.0175	3.0358
39	2.9100	3.1800	3.0900	3.0520	3.0840
40	2.8765	3.0464	2.9898	2.9850	2.9861
41	2.9696	3.2412	3.1507	3.1813	3.1769
42	2.9961	3.2784	3.1843	3.2164	3.2370
43	2.9042	3.1439	3.0640	3.0121	3.0250
44	2.9292	3.1741	3.0925	3.0596	3.0715
45	2.9510	3.2009	3.1176	3.1332	3.1243
46	2.9207	3.1700	3.0869	3.0357	3.0594
47	2.9795	3.2486	3.1589	3.1889	3.1828
48	2.9796	3.2284	3.1454	3.1520	3.1549
49	3.1059	3.2656	3.2124	3.2288	3.2284
50	2.9680	3.2242	3.1388	3.1482	3.1469
51	2.9504	3.2014	3.1177	3.1053	3.1092
52	2.9555	3.2076	3.1236	3.1132	3.1171
53	2.9436	3.1796	3.1009	3.0736	3.0788
54	2.9256	3.1317	3.0630	3.0305	3.0383
55	2.9243	3.2725	3.1565	3.1677	3.1330
56	2.9328	3.1732	3.0931	3.0568	3.0740
57	3.0000	3.3234	3.2156	3.2475	3.2463
58	2.9675	3.2415	3.1502	3.1526	3.1579
59	2.9008	2.9477	2.9320	2.9947	2.9739
60	2.9253	3.1673	3.0866	3.0397	3.0540
61	2.8000	3.1100	3.0667	2.28 60	2.579 0
62	2.8546	2.8546	2.8546	2.8785	2.9108
63	2.8583	2.8583	2.8583	2.8583	2.8993
64	2.8900	2.9900	2.9570	2.98 60	2.978 0
65	2.8517	2.8517	2.8517	2.9320	2.9120
66	2.9088	3.0805	3.0233	3.0153	3.0164
67	2.8839	2.9963	2.9588	2.9883	2.9781
68	2.9000	2.9300	2.9200	3.0020	2.978 0
69	2.9049	3.1107	3.0421	3.0197	3.0241
70	2.8856	2.9934	2.9574	3.0024	2.9972

Appendix IV- continued

Sample Number	Mz1	Mz2	Mz3	Mz4	Mz
71	2.8870	2.8870	2.8870	2.9832	2.9520
72	2.8854	3.1322	3.0499	3.0104	3.0157
73	2.9695	3.2457	3.1536	3.1837	3.1684
74	2.8000	2.9500	2.9000	2.4500	2.6760
75	2.8700	2.9186	2.9024	2.9714	2.9495
76	2.9064	3.0955	3.0324	3.0185	3.0219
77	2.8000	3.0000	2.9333	2.9660	2.9910
78	2.9055	3.1695	3.0815	3.0352	3.0408
79	2.8826	3.1233	3.0430	2.9918	2.9945
80	2.9216	3.1767	3.0916	3.0318	3.0685
81	2.4100	2.4550	2.4400	2.5420	2.5340
82	2.9250	3.1837	3.0975	3.0442	3.0624
83	2.8954	2.9792	2.9513	3.0069	2.9960
84	2.8928	2.9526	2.9326	2.9931	2.9741
85	2.8949	3.0715	3.0126	3.0096	3.0130
86	2.9417	3.2133	3.1227	3.0936	3.1126
87	2.9144	3.1516	3.0725	3.0228	3.0256
88	2.8409	2.9819	2.9349	2.9429	2.9381
89	2.8502	2.3502	2.8502	2.9432	2.9198
90	2.8454	2.9745	2.9315	2.9455	2.9377
91	2.8706	3.0170	2.9682	2.9889	2.9906
92	2.9048	3.1829	3.0902	3.0350	3.0803
93	2.8904	2.9689	2.9427	2.9941	2.9778
94	2.9179	3.1770	3.0906	3.0433	3.0538
95	2.9195	3.1765	3.0909	3.0444	3.0543
96	2.8856	3.0523	2.9967	2.9968	2.9980
97	2.9044	3.1499	3.0680	3.0255	3.0302
98	2.9101	3.1512	3.0708	3.0172	3.0194
99	2.8906	2.9422	2.9250	2.9980	2.9801
100	2.8426	2.9140	2.8902	2.9479	2.9330
101	2.9217	3.1796	3.0936	3.0347	3.0627
102	2.8693	2.8693	2.8693	2.9689	2.9308
103	2.8955	3.0785	3.0175	3.0032	3.0060
104	1.4200	1.9500	1.7733	1.6660	1.7690

Appendix V- Standard deviation values (phi units) as estimated by different formulae

Sample Number	σ_1	σ_2	σ_3	σ_4	σ
1	.1333	.8850	.8364	.8204	.7440
2	.6092	.5580	.6711	.8777	.7146
3	.1342	.1336	.2134	.2307	.2280
4	.1263	.1258	.1980	.2137	.1894
5	.1425	.2875	.3041	.3177	.2721
6	.1294	.1288	.2120	.2301	.2161
7	.1471	.1826	.2621	.3006	.2833
8	.1585	.1578	.2426	.2742	.2776
9	.1366	.1360	.2070	.2224	.2214
10	.1310	.1304	.2136	.2359	.2456
11	.1349	.1343	.1922	.2047	.2044
12	.5352	.4425	.4053	.3928	.4016
13	.2014	.2005	.3121	.3363	.3961
14	.1437	.2793	.2999	.3165	.2686
15	.1464	.3811	.3533	.3438	.3024
16	.1429	.3835	.3559	.3464	.3093
17	.1170	.1165	.1241	.1254	.1334
18	.1453	.3906	.3585	.3477	.2740
19	.1635	.3854	.3527	.3418	.3091
20	.1945	.3995	.3669	.3559	.3298
21	.1551	.3910	.3606	.3502	.3003
22	.6434	.5571	.6941	.7201	.7263
23	.1106	.8702	.4097	.7415	.0371
24	.1262	.2667	.2845	.3037	.2510
25	.1414	.3691	.3447	.3362	.2978
26	.4511	.4038	.3693	.3578	.3538
27	.1444	.3226	.3277	.3409	.2822
28	.3721	.3907	.3617	.3518	.3392
29	.5331	.4627	.4349	.4251	.4215
30	.5656	.4533	.4080	.3930	.4255
31	.2148	.3750	.3820	.3889	.3500
32	.0776	.0772	.0774	.0772	.0773
33	.4860	.4093	.3787	.3683	.3776
34	.3837	.4291	.4025	.3932	.3681
35	.1727	.3971	.3784	.3735	.3173

Appendix V- continued

Sample Number	σ_1	σ_2	σ_3	σ_4	σ
36	.3359	.4554	.4383	.4318	.3902
37	.5086	.4211	.3860	.3742	.3809
38	.2751	.4056	.3757	.3654	.3423
39	.2222	.3700	.3805	.3852	.3571
40	.1430	.3122	.3257	.3452	.2809
41	.5423	.4471	.4089	.3961	.4237
42	.5576	.4566	.4161	.4026	.4297
43	.2344	.3955	.3690	.3599	.3302
44	.3900	.4029	.3736	.3636	.3528
45	.5276	.4410	.4065	.3948	.4130
46	.2986	.3949	.3723	.3643	.3401
47	.5153	.4233	.3864	.3741	.4007
48	.4483	.3721	.3417	.3314	.3426
49	.4792	.3904	.3547	.3428	.3685
50	.4795	.4005	.3690	.3583	.3714
51	.4268	.3958	.3685	.3591	.3583
52	.4226	.3885	.3611	.3517	.3521
53	.3509	.3749	.3461	.3363	.3285
54	.1497	.3225	.3145	.3166	.2762
55	.6141	.5709	.5084	.4915	.5007
56	.2861	.3763	.3645	.3598	.3344
57	.4066	.3234	.2899	.2789	.3029
58	.4476	.4058	.3867	.3797	.3541
59	.1069	.1533	.2179	.2418	.2297
60	.2035	.3656	.3483	.3420	.3080
61	.2741	.3900	1.0223	1.1222	1.1692
62	.1199	.1194	.2047	.2233	.2103
63	.1023	.1019	.1641	.1776	.1713
64	.1333	.2200	.2630	.2870	.2505
65	.1442	.1436	.2327	.2551	.2625
66	.1288	.3000	.3177	.3273	.2902
67	.1289	.2408	.2784	.3026	.2606
68	.9630	.7750	.6920	.6704	.7319
69	.1148	.3202	.3248	.3350	.2690
70	.1247	.2320	.2974	.3309	.2856

Appendix V- continued

Sample Number	σ_1	σ_2	σ_3	σ_4	σ
71	.1070	.1066	.2053	.2269	.2431
72	.1428	.3889	.3855	.3834	.3181
73	.5005	.4108	.3748	.3627	.3887
74	.3333	.4000	.7833	.9167	.9637
75	.1356	.1837	.2485	.2822	.2612
76	.1212	.3098	.3224	.3345	.2835
77	.2148	.3000	.2879	.3296	.3495
78	.1459	.4038	.3933	.3889	.3495
79	.1581	.3982	.3732	.3645	.3187
80	.4060	.4017	.3657	.3537	.3310
81	.1111	.1450	.2210	.3204	.2637
82	.2345	.3824	.3587	.3504	.3252
83	.1126	.1958	.2654	.2982	.2668
84	.1151	.1744	.2379	.2651	.2456
85	.1364	.3124	.3397	.3544	.3050
86	.4797	.3989	.3665	.3556	.3474
87	.1131	.3498	.3264	.3184	.2664
88	.1796	.3199	.3379	.3586	.3043
89	.1374	.1368	.2424	.2655	.2805
90	.1779	.3062	.3296	.3477	.3015
91	.1427	.2885	.3319	.3641	.3020
92	.5406	.4613	.4298	.4189	.3946
93	.1174	.1954	.2492	.2787	.2482
94	.1718	.3854	.3718	.3665	.3332
95	.1636	.3804	.3679	.3630	.3281
96	.1321	.2982	.3185	.3395	.2769
97	.1195	.3644	.3555	.3517	.2917
98	.1306	.3712	.3422	.3324	.2939
99	.1142	.1653	.2425	.2793	.2575
100	.1661	.2369	.2980	.3327	.3015
101	.3288	.3935	.3598	.3485	.3250
102	.1209	.1204	.2137	.2341	.2511
103	.1204	.3029	.3062	.3243	.2539
104	.7630	.6800	.6476	.6388	.5879

Appendix VI- Skewness values as estimated by
different formulae

Sample Number	Sk1	Sk2	Sk3	Sk
1	.0000	.8531	1.2316	.8458
2	.1882	.4108	-.3837	.1226
3	0.0000	0.0000	1.9637	.2713
4	0.0000	0.0000	1.8911	.2666
5	0.0000	.5064	1.0245	.5314
6	0.0000	0.0000	2.1256	.2811
7	0.0000	.1978	1.7607	.3840
8	0.0000	0.0000	1.7685	.2583
9	-.0000	-.0000	1.7181	.2547
10	0.0000	0.0000	2.0988	.2796
11	0.0000	0.0000	1.4178	.2307
12	.2160	.5159	.5721	.4663
13	0.0000	0.0000	.6565	.0941
14	0.0000	.4875	1.0462	.5199
15	0.0000	.6174	.7765	.5842
16	0.0000	.6288	.7983	.5970
17	0.0000	0.0000	.2095	.0562
18	0.0000	.6296	.7661	.5926
19	.0119	.6230	.7466	.5839
20	.0260	.6112	.7377	.5727
21	0.0000	.6048	.7397	.5678
22	.2486	.5083	-.4734	.1579
23	-.4689	-.5240	-2.1913	-.6754
24	0.0000	.5287	1.0900	.5558
25	.0071	.6472	.8475	.6196
26	.1980	.6109	.7246	.5702
27	0.0000	.5544	.9647	.5606
28	.1556	.6391	.8082	.6071
29	.2336	.5976	.7860	.5695
30	-.1411	-.3022	-.2833	-.2583
31	.0550	.6800	.6400	.5260
32	0.0000	0.0000	0.0000	0.0000
33	.2389	.6789	.8723	.6502
34	.1460	.6115	.8029	.5834
35	0.0000	.5669	.7774	.5437

Appendix VI- continued

Sample Number	Sk1	Sk2	Sk3	Sk
36	.1100	.6221	.9004	.6061
37	.2352	.6215	.7493	.5831
38	.0803	.6167	.7719	.5828
39	.0900	.7297	1.2027	.7098
40	0.0000	.5440	1.0383	.5616
41	.2471	.6075	.7190	.5665
42	.2581	.6181	.7255	.5763
43	.0526	.6059	.7771	.5749
44	.1561	.6076	.7611	.5737
45	.2264	.5663	.6740	.5254
46	.1027	.6310	.8506	.6066
47	.2432	.6356	.7596	.5965
48	.2189	.6683	.8311	.6353
49	.1382	.4091	.5208	.3977
50	.2257	.6395	.7935	.6052
51	.1899	.6342	.8170	.6043
52	.1927	.6489	.8363	.6195
53	.1427	.6295	.7835	.5953
54	.0222	.6392	.9717	.6293
55	.2636	.6100	.6437	.5547
56	.1009	.6388	.9487	.6261
57	.2744	1.0000	1.3080	1.0000
58	.2127	.6750	.9566	.6576
59	0.0000	.3058	1.8905	.4639
60	.0535	.6618	.9342	.6436
61	-0.0150	-0.2627	-2.2881	-0.0186
62	0.0000	0.0000	2.3544	.2936
63	0.0000	0.0000	2.0110	.2743
64	0.0000	.4545	-1.3864	.5045
65	0.0000	0.0000	2.0421	.2762
66	0.0000	.5723	1.1373	.5944
67	0.0000	.4668	1.2827	.5297
68	0.0000	.2600	.8333	.5417
69	0.0000	.6428	1.1072	.6474
70	0.0000	.4645	1.6947	.5606

Appendix VI- continued

Sample Number	Sk1	Sk2	Sk3	Sk
71	0.0000	0.0000	3.0499	.3241
72	0.0000	.6343	1.0162	.6305
73	.2466	.6723	.8188	.6370
74	.0250	.3750	-2.1875	-.0398
75	0.0000	.2650	1.5998	.4166
76	0.0000	.6104	1.1401	.6246
77	.0255	.6111	1.9221	.6632
78	.0037	.6536	.9908	.6435
79	0.0000	.6044	.7886	.5755
80	.1746	.6348	.7506	.5944
81	.0150	.3103	2.0690	.4613
82	.0744	.6766	.9103	.6532
83	0.0000	.4274	1.8751	.5459
84	0.0000	.3429	1.7656	.4809
85	0.0000	.5652	1.2195	.5971
86	.2375	.6808	.8542	.6494
87	0.0000	.6780	.8970	.6527
88	0.0000	.4407	.9106	.4683
89	0.0000	0.0000	2.5409	.3028
90	0.0000	.4214	.9455	.4592
91	0.0000	.5075	1.3320	.5640
92	.2406	.6027	.7673	.5706
93	0.0000	.4014	1.5688	.5072
94	.0302	.6720	.9909	.6591
95	.0267	.6754	1.0045	.6635
96	0.0000	.5587	1.1449	.5847
97	0.0000	.6735	1.0289	.6646
98	0.0000	.6495	.8124	.6165
99	0.0000	.3120	2.0536	.4777
100	0.0000	.3016	1.3462	.4198
101	.1300	.6553	.7972	.6191
102	0.0000	0.0000	2.5519	.3033
103	0.0000	.6042	1.0311	.6079
104	.4150	.7794	1.1250	.7566

=SK

Appendix VII- Kurtosis values as estimated
by different formulae

Sample Number	Ku1	Ku2	Ku
1	.0435	.508 5	5.9 199
2	.1766	1.3186	1.2896
3	.1506	2.6182	2.1872
4	.2630	2.5456	2.1433
5	.1105	.8411	2.2549
6	.1751	2.7801	2.2851
7	.1103	2.0879	2.3269
8	.1205	2.4230	2.0692
9	.1396	2.3725	2.0387
10	.1133	2.7533	2.2688
11	.2630	2.0722	1.8571
12	.3505	.3729	.6891
13	.1610	2.4860	2.1073
14	.1109	.8940	2.2344
15	.1098	.4093	2.2272
16	.1064	.4124	2.3004
17	.2630	.8640	1.1267
18	.1075	.3788	2.2508
19	.1231	.3702	1.9605
20	.1406	.3807	1.7219
21	.1141	.3934	2.1316
22	.3254	1.4610	1.2938
23	.3420	6.4878	3.5621
24	.1018	.8697	2.3983
25	.1086	.4312	2.2676
26	.3242	.3682	.7436
27	.1084	.7019	2.3090
28	.2726	.4053	.8958
29	.3241	.4517	.7650
30	.3689	.3205	.6425
31	.1405	.720 0	1.8230
32	.2630	.6544	1.0001
33	.3401	.4035	.7177
34	.2522	.4456	.9814
35	.1197	.4938	2.0854

Appendix VII- continued

Sample Number	Ku1	Ku2	Ku
36	.2012	.5256	1.2559
37	.3496	.3754	.6914
38	.1941	.4060	1.2585
39	.1485	.7432	1.7623
40	.1061	.7926	2.3767
41	.3521	.3683	.6849
42	.3559	.3573	.6750
43	.1682	.4290	1.4637
44	.2766	.4102	.8844
45	.3442	.3914	.7063
46	.2120	.4610	1.1733
47	.3541	.3624	.6795
48	.3481	.3798	.6955
49	.3590	.3483	.6669
50	.3447	.3899	.7049
51	.3067	.4221	.8008
52	.3099	.4172	.7911
53	.2688	.3964	.9058
54	.1226	.5686	2.0508
55	.3031	.2889	.7274
56	.2067	.5463	1.2348
57	.3734	.3080	.6318
58	.3056	.4942	.8226
59	.0969	2.0390	2.6464
60	.1542	.4937	1.6289
61	.0327	.0678	.3168
62	.1895	3.0089	2.4234
63	.2629	2.6655	2.2158
64	.1098	1.2955	2.2996
65	.1261	2.6965	2.2345
66	.1007	.8447	2.6079
67	.1020	1.1647	2.4546
68	.0921	3.0417	2.8395
69	.0892	.6981	2.8744
70	.0931	1.5806	2.9133

Appendix VII- continued

Sample Number	Ku1	Ku2	Ku
71	.0956	3.7044	2.8438
72	.0972	.6212	2.6800
73	.3547	.3608	.6781
74	.0584	3.8125	3.5064
75	.1070	1.8157	2.3159
76	.0938	.7846	2.7692
77	.1330	.5167	1.2860
78	.0976	.5638	2.6265
79	.1121	.4429	2.2054
80	.2949	.3546	.8137
81	.0789	2.3793	2.6776
82	.1729	.4454	1.4309
83	.0898	1.8223	2.9800
84	.0974	1.8528	2.6245
85	.0996	.9388	2.6957
86	.3473	.3823	.6977
87	.0917	.4297	2.6842
88	.1248	.8359	1.9844
89	.1134	3.1953	2.5361
90	.1254	.9026	1.9881
91	.1005	1.1467	2.6351
92	.3330	.4245	.7380
93	.0967	1.5590	2.5845
94	.1217	.5334	2.0888
95	.1171	.5414	2.1762
96	.0996	.8749	2.5087
97	.0884	.5690	2.9054
98	.1012	.3921	2.4016
99	.0928	2.1917	2.8047
100	.1176	1.5016	2.1654
101	.2426	.3674	.9935
102	.1010	3.2064	2.5428
103	.0958	.6859	2.5749
104	.3140	.4926	.8077

Appendix VIII- Metric values of median (Md), standard deviation (QDa) and skewness (Ska) for use in diagrams of Buller and McManus (1972)

Sample Number	Md (mm)	QDa (mm)	Ska
1	0.375	0.079	
2	0.139	0.035	0.057
3	0.138	0.009	-0.012
4	0.142	0.009	0.000
5	0.136	0.009	0.002
6	0.139	0.009	0.000
7	0.138	0.009	0.001
8	0.140	0.010	0.001
9	0.139	0.010	0.000
10	0.137	0.009	0.001
11	0.143	0.009	-0.001
12	0.131	0.009	0.003
13	0.146	0.029	-0.015
14	0.136	0.014	0.005
15	0.134	0.010	0.005
16	0.134	0.010	0.001
17	0.142	0.009	0.000
18	0.137	0.008	0.001
19	0.134	0.010	0.001
20	0.134	0.010	-0.001
21	0.136	0.012	-0.002
22	0.134	0.010	0.000
23	0.177	0.035	-0.016
24	0.134	0.134	0.102
25	0.133	0.008	0.001
26	0.131	0.009	-0.001
27	0.136	0.025	-0.015
28	0.131	0.009	-0.000
29	0.131	0.046	0.014
30	0.094	0.028	-0.016
31	0.132	0.028	0.014
32	0.198	0.012	-0.004
33	0.128	0.007	0.000
34	0.133	0.025	-0.017
		0.021	-0.017

Appendix VIII- continued

Sample Number	Md (mm)	QDa (mm)	Ska
35	0.137	0.012	0.001
36	0.134	0.020	-0.008
37	0.130	0.027	-0.016
38	0.133	0.017	-0.006
39	0.130	0.026	-0.017
40	0.136	0.010	0.001
41	0.128	0.028	-0.017
42	0.125	0.028	-0.017
43	0.135	0.015	-0.005
44	0.131	0.022	-0.012
45	0.129	0.028	-0.015
46	0.132	0.018	-0.007
47	0.127	0.026	-0.017
48	0.127	0.023	-0.016
49	0.166	0.024	-0.008
50	0.128	0.025	-0.016
51	0.129	0.023	-0.013
52	0.129	0.022	-0.014
53	0.130	0.020	-0.011
54	0.132	0.009	-0.002
55	0.132	0.032	-0.018
56	0.131	0.017	-0.008
57	0.125	0.020	-0.020
58	0.127	0.021	-0.018
59	0.134	0.007	-0.000
60	0.132	0.013	-0.005
61	0.144	0.018	0.002
62	0.138	0.009	0.001
63	0.138	0.007	0.000
64	0.136	0.008	0.000
65	0.139	0.010	-0.001
66	0.133	0.009	0.001
67	0.136	0.008	0.000
68	0.135	0.007	0.000
69	0.134	0.007	0.000
70	0.135	0.008	0.001

Appendix VIII- continued

Sample Number	Md (mm)	QDa (mm)	Ska
71	0.135	0.007	0.001
72	0.135	0.009	0.001
73	0.128	0.026	-0.018
74	0.141	0.011	-0.001
75	0.136	0.009	0.001
76	0.133	0.008	0.001
77	0.132	0.018	-0.008
78	0.134	0.010	-0.001
79	0.136	0.010	0.000
80	0.132	0.022	-0.013
81	0.133	0.018	-0.008
82	0.132	0.014	-0.005
83	0.135	0.007	0.001
84	0.135	0.052	-0.045
85	0.135	0.009	-0.001
86	0.130	0.025	-0.017
87	0.133	0.007	0.000
88	0.140	0.012	0.000
89	0.139	0.009	-0.001
90	0.139	0.012	0.001
91	0.137	0.009	0.000
92	0.134	0.029	-0.017
93	0.134	0.007	0.001
94	0.132	0.010	-0.002
95	0.132	0.010	-0.002
96	0.135	0.008	0.000
97	0.134	0.008	-0.001
98	0.133	0.009	0.001
99	0.134	0.007	0.001
100	0.139	0.011	0.001
101	0.132	0.019	-0.010
102	0.137	0.008	0.001
103	0.134	0.008	0.001
104	0.385	0.088	-0.053